MODIFIED POLYSACCHARIDE-BASED PARTICLES FOR STRENGTHENING PAPER

by

Johannes Christoffel Terblanche

Dissertation presented for the Degree

of

DOCTOR OF PHILOSOPHY
(Chemical Engineering)

in the Department of Process Engineering
at the University of Stellenbosch

Promoters

Prof. J.H. Knoetze
Department of Process Engineering
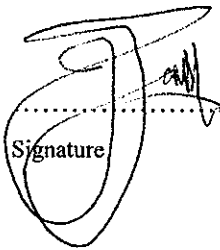University of Stellenbosch

Prof. R.D. Sanderson
Institute for Polymer science
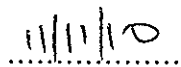University of Stellenbosch

STELLENBOSCH

December 2010

Declaration

I, the undersigned, hereby declare that the work contained in this dissertation is my own original work and that I have not previously in its entirety or in part submitted it at any university for a degree.

.... Signature

.... Date

Abstract

The ongoing trend in papermaking industries is to lower production costs by increasing the low cost filler content in the sheets. However, the disruption of inter-fibre bonding is accompanied by a deterioration of paper stiffness and mechanical properties if filler content exceeds 18 wt%. Polysaccharide solutions, such as starch, are often used as a low cost biodegradable additive to improve internal sheet strength when added to the wet-end of production. The amount of starch that can be added is however limited as only a small percentage will be retained in the paper web.

A dual additive multifunctional polysaccharide system was developed to allow higher filler loading levels without detrimental deterioration in paper properties. In order to achieve a larger surface area for fibre/filler interaction and to reduce drainage losses, at least one of these additives was in particulate form. Anionic, cationic, and unsaturated derivatives were prepared using sodium monochloroacetate, 3-chloro-2-hydroxypropyltrimethylammonium chloride, and allyl bromide, respectively. The degree of substitution was determined by ^{1}H-NMR spectroscopy and back titration methods and the interaction of the ionic modified derivatives with paper components was determined using fluorescence microscopy.

Anionic modified polysaccharide particles were prepared using techniques such as macrogel ultrasonification, water-in-water emulsification, and in-situ cross-linking and carboxymethylation of granular starch. A process of adding sequential layers of oppositely charged polyelectrolyte layers onto the filler particles was also investigated. A novel approach of preparing modified particles with tailored size and distribution using microfluidics was studied and modelled using response surface methodology.

Hand sheets were prepared using the dual additive system and improvements in stiffness, tear resistance, breaking length, and folding endurance were observed. The modified granular maize starch particles had a pre-eminent effect on improving stiffness at higher filler loadings (14% improvement at 30 wt% filler loading), while bulky particles prepared using microfluidics showed a more consistent improvement (between 6% and 10%) across the loading range.

Overall improvements gained by the introduction of multi-layered soluble polymers onto fillers suggest that the introduction of nanotechnology to the papermaking process should be of potential benefit to the industry. Furthermore, the dual additive system developed during the course of this study should also be tested on a continuous pilot plant papermaking process.

Opsomming

Die papierindustrie neig voortdurend daarna om produksiekostes te verlaag deur die persentasie lae koste vulstof wat gebruik word te verhoog. Aangesien die vulstof vesel kontak belemmer, gaan hoër vlakke (> 18 wt%) egter gepaard met 'n verlaging in papier styfheid en meganiese eienskappe. Polisakkaried oplossings, soos byvoorbeeld stysel, word dikwels gebruik as lae koste vergaanbare bymiddel om papier intern te versterk wanneer dit voor die vormingsproses bygevoeg word. Slegs 'n beperkte hoeveelheid stysel word egter behou in die papier matriks en oormatige oplossings ontsnap tydens dreinering in die afvalwater.

'n Dubbele multi-funksionele polisakkaried bymiddelsisteem was ontwikkel wat ongewensde verwakking in papiereienskappe verminder tydens vulstof verhogings. Ten minste een van die bymiddels was in partikelvorm om sodoende 'n groter oppervlak te bied vir vesel/vulstof interaksie en om dreineringsverliese te verminder. Anioniese, kationiese, sowel as onversadigde derivate was berei deur onderskeidelik gebruik te maak van natrium monochloroasetaat, 3-chloro-2-hidroksiepropieltrimetielammonium chloried, en alliel bromied. Die graad van substitutiese was bepaal met behulp van ^{1}H-KMR spektroskopie sowel as titrasie tegnieke terwyl die ioniese interaksie van die gemodifiseerde stysels met die papierkomponente ondersoek was met behulp van fluoressensie mikroskopie.

Anioniese polisakkaried partikels was berei met tegnieke soos makro-jel ultrasonifikasie, water-in-water emulsifikasie, en in-situ kruisbinding en karboksiemetielasie van stysel granulate. 'n Proses was ook ondersoek waar vulstof partikels omhul was in verskeie lae poliëlektroliet oplossings. 'n Nuwe benadering was toegepas waar gemodifiseerde partikels met voorafbepaalde grootte en verspreiding berei is deur gebruik te maak van mikrofluïdika en gemodelleer met behulp van oppervlakte ontwerp metodeleer.

Papier toetse was uitgevoer met die bymiddelsisteem en algehele verbetering in styfheid, skeurweerstand, breeklengte, en voulydsaamheid is waargeneem. Die gemodifiseerde stysel granulate het die grootste verbetering in styfheid by hoë vulstofladings getoon (14% verbetering by 30 wt% vulstoflading) terwyl die groter mikrofluïdika-bereide partikels algehele verbetering (tussen 6% en 10%) getoon het oor die hele vulstoflading reeks.

Die verbeteringe in styfheid sowel as meganiese eienskappe van papier voorberei met poliëlektroliet omhulde vulstof toon dat aanwending van nanotegnologie in hierdie bedryf potensieel voordelig kan wees. Opskalering van die polisakkaried bymiddels ontwikkel gedurende hierdie studie behoort uitgevoer te word vir verdere toetse op 'n kontinue papier loodsaanleg.

Acknowledgements

I would like to express my sincere thanks to the following people:

Prof. R.D. Sanderson and Prof. J.H. Knoetze who supervised my dissertation and contributed to ideas, provided guidance, and assisted me throughout this study. I also thank you for your motivation and friendship throughout the years.

Dr. A. Kornherr, Dr. F. Eder, and Dr. B.J.H. Janse for providing continuous support, feedback, and funding for this project. I will be eternally grateful for everything and it was a privilege working with you.

I would also like to thank Prof. V. Hessel and his colleagues at IMM (Mainz, Germany) for their kind assistance and warm reception during my visit to their facilities.

Hanlie Botha, Elsa Malherbe, Pauline Skillington, Miranda Waldron, and Illana Bergh for all their assistance with analytical work.

To all my colleagues and friends from the Mondi BP team in Stellenbosch I must express my sincere gratitude. Thank you Mingxuan Zou, Marehette le Grange, Carin Aston, Howard Matahwa, Helen Chirowodza, and Ashwell Makan for all your hard work and assistance on the Mondi projects. Also a special thanks to Donna-Leigh D'Aguiar for her assistance in the fluorescence studies.

To my Heavenly Father for His guidance.

Contents

<u>Glossary</u>

Abbreviation	Description
AgCl	Silver chloride
AgNO$_3$	Silver nitrate
AGU	Anhydroglucose unit
A$_i$	^{1}H-NMR peak integration area of position i
ANOVA	Analysis of variance
APS	Average particle size
APS$_{ds}$	Average particle size of dry starch
APS$_{ss}$	Average particle size of swollen starch granules
CCD	Charge-coupled device
CHPTMAC	3-chloro-2-hydroxypropyltrimethylammonium chloride
CMS	Carboxymethyl starch
D$_2$O	Deuterium oxide
DBTD	Dibutyltin dilaurate
DCl	Deuterium chloride
DDI	Distilled deionised
dex-HEMA	Hydroxyethyl methacrylate modified dextran
dex-MA	Methacrylated dextran
DF	Degrees of freedom
DMAc	Dimethylacetamide
DMF	Dimethyl formamide
DS	Degree of substitution
DS$_{allyl}$	Degree of substitution by allyl groups
DS$_{anionic}$	Degree of substitution by anionic groups
DS$_{cationic}$	Degree of substitution by cationic groups
DS$_{exp}$	Experimental degree of substitution
DSS	3-(trimethylsilyl)-1-propanesulfonic acid sodium salt
DS$_{th}$	Theoretical degree of substitution
ECH	Epichlorohydrin
FA	Folic acid
FITC	Fluorescein isothiocyanate
FPR	Phenolic formaldehyde resin
FTIR	Fourier transform infrared
GCC	Ground calcium carbonate
HCl	Hydrochloric acid
HES	Hydroxyethylmethacrylate
HES-HEMA	Hydroxyethylmethacrylate-hydroxyethyl starch
HLB	Hydrophilic-lipophilic balance
ISXL	In-situ cross-linked
KOH	Potassium hydroxide
LbL	Layer-by-layer
LDPE	Low density polyethylene
LiCl	Lithium chloride
MBA	*N,N*-methylene bisacrylamide
MS	Mean square
Na$_2$SO$_4$	Sodium sulphate
NaBH$_4$	Sodium borohydrate
NaCl	Sodium chloride
NaOH	Sodium hydroxide
PAC	Polyaluminium chloride

PCC	Precipitated calcium carbonate	
PCC-LBL0.05	Precipitated calcium carbonate encapsulated in ionic modified starch with DS of 0.05	
PCC-LBL0.40	Precipitated calcium carbonate encapsulated in ionic modified starch with DS of 0.40	
pDADMAC	Polydiallyldimethylammonium chloride	
PDI	Potential determining ions	
PEG	Poly(ethylene glycol)	
PEI	Polyethylenimine	
PEO	Poly(ethylene oxide)	
PNS	Polynaphthalene sulfonate	
$POCl_3$	Phosphorus oxychloride	
Ppm	parts per million	
PRESS	Predicted residual sum of squares	
PSS	Polystyrene sulfonate	
PVA	Polyvinyl alcohol	
RE	Reaction efficiency	
RE_{allyl}	Reaction efficiency of allyl substitution reaction	
$RE_{anionic}$	Reaction efficiency of anionic substitution reaction	
$RE_{cationic}$	Reaction efficiency of anionic substitution reaction	
RITC	Rhodamine B isothiocyanate	
RSM	Response surface methodology	
SEM	Scanning electron microscope	
SISXL	Self in-situ cross-linked	
SMCA	Sodium monochloroacetate	
SMCF	Starch microcellular foam	
SS	Stainless steel	
SSE	Sum of squares	
STDev	Standard deviation	
STMP	Sodium trimetaphosphate	
TA	Tannic acid	
TEMED	*N,N,N',N'*-tetramethylethylenediamine	
TGA	Thermogravimetric analysis	
TSC	Total solids content	
TSDC	Thermally stimulated depolarisation current	
UV	Ultraviolet	
W/O	Water-in-oil	
W/W	Water-in-water	
XRD	X-ray diffraction	

Symbols	Description	Units
μ	Electrophoretic mobility	$[m^2V^{-1}s^{-1}]$
c_i	Molar concentration of i	$[mol/dm^3]$
M_w	Molecular weight	$[g/mol]$
n_i	Molar amount of group i	$[mol]$
R^2	Coefficient of determination	$[-]$
T	Temperature	$[^oC]$
V	Volume	$[cm^3]$
v/v	Volume per unit volume	$[-]$
v_j	Volume fraction of component j	$[-]$
w/w	Weight per unit weight	$[-]$
ΔG_{mix}	Gibbs free energy of mixing	$[J/mol]$
ΔH_{mix}	Enthalpy of mixing	$[J/mol]$
ΔS_{mix}	Entropy of mixing	$[J/mol]$

ε	Permittivity	[F/m]
η	Viscosity	[Nsm^{-2}]
λ	Wavelength	[nm]
ξ	Zeta potential	[mV]
χ$_{ij}$	Interaction parameter between i and j	[-]

Chapter 1: Introduction

1.1 General introduction

Polysaccharides are natural macromolecules of universal occurrence in many living organisms, performing a wide variety of functions of which many are still not fully understood[1]. It forms the skeletal substance in higher plant and seaweed cell walls where it provides reserve food supplies and in some cases acts as a protective substance in the form of exudate gums, which can seal off injury sites. Its economic importance is mostly derived from the plant kingdom. For example, cellulose is by far the most abundant of all polysaccharides and has direct application as fibres in cotton, hemp, ramie, and as wood pulp for papermaking. It is also used as starting material for the formation of derivatives used in the manufacture of rayons and other fibres, films, sheeting, and even certain plastics.

Starch is the main polysaccharide used for human consumption, most notably in the form of cereal grains (eg. maize) and root crops (eg. potatoes), and stored as a more permanent reserve with the crop consisting of up to 70% starch[2]. It is also found, to a lesser extent, in seeds, fruits, leaves, and plant tubers, which contains up to 30% starch. Although starch from various sources receives widespread academic interest to advance the understanding of starch chemistry, only those that can be obtained in high yields from plants, which can be cultivated in abundance, are more of industrial importance. The work reported in this study is concerned with the latter variety, with the main focus on maize starch, representing the major commercial source of starch worldwide and an inexpensive renewable chemical feedstock.[3]

1.2 Modified polysaccharides

Modified polysaccharides have been developed over the last century in order to overcome one or more of its shortcomings, thereby expanding its usefulness for a myriad of industrial applications[4]. It has found uses in both food and non-food applications, though it is somewhat limited in the former where polysaccharides are chemically modified. This is due to possible toxicological restraints. Chemical modifications are introduced to alter the nature

1

of the interactions between the macromolecular chains and conducted predominantly by grafting or substituting the hydroxyl groups on the polysaccharide backbone with functional groups. Oxidation, alkylation, or esterification of the glucose hydroxyl groups can affect the hydrogen bonding, charge interaction (eg. by introducing phosphate groups), and hydrophobic character (eg. highly esterified starch solubility in organic solvents). Cross-linked polysaccharides have been found to improve stability to heat, pH, and freeze-thaw cycles, compared to native polysaccharides and used in, for example, a wide range of canned and frozen foods[5, 6] as well as biodegradable plastics[7]. Polymeric starch derivatives commonly used on industrial scale include starch xanthates as rubber substitutes[8] and starch esters as biodegradable detergents[9]. Copolymers of starch have also received substantial interest in the production of super absorbents, possessing the unusual property of absorbing several hundred times its own weight in water. This offers considerable potential in horticultural mulches and sanitary products[9, 10]. Enzymatic and/or acid hydrolysis of starches to lower molecular weights also represent a significant portion of commercial polysaccharide utilisation and it is used to produce glucose syrup that can be further converted to products such as ethanol (by fermentation)[11] or fructose (by isomerisation)[12].

1.3 Polysaccharide-based microparticles

Polymer-based microparticles have gained interest as delivery vehicle in the food and predominantly the pharmaceutical industries. In the food industry it is used to encapsulate or absorb ingredients such as vitamins, probiotics, flavours, bioactive peptides, and antioxidants[13]. In the pharmaceutical industry it is used as a carrier of nutrients, proteins, peptides, and other drugs[14]. These types of microparticles can be used for masking unpleasant tastes and/or ensure controlled release of the active substances as it moves through the digestive system of the body. Additionally, they are used to protect potentially reactive or unstable substances against environmental conditions during storage (eg. moisture) and/or after administration (eg. pH). The microgel particles prepared usually require cross-linking in order to render them water-insoluble until the polysaccharides hydrolyse systematically within the body, releasing the active substance.

Various techniques for preparing polysaccharide microparticles have been reported in literature and include spray drying, crystallisation, and water-in-oil (W/O) emulsification[15-17].

1.4 The paper industry

Paper production is based mainly on fibrous raw materials (such as wood fibres) and fillers. As regular mineral fillers are, in general, lower in price than typical papermaking fibres, partial replacement with fillers usually provides better papermaking economics (see Section 1.5). The main mineral fillers (in terms of quantity added in paper) are hydrous kaolin, talc, ground calcium carbonate (GCC), and precipitated calcium carbonate (PCC), the latter comprising about 39% of the global consumption of all types of virgin fillers applied in papermaking (source: Omya, 2004)[18]. The introduction of fillers offers benefits such as improved optical properties, printability, and dimensional stability while efforts are continuously made to include as much low cost filler as possible to support economic demands. However, fillers disrupt the tightly woven fibre network and the limit in terms of filler loading are set primarily by an accompanying reduction in paper strength properties (eg. stiffness and breaking length) (Figure 1.1).

Figure 1.1: Impact of filler loading degree on some important paper properties (pilot study, GCC as filler, wood-free filler furnish, grammage of 80 g/m^2 (picture redrawn)[18].
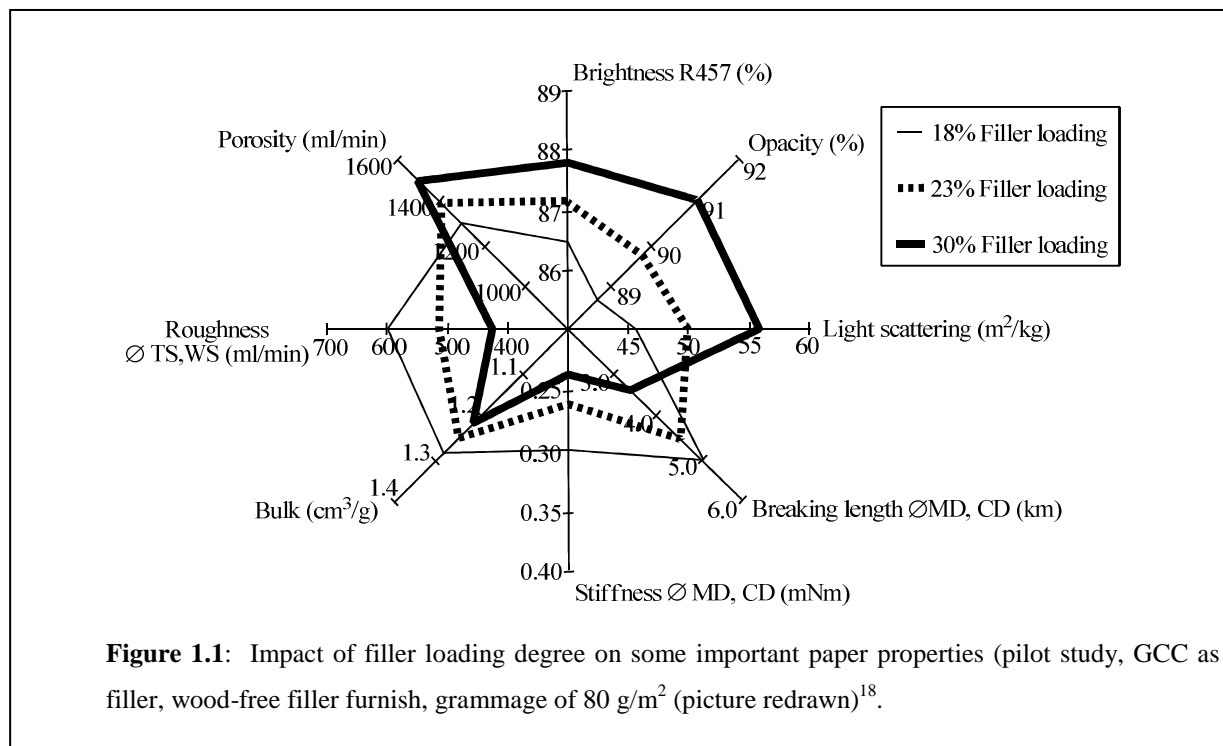
Natural chemical additives, particularly starch, play a dominant role in manufacturing paper and board and were used even before the existence of handmade paper, being present in sheets of papyrus prepared by the ancient Egyptians[4]. The bond strength of starch to fibre is

known to be greater than fiber-fiber bonding and is used to improve paper strength properties. However, native starch as such is not very suitable for wet-end application in the papermaking process since it is not well retained during drainage, making it undesirable from both an economic and environmental standpoint. The multifunctional character of cationic modified starch solutions enable papermakers to overcome some disadvantages inherent to unmodified starch, since it is retained more fully and consistently on a variety of filler surfaces. However, it has been shown that the amount retained is often also limited and higher additions will not necessarily be accompanied with an increase in sheet strength[19].

1.5 Considerations

Filler (eg. PCC) loading levels used in most European paper industries today typically range between 12 – 20 wt% (depending on the desired paper quality), with the remaining percentage comprising mainly of fibres[18]. Even with the addition of strengthening additives such as cationic starch at the wet end of the process, paper strength inevitably starts to deteriorate significantly as filler loadings exceed 18 wt%. For printing paper the loss in bending stiffness is usually the primary limit since it quickly weakens to below its minimum specification value. However, a suitable additive system that could effectively bridge and improve fibre-fibre, fibre-filler, as well as filler-filler bonding should allow adequate stiffness to be retained even if the filler loading increases above 20 wt%.

Table 1.1 shows the potential formulation cost saving if an existing printing paper grade (manufactured in Europe) containing 18 wt% PCC was increased to 20, 25, and 30 wt%, respectively.

Table 1.1: Example of the impact of PCC (filler) loading increase on printing paper formulating cost.

	PCC loading increase		
	18 → 20 wt%	**18 → 25 wt%**	**18 → 30 wt%**
Cost Saving/kg	1.4%	5.8%	10.2%

Even though a 2 wt% increase appears to show only a marginal percentage saving per unit weight, it should also be considered that paper manufacture involves a high volume

production process and even minor unit savings would amount to very significant economic importance for the industry.

An additive system that would make it possible to retain a higher percentage starch in paper, resulting in improved sheet strength, would ultimately allow higher filler loadings to be used to the advantage of the papermaker. However, polysaccharides such as starch are an essential food source for humans and resources are becoming under increased pressure as the demand from the biotechnology industry grows[20]. Subsequently the question arises of how greater starch absorption by the paper industry would affect the rest of the world. In essence printing paper currently consists of less than 1% modified starch and even if this small percentage is doubled, it would be easily justified if it would be accompanied by a significant preservation of forestry required for producing paper fibres.

1.6 Objectives

The main aim of this study was to develop an additive system that would allow PCC filler loadings in printing paper to be increased above 20 wt% without causing detrimental deterioration in paper strength. The major emphasis was on gaining improvements in bending stiffness when compared to standard paper containing similar loadings.

A new approach was taken whereby a dual additive polysaccharide-based system could be added to both the filler and fibre, consisting of a cationic as well as anionic polymer and where at least one of these additives were in particulate form. The rationale behind this was that multi-functional microgel particles offer a larger surface area for interaction between individual components as opposed to macromolecules alone. Apart from exclusively relying on electrostatic interactions to retain the polysaccharides in the paper matrix, microgel particles will escape more arduously through the drainage wire mesh during production. Methods for preparing ionic modified microgel particles had to be investigated and its performance in improving the strength of paper hand sheets evaluated and compared.

The objectives of this study were as follows:

1). Conduct a literature survey on the physicochemical properties of paper components and polysaccharides in order to gain insight on how it can be integrated to improve paper strength. Investigate available techniques for chemically modifying polysaccharides and preparing microgel particles.

2). Conceptualise the approach of incorporating ionic modified cross-linked particles as additives in paper. Synthesise a more familiar polyester-based particulate system containing both anionic and cationic charges. Treat these particles individually as well as simultaneously to paper components and conduct hand sheet trials with filler loadings increased above 20 wt%. Evaluate the effect of these additions on paper strength properties, including stiffness.

3). Chemically modify polysaccharides to contain either anionic or cationic charges. Also synthesise polysaccharide derivatives that can be cross-linked to form microgels. Find methods to determine the degree of modification.

4). Research techniques that can demonstrate the interaction of anionic and cationic modified polysaccharide species with paper components (fibres and fillers).

5). Find conventional techniques for preparing ionic modified (including different degrees of modification) polysaccharide particles suitable for application as additive in paper. Keep the complexity of processes and equipment to a minimum thereby allowing room for a more economical approach to be taken towards possible future scale-up.

6). Investigate a novel processing technique for preparing ionic modified polysaccharide particles. Consider microfluidic devices and construct a set-up, develop a suitable formulation, and test the process. Model the effect of flow conditions on particle size and distribution.

7). Conduct hand sheet trials with the separate ionic polysaccharide particles incorporated as additives. Use filler loadings above 18 wt% and report improvements made in paper strength

properties compared to standard sheets (excluding additive). Draw meaningful conclusions from all results.

1.7 Layout of dissertation

The dissertation consists of seven chapters and the flow diagram is presented in Figure 1.2. The second chapter presents a more detailed description of the basic papermaking process as well as the physicochemical properties of its components. Physicochemical properties of polysaccharides are also discussed, with the emphasis on starch. Various reported literature relating to processes that have been applied for preparing polysaccharide-based particles are summarised.
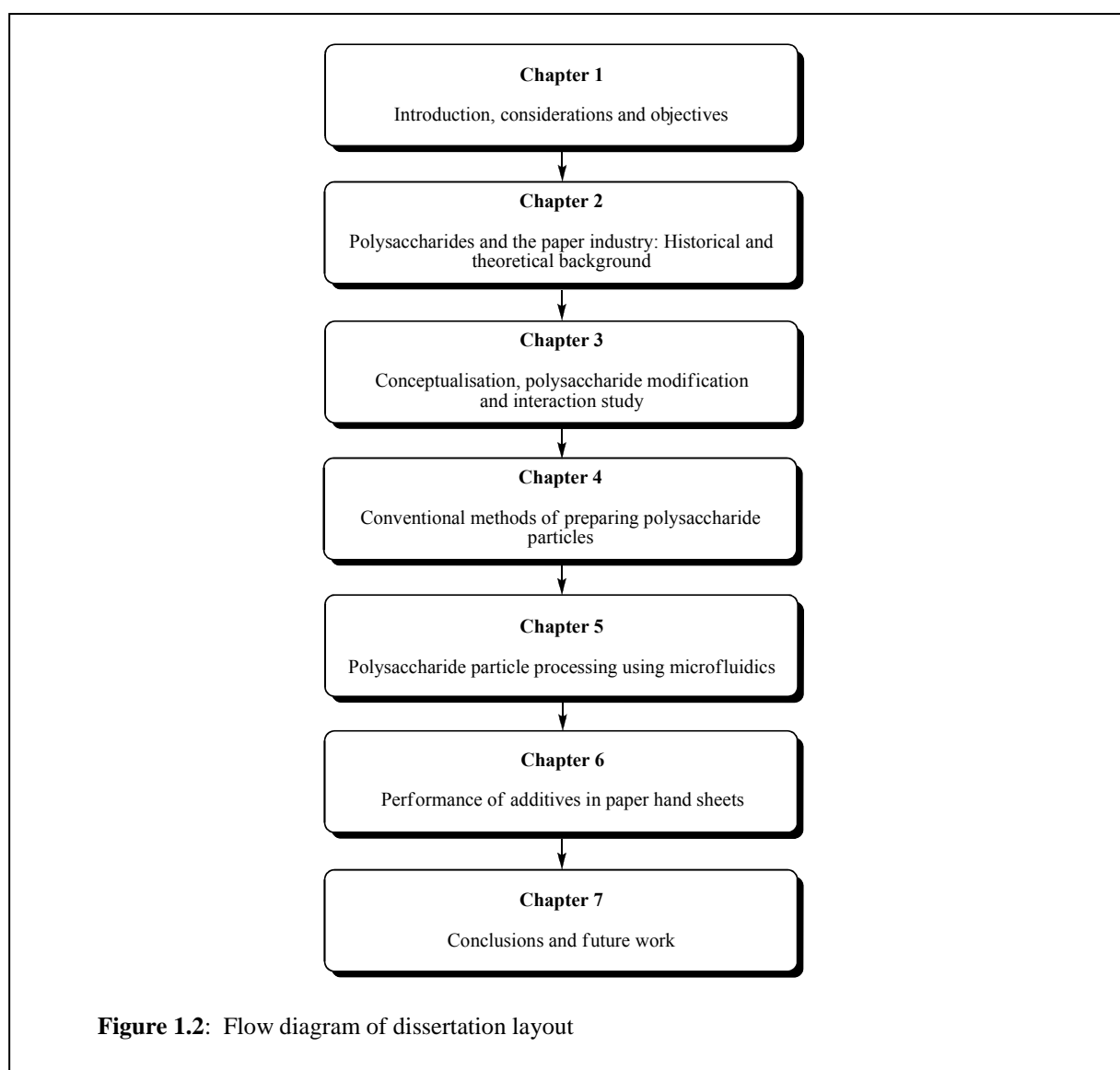
Figure 1.2: Flow diagram of dissertation layout

In Chapter 3, methods are described for preparing anionic and cationic modified polyester particles, which were used at the start of this study to illustrate the concept of introducing charged particulates to enhance the mechanical properties of paper. The procedures used for modifying polysaccharides are explained and characterised using ^{1}H-NMR spectroscopy. By utilising fluorescence microscopy, a methodology is described for studying the interactions of the individual ionic modified polysaccharides with both fibre and PCC.

Different techniques for preparing modified polysaccharide particles using conventional apparatus are discussed in Chapter 4. Since cationic starch solutions already form part of the current papermaking process, the discussion is more focused on preparing anionic modified microgel particles to form part of a dual retention aid system.

A novel technique for preparing W/O polysaccharide particles using a microfluidic device is discussed in Chapter 5. Device-type selection as well as suitable modified polysaccharides and emulsifiers for the system are described. The effect of individual water and oil flow rates and emulsifier level on particle size and distribution are presented using response surface methodology (RSM).

Results of hand sheets prepared using various synthesised polysaccharide particles are presented in Chapter 6. These results include paper bending stiffness, tear resistance, folding endurance, and tear strength. The procedure involved increasing the filler loading between nominal values of 20% and 30% and comparing deterioration strength trends to hand sheet standards.

The study is concluded in Chapter 7 with some recommendations made for possible further studies.

1.8 References

1.   G. O. Aspinall, *Polysaccharides*. Pergamon Press: Oxford, **1970**.

2.   R. W. Kerr, *Chemistry and Industry of Starch*. 2nd ed.; Academic Press Inc.: New York, **1950**.

3.   T. Gallaird, *Starch: Properties and Uses*. John Wiley & Sons: Great Britain, **1987**; Vol. 13.

4.   O. B. Wurzburg, *Modified Starches: Properties and Uses*. CRC Press, Inc.: **1986**.

5.   M. Nayouf; C. Loisel; J. L. Doublier, *Journal of Food Engineering*, **2003**, 59, 209-219.

6.   P. Deetae; S. Shobsngob; W. Varanyanond, et al., *Carbohydrate Polymers*, **2008**, 73, 351-358.

7.   M. Kim; S. J. Lee, *Carbohydrate Polymers*, **2002**, 50, 331-337.

8.   Z. Wang; Z. Peng; S. Li, et al., *Composites Science and Technology*, **2009**, 69, 1797-1803.

9.   D. Horton, *Advances in Carbohydrate Chemistry*. 1st ed.; Elsevier Inc.: San Diego, **2004**; Vol. 59.

10.   A. Li; J. Zhang; A. Wang, *Bioresource Technology*, **2007**, 98, 327-332.

11.   K. R. Szulczyk; B. A. McCarl; G. Cornforth, *Renewable and Sustainable Energy Reviews*, **2010**, 14, 394-403.

12.   K. Buchholz; J. Seibel, *Carbohydrate Research*, **2008**, 343, 1966-1979.

13.   B. Li; L. Wang; D. Li, et al., *Journal of Food Engineering*, **2009**, 92, 255-260.

14.   O. Franssen; O. P. Vos; W. E. Hennink, *Journal of Controlled Release*, **1997**, 44, 237-245.

15.   S. Krishnan; A. C. Kshirsagar; R. S. Singhal, *Carbohydrate Polymers*, **2005**, 62, 309-315.

16.   L. Elfstrand; A. C. Eliasson; M. Jönsson, et al., *Carbohydrate Polymers*, **2007**, 69, 732-741.

17.   G. Hamdi; G. Ponchel; D. Duchene, *Journal of Microencapsulation*, **2001**, 18, 373-383.

18.   H. Holik, *Handbook of Paper and Board*. Wiley-VCH GmbH & Co.: Weinheim, **2006**.

19.   M. Laleg, Swollen Starch-Latex Compositions for use in Papermaking, Patent: US 7,074,845 B2, **2006**.

20.   G. Entwistle; S. Bachelor; E. Booth, et al., *Industrial Crops and Products*, **1998**, 7, 175-186.

Chapter 2: Historical and theoretical background

2.1 Introduction to papermaking

Since the start of civilization, the human race had the need to communicate and document historical events in the form of writing. In ancient Egypt, papyrus plants, which grew abundantly along the Nile River, were used to make the written word more portable. Some of these artefacts were found in tombs dating back to 3500 BC[1-3]. The inner fibrous stem of the papyrus (where the name "paper" also originates) were laid out flat on a surface and weaved to form a flat sheet, which was then dampened in water and pressed. The glue-like sap of the plant bonded the woven fibres together as the sheet dried. During the first half of the 2nd century BC, writing on parchments, which is the skin of sheep or calves, gained popularity mainly because of problems with the supply of papyrus from Egypt. Wood, stone, wax, metal, pottery, clay, and other materials were all used as writing materials, but it was only in 105 AD that Tr'ai Lun, an official attached to the imperial court of China, made the first piece of paper from mulberry and other bast fibres combined with old rags, fishnets and hemp waste. The discovery and art of papermaking remained in China for over 500 years.

By the 14th century there were already paper mills operational around Europe, especially France, Spain, Germany and Italy, which mainly converted white linen and cotton rags into paper. However, the invention of the printing press by the Germans in 1450 significantly increased the demand for paper, which by the 17th century caused raw material shortages. A more abundant substitute for linen and cotton was required. It wasn't until 1719 that a Frenchman, René de Reamur, after watching American wasps making nests from chewed up wood fibre, commented that this should be the ideal method of making paper. However, it was only in the mid 19th century that wood pulp became commonly used for papermaking.

2.2 The pulp and paper making process

Until 1799 the paper manufacturing process involved dipping a mould in a suspension of fibres[3]. The mould consisted of a shallow box with removable sides and a screen bottom.

Operators skilfully had to pick up the correct amount of fibre from the suspension and shake it to drain excess water and distribute fibres evenly. The wet sheet subsequently had to be removed from the mesh, pressed, and dried. In 1800 the Fourdrinier brothers developed a process for making continuous sheets of paper based on the invention that Roberts developed a year before. This involved the pulp suspension being fed onto a travelling screen belt whilst the water was removed by suction below the screen wire after which the sheet was fed through a series of rollers and steam heated cylinders which press, dry, and form the final paper sheet.

Today pulp and paper mills can mainly be divided into two types:
- Integrated mills – where the pulp and paper mill are built on the same site and the pulp directly fed to the paper mill.
- Non-integrated mills – where the supply of 'virgin' dry pulp bales are purchased as raw material from domestic or foreign sources.

2.2.1 Pulp processing

Selected properties required from manufactured paper or board depend to a large extent on the selection of wood used. In the past, industry mostly used softwoods such as pine, spruce, cedar, and fir. Softwoods provide long strong cellulose fibres that provide added strength to paper. Hardwoods, including birch and aspen have shorter fibres that provide bulk, opacity, and smoothness to paper. Eucaluptus, a fast growing hardwood, most widely used for the manufacture of printing paper is successfully cultivated in places like Northern Spain, Portugal, and Brazil and provides the papermaker with a very high quality pulp.

Raw wood fibre walls contains cellulose, hemicellulose, and lignin[4]. The structural body of the fibre is made up from cellulose, whilst the hemicellulose and lignin act as a gel that binds the fibres together. The presence of hemicellulose is important as it assists in internal fibrillation, adding strength to the network structure of the final sheet[5], but lignin, which comprises about 24% in hardwoods and 28% in softwoods, needs to be removed to improve digestibility of the pulp[6] and avoid discolouration of the paper due to its reaction with ultra-violet light.

Pulp characteristics also depend strongly on what process is used to reduce the wood to its component fibres. Generally there are three pulping methods, which are mechanical, chemical, and semi-chemical pulping[3].

Mechanical pulp or "groundwood" is made by grinding debarked logs against an abrasive rotating stone in the presence of water to form small wood fibre bundles. It is an energy intensive process which can partially be offset by using the removed bark as fuel. The pulp obtained has essentially the same composition as the wood and the presence of lignin, which remains strongly associated to the fibres, will make it weak and yellow over time if exposed to sunlight. Generally this type of pulp will be used in low quality paper products such as wrapping paper or newspaper.

Chemical pulp or "kraft" is mostly produced using the sulphate process. Debarked logs are fed to a digester and dissolved in caustic soda and sulphur at high temperature and pressure, forming a pulp with a brown discolouration due to the effect of chemical interaction with the lignin and wood sap that requires further washing and bleaching to improve the pulp brightness.

Semichemical pulp is a combination of chemical and mechanical pulp where debarked woodchips are impregnated with a mild inorganic chemical such as neutral sodium sulphite at high temperature and subsequently fed through disk refiners to loosen the fibres further to pulp. The pulp is then washed to remove excess chemicals and lignin and bleached. Compared to full chemical pulping, this process requires lower chemical concentrations, shorter cooking cycles, and less energy since it is operated at lower temperature and pressure.

The cooking process in chemical and semichemical pulping ensures the freeing of the fibres in the wood thereby ensuring most lignin is removed[3]. There is however a small percentage that remains after washing and progressive delignification and brightening of pulp can be performed using a multistage bleaching process. It is imperative that bleaching agents do not attack the cellulose constituent during the process and the most widely used compounds include chlorine (low cost), sodium hypochlorite, chlorine dioxide (high available chlorine), hydrogen peroxide (mostly used for groundwood), ozone, or any combinations of the above.

After the bleached pulp is thoroughly washed, the pulp can directly be used for stock preparation in an integrated mill, or pressed to remove water and dried into dry sheets and transferred to the paper mills. This drying process is also referred to as lapping[5].

2.2.2 Paper processing

The first step in producing paper is to prepare a stock solution where the pulp is diluted in water to the proper consistency and treated mechanically and, in some cases, chemically by addition of additives in order to make it ready for sheet forming. Mechanical treatment mainly consists of two processes, beating and refining. Beating, usually a batch process, involves flattening the individual stiff, smooth fibres. This is done to increase the surface area of the fibres, allowing better interaction between neighbouring fibres when formed into a sheet, thereby contributing to dry sheet strength. Refining, usually a continuous process, can be used alone or after beating to further shorten and fibrillate fibres to further enhance bonding properties of the sheets[5]. After refining additional dyes, additives, and internal sizing agents are added to give the final paper the desired properties. This solution is also referred to as the furnish.

The furnish, consisting of 97.5 – 99.5 wt% water is passed through a headbox (Figure 2.1A), which ensures that an even fibre suspension is spread onto machine screens, also referred to as the Fourdrinier wire (Figurer 2.1B), consisting of framework supports, a finely woven metal cloth that allows drainage, suction boxes, and table rolls[3]. The suction boxes draw water from the furnish through the wire, travelling at a few hundred up to 2,000 m/min, causing longer fibres to quickly form a skeleton fibre sheet on which the shorter fibres, fillers, and other additives deposits[4]. The water content after passing over the screens is typically about 83 wt%.

After the sheet is formed, additional water is removed in the press section (Figure 2.1C) where moisture is squeezed out as the sheet passes through a series of press rollers and during this operation, the water content will typically reduce to about 50 wt%.

Sheets are now further dried in a drying section (Figure 2.1D) and at this point heat is required to lower the moisture content further. Up to 100 steam-heated dryers may be needed

to ensure adequate drying and as the sheet dries, it starts to shrink. To compensate for this shrinkage, each roller in different sections is set to a slightly different speed. A dryer felt is also used to hold the paper sheet in contact with the hot dryers. The moisture content after this stage normally is about 10 wt%.

Figure 2.1: Diagram of operations on a Fourdrinier papermaking machine.
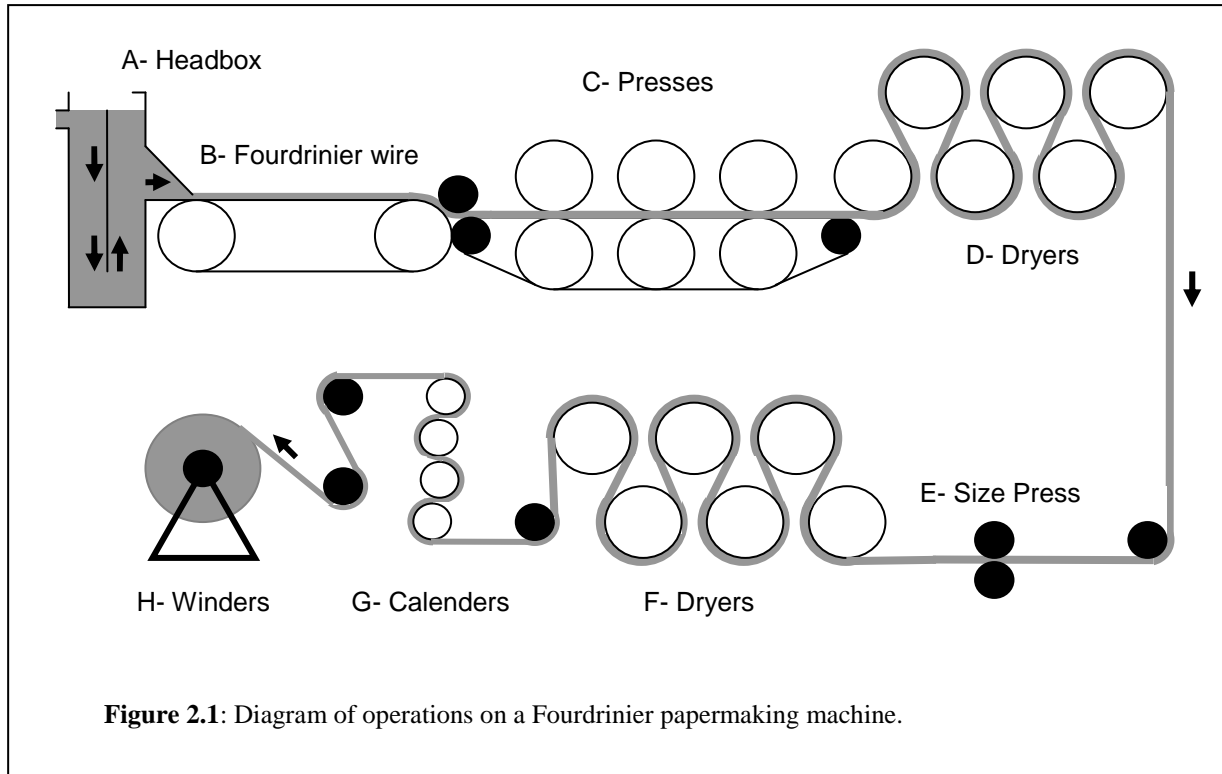
The size press (Figure 2.1E) is a surface treatment stage where a sizing agent is applied to both sides of the paper sheet. Surface sizing is applied to improve paper properties such as ink and/or water absorption, smoothness, texture, hardness, etc. These additives are applied in an aqueous medium and this subsequently means that the moisture content in the paper web will increase by about 10 wt%. In order to remove this moisture again, the sheet is passed a second time through a series of drying presses (Figure 2.1F) until the moisture content is about 5 – 5.5 wt%.

Since there is a tendency for fibres to lift from the sheet during drying, a calendering step (Figure 2.1G) is used to compress the dry sheet on both sides, which smoothens the finish.

The calender reels are also chilled, which cools the sheet down, thereby ensuring that the sheet can support itself.

Since the papermaking process is a continuous process starting at the headbox, it needs to be collected in a form that is easily transported and handled. This is done by winding the sheet into a large reel (Figure 2.1H). These reels can be stored or continue to be inspected, cut into reams, counted and sealed for consumer use.

2.3 Paper composition

For the purpose of this study, paper composition will be divided into 3 categories, which is fibres, fillers, and additives.

2.3.1 Fibres

Chemically, wood fibres consist of high molecular weight carbohydrates and lignin. The carbohydrate portion can further be broken down into cellulose and hemicellulose. Small amounts of waxes, fats, and tannins are also known to be present in fibres and known as extractives. Studying its structure, four distinct walls are found surrounding the central cavity of the fibre[4].
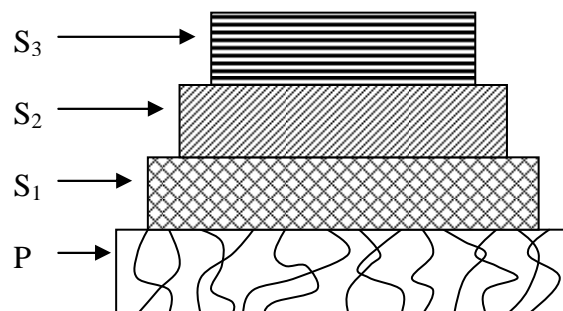
Figure 2.2: Transverse section of fibre. P represents the primary wall, S_1 the outer secondary wall, S_2 the middle secondary wall, and S_3 the inner secondary wall.

The primary wall (P, Figure 2.2) represents the original cambial layer and consists mainly of fine, thinly fibrillated networks of cellulose, hemicellulose as well as lignin. Within the primary wall the secondary wall is found, consisting of three principal divisions that mainly consist of high molecular weight cellulose microfibrils. The difference between the secondary layers is the manner in which the microfibrils are orientated and also at which angle the microfibrils are orientated from the longitudinal axes of the cell[7]. The inner secondary wall (S_3, Figure 2.2) has an interwoven or mesh-like fibrillar region[8], whilst the middle secondary wall (S_2, Figure 2.2) contains the bulk of the cellulose fibrils and is arranged in a series of coaxial lamellae. The outer secondary wall (S_3, Figure 2.2) is a thin outer skin-like layer with fibrils forming a counter rotating helix around the S_2 layer.

Cellulose, which falls in the carbohydrate family, is a compound that comprises carbon, hydrogen, and oxygen. It has a linear β-1,4-D glucan structure[9] (Figure 2.3) and is by far the most abundant polysaccharide available in the world today.

Figure 2.3: Cellulose structure.
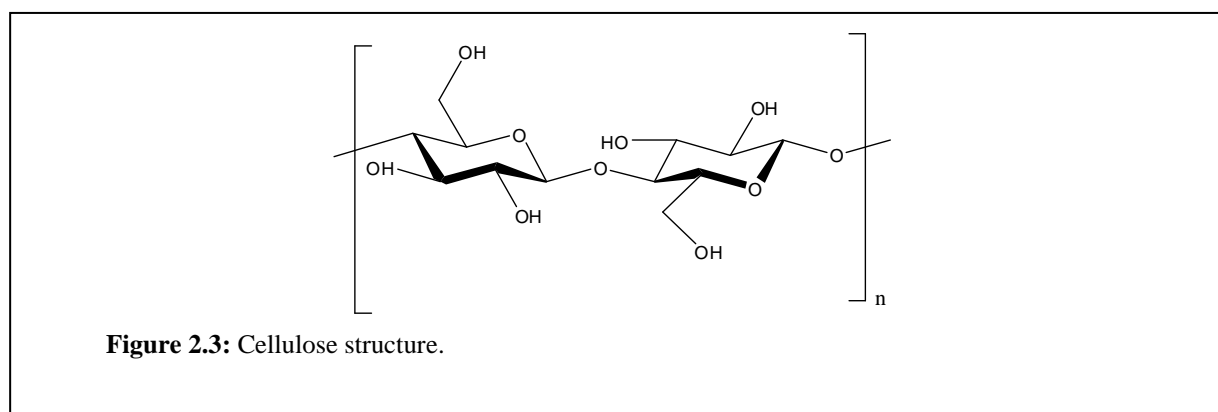
The hydrogen and oxygen in cellulose are in similar ratio as they combine to form water and this results in high swellability of cellulose in the presence of water. This is a very important property, and allows the amorphous cellulose in the structured (crystalline) microfibrils to become detangled and free in solution. During the drying process of sheet formation, the microfibrils, predominantly from the S_2 region, become entangled and interwoven, giving wet strength properties to the sheet. As it continues drying neighbouring fibres are linked by hydrogen bonding. Due to the large number of free hydroxyl groups on the cellulose backbone, the oxygen groups are able to hydrogen bond to hydrogen atoms on adjacent fibre

surfaces. Inter-fibre bonding is essential as this is the "glue" that keeps a dry paper sheet intact, whilst also adding to its strength and stiffness.

Xylans, a generic term used for describing a wide variety of highly complex polysaccharides found in plant cell walls, form a major portion of hemicellulose[10]. 4-*O*-methyl-D-glucuronic acid groups are found on the backbone of xylans[11] and the carboxyl groups of the uronic acid provide the fibre with a slight anionic charge. Carboxyl groups can also be found in oxidised lignin, resin, and fatty acids present in wood. Alkaline treatment as well as bleaching of the fibres can even increase the amount of carboxylic groups on the fibre surface due to the lignin oxidation and de-methylation of pectins[12], a hetero-polysaccharide also found in plant cells.

The carboxyl group content of pulp used in the papermaking process is very important, since it enhances the swelling of fibres in water and increases the specific bond strength. Furthermore these groups can interact with added wet-end chemicals such as cationic starch and other sizing or retention aids that will assist in retaining fillers and fines in the paper sheet.

2.3.2 Fillers

Mineral and non-mineral substances are added during the wet-end of paper production in order to enhance various properties of the sheets. Generally these substances are also referred to as fillers in the paper coatings, paints, and rubber industries and are well chosen to differentiate between white pigments, used for loading, and coloured pigments, which are applied for colouring paper[5].

A web consisting of long interwoven fibres will exclusively have a discontinuous surface with random voids and uneven surfaces. Filler particles between 0.3 and 10 µm are very small compared to these fibres, which length varies between 500 and 2,000 µm. The filler particles fit very well between the long fibre matrix, giving the paper a much more attractive closed texture. The reasons for including fillers especially in the printing paper industry include[4]:

- To improve the whiteness, opacity, and brightness.
- To improve the smoothness and texture
- To improve the print quality.

- As an aid to control special paper properties, such as controlled rate of burning.
- Reduction in cost of raw materials (if less expensive fillers are used).

The types of fillers used in the paper industry include clay, calcium carbonate, titanium dioxide, zinc sulphide, calcium sulphite, calcium silicate, barium sulphate, magnesium silicates, diatomaceous earth, and combinations of some of the above materials. The selection of the type of fillers is influenced by its cost, refractive index, specific gravity, particle size, and particle shape.

Clays consist of finer particles and possesses a very desirable high brightness[5]. It essentially consists of kaolinite and the presence of quartz, mica, and other components which drastically increases its abrasiveness, rendering it applicable only in special papers at low filler content. Synthetic silicates offers good light scattering efficiency, but can become costly. Calcium sulfite is a very white filler, but can react with alum to release sulphurous acid. This demands that corrosion resistant paper machine wires and specialised equipment be used and is the reason why this filler is not widely used. Calcium sulphate appears to be attractive because of its high brightness and low cost, but due to its high solubility in water, large quantities get lost in the white water during paper manufacture. Barium sulphate, zinc sulphide and titanium dioxide offer excellent brightness and opacity, but are very costly.

2.3.2.1 Calcium carbonate

Calcium carbonate constitutes about 1% of the earth's crust and is one of the most abundant sedimentary minerals on our planet[13] and if carefully prepared, the most practical for use in the printing paper industry due to the high opacity and brightness it imparts on paper at minimum cost[14]. It has an alkaline reaction, and in the quantities used for filler, has a high capacity for neutralising acids. Ageing of paper sheets containing calcium carbonate indicates that lignin-based organic acids that form over time and normally causes degradation of mechanical properties of paper, are neutralised by this filler [15]. It also masks yellowing caused by lignin, cellulose and hemicellulose degradation during ageing.

Calcium carbonate, as used in industry, can be extracted by mining and quarrying and involves crushing and processing limestone. This natural form is also referred to as "ground calcium carbonate" or GCC. Another method is to manufacture the filler using a process of precipitation and the product is also known as "precipitated calcium carbonate" or PCC. High-calcium content quicklime is hydrated and white slurry, also known as "milk of lime", is reacted with carbon dioxide. PCC is the preferred filler[16, 17] firstly because it can be produced with various crystal habits, each with unique properties and advantages in paper. Properties such as particle size, surface area, particle shape, and surface chemistry can be optimised by varying the reaction conditions. Secondly, PCC can be produced in slurries at satellite plants located near the paper mill, using carbon dioxide emitted by the mill as raw material. This not only creates a more economic and environmentally friendly production plant, but also makes the filler available with little or no transportation cost. PCC generally possesses a rosette (scalenohedral) crystal structure, depending on reaction conditions, but can also form blocky (rhombohedral), needle-like (acicular), or various intermediate structures. Rosette crystal structures tend to form bulkier sheets of paper with improved smoothness after calendering, whilst the much denser calcite structure of GCC tends to produce a denser paper sheet with higher tensile strength.

The surface electrical properties of calcium carbonate have been studied extensively over the years due to its importance in various industries. Unlike oxide minerals where the potential determining ions (PDI) are generally H^+ and OH^- ions (regulated by changes in pH), calcium carbonate has a Ca^{2+} and CO_3^{2-} predominant PDI, also referred to as a calco-carbonic equilibration system[13]. At a lower alkaline pH range, CO_3^{2-} ions are unstable and hydrolyse to HCO_3^- and further to dissolved CO_2, which subsequently outgases from the system. Consequently the Ca^{2+} ion activity exceeds the activity of CO_3^{2-}, resulting in a slightly positively charged calcium carbonate surface. This is of significant importance in papermaking, since the surface electrical properties of calcium carbonate affects its colloidal interaction with other ionic species in the paper matrix, such as the fibre surface.

19

2.3.2.2 Filler retention

The addition of fillers during the wet end of the papermaking process is a sensitive process as these fillers may be removed from the paper web during the water removal stages. The aim is to ensure that the maximum amount of filler is retained in the fibre matrix and not lost in the white water. The efficiency with which fillers are retained in a paper sheet effects the quality and therefore also the cost of the product, the cleanliness of the system as well as the pollution load of the disposal system[18]. The mechanism of filler retention by stock on the machine wire is very complicated and relies on a combination of mechanical, chemical, and physical attractive forces brought about by the prevailing conditions during fibre treatment[4]. Filler is retained by two actions, filtration and adsorption. Larger particle size fillers show an increase in retention due to filtration, i.e. particles get entrapped in the paper matrix and can not travel through the machine wire. Smaller particles on the other hand show an increase in adsorption onto the fibre surfaces due to colloidal interactions. However, smaller particles also have a poor filtration retention action since it can easily pass through the inter-fibre spaces and machine wire. Generally medium-sized filler particles are most efficiently retained, since retention is facilitated by both filtration and adsorption actions. Filler particles in the region of about 9 µm are ideal, since it will settle in water at the same rate as the fibres, ensuring a much more even filler-fibre distribution.

Factors that affect and influence particle retention are[4]:

- The particle size of the filler.
- The pH of the stock.
- The rate at which stock flows over the machine wire.
- The mesh size of the wire.
- The substance of the paper.
- The type of stock, which includes the length of the fibre, degree of fibre beating, etc.

The tendency in industry over the last decades has been to increase filler loading and retention, primarily because of economic reasons. Fillers, such as calcium carbonate, are substantially cheaper than the high fluctuating cost of pulp[19]. However, using excess fillers can result in very undesirable effects in the finished paper, which include[20]:

- Loss in strength of paper sheet since filler particles in the paper matrix interfere with inter-fibre bonding.

- Loss in paper stiffness.

- Dusting of paper occurs, where overloaded, unattached fillers separate from the sheet.

- Paper may become abrasive on the surface and cause wear on printer plates.

Flocculation of fillers is often used as an aid to improve retention by filtration action, omitting the effect of electronic filler-fibre forces.

2.3.3 Retention aids

Wet end additives are commonly used in papermaking to attach fine filler particles onto fibres. This can be done by forming an agglomeration of fibres and fine mineral filler particles, allowing it to be trapped by the forming wire. Retention aids can be used either to promote the flocculation of fine fillers and/or fibres, making it difficult for aggregates to travel through the machine wire, or as a bridging mechanism to adsorb mineral fillers to fibre surfaces. Considering the speed with which water drainage and web formation occurs after the pulp is dispensed onto the machine wire, the kinetics of flocculation and adsorption induced by a retention aid is of great importance in determining its efficiency[21]. Formation, drainage, and retention are also affected by production shear stress as well as the stock characteristics (such as composition and ionic content) as this will determine the flocculation and adsorption mechanism[22]. If the flocs formed are too large, it could lead to blockage of channels in the forming sheet making it difficult for water to pass through and therefore causing a reduction in drainage.

Most retention aid systems can be divided into two categories, those that rely on macromolecular bridging and those that function by charge modification. Macromolecular bridging occurs when a high molecular weight polyelectrolyte with an appreciable charge density adsorbs on a surface[23]. If these are long enough to extend beyond the double layer, they will be available for bonding with another surface and when collision occurs, the particles will flocculate (Figure 2.4A). This type of adsorption is very strong and difficult to break up even under significant shear stress. Examples of macromolecular bridging aids include poly(ethylene oxide) (PEO) with an attached co-factor. By itself PEO does not adsorb onto fibre and only poorly adsorbs onto PCC filler. The cofactor chosen should associate with PEO and the association complex needs to act as an effective bridging agent.

Co-factors can consist of compounds containing a phenolic group that is able to form hydrogen bonding with PEO, such as phenolic formaldehyde resin (FPR), tannic acid (TA) and sulfonated kraft lignin (SKL) or compounds lacking phenolic structures, such as polynaphthalene sulfonate (PNS), polystyrene sulfonate (PSS) and folic acid (FA)[24]. Another type of very effective macromolecular bridging aid is low charge density cationic polyacrylamide (cPAM)[25].

Figure 2.4: Macromolecular bridging (**A**) and charge modification (**B**) retention aid systems.
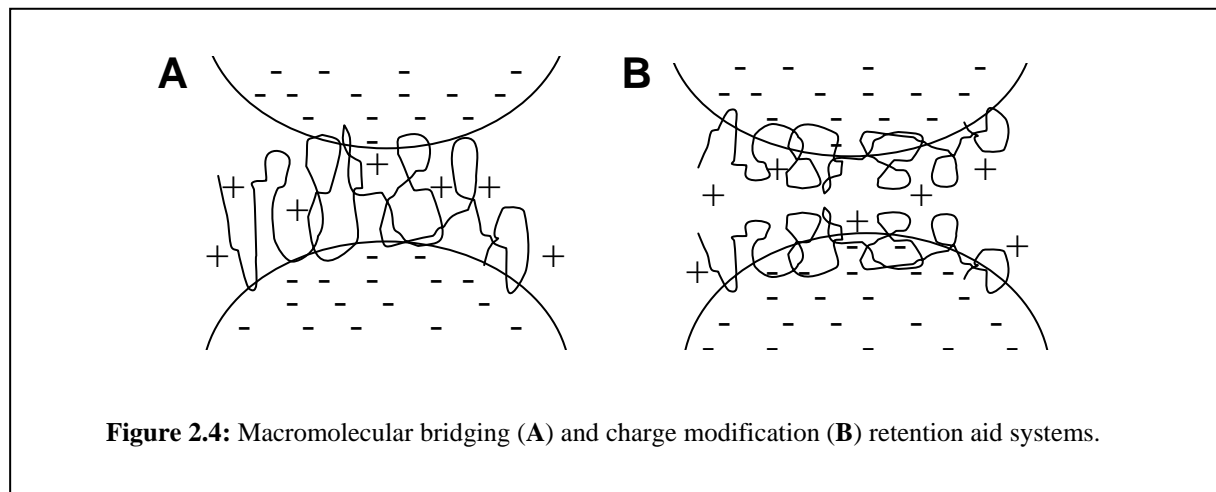
In charge modification the electrical charge at the surface interface is cancelled out through ion exchange with polycations in stoichiometric proportions, and flocculation occurs due to Van der Waals forces between the uncharged particles[26]. Flocculation in this case is reversible and can easily be re-dispersed by applying shear. Examples of these types of retention aids include polydiallyldimethylammonium chloride (pDADMAC)[27], polyethylenimine (PEI)[28], and polyaluminium chloride (PAC)[29].

Retention aids that are based on natural organic polymers are also successfully used since they are environmentally friendly, biodegradable, and inexpensive. Cationic starch or cationic guar gum are commonly added to paper stock in order to improve the dry strength of paper and the improvement it imparts on retention is a welcomed side effect[26, 30]. Chitosan, which has a chemical structure very close to starch, is a linear copolymer of β-(1-4)-2-acetamido-2-deoxy-D-glucopyranose and β-(1-4)-2-amino-2-deoxy-D-glucopyranose and is one of the most abundant polysaccharides found in nature[31]. Huang Chi et al.[32] describe the use of cationic chitosan, such as N-(2-hydroxyl-3-trimethylammonio)-propyl chitosan as an

effective retention aid that also improves the physicomechanical properties of paper. El-Sayed[33] described the use of cationic pyrodextrins and Modgi et al.[34] the use of cationic tapioca and potato starch as alternatives to conventionally used cationic starch.

2.4 Introduction to starch

Carbohydrates (also known as saccharides or glycans) are natural occurring organic compounds and a vital energy source for humans and plant-eating animals. It originates as products of photosynthesis in plants where an endothermic reductive condensation of carbon dioxide and water in the presence of chlorophyll pigment and light takes place[35]. The formula of carbohydrates generally can be written as carbon hydrates [or $C_n(H_2O)_n$], from there the name.

The building blocks of carbohydrates are monosaccharides of which glucose (or simple sugar) is the most commonly known. Two stereoisomers exist for glucose, namely L-glucose and D-glucose[36], the two structures being mirror images of each other, but D-glucose is the most commonly existing structure. Cyclic glucose exists as two anomers and differs structurally by the relative positioning of the hydroxyl group at C-1 to the one at C-6 (Figure 2.5). For α-glucose the hydroxyl groups exist on opposite sides of the cyclic plane, whilst β-glucose are on the same side.
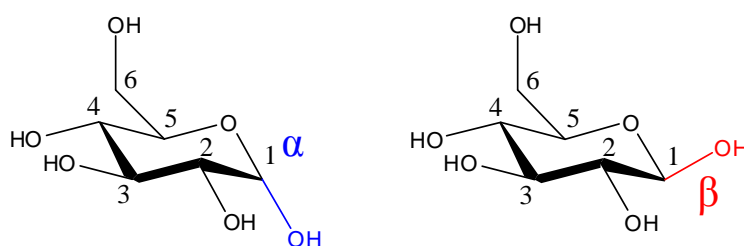
Figure 2.5: Anomers of cyclic D-glucose.

Starch is a polysaccharide (usually with particle size ranging between 1-100 µm[37]) consisting of repeated units of α-D-glucose. The repeating units of starch are also known as

anhydroglucose units (AGU's)[38]. It consists mainly of two types of molecules, amylose (20-30%) and amylopectin (70-80%), both polymers bonded together primarily through α-D-(1→4) glucosidic bonds. It has been established that these two molecules form a heterogeneous starch structure, together making up about 98-99% of the dry weight of native granules[39]. The remainder essentially consists of small amounts of lipids, minerals and phosphate groups.

Amylose is a linear low molecular weight polymer with 200–2,000 α-D-(1→4) AGU's, depending on the source[38] and a molecular weight ranging between 2×10^5 and 2×10^6 g/mol (Figure 2.6A). The linearity of amylose allows the molecules to have high mobility upon heating and will readily leech out from the particle in a suitable solvent system such as water. The high concentration of hydroxyl groups, together with its linearity and mobility, allows amylose to easily orientate itself in a parallel fashion and approach each other very closely to permit hydrogen bonding between hydroxyls on adjacent groups. Due to this bonding mechanism, the water affinity of amylose is reduced at low concentrations in water, and may even form precipitates. At higher concentrations steric hindrance interferes with the self association mechanism, causing obstruction for hydrogen bonding to occur. This produces a strong gel consisting of a three-dimensional network held together by limited hydrogen bonding. This phenomenon of intermolecular association is generally referred to as retrogradation[40]. Amylose molecules may form an extended shape (hydrodynamic radius 7-22 nm[41]), but the chains tends to wind up into helices[42].

Amylopectin is a high molecular weight branched polymer containing, in addition to the α-D-(1→4) glucosidic bonds, periodic branches at the C-6 position and these are linked by α-D-(1→6) glucosidic bonds[38] (Figure 2.6B). These branch points normally consist of 5-6% of all glucosidic bonds[39, 42] and each branch contains about 20-30 AGU's. The large size and branched nature of amylopectin causes the molecules to have poor mobility and therefore interferes with its tendency to orientate itself close enough to adjacent hydroxyl groups to allow high levels of hydrogen bonding. Aqueous solutions of amylopectin are therefore characterised by its clarity and stability as measured by its resistance to form gels during aging. Amylopectin has a hydrodynamic radius of about 21-75 nm[43].

Figure 2.6: Structures of linear amylose (**A**) with α-D-(1→4) glucosidic bonds that forms a helical complex, and branched amylopectin (**B**) with similar bonds as well as α-D-(1→6) glucosidic branching points.
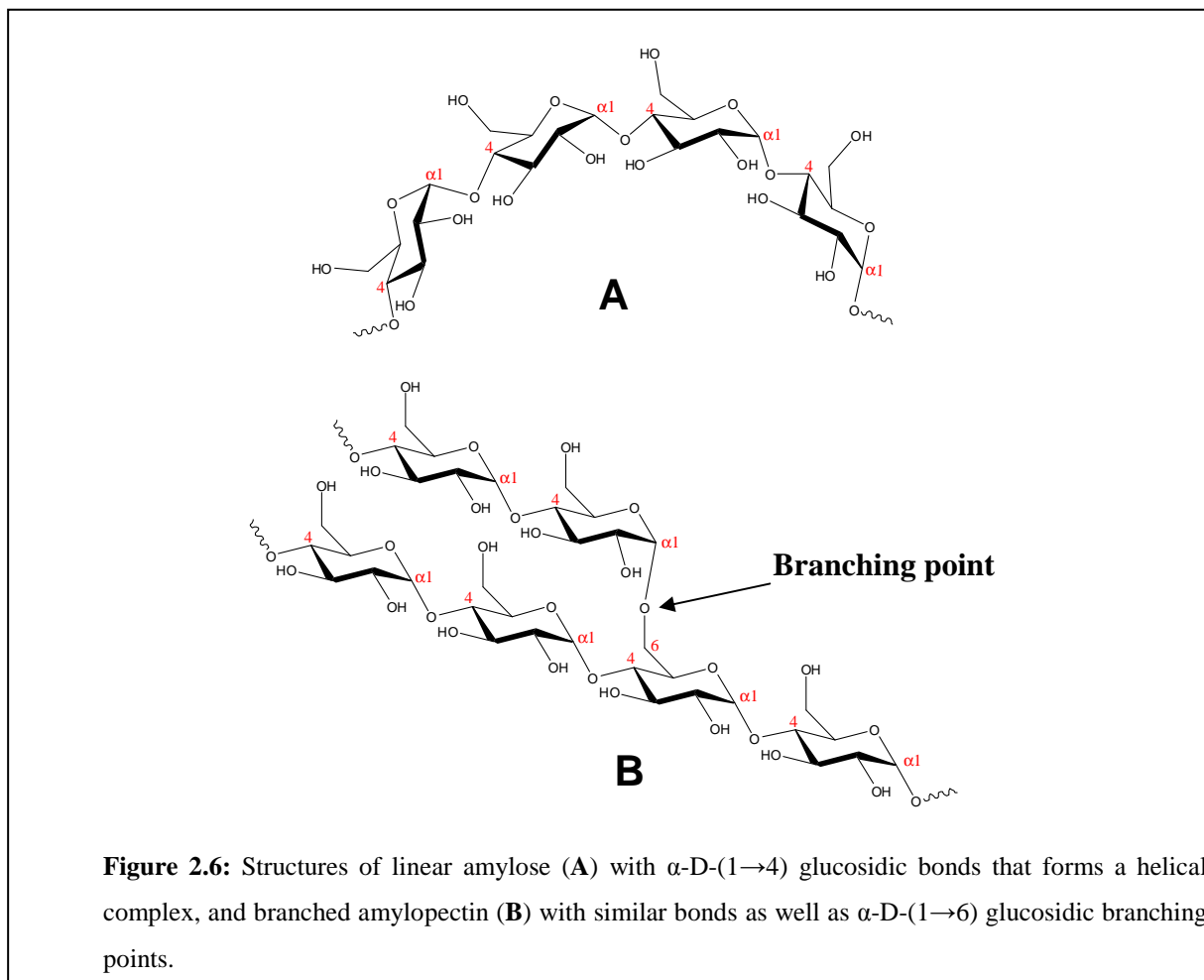
It has been found that branched amylopectin exists as a tree-like structure. Even though the amylopectin branches on average have 20-30 AGU's, it has further been found that two types of branched chains exist, the more abundant type with about 15 AGU's (Type A) and the lower concentration type with about 40 AGU's (Type B)[44]. The amylopectin skeleton essentially consists of single branched A chains with a cluster of B branches (Figure 2.7A).

Each amylopectin molecule has one primary reducing end, also known as Type C. Studies indicate that the molecules are orientated radially within starch particles around a center point, known as the hilum (Figure 2.7B). The shorter Type B chain clusters are distributed in the starch particle skeleton, forming highly branched concentric areas that are amorphous with shorter, more structured (due to linearity) Type A chains that form a crystalline region. The degree of crystallinity of starch granules can vary between 20% and 45%, depending on its

biological origin and can be measured using methods such as X-ray diffraction[45] and thermally stimulated depolarization current (TSDC) experiments[46].

Figure 2.7: Skeletal structure of amylopectin showing the tree-like structure of the molecule with A-, B-, and C-type branching (**A**). The A- and B-type branching causes amorphous and crystalline concentric areas with a radial distribution in starch granules (**B**) (picture redrawn)[44].
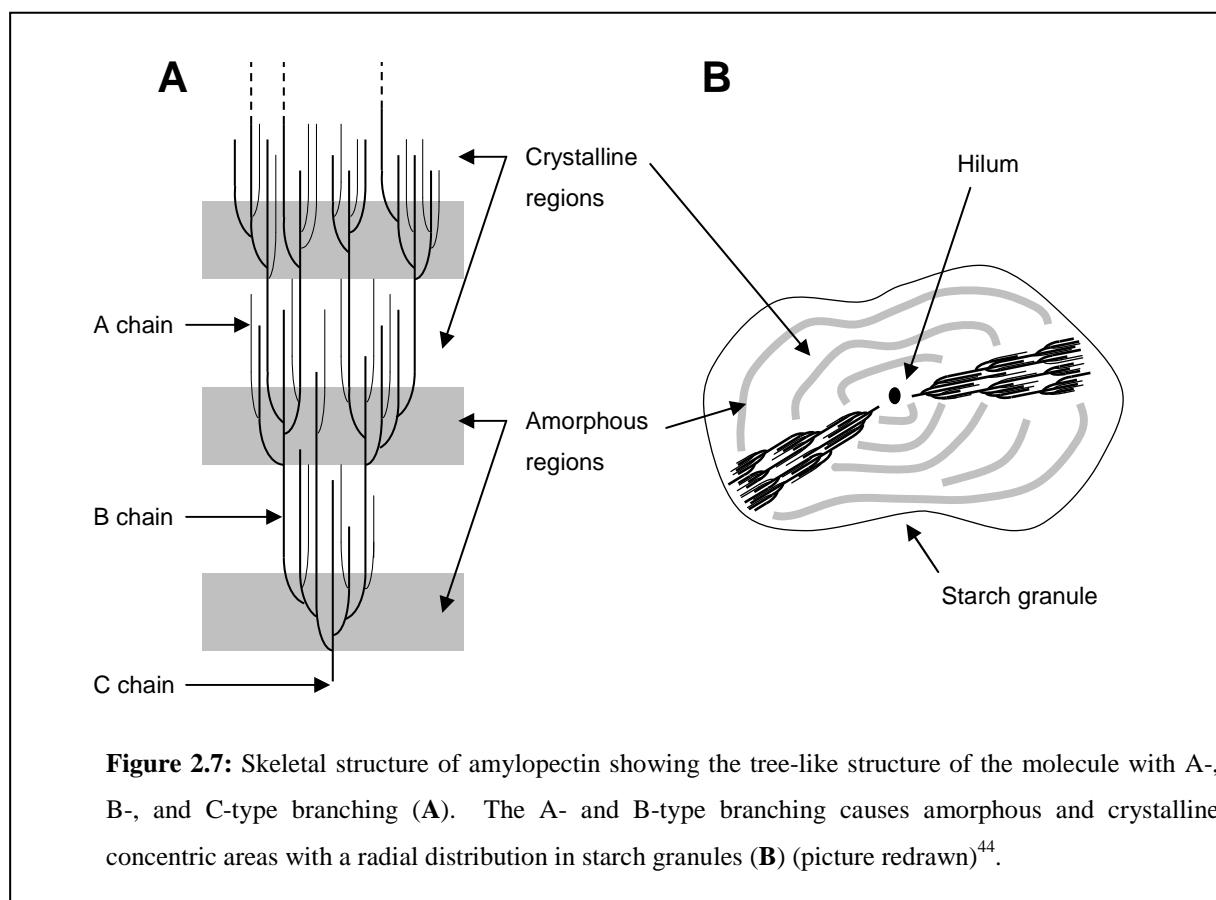
2.4.1 Properties and uses

Pure starch is a white, relatively low taste substance that is built up in the fruit, bulbs and tubers of various plants. Although found throughout the plant world, only limited sources are utilized for the production of commercial starch. Maize is by far the major source of starch produced[38]. Other sources include potatoes, wheat, sorghum, tapioca, cassava, and rice. If viewed under the microscope, it can be seen that starch consists of small spherules or granules, the shape and size of which are unique to their source[47]. Granular starch is completely insoluble in cold water, but once heated, interesting physical changes occur. Energy interferes with the hydrogen bonding of adjacent starch hydroxyl groups, allowing water to hydrate the starch molecules. The granules start to swell, originating at the hilum and progressing to the periphery, while still maintaining their original shape. During

swelling, the viscosity of the solutions start to increase. However, when the aqueous solution reaches a critical temperature, gelatinisation occurs where the swollen balloon-like granules collapse, allowing the starch molecules to become mobile as a gel paste. Viscosity increases up to the gelatinisation point after which it decreases again as the granules collapse.

The ability of starch to swell and form a gel is its most important practical property and used widely in industry. Table 2.1 shows a summary of industrial uses of starch[48].

Table 2.1: Industrial uses of starch[48].

Industry	Use of starch/ modified starch
Adhesive	Adhesive production
Agrochemical	Mulches, pesticide delivery, seed coatings
Cosmetics	Face and talcum powders
Detergents	Surfactants, builders, co-builders, bleaching agents and bleaching activators
Food	Viscosity modifier, glazing agent
Medical	Plasma extender/replacer, transplant organ preservation, absorbent sanitary products
Oil drilling	Viscosity modifier
Paper and board	Binding, sizing, coating
Pharmaceuticals	Diluent, binder, drug delivery
Plastics	Biodegradable filler
Purification	Flocculant
Textile	Sizing, finishing and printing, fire resistance

The main application areas of starch in the paper industry include[49]:

- Furnish preparation prior to web formation, where it functions as a flocculation aid, retention aid, internal sheet strengthening aid, and drainage aid.
- Surface sizing, where it is used as an adhesive to bond loose fibres to enhance paper strength and stiffness, which aids in improving printability and dimensional stability.
- Coating, where it can be used to bind fine pigments that can also improve printability as well as sheet smoothness and gloss.
- Effluent treatment, where cationic starch can be used to flocculate any loose fibres and/or pigments that escape to the waste water.
- Conversion of paperboard to packaging grades, where it is used as an adhesive to attach multiple boards or corrugated board together.

2.5 Chemical modification of starch

Native starch varies greatly in form and functionality between and within source species, and can even vary as a result of the conditions under which it was grown[39]. This variability can cause inconsistencies in the raw materials and ultimately in properties of the product it is added to, such as paper. Chemically modified starch can be extensively used to overcome this variability. Unmodified starch is widely used, but most of the starch produced today is further processed and modified. Modified starch includes any changes made in the physical and chemical properties of native starch by significant molecular scission, molecular rearrangement, oxidation, or introduction of substituent chemical groups onto the starch molecules[38]. In the development of multi-functional polysaccharide particles the main chemical modifications investigated during the course of this study included cross-linking as well as anionic and cationic derivatisation.

2.5.1 Cross-linked starch

Cross-linked starch granules that are prepared under atmospheric conditions will swell, but not break, so it is expected that this would serve as an effective internal size for paper, since it will be largely retained in the sheet as it is formed[50]. In the textile industry it would also remain near the surface in sizing textile yarns, giving enhanced abrasion resistance. Cross-linked starch is also widely used in adhesive applications for corrugating and paper coating formulations due to its ability to withstand high shear in recirculating systems. Other application areas include oil well drilling mud, paints, printing inks, ceramics, and charcoal briquettes.

2.5.1.1 Epichlorohydrin cross-linked starch

Epichlorohydrin (ECH) is the most commonly used agent for cross-linking polysaccharides, since it is a bifunctional reagent that reacts with the hydroxyl groups of glucose monomers[51]. Simkovic *et al.*[52] described a process of preparing a weak basic ion exchanger in which ECH is premixed with ammonium hydroxide (NH_4OH) and NaOH solutions prior to reacting it with water-insoluble wheat starch.

Under the right conditions a poly(hydroxypropylamine)-modified starch is produced (Figure 2.8), which can be used as a cheaper, biodegradable ion-exchange alternative to synthetic, petroleum-based anion-exchange resins.

NH_3 + CH_2—$CHCH_2Cl$ + starch—OH → OH^- +
                starch—O—$[CH_2CH(OH)CH_2N(CH_2CH(OH)CH_2)_2]_n$—O—starch
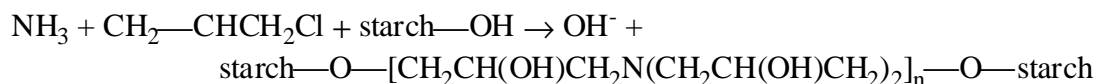
Figure 2.8: Mechanism for preparing weakly basic ion-exchanger by cross-linking starch with epichlorohydrin and NH_4OH[52].

Griffin[53] proposed a process for preparing low density polyethylene (LDPE) blown films that contain native and modified starch. In later years, Kim *et al.*[54] found that by using cross-linked potato starch, prepared by combining potato starch and ECH in an alkali aqueous solution and allowing cross-linking to occur at ambient temperature for 24h under constant stirring, the mechanical properties (tensile strength and strain energy) of plastic films improved significantly. Cross-linked starch-LDPE was prepared by single screw extrusion in the presence of a pro-oxidant.

Chen et al[55] described a process for preparing cross-linked oxidised starch for use as a calcium ion absorbent in waste water treatment. Cornstarch was slurried in water containing sodium sulphate and NaOH. After allowing for cross-linking to be completed, the pH of the solution was neutralised and supplemented with copper sulphate and oxidized with hydrogen peroxide. Cross-linked oxidized starch can be applied as a non-toxic alternative to tripolyphosphate, which is widely used in detergents.

2.5.1.2 Allyl starch

Huijbrechts *et al.*[56] reported the synthesis of 1-allyloxy-2-hydroxy-propyl-starch in an aqueous medium. Allyl glycidyl ether was added to distilled water containing waxy maize starch, NaOH and sodium sulphate (Na_2SO_4) and the reaction mixture was left for 48 hours for coupling to occur (Figure 2.9).

Figure 2.9: Synthesis of 1-allyloxy-2-hydroxy-propyl-starch[56].
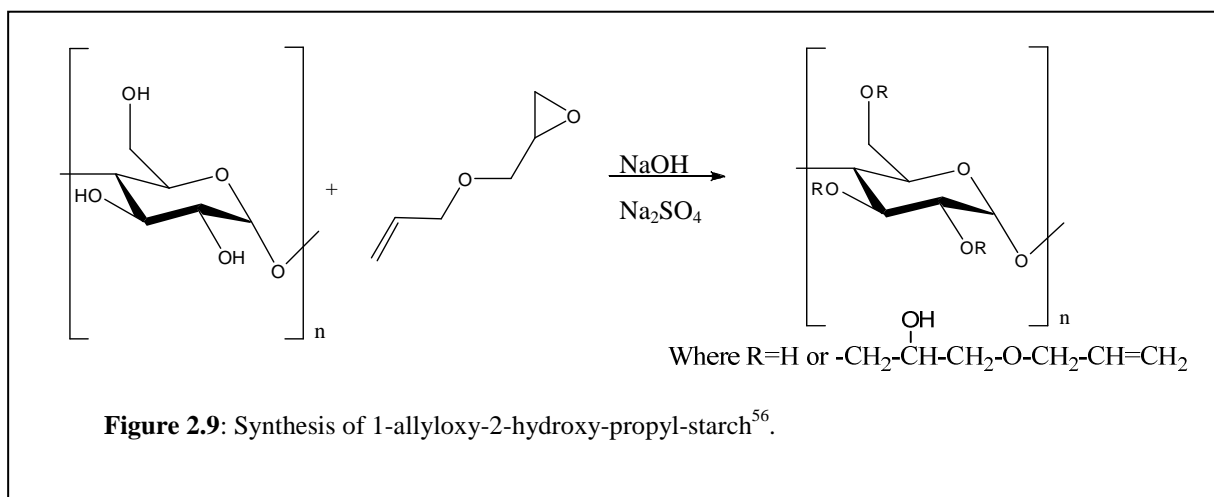
Jaworek *et al.*[57] described a simple method of preparing starch allyl ethers as an intermediate step for binding biologically active proteins onto insoluble activated polysaccharide carriers. Soluble starch was slurried in a mixture of acetone and deionised water treated with NaOH. Allyl bromide was added dropwise under a nitrogen blanket and the reaction allowed to complete (Figure 2.10).

Figure 2.10: Synthesis of starch allyl ether[57].
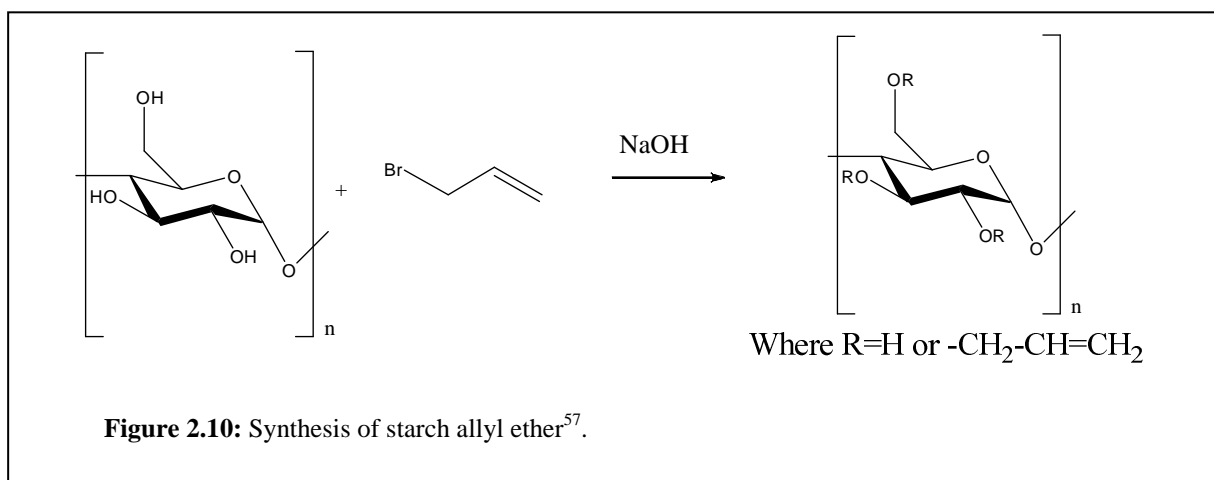
2.5.1.3 Other cross-linked starch

Seker *et al.*[58] reported the cross-linking of starch by phosphorylation using sodium trimetaphosphate and NaOH in a single-screw extruder. Phosphorylation can also be performed using phosphorus oxychloride $(POCl_3)$[59, 60] or mixtures of sodium trimetaphosphate and sodium tripolyphosphate[61, 62]. Other cross-linking agents include

acrylates[63-66], aldehydes[67, 68], vinyl sulfone[69], di-epoxides[70] and various urea-formaldehyde resins are also effective cross-linking agents. Generally any molecule that is capable of reacting with at least two hydroxyl groups can cross-link starch, although unreactive molecules such as aliphatic dihalides may cause damage to the starch structure[50].

2.5.2 Anionic modified starch

The most common anionic modified starch is carboxymethyl starch (CMS) which is obtained as a product from the reaction of starch with sodium monochloroacetate (SMCA) in the presence of NaOH (Figure 2.11). This method is based on Williamson's ether synthesis[71].
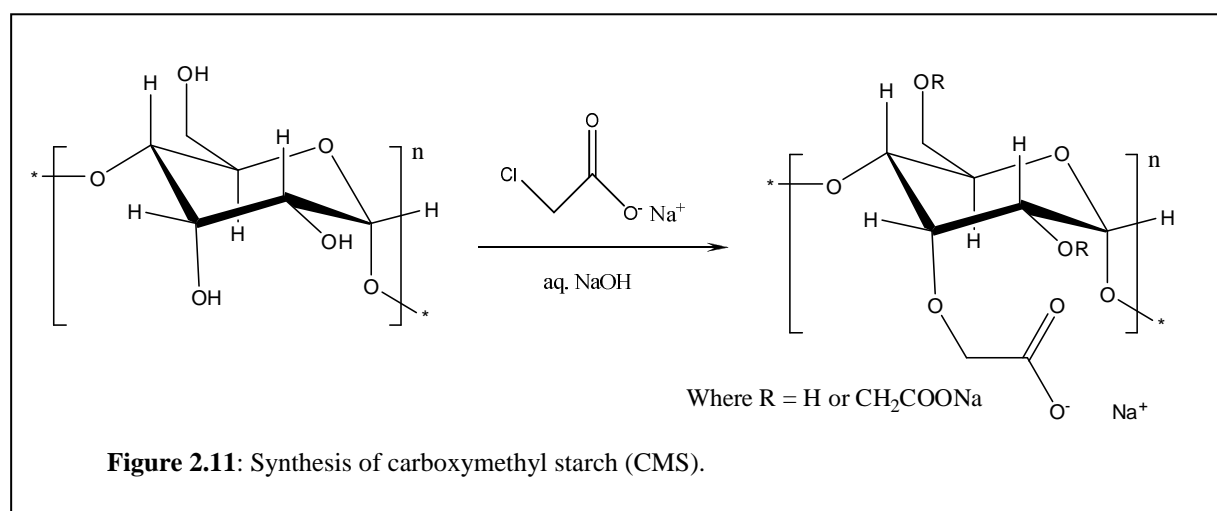
Figure 2.11: Synthesis of carboxymethyl starch (CMS).

It is widely employed as an additive in the paper industry, as a thickener in food and in the formulation of textile printing pastes[72], and as protective colloids in the building industry[73] (refer to Figure 2.12 for an overview)[74]. The use of CMS in enhanced oil recovery systems is also gaining increased attention.

The natural ability of native starch to undergo retrogradation can be prevented by introducing more hydrophilic groups, such as carboxymethyl groups, ensuring more stable starch solutions. Carboxymethyl starch is not harmful to humans and therefore can be used for medical applications such as anions in salts of certain drugs[38]. Other benefits over native starch include increased resistance to heat and bacterial degradation; it is cold water soluble,

with increased swellability, which makes it useful as super-absorbents especially in the medical industry[75]. It is also compatible with many hydrophilic sizing agents, such as polyvinyl alcohol, used in papermaking and significantly contributes to oil resistance and water insolubility[38].

Sodium monochloroacetate is a crystalline solid, soluble in water, alcohols and benzene, but starch modification is usually conducted in an aqueous medium, although a number of papers report carboxymethylation of starch in its granular form[74, 76-78]. This is done in a mixture of water and a water-miscible solvent such as methanol or isopropanol, blended in a ratio that does not allow the granules to rupture during the modification process.

Figure 2.12: Industrial applications of carboxymethyl starch (CMS) (picture redrawn)[77].
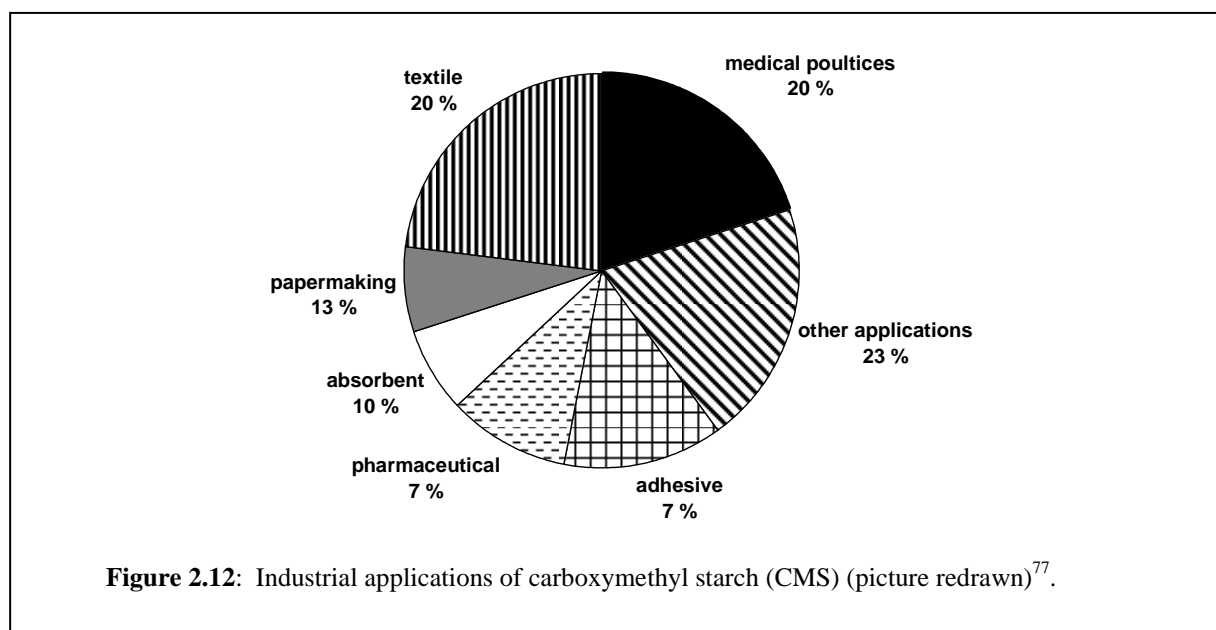
2.5.3 Cationic modified starch

Cationic starch can be produced by the chemical reaction of starch with reagents containing amino, imino, ammonium, sulfonium, or phosphonium groups, all of which contain a positive charge[38, 79, 80]. Commercially significant derivatives contain either tertiary amino or quaternary ammonium starch ethers, of which 3-chloro-2-hydroxypropyltrimethylammonium chloride and 2,3-epoxypropyltrimethylammonium chloride is best known in the art[81-85].

32

Cationic modification can also be performed using Williamson's ether synthesis where the starch and cationic derivative is combined in the presence of excess NaOH (Figure 2.13).
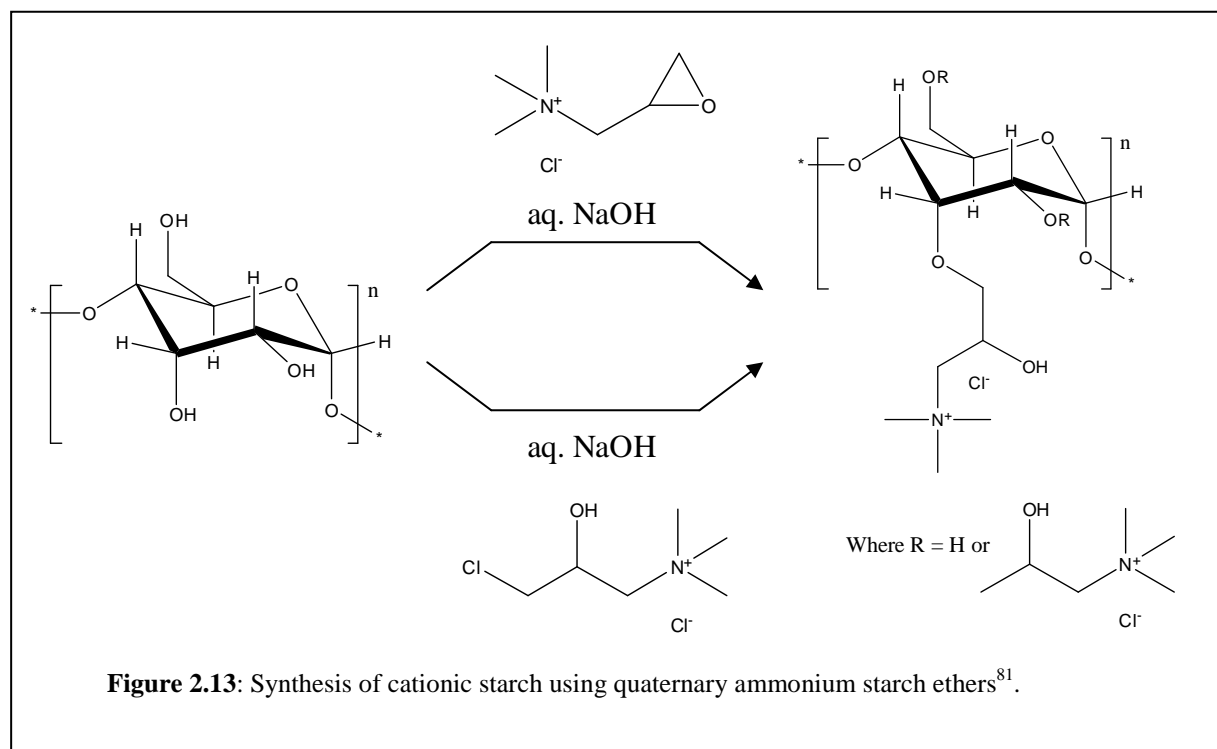
Figure 2.13: Synthesis of cationic starch using quaternary ammonium starch ethers[81].

Cationic starch is extensively used as flocculation polyelectrolyte in the paper industry, as raw and wastewater clarifier, for sludge dewatering, and in mineral processing to obtain good colloidal stability[80, 81, 86-88]. It has gained significant interest in industry since synthetic polymers such as polyacrylamide, polyethylenimine, and poly(N-dimethylaminomethyl-acrylamide) are not biodegradable and may contain toxic monomeric residues. Cationic starch is also extensively used as internal binder in the paper industry, improving inter-fibre bonding by neutralising the anionic charge on the fibre surface, resulting in enhanced physical paper properties, such as tensile strength, elongation, fold endurance and pick resistance[38, 89, 90]. Half of the starch used in the paper industry is chemically modified, of which almost 20% is cationic modified[83].

Four processes for preparing cationic starch have been reported[91] using the Williamson's ether synthesis process. The first involves preparing a slurry of partially swollen starch. Granular swelling is controlled by adding a sodium sulphate (Na_2SO_4) retardant before

treatment with NaOH and a quaternary ammonium chloride reagent. The starch slurry is typically 40% dry substance. The second process is performed by completely gelatinizing the starch to an aqueous paste (approximately 40% dry substance) before treatment. The third process is a semi-dry process where the starch powder (starch concentration approximately 80% dry substance) is treated with NaOH and the etherification agent and the reaction left for at least 48 hours. The last process is conducted using a twin screw extruder[79] containing 7 sections. The starch and NaOH is added in the first section and the etherification agent added at the second. The temperature is increased from 20°C in the first section to 125°C in the last. Reactive extrusion is becoming increasingly popular since this is a continuous process and it has been shown that the lower viscosity of the cationic starch, caused by chain degradation during extrusion, is an advantage in the papermaking process[79].

2.6 Microgel starch particles

2.6.1 Introduction

The application of modified swollen starch particles in the paper industry is not well documented, but it has been widely studied in the medical and pharmaceutical fields as a drug carrier due to its biodegradability, biocompatibility, non-toxicity, storage stability, and cost-effective fabrication method[92]. After administering drug-enriched or encapsulated microspheres to the body, it starts to swell significantly to form a gel-like structure, allowing controlled drug release at a predetermined rate as it passes and degrades through the digestive tract.

Schwoerer *et al.*[93] described the use of cross-linked hydroxyethylmethacrylate-hydroxyethyl starch (HES-HEMA) as a carrier system for proteins. Hydroxyethylmethacrylate (HES) has also been used extensively in the past as substitute for plasma. Mundargi *et al.*[94] reported on the encapsulation of ampicillin, a broad spectrum antibiotic, in starch-based tableted microspheres, while Silva *et al.*[95] used microparticles as carriers of stem/progenitor cells for bone-tissue engineering applications.

Starch microparticles are also being considered for agricultural applications. Roy *et al.*[96] recently also demonstrated the suitability of using starch and alginate, a polysaccharide

consisting of an unbranched binary copolymer constituted of (1→4) linked α-L-guluronic acid and β-D-mannuronic acid, as a carrier for swelling and erosion controlled release of the insecticide chlorpyrifos.

Various processes of preparing starch microspheres have been reported and some of these techniques include conventional water-in-oil emulsification, water-in-water emulsification, crystallisation, solvent exchange, spray drying, and a novel procedure of using microfluidic devices.

2.6.2 Water-in-oil emulsification processing

The suspension polymerisation of aqueous starch solutions in a hydrophobic organic phase is the most commonly documented and used process for preparing starch microparticles. Hamdi *et al.*[97] described a process of dissolving low molecular weight soluble starch in an alkaline aqueous solution and emulsifying it in a cyclohexane/chloroform (4:1 v/v) mixture containing varying amounts of an emulsifying agent, such as sorbitan mono-oleate (commercially referred to as Span 80). Emulsification was performed using a low shear laboratory stirrer or a high speed homogeniser, depending on the particle size requirement. Varying amounts of epichlorohydrin (ECH) was added to initiate cross-linking and the reaction mixture left for a period of 18 hours at 40°C. The particles were isolated by centrifugation and subsequent washing in cyclohexane and lyophilised (freeze dried) to a dry powder. Dziechciarek *et al.*[98] described a similar process, but added the ECH directly to an aqueous potato starch solution before emulsification in a pure cyclohexane continuous phase. Mundargi *et al.*[94] replaced cyclohexane with petroleum ether combined with a light liquid petroleum mixture (40:60 v/v). Fundueanu *et al.*[99] dissolved a combination of maltodextrin and cyclodextrin in water treated with NaOH and sodium borohydrate ($NaBH_4$) before emulsification in a 1,2-dichloroethane solvent system containing a cellulose acetate butyrate dispersion agent. After 1 hour emulsification, ECH was added and cross-linked for 20 hours at 50°C. Other cross-linking agents have also been investigated and include sodium trimetaphosphate (STMP)[92], phosphorous chloride oxide ($POCl_3$)[100], glutaraldehyde[68] and formaldehyde[68, 101].

2.6.3 Water-in-water emulsification process

Although the water-in-oil emulsification technique is the most popular process for preparing starch microparticles, it has some disadvantages especially for the pharmaceutical industry. Firstly organic solvents are required for the preparation of the drug-loaded system and secondly, highly alkaline conditions are required for cross-linking which may cause the microparticle core to have a low pH. Both effects have been known to adversely affect the stability of encapsulated proteins[102, 103]. Franssen and Hennink[104] developed an innovative technique of preparing starch hydrogel particles in a completely aqueous system. Aqueous polymer immiscibility is known to occur in many combinations of water-soluble polymers. These include mixtures of dextran, poly(ethylene glycol) (PEG), poly(vinyl alcohol), poly(vinylpyrrolidone), gelatine, and soluble starch. These polymers will remain in solution, but separate above a certain concentration and/or molecular weight. From a thermodynamic point of view, phase separation will occur when the Gibbs free energy of mixing (ΔG_{mix}) is positive. Gibbs free energy is calculated by the following equation[104]:

$$\Delta G_{mix} = \Delta H_{mix} - T\Delta S_{mix} \qquad\qquad \text{equation 2.1}$$

where ΔH_{mix} is the enthalpy of mixing, T the absolute temperature and ΔS_{mix} is the entropy of mixing. Furthermore the enthalpy and entropy of mixing can respectively be given by:

$$\Delta H_{mix} = kT \Sigma n_i v_j \chi_{ij} \qquad\qquad \text{equation 2.2}$$

$$\Delta S_{mix} = - k \Sigma n_i \ln v_i \qquad\qquad \text{equation 2.3}$$

where k is Boltzmann's constant, n_i the number of molecules of component I, v_j the volume fraction of component j, and χ_{ij} the interaction parameter between component i and j.

In an aqueous system containing dextran and PEG, phase separation will occur, caused by an unfavourable interaction parameter (large χ parameter). In other words, when the gain in entropy of mixing is not large enough to compensate for the repulsive dextran/PEG interaction enthalpy, mixing of the polymers is not thermodynamically favourable, resulting in phase separation[105].

A general procedure for preparing methacrylated dextrans (dex-MA) in various molecular weight (4,000 – 20,000 g/mol) PEG solutions have been reported[102-109]. Deoxygenated aqueous solutions of dex-MA have been homogenised under an argon atmosphere and allowed to stabilise for 10 – 20 minutes. Potassium persulfate (KPS) and *N,N,N',N'*-tetramethyl ethylenediamine (TEMED) were subsequently added to initiate polymerisation of the methacryloyl moieties on the dextran chains. After a 30 minute incubation period, the cross-linked microspheres were separated by centrifugation and washed several times to remove traces of PEG. Proteins, such as immunoglobulin, are normally encapsulated by mixing it with dex-MA prior to emulsification.

2.6.4 Crystallisation

The colloidal properties of aqueous starch solutions together with its natural ability to rebuild its crystalline structure upon storage can be applied to prepare starch composites without the need to use chemical cross-linking agents[110, 111]. Crystalline starch microspheres can be precipitated from aqueous solutions by application of a time/temperature incubation step during manufacture. It is hypothesized that the crystallites/precipitates form due to intermolecular cross-linking of starch chains caused by hydrogen bonding[112]. Fanta *et al.*[113] described using steam jet cooking to heat aqueous starch solutions (4 wt%) to 140 $^{\circ}$C in order to ensure complete dissolution. The solutions were slowly cooled, allowing sufficient time for starch crystallization to occur. It was found that the cooling rate had a significant effect on the particle size, morphology, and crystal structure.

2.6.5 Solvent exchange

Starch microcellular foam (SMCF) has received considerable attention as a method to encapsulate volatile compounds, prepare light weight concrete, and as an additive in wood adhesives[67]. It essentially consists of a starch based porous matrix containing pores ranging from about 2 μm to sub-micrometer size, possessing a very high air-solid area interface. These pores also provide the composite with an excellent ability to scatter light, making it suitable for use as an opacifying agent for use as pigment in biodegradable plastics manufacture.

Starch microcellular foam was prepared by the exchange of water in rigid starch aquagels with a liquid containing a lower surface tension. Hydrolysed maize starch was heated in water to 95 ^{o}C and cooked for 30 minutes under continuous stirring, before being cooled to 50 ^{o}C. Glutaraldehyde was added in an acidic medium and the cross-linking reaction allowed to proceed for about 2 hours. A lower surface tension solvent, such as anhydrous ethanol was slowly added under vigorous stirring to precipitate and form the SMCF. The foam particles were subsequently filtered and air dried to a dry powder. Particles prepared using this technique was generally non-spherical since its formation relied on the destruction of an already cross-linked composite using high shear stirring during precipitation.

2.6.6 Spray drying

Krishnan *et al.*[114] reported the use of starch microparticles to encapsulate and preserve oleoresins of spices. Oleoresins are the extracted oil that contains the unique flavour of the particular spice. Microencapsulation protects the oleoresin from destructive environments such as low pH, high temperatures, and oxidation and also converts the extractive to a free flowing powder.

Aqueous gum arabic, maltodextrin, or starch solutions were prepared after which the oleoresin were added. The oil-in-water system was dispersed using a homogeniser and adding Tween 80 as emulsifying agent followed by spray drying using a mini spray dryer equipped with a 0.5 mm diameter nozzle. The pressure of compressed air flow was adjusted to 5 bar and the inlet and outlet temperatures was maintained at 178 ^{o}C and 120 ^{o}C, respectively. The encapsulated oleoresin microspheres possessed enhanced resistance to light, heat, and oxidation.

Limwong *et al.*[115] also reported the use of spray drying techniques to prepare composite starch particles. Rice starch solutions were atomised using a rotating centrifugal wheel atomiser with an atomising pressure of 2 bar and inlet temperature of 130 ^{o}C. The particles exhibited high compressibility and flow ability and were successfully used in preparing compressed tablets.

2.6.7 Microfluidics

Polymeric microspheres with uniform size particle diameter ranging between 10 – 100 µm have significant application importance in diverse fields. For example, emulsions that have a very low poly-dispersity have been used to produce templates for sol-gel chemistry where the droplets spontaneously order into regular packings or where electro-optical materials such as liquid crystal needed to be encapsulated[116]. Conventional emulsion polymerisation can typically only produce mono-disperse particles below 1 µm, while dispersion polymerisation under certain conditions can be used to produce mono-disperse particles up to 10 µm. Above 10 µm, dispersion polymerisation yields poly-disperse particles that can only be classified into lower distribution size using tedious and only marginally effective fractionation[117]. Microfluidic systems have recently become available as an effective tool for preparing mono-dispersed particles and emulsions. Two immiscible fluids are introduced into separate microchannels and forced together at a junction to form micro droplets one at a time. Particle formation is rapid and reproducible and droplet size can be controlled by varying the flow conditions.

T-junction devices are the simplest type of microfluidic devices, where two fluids are joined at right angles in a T-section[116-119] (Figure 2.14A). Depending on the individual flow rates, the droplet size and distribution can be controlled.

Jeong *et al*[120] prepared hydrogel biocatalyst particles consisting of a blend of 4-hydroxybutyl acrylate, acrylic acid, ethyleneglycol dimethacrylate 2,2-dimethoxy-2-phenyl-acetophenone in a mineral carrier oil. This was performed using a two inlet channel microfluidic system as shown in Figure 2.14B. Droplet formation is followed by an in-line UV light source, used to initiate cross-linking by photopolymerisation.

Utada *et al.*[121] developed a process for preparing double emulsions in a single step using a three inlet microfluidic system (Figure 2.14C). Double emulsifications separate the inner most fluid from the outer fluid through encapsulation by an intermediate fluid. These types of emulsions are highly desirable for applications in controlled release of substances, separation, and encapsulation of nutrients and flavours for food additives and personal care items[122]. Furthermore, since there is much better control over the particle size and poly-dispersity of

the particles prepared, precise control is gained over the release of active substances encapsulated. Additionally, the core to shell concentration ratio can be controlled by adjusting the individual fluid flow rates.

Figure 2.14: Schematic illustration of different types of microfluidic devices which includes a simple T-junction layout (**A**), a two inlet channel system (**B**), and a three inlet channel structure used for double emulsification (**C**).
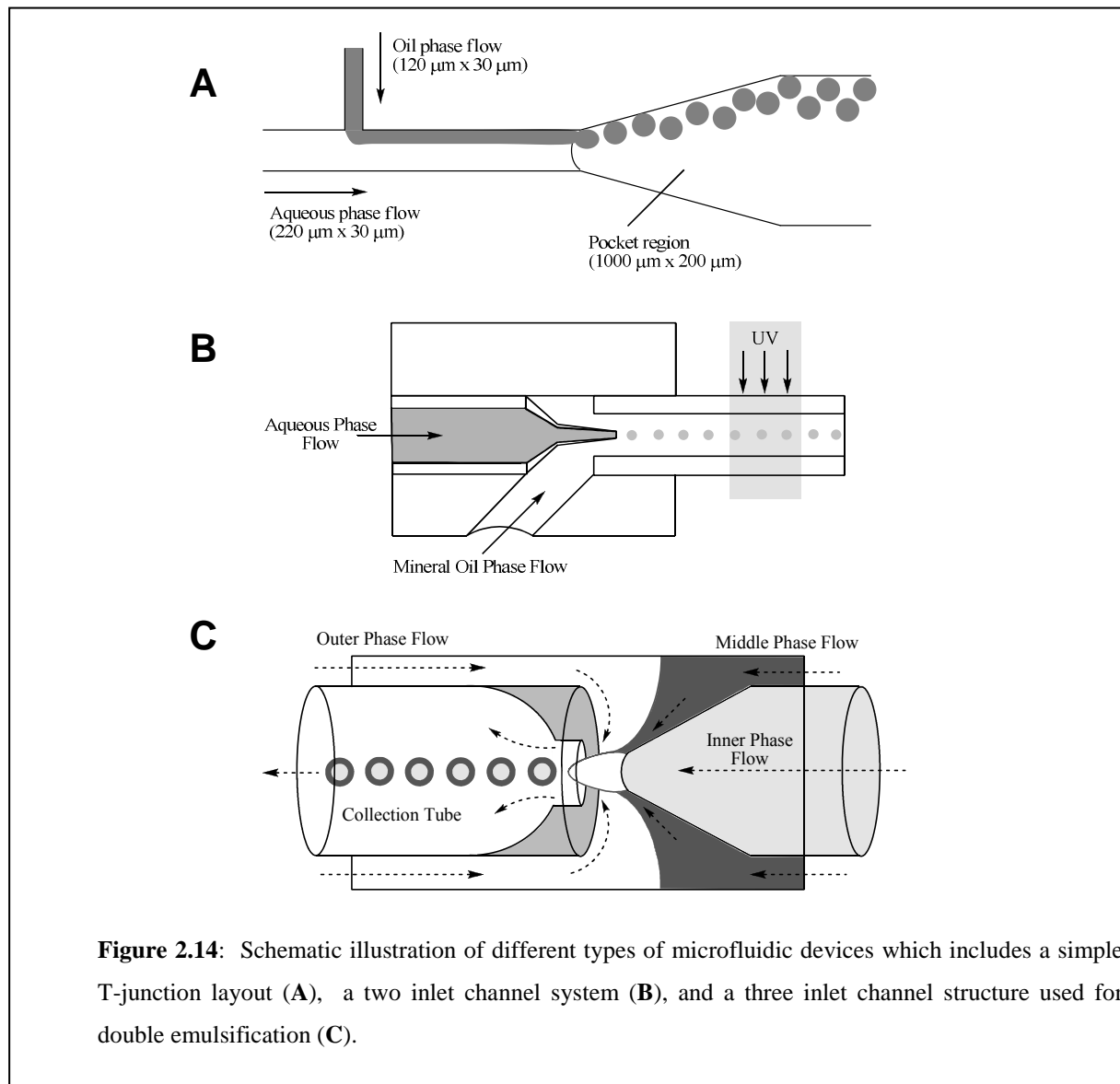
De Geest *et al.*[123] investigated the preparation of dextran hydrogel particles on a two inlet channel microfluidic system. Aqueous hydroxyethyl methacrylate modified dextran (dex-HEMA) solutions were treated with a photoinitiator and emulsified in mineral oil containing a non-ionic (cetyl dimethicone copolymer) surfactant. After passing through the microfluidic system, the methacrylate groups were polymerised by UV irradiation.

Generally it was found that droplet formation is more mono-dispersed when the dex-HEMA flow was at low pressure compared to the oil flow. If the system remained at low Reynolds number the droplets moved in an ordered way through the channel causing minimal impact that may result in coalescence. After photopolymerisation, the hydrogel microparticles could be separated from the oil by centrifugation, followed by several washing steps with deionised water.

Studies were also conducted on preparing water-in-water emulsions by combining dex-HEMA with an aqueous PEG solution based on the work of Franssen and Hennink[104], but it was impossible to generate aqueous dex-HEMA droplets due to the lack of shear between the two phases upon formation.

A further introduction and discussion of applying microfluidics for preparing modified polysaccharide particles follows in Chapter 5.

2.7 Conclusions

The paper industry often relies on additives to improve the interaction and retention of fibres and fillers in paper. Polysaccharides, starch being the most common, are widely used for improving the strength and smoothness of paper and incorporated as a wet-end additive and/or a sizing agent. It is attractive in the selection of additives owing to its non-toxicity, biodegradability, and low cost. Chemical modifications offer further advantages and cationic charged starch is commonly used to flocculate and retain anionic charged fibres. Processing of polysaccharide microgel particles have also been widely reported with the major application areas being in the pharmaceutical industry for the purpose of encapsulating drugs for controlled release and adhesive carrier systems. To date, modified polysaccharide particle processing for application in the papermaking industry is still specifically unknown.

2.8 References

1.   M. Rice, *New Techniques for Continuous Chemical Analysis in the Pulp & Paper Industry*. Universitetsservice US AB, Stockholm, 2001: Stockholm, Sweden, **2001**.

2. N. Wilson, *Encyclopedia of Ancient Greece*. Routledge: **2005**.

3. J. B. Calkin, *Modern Pulp and Paper Making*. 3rd ed.; Reinhold Publishing Corporation: New York, **1957**.

4. R. R. A. Higham, *A Handbook of Papermaking- the Technology of Pulp, Paper and Board Manufacture*. 2nd ed.; Business Books Limited: London, **1968**.

5. C. E. Libby, *Pulp and Paper Science and Technology*. McGraw-Hill Book Company: New York, **1962**; Vol. 2 - Paper.

6. A. J. Baker, *Journal of Animal Science*, **1973**, 36, 768 - 771.

7. W. C. Dickison, *Integrated Plant Anatomy*. Academic Press: United States of America, **2000**.

8. *Elements of Wood, Fiber Structure and Fiber Bonding*; U.S. Department of Agriculture: Madison, WS, May 1963.

9. Y. Song; J. Zhou; Q. Li, et al., *Carbohydrate Research*, **2009**, 344, 1332-1339.

10. K. B. Bastawde, *World Journal of Microbiology and Biotechnology*, **2005**, 8, 353 - 368.

11. E. Sjostrom, *Journal of Wood Chemistry and Technology*, **2006**, 26, 283 - 288.

12. A. Sundberg, *Journal of Wood Chemistry and Technology*, **2000**, 20, 71 - 92.

13. S. Knez, *Chemical Engineering Science*, **2006**, 61, 5867-5880.

14. R. L. Ain, *Alkaline Paper Advocate*, **1996**, 10.

15. J. S. Bond, *The Aging of Lignin Rich Papers Upon Exposure to Light: Its Quantification and Prediction*, Proceedings of the 10th International Symposium on Wood and Pulping Chemistry, Yokohama, Japan, TAPPI Press: **1999**; pp 500-504.

16. R. A. Gill, *Paperboard Filling Experiences with Precipitated Calcium Carbonate (PCC) for the New Millenium*, Papermaking Conference, **2000**; pp 811-821.

17. E. Antunes, *Chemical Engineering Research and Design*, **2008**, 86, 1155-1160.

18. R. Vengimalla, *Separation and Purification Technology*, **1999**, 15, 153-161.

19. S. Bratskaya, *Industrial & Engineering Chemistry Research*, **2006**, 45, 7374-7379.

20. R. Gaudreault, *Colloids and Surfaces A-Physicochemical and Engineering Aspects*, **2009**, 340, 56-65.

21. M. Cadotte, *The Canadian Journal of Chemical Engineering*, **2007**, 85, 240-248.

22. M. A. Hubbe, *Solutions*, **2004**, 87, 23-25.

23. J. E. Unbehend, *Industrial & Engineering Chemistry Product Research and Development*, **1982**, 21, 150-153.

24. T. G. M. van de Ven, *Advances in Colloid and Interface Science*, **2005**, 114-115, 147-157.

25. M. Kamiti, *Macromolecules*, **1996**, 29, 1191-1194.

26. J. C. Roberts, *Paper Chemistry*. 2nd ed.; Chapman & Hall: **1996**.

27. H. Ichiura, *Journal of Materials Science*, **2001**, 36, 913-917.

28. S. Akari, *Langmuir*, **1996**, 12, 857-860.

29. Y. Zou, *TAPPI Journal Online Exclusive*, **2004**, 3, E41-E59.

30. M. Zhang; B. Ju; S. Zhang, et al., *Carbohydrate Polymers*, **2007**, 69, 123-129.

31. H. Li, *Colloids and Surfaces A-Physicochemical and Engineering Aspects*, **2004**, 242, 1-8.

32. H. Chi, *Colloids and Surfaces*, **2007**, 297, 147-153.

33. E. S. A. El-Sayed, *Pigment & Resin Technology*, **2005**, 34/2, 88-93.

34. S. Modgi; M. E. McQuaid; R. Englezos, *Journal of Pulp and Paper Science*, **2007**, 33, 156-162.

35. H. W. Heldt, *Plant Biochemistry*. 3rd ed.; Elsevier Academic Press: **2005**.

36. M. Shiozaki, *Journal of Organic Chemistry*, **1991**, 56, 528-532.

37. L. Copeland; J. Blazek; H. Salman, et al., *Food Hydrocolloids*, **2009**, 23, 1527-1534.

38. O. B. Wurzburg, *Modified Starches: Properties and Uses*. CRC Press, Inc.: **1986**.

39. J. B. Les Copeland, Hayfa Salman, Mary Chiming Tang, *Food Hydrocolloids*, **2009**, 23, 1527-1534.

40. Y. Tian; Y. Li; F. A. Manthey, et al., *Food Chemistry*, **2009**, 116, 54-58.

41. Y. A. L. Gouellec; D. Cornwell, *A Novel Approach to Seawater Desalination Using Dual-Staged Nanofiltration*. illustrated ed.; American Water Works Association: **2006**; p 164.

42. A. Buleon; P. Colonna; V. Planchot, et al., *International Journal of Biological Macromolecules*, **1998**, 23, 85-112.

43. W. P. Edwards, *The Science of Bakery Products*. The Royal Society of Chemistry: **2007**.

44. T. P. Coultate, *Food: The Chemistry of its Components*. 5th ed.; The Royal Society of Chemistry: **2009**.

45. C. M. O. Muller; J. B. Laurindo; F. Yamashita, *Carbohydrate Polymers*, **2009**, 77, 293-299.

46. E. Laredo; D. Newman; A. Bello, et al., *European Polymer Journal*, **2009**, 45, 1506-1515.

47. J. W. Knight, *The Starch Industry*. 1st ed.; Pergamon Press Ltd.: **1969**.

48. R. P. Ellis; M. P. Cochrane; M. F. B. Dale, *Journal of the Science of Food and Agriculture*, **1998**, 77, 289-311.

49. H. W. Maurer; R. L. Kearney, *Starch-Starke*, **1998**, 50, 396-402.

50. R. L. Whistler; E. F. Paschall, *Starch Chemistry and Technology*. 1st ed.; Academic Press: **1967**; Vol. 2.

51. H. Rozie; W. Somers; K. van't Riet, et al., *Carbohydrate Polymers*, **1991**, 15, 349-365.

52. I. Simkovic; J. A. Laszlo; A. R. Thompson, *Carbohydrate Polymers*, **1996**, 30, 25-30.

53. G. J. L. Griffin, *Advances in Chemistry Series*, **1974**, 134, 159-170.

54. M. Kim; S. J. Lee, *Carbohydrate Polymers*, **2002**, 50, 331-337.

55. Y. X. Chen; G. Y. Wang, *Journal of Applied Polymer Science*, **2006**, 102, 1539-1546.

56. A. M. L. Huijbrechts; M. Desse; T. Budtova, *Carbohydrate Polymers*, **2008**, 74, 170-184.

57. D. Jaworek; J. Maier; M. Nelbock-Hochstetter, Process for Binding Biologically Active Proteins, Patent: U.S. 4,038,140, **1977**.

58. M. Seker; M. A. Hanna, *Carbohydrate Polymers*, **2005**, 59, 541-544.

59. T. Yoneya; K. Ishibashi; K. Hironaka, et al., *Carbohydrate Polymers*, **2003**, 53, 447-457.

60. T. Kasemsuwan; J. Jane, *Cereal Chemistry*, **1994**, 71, 282-287.

61. K. S. Woo; P. A. Seib, *Cereal Chemistry*, **2002**, 79, 819-825.

62. S. Wattanachant; K. Muhammad; D. M. Hashim, et al., *Food Chemistry*, **2003**, 80, 463-471.

63. S. H. Kim; C. Y. Won; C. C. Chu, *Carbohydrate Polymers*, **1999**, 40, 183-190.

64. B. D. Martin; S. A. Ampofo; R. J. Linhardt, *Macromolecules*, **1992**, 25, 7081-7085.

65. B. D. Martin; R. J. Linhardt; J. S. Dordick, *Biomaterials*, **1998**, 19, 69-76.

66. W. N. E. van Dijk- Wolthuis; O. Franssen; H. Talsma, et al., *Macromolecules*, **1995**, 28, 6317-6322.

67. K. El-Tahlawy; R. A. Venditti; J. J. Pawlak, *Carbohydrate Polymers*, **2007**, 67, 319-331.

68. F. Atyabi; S. Manoochehri; S. H. Moghadam, et al., *Archives of Pharmacal Research*, **2006**, 29, 1179-1186.

69. R. M. Kriegel, Divinyl Sulfone Crosslinking Agents and Methods of use in Subterranean Applications, Patent: U.S. 7,131,492, **2006**.

70. I. Simkovic; M. Hricovini; R. Mendichi, *Carbohydrate Polymers*, **2004**, 55, 299-305.

71. O. S. Lawal; M. D. Lechner; B. Hartmann, et al., *Starch-Starke*, **2007**, 59, 224-233.

72. Z. Stojanovic; K. Jeremic; S. Jovanovic, *Starch-Starke*, **2000**, 52, 413-419.

73. B. Volkert; F. Loth; W. Lazik, et al., *Starch-Starke*, **2004**, 56, 307-314.

74. C. J. Tijsen; H. J. Kolk; E. J. Stamhuis, et al., *Carbohydrate Polymers*, **2001**, 45, 219-226.

75. J. K. Dutkiewicz, *Journal of Biomedical Materials Research*, **2002**, 63, 373-381.

76. J. Yao; W. R. Chen; R. M. Manurung, et al., *Starch-Starke*, **2004**, 56, 100-107.

77. C. J. Tijsen; R. M. Voncken; A. Beenackers, *Chemical Engineering Science*, **2001**, 56, 411-418.

78. W. Lazik; T. Heinze; K. Pfeiffer, et al., *Journal of Applied Polymer Science*, **2002**, 86, 743-752.

79. A. Tara; F. Berzin; L. Tighzert, et al., *Journal of Applied Polymer Science*, **2004**, 93, 201-208.

80. S. Pal; D. Mal; R. P. Singh, *Carbohydrate Polymers*, **2005**, 59, 417-423.

81. V. Haack; T. Heinze; G. Oelmeyer, et al., *Macromolecular Materials and Engineering*, **2002**, 287, 495-502.

82. T. Heinze; V. Haack; S. Rensing, *Starch-Starke*, **2004**, 56, 288-296.

83. J. Bendoraitiene; R. Kavaliauskaite; R. Klimaviciute, et al., *Starch-Starke*, **2006**, 58, 623-631.

84. V. Goclik; P. Mischnick, *Carbohydrate Research*, **2003**, 338, 733-741.

85. A. Ayoub; S. Gruyer; C. Bliard, *International Journal of Biological Macromolecules*, **2003**, 32, 209-216.

86. Y. X. Chen; S. Y. Liu; G. Y. Wang, *Journal of Applied Polymer Science*, **2007**, 105, 2841-2849.

87. V. Bobacka; D. Eklund, *Colloids and Surfaces A-Physicochemical and Engineering Aspects*, **1999**, 152, 285-291.

88. M. I. Khalil; A. A. Aly, *Journal of Applied Polymer Science*, **2004**, 93, 227-234.

89. R. Nystrom; G. Hedstrom; J. Gustafsson, et al., *Colloids and Surfaces A-Physicochemical and Engineering Aspects*, **2004**, 234, 85-93.

90. H. Grano; J. Yli-Kauhaluoma; T. Suortti, et al., *Carbohydrate Polymers*, **2000**, 41, 277-283.

91. S. Radosta; W. Vorwerg; A. Ebert, et al., *Starch-Starke*, **2004**, 56, 277-287.

92. Y. Fang; L. Wang; D. Li, *Carbohydrate Polymers*, **2008**, 74, 379-384.

93. A. Schwoerer; S. Harling; H. Menzel, *Journal of Controlled Release*, **2008**, 132, e1-e18.

94. R. C. Mundargi; N. B. Shelke; A. P. Rokhade, *Carbohydrate Polymers*, **2008**, 71, 42-53.

95. G. A. Silva; O. P. Coutinho; P. Ducheyne, *Biomaterials*, **2007**, 28, 326-334.

96. A. Roy; J. Bajpai; A. K. Bajpai, *Carbohydrate Polymers*, **2009**, 76, 222-231.

97. G. Hamdi; G. Ponchel; D. Duchene, *Journal of Microencapsulation*, **2001**, 18, 373-383.

98. Y. Dziechciarek; J. J. G. van Soest; A. P. Philipse, *Journal of Colloid and Interface Science*, **2002**, 246, 48-59.

99. G. Fundueanu; M. Constantin; A. Dalpiaz, *Biomaterials*, **2004**, 25, 159-170.

100. S. Y. Xiao; C. Y. Tong; X. M. Liu, et al., *Chinese Science Bulletin*, **2006**, 51, 1693-1697.

101. H. Selek; S. Sahin; H. S. Kas, et al., *Drug Development and Industrial Pharmacy*, **2007**, 33, 147-154.

102. R. J. H. Stenekes; W. E. Hennink, *Polymer*, **2000**, 41, 5563-5569.

103. O. Franssen; R. J. H. Stenekes; W. E. Hennink, *Journal of Controlled Release*, **1999**, 59, 219-228.

104. O. Franssen; W. E. Hennink, *International Journal of Pharmaceutics*, **1998**, 168, 1-7.

105. R. J. H. Stenekes; O. Franssen; E. M. G. van Bommel, et al., *Pharmaceutical Research*, **1998**, 15, 557-561.

106. R. J. H. Stenekes; O. Franssen; E. M. G. van Bommel, et al., *International Journal of Pharmaceutics*, **1999**, 183, 29-32.

107. O. Franssen; R. D. van Ooijen; D. de Boer, et al., *Macromolecules*, **1997**, 30, 7408-7413.

108. W. N. E. van Dijk-Wolthuis; M. J. van Steenbergen; W. J. M. Underberg, et al., *Journal of Pharmaceutical Sciences*, **1997**, 86, 413-417.

109. L. Elfstrand; A. C. Eliasson; M. Jönsson, et al., *Starch-Starke*, **2006**, 58, 381-390.

110. L. Elfstrand; A. C. Eliasson; M. Jönsson, et al., *Carbohydrate Polymers*, **2007**, 68, 568-576.

111. L. Elfstrand; A. C. Eliasson; M. Jönsson, et al., *Carbohydrate Polymers*, **2007**, 69, 732-741.

112. R. J. H. Stenekes; H. Talsma; W. E. Hennink, *Biomaterials*, **2001**, 22, 1891-1898.

113. G. F. Fanta; F. C. Felker; R. L. Shogren, et al., *Carbohydrate Polymers*, **2005**, 61, 222-230.

114. S. Krishnan; A. C. Kshirsagar; R. S. Singhal, *Carbohydrate Polymers*, **2005**, 62, 309-315.

115. V. Limwong; N. Sutanthavibul; P. Kulvanich, *Aaps Pharmscitech*, **2004**, 5.

116. D. R. Link; S. L. Anna; D. A. Weitz, *Physical Review Letters*, **2004**, 92, 054503-1 to 4.

117. T. Nisisako; T. Torii; T. Higuchi, *Chemical Engineering Journal*, **2004**, 101, 23-29.

118. T. Nisisako; T. Torii; T. Higuchi, *Lab on a Chip*, **2002**, 2, 24-26.

119. T. Iwasaki; J. Yoshida, *Macromolecules*, **2005**, 38, 1159-1163.

120. W. J. Jeong; J. Y. Kim; J. Choo, *Langmuir*, **2005**, 21, 3738-3741.

121. A. S. Utada; E. Lorenceau; D. R. Link, *Science*, **2005**, 308, 537-541.

122. S. Okushima; T. Nisisako; T. Torii, et al., *Langmuir*, **2004**, 20, 9905-9908.

123. B. G. De Geest; J. P. Urbanski; T. Thorsen, et al., *Langmuir*, **2005**, 21, 10275-10279.

Chapter 3: Conceptualisation and methodology

3.1 Introduction

Producing paper with higher filler content requires an efficient retention aid system since the replacement of fibres with filler particles, such as precipitated calcium carbonate (PCC) inevitably reduces the paper strength. This is not only because there are less fibres in the sheet which reduces the number of fibre-fibre bonds, but also because the presence of fillers reduces the area of contact between the remaining fibres. Retention aids assist in attaching the fillers onto the long fibres. The cationic starch used in the wet end of the papermaking process is usually first dispersed in cold water at a concentration of about 2–6 wt% whereupon full gelatinisation in either batch cookers (96–100 ^{o}C) or jet cookers (120-140 ^{o}C) is performed, prior to treatment to pulp suspensions where it easily adsorbs onto the negatively charged fibres. Unfortunately, when used in chemical pulp furnishes, the improvement in paper strength is often low and addition of higher levels does not necessarily provide improved strength[1]. This is related to the amount of starch that can adsorb on the fibres. It appears that once the negative charge on the fibre surface is neutralised by the cationic charge, no further starch adsorbs, and higher dosage levels only results in loss in the waste water system.

One approach for improving filler retention, strength and sizing performance is to make use of a dual retention system. Since PCC has a slight positive surface charge, an anionic additive can be added to the filler solution prior to mixing it with the pulp stock. The anionic additive attaches to the filler particles and promotes flocculation, which usually improves retention since the flocs are effectively trapped in the fibre matrix. Additionally, once the anionic modified filler is added to the pulp stock, strong interaction will occur with cationic modified fibres, resulting in improved strength and retention.

Theoretically, a further improvement in paper strength can be realised if the retention aids are in the form of micro-particles as opposed to high molecular weight polymers such as starch gels. Sheet formation during the papermaking process is a very fast, turbulent process with

high shear exerted on the furnish during drainage[2]. Conventional retention aids often fail to bridge filler-fibre interaction under these harsh conditions since it relies on weak single polymer chain bridging mechanisms. The use of micro-particles as retention aids offer a larger multi-functional group surface area for interaction and should be more effective in binding filler particles to fibres (Figure 3.1). Furthermore, the bulky particles should be more easily captured and retained in the paper web, allowing the use of higher dosage levels, whilst densely cross-linked micro-particles embedded in the paper sheet should effectively improve the stiffness and mechanical properties of paper.

Figure 3.1: Schematic illustration of starch polymer and particle bridging mechanism between fibre and filler.
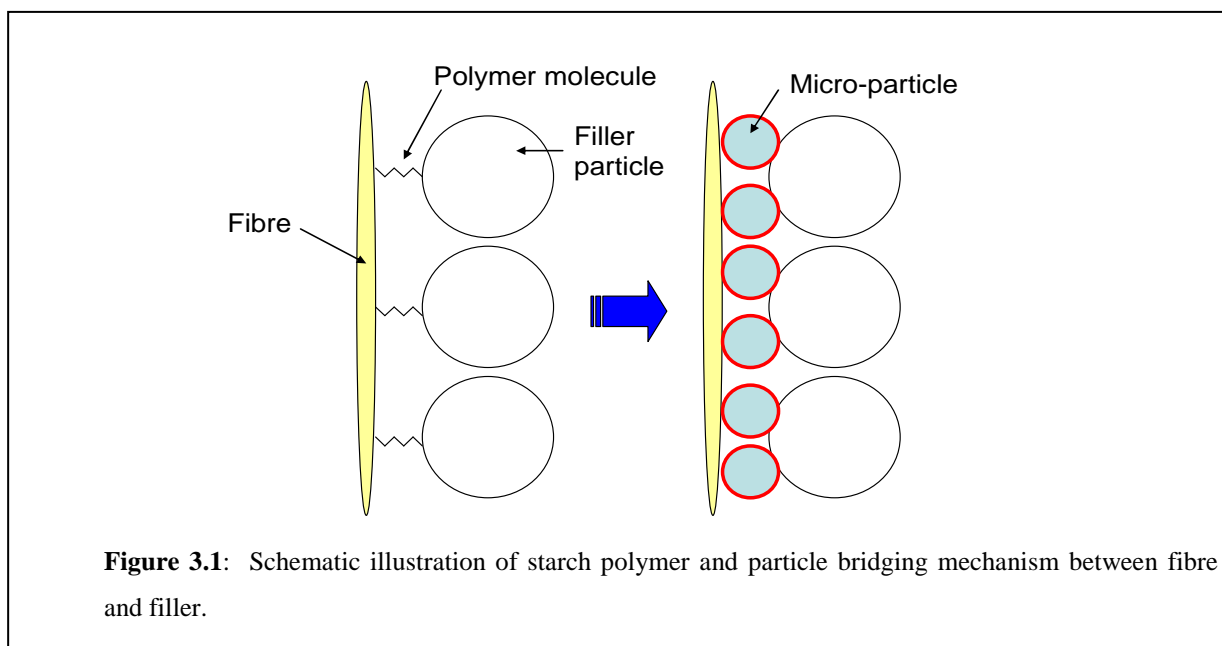
3.2 Modified polyester particles

3.2.1 Background

In order to investigate if the mechanism depicted in Figure 3.1 is indeed valid, the study was started off using a more familiar micro-particle system. Vesiculated particles are synthetic, opaque, highly cross-linked beads containing multiple microvoids encapsulated in an insoluble polyester shell[3]. These beads are typically held stable in a continuous aqueous phase containing water soluble stabilisers. When dried, the water-filled vesicles in the polyester casing become hollow, causing the beads to develop hiding power due to the difference in refractive index between the air and polymeric beads. These particles are mostly

incorporated in paint as a low cost extender to partially substitute high cost titanium dioxide pigment, which is the primary whitening pigment used in the industry.

Gunning *et al.*[4] and Karickhoff[5] published patents describing processes for preparing vesiculated beads. The polyesters used were caboxylated unsaturated resins prepared by the condensation polymerisation of either fumaric acid, itaconic acid, and maleic acid or maleic anhydride, phthalic acid, and propylene glycol. The condensation product was diluted in a water-insoluble monomer such as styrene and the final acid value of the resin has to be between 10 and 45 mg KOH/g polyester.

Water was initially dispersed in the polyester in conjunction with a co-monomer, which can be any water-insoluble monomer (less than 5 wt% solubility in water at 20 ^{o}C) such as ethyl acrylate, *n*-butyl methacrylate, acrylonitrile, or styrene. The water was stabilised in the polyester by adding a polyamine with at least 3 amine groups per molecule. A small amount of titanium dioxide could also be added to the resin to enhance whiteness.

The water-in-oil solution was subsequently added to a secondary aqueous phase and dispersed using high shear agitation. The water-in-oil globules formed were held stable with colloid stabilisers added to the secondary aqueous phase and typically consisted of partially hydrolysed polyvinyl acetate and/or hydroxyethyl cellulose.

The water-in-oil-in-water emulsion was subsequently polymerised by free radical initiation, either using organic peroxides, such as benzoyl peroxide or cumene peroxide, in combination with a free radical initiator, or ultra-voilet radiation. The most useful initiation system found was a combination of diethylene triamine and cumene hydroperoxide, which was triggered by ferrous ions[4]. The cross-linked vesiculated beads prepared using this method typically had a highly poly-disperse particle size range with average diameters ranging between 0.1 to 500µm and possessed extremely high dimensional stability.

Since it is not one of the objectives to improve the whiteness of paper, using a double emulsification system to encapsulate aqueous microdroplets in the polyester resin is not necessary. Therefore a single oil-in-water emulsification technique was used where a co-

monomer is combined with the polyester prior to dispersion in a stabilised aqueous system and catalysis. The co-monomers selected essentially required an ionic charge and acrylic acid was selected as anionic monomer and 3-[(methacryloylamino)propyl]trimethylammonium chloride was used as cationic monomer.

3.2.2 Experimental

3.2.2.1 Materials

The unsaturated polyester resin used was the condensation products of maleic anhydride, phthalic anhydride and propylene glycol (M_w = 5,000 g/mol; acid value = 24-28 mg KOH/g; from storage) and diluted in styrene to a concentration of 68 wt% (supplied by Barloworld Coatings Research Centre). Acrylic acid (Acros, Cat: 16,425) was vacuum-distilled at 30 ^{o}C and stored at -5 ^{o}C prior to use, while the 3-[(methacryloylamino)-propyl]trimethylammonium chloride (Aldrich, Cat: 280,658) was used as received. The colloid stabiliser system selected consists of a blend of partially hydrolysed polyvinyl alcohol (M_w = 146,000 – 186, 000 g/mol; 87 - 89% hydrolysed) (Aldrich, Cat: 363,103) and hydroxyethyl cellulose (Natrosol$^®$ 250, supplied by Aqualon). The catalyst system consisted of a combination of diethylene triamine (99%) (Aldrich, Cat: D93,856), cumene hydroperoxide (Aldrich, Cat: 513,296) and anhydrous ferrous sulphate (Merck, Cat: SAAR2345860 EM).

3.2.2.2 Preparation of anionic polyester particles

The unsaturated polyester (13.22 g) was blended with 5.64 g acrylic acid (Figure 3.2A) and 0.20 g diethylene triamine for a period of at least 5 minutes. In a separate container the aqueous phase was prepared, consisting of 71.8 g distilled deionised (DDI) water, 1.34 g polyvinyl alcohol and 0.26 g hydroxyethyl cellulose. The solution was heated to 85 ^{o}C under reflux and continuous stirring for 1 hour to completely solubilise the colloid stabilisers after which it was cooled down to ambient temperature. In order to avoid pH shock that may result in emulsion destabilisation, the aqueous phase was also treated with 0.05 g diethylene triamine.

The two phases were combined and emulsified in a Silverson (Model L4R) homogeniser at 5,500 rpm for 2 minutes. The mixture was placed in an oilbath (50 ^{o}C) under continuous stirring and treated with ferrous sulphate (0.01 g) followed by cumene hydroperoxide (80 wt%) (0.1 g). The combination of organic peroxide and metal redox activator initiated polymerisation and the mixture was left overnight for the reaction to complete. The total solids content of the mixture was 22.1 wt%.

Figure 3.2: Structures of acrylic acid (anionic monomer) (**A**) and 3-[(methacryloylamino)propyl]-trimethylammonium chloride (cationic monomer) (**B**).
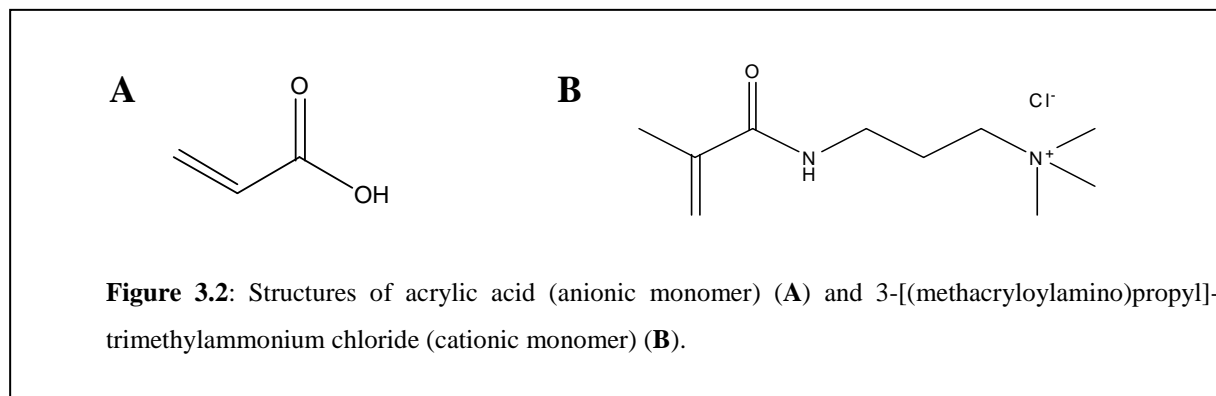
3.2.2.3 Cationic polyester particles

Exactly the same procedure was followed as above, but the acrylic acid was replaced with 3-[(methacryloylamino)propyl]trimethylammonium chloride (Figure 3.2B).

3.2.2.4 Combination of modified polyester particles with filler and fibre

The anionic and cationic modified polyester particles were both centrifuged and washed 3 times with DDI water to isolate the particles. The final total solids content for both particles were adjusted to 5 wt%.

Fibre sheets (supplied by Mondi) were dried in an oven at 50 ^{o}C overnight to remove any excess moisture. A 0.5 wt% fibre solution in DDI water was prepared and mixed for 2 hours on a magnetic stirrer to ensure complete fibril detanglement.

Precipitated calcium carbonate was also supplied by Mondi as an aqueous slurry with a concentration of 22.5 wt%.

The anionic polyester particles were added to the PCC solution at a concentration of 2 wt% (dry particles/ dry PCC) and placed on a magnetic stirrer for a period of 24 hours to ensure effective time for ionic interaction.

Similarly, the cationic polyester particles were added to the fibre solution at the same concentration (2 wt% dry particles/dry fibre) and mixed for the same period of time.

3.2.3 Analysis

3.2.3.1 Particle size analysis

The average particle size of the polyester particles was determined by static laser light scattering, using a Saturn DigiSizer 5200 from Micrometrics Instrument Corporation. The instrument uses a laser in conjunction with a charge-coupled device (CCD) that contains over one million detector elements to measure particle size. These detector elements are placed so that they can measure the intensity of light scattered by particles at various angles. Light is scattered by particles in a pattern dependent on their size, shape, refractive index and wave length of incident light and based on the Mie theory[6], the particle size distribution is calculated from the angle distribution of the scattered light intensity collected by detectors.

3.2.3.2 Optical microscopy

Optical microscopy of wet samples was performed at the Freeworld Coatings Research Centre on an Olympus SZX12 Zoom Stereo microscope with a 1.6x objective and a 10x eyepiece with an effective zoom range of 3.5x to 144x and fitted with an SIS view Firewall camera for image capturing.

3.2.3.3 Scanning electron microscopy

Wet samples of the prepared cationic polyesters treated to the fibre and anionic polyester particles with the PCC filler were placed directly onto carbon tape and oven dried at a temperature of 50 ^{o}C for 4 hours. Imaging was performed using a Leo 1430VP Scanning Electron microscope fitted with a variable pressure detector.

3.2.4 Results and discussion

Figure 3.3 presents the particle size distribution of the cationic and anionic modified polyester particles with average particle sizes of 2.3µm and 6.0µm respectively, the latter having a significantly higher poly-dispersity. In order to validate if these particles indeed had flocculating capability, a 50:50 (w/w) combination of the two particles was made. Instantaneous particle flocculation was observed.
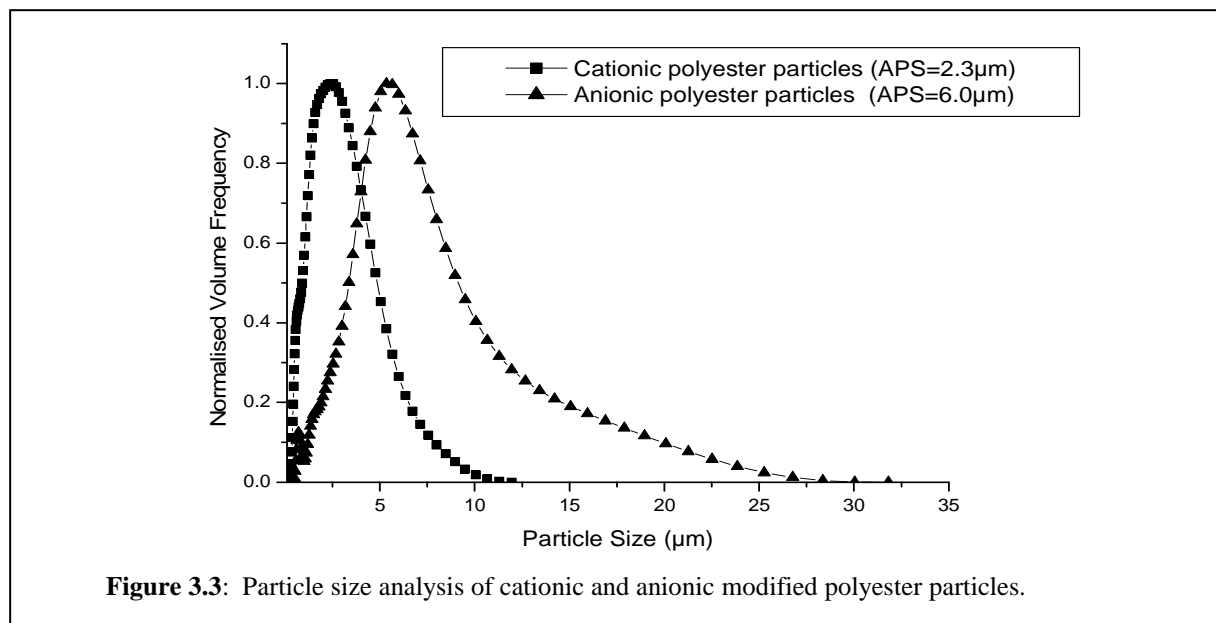
Figure 3.3: Particle size analysis of cationic and anionic modified polyester particles.

Addition of anionic charged polyester particles to the PCC also showed immediate flocculation and scanning electron microscopy was used to study the position of the polyester particles in the system. Although it was not easy to observe the particles in the densely flocculated system, some protruding polyester particles could be detected on the surface (Figure 3.4).

Similarly it was observed that there was definite adsorption of cationic polyester particles onto the surface of fibre (Figure 3.5), with certain areas more enriched with a cluster of particles than others. This phenomenon will be investigated later in this chapter.
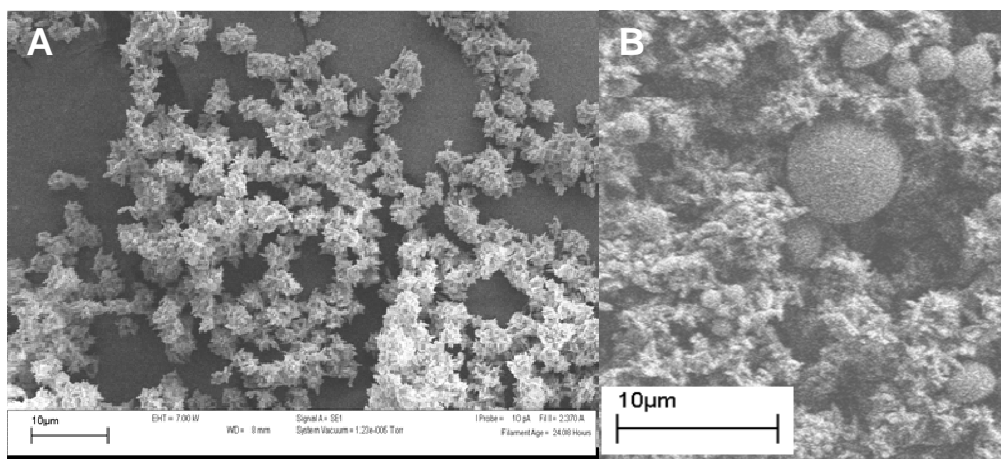
Figure 3.4: SEM imaging showing pure PCC particles (control) (**A**), and flocculated PCC treated with 2 wt% (dry particles/dry PCC) anionic polyester particles (**B**) (scale bars=10µm).
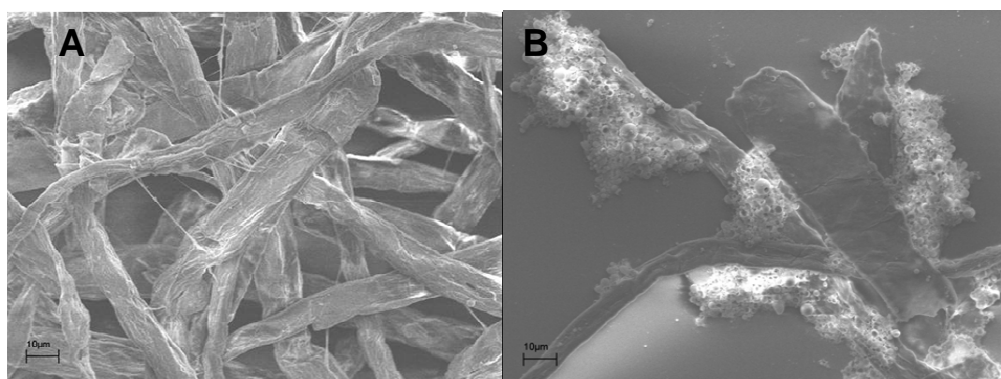
Figure 3.5: SEM imaging showing (**A**) pure fibres (control), and (**B**) fibres treated with 2 wt% (dry particles/dry fibre) cationic polyester particles (scale bars = 10µm).

Subsequently, a combined system was prepared consisting of PCC (22.5 wt%) treated with 2 wt% cationic particles (based on dry PCC), which were added to a 0.5 wt% fibre solution containing 2 wt% anionic particles (based on dry fibre). The system contained in total 20 wt% dry PCC based on dry fibre, this concentration being typical of that used in the paper industry.

Figure 3.6 shows a control sample prepared similarly, but without any particles, compared to the sample including particles. The control sample image (Figure 3.6A) shows the presence of PCC adsorbed onto the fibre surface as expected, since there does exist a weak ionic interaction between the anionic charged fibre and the cationic PCC, but a significant amount

55

of free PCC particles are detected around the vicinity of the fibre as well. This would typically represent filler that might filter through the filler matrix during paper making, ending up in the waste water.

Figure 3.6: SEM imaging of control sample of fibre treated with 20 wt% (dry PCC/dry fibre) PCC (**A**), and a similar sample where PCC is pretreated with 2 wt% anionic polyester particles and the fibre with 2 wt% cationic polyester particles (**B**) (scale bars = 100µm).
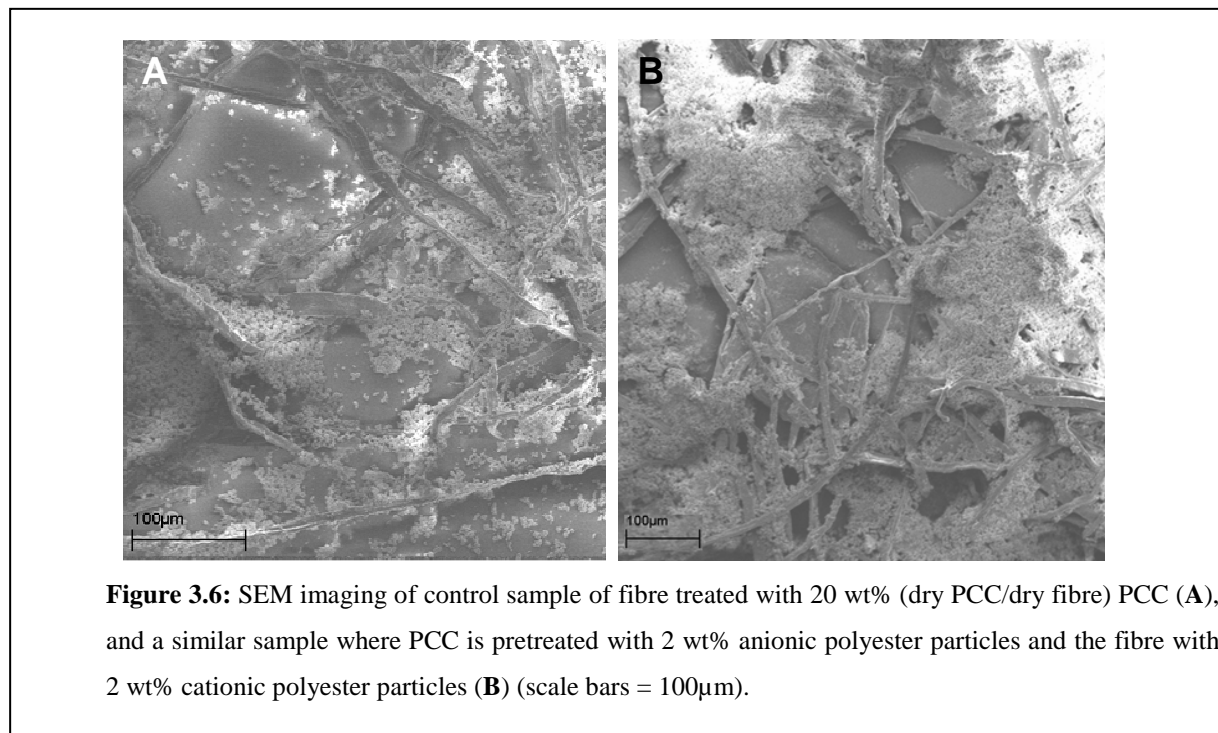
The sample that includes the modified particles shows significantly improved filler attachment with almost all PCC bound in clusters on top of the fibres and hardly any free particles on the pore surface. A close-up view of the fibre surface (Figure 3.7) clearly shows the presence of polyester particles on the fibre surface with attached filler surrounding it. Note that some of the polyester particles appear to have collapsed and this could be attributed to large vesicules entrapped within the polyester shell, causing the particle wall to weaken and fall in upon drying.

Even though the systems discussed in this section were only used to demonstrate the concept of using ionic modified particles in paper and its potential location in a paper sheet, samples of each of the modified polyester particles were sent to Mondi, Austria for testing in paper hand sheets. Results will be presented and discussed in Chapter 6.
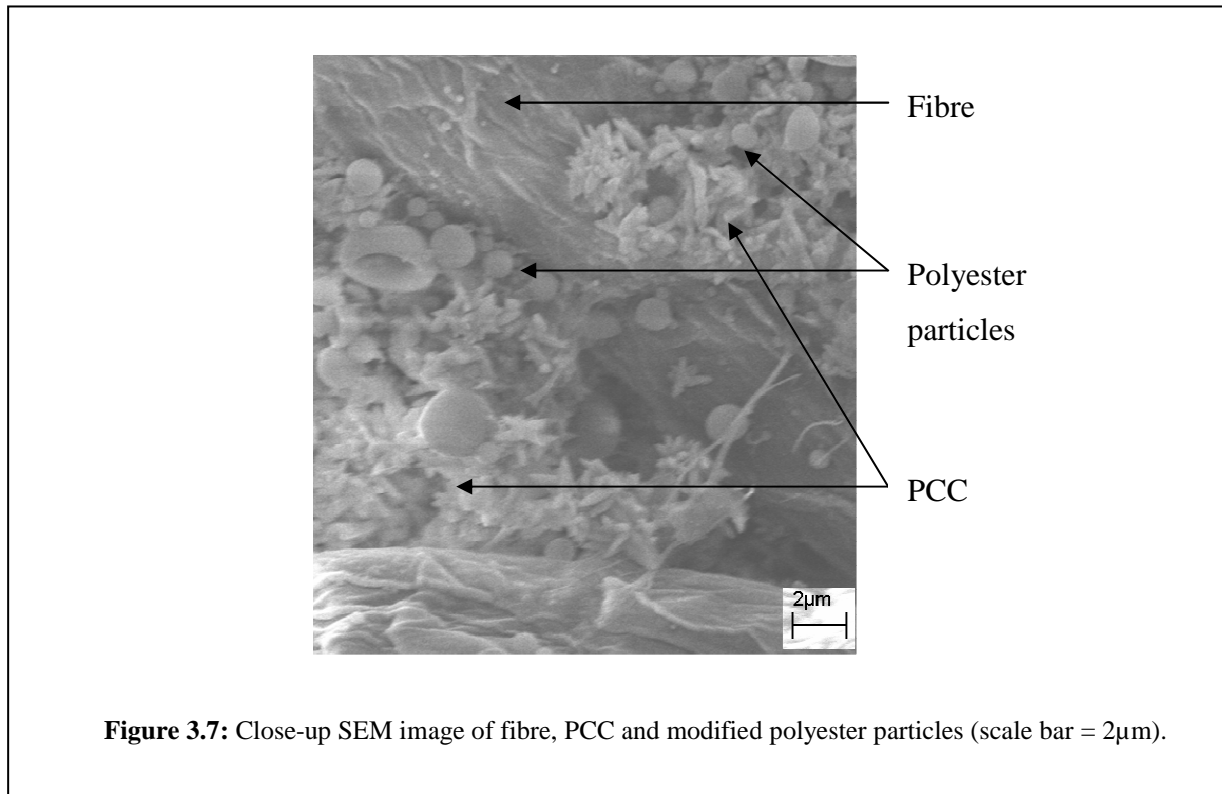
Figure 3.7: Close-up SEM image of fibre, PCC and modified polyester particles (scale bar = 2µm).

3.3 Modification of starch

3.3.1 Degree of substitution

In the modification of starch, the degree of substitution (DS) relates to the average number of sites per anhydroglucose unit (AGU) on which the hydroxide groups are replaced by substituent groups[7]. In other words, if one of the hydroxyl groups on each AGU is replaced with another functional group, the DS would be 1. A DS of 0.1 would therefore signify that 1 hydroxyl group out of every 10 AGU's is substituted and since there are only 3 hydroxyl groups available for modification per AGU, the maximum DS that can be obtained is 3. The formula for calculating the DS will vary depending on the molecular weight and functionality of the substituent group, thus, for sodium carboxymethyl starch:

$$DS_{th} = \frac{162 \times (n_{-CH_2COONa})}{m_s - (80 \times n_{-CH_2COONa})}$$

equation 3.1

where DS_{th} is the theoretical degree of substitution, 162 g/mol is the molar mass of an AGU, $n_{-CH2COONa}$ is the molar amount of sodium carboxymethyl groups attached to each AGU, m_s is the total mass of the dry starch sample and 80 g/mol is the nett increase in the mass of an AGU for each sodium carboxymethyl group substituted[8].

Reaction efficiency (RE) indicates the percentage of added reagent that has potentially reacted with the starch and is defined as:

$$RE = \frac{DS}{DS_{th}} \times 100(\%)$$
equation 3.2

with DS being the actual degree of substitution[9].

Commercially available modified starches normally have low DS values ranging up to about 0.1.

3.3.2 Experimental

3.3.2.1 Materials

Being readily available, extra pure maize starch (Acros, Cat: 24,073) was selected for the study and was dried before use. Sodium monochloroacetate (SMCA) (Fluka, Cat: 24,610), sodium hydroxide (NaOH) (Merck, Cat: SAAR5823160 EM), 32% hydrochloric acid (HCl) (Merck, Cat: SAAR3063040 LP) and 3-chloro-2-hydroxypropyl-trimethylammonium chloride (CHPTMAC) (Aldrich, Cat: 348,287) were used as received. Allyl bromide (Aldrich, Cat: A29585) was stored at 4 $^{\circ}$C. Acetone (Kimix, CP grade) and silver nitrate ($AgNO_3$) (N.T. Analytical Reagents, Cat: R2810) were used as received.

3.3.2.2 Carboxymethyl starch gel synthesis

Carboxymethyl starch with DS = 0.4 was prepared using the Williamson ether synthesis[10] (Figure 3.8A) and the laboratory set-up is shown in Figure 3.9. Maize starch (20 g) was loaded to a 250 ml round bottom flask fitted with a condenser and slurried in acetone (25 ml) at 300 rpm while 103.43 g of a 3.55 wt% aqueous NaOH solution was slowly added. This concentration was 10 wt% higher than the stoichiometric amount required for full conversion.

The introduction of NaOH significantly increased the cold water insoluble starch granules' affinity to water, inducing swelling and resulting in an increase in its particle size[11].

Figure 3.8: Modification of starch using Williamson ether synthesis with sodium monochloroacetate for anionic carboxymethyl starch (**A**), 3-chloro-2-hydroxypropyltrimethylammonium chloride for cationic starch (**B**), and allyl bromide for cross-linkable allyl starch (**C**).
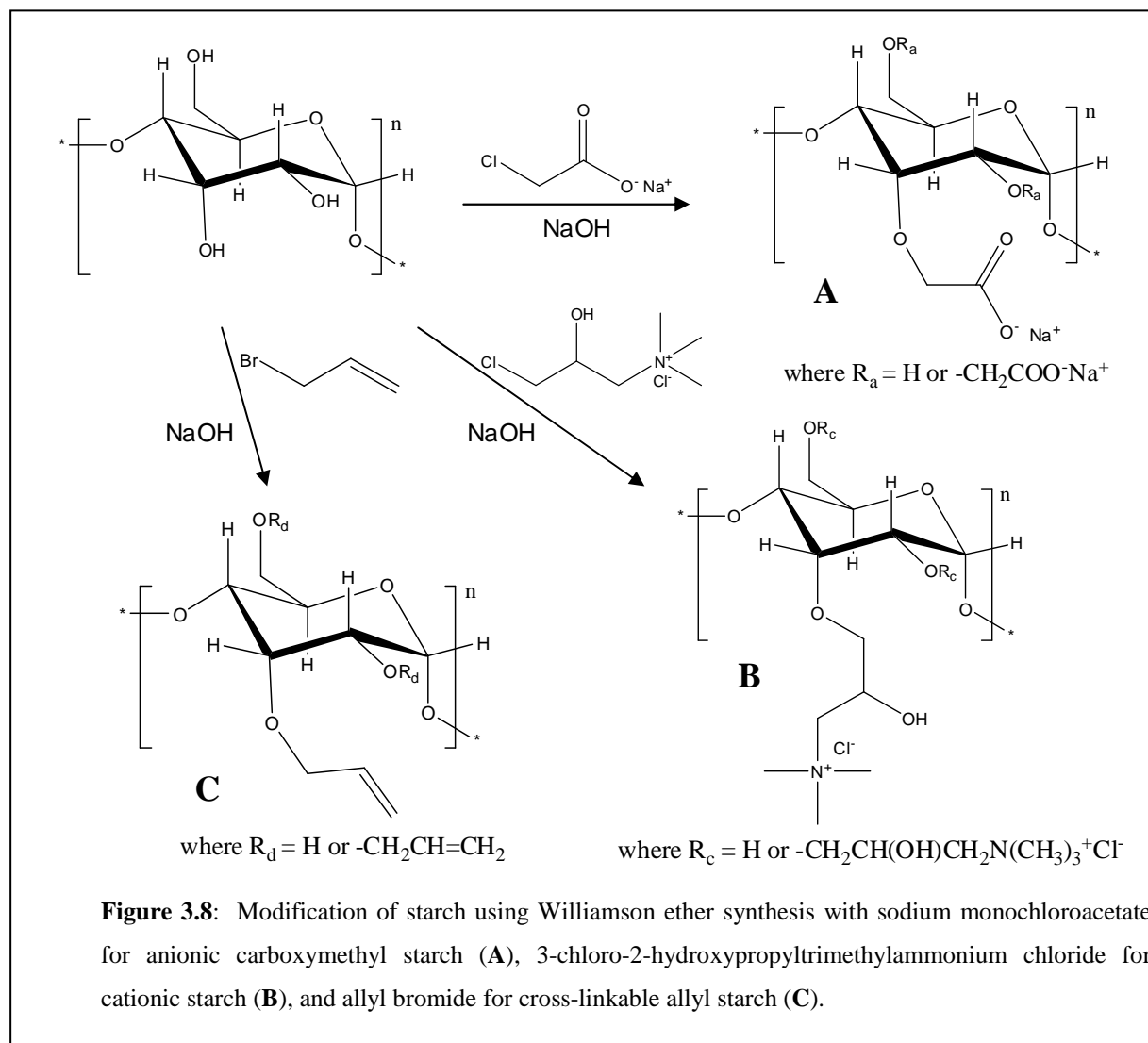
The mixture was heated to 55 ^{o}C in order to completely gel the starch after which 5.75 g SMCA was added to the flask. The reaction mixture was allowed to react for a period of 2 hours after which heating was removed and the reaction stopped by neutralising the pH with the addition of 4.16 g HCl. The mixture was allowed to cool overnight under continuous stirring at 200 rpm. Subsequently the modified starch was precipitated in 500 ml acetone, filtered off, and re-dissolved in DDI water. The precipitation and re-dissolving (washing) steps were repeated until no chloride was present, which could be detected by silver chloride (AgCl) precipitation when $AgNO_3$ was added to a small amount of the acetone filtrate.

Once the sample was essentially chloride free, the filtered starch was placed in a vacuum oven and dried overnight at 50 $^{\circ}$C. The dry sample was ground into a powder and stored in a sealed container.
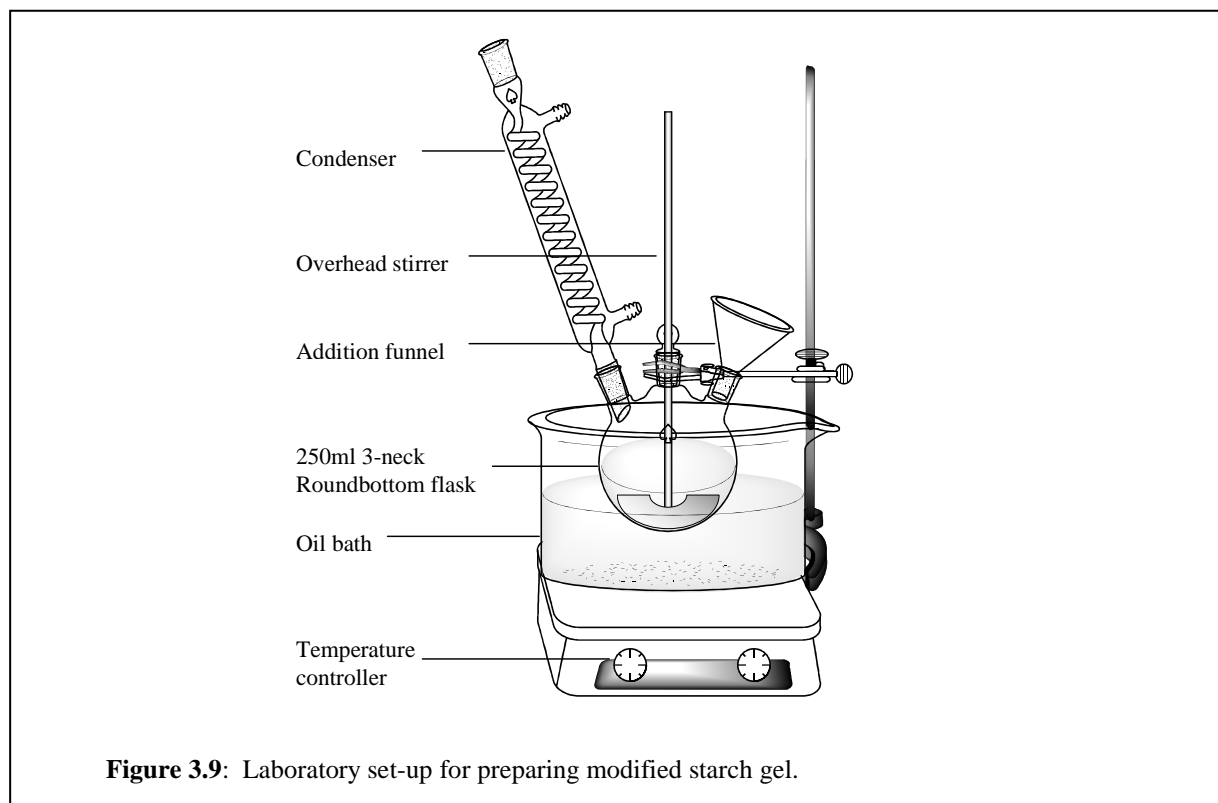
Figure 3.9: Laboratory set-up for preparing modified starch gel.

The carboxymethylation of starch occurs as a two-step reaction, the first being the alkalisation of starch to form an activated starch alkoxide[12]:

$$St\text{-}OH + NaOH \quad \rightarrow \quad St\text{-}O^-Na^+ + H_2O \tag{1}$$
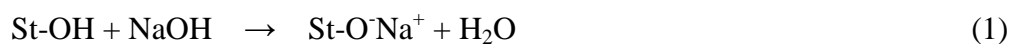
In the second step etherification occurs:

$$St\text{-}O^-Na^+ + ClCH_2COONa \quad \rightarrow \quad St\text{-}O\text{-}CH_2COONa + NaCl \tag{2}$$
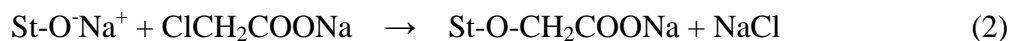
Additionally, an undesired side reaction of SMCA with NaOH can also take place in the presence of water, resulting in hydrolysis of SMCA to sodium glycolate:

$$NaOH + Cl\text{-}CH_2COONa \quad \overset{H_2O}{\rightarrow} \quad HO\text{-}CH_2COONa + NaCl \tag{3}$$
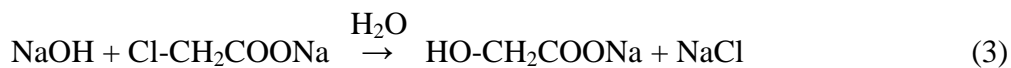
Formulations for preparing CMS solutions with various DS values appear in Table A1, Appendix A.

3.3.2.3 Cationic starch gel synthesis

Cationic modified starch (Figure 3.8B) with DS = 0.4 was prepared similar to the procedure for preparing CMS. After heating the maize starch, acetone, and aqueous NaOH solution to 55 $^{\circ}$C, 15.47 g 3-chloro-2-hydroxypropyltrimethylammonium chloride was added and neutralised with 3.9 g HCl solution after 2 hours reaction time. Formulations for preparing cationic starch solutions with different DS values appear in Table A2, Appendix A.

3.3.2.4 Allyl starch gel synthesis

Unsaturated allyl maize starch was prepared with DS = 0.4. Dry maize starch (20 g) was slurried at 300 rpm in 25 ml acetone while 73 g 4.1 wt% aqueous NaOH solution was added. The mixture was flushed with nitrogen and heated to 40 $^{\circ}$C. In the course of 15 minutes 6 g allyl bromide was added dropwise after which the reaction mixture was maintained at 55 $^{\circ}$C for 2 hours. The reaction was stopped by neutralising the pH with 2.9 g HCl solution. The modified starch was repeatedly precipitated and washed with DDI water until no trace of chloride ions was present. The precipitated clean starch was dissolved in 100 ml DDI water and vacuum distilled at 50 $^{\circ}$C to remove residual acetone from the system. The solids content of the solution was subsequently adjusted to 10 wt% and stored at 4 $^{\circ}$C. Although the allyl starch can be vacuum dried at low temperature, it was observed that it could not be dissolved again in water after extended storage times, possibly due to polymerisation occurring in the presence of air/light.

3.3.3 Analysis

3.3.3.1 NMR analysis

Both the experimental (actual) DS as well as distribution (where the substitution occurs) of substituents can be determined by ^{1}H-NMR and/or ^{13}C-NMR, as reported in literature[13, 14]. In this study ^{1}H-NMR was selected since it was shown to be the most convenient and reliable

method to calculate DS for both anionic and cationic starch as well as allyl starch. Due to the high viscosity of starch, it was found preferable to first hydrolyse the starch with acid prior to analysis.

Dry starch (10 mg) was weighed off in an NMR tube and dissolved in a deuterium oxide (D_2O) (Merck, Cat: 1.13366.0010) and deuterium chloride (DCl) (35 wt% in D_2O) (Aldrich, Cat: 543,047) solvent system in a ratio of 4:1 (v/v). As internal standard, 3-(trimethylsilyl)-1-propanesulfonic acid sodium salt (DSS) (Aldrich, Cat: 178,837) was used. The turbid viscous solution was heated to 70 ^{o}C in an oil bath and left overnight in order to allow sufficient time for starch hydrolysis to form a homogenous and completely clear aqueous solution.

Samples were submitted for ^{1}H-NMR on a Varian Anova NMR spectrometer at 600 MHz. Integration of spectra was carried out using MestReC 4.7.0.0 NMR data processing software.

3.3.4 Results and discussion

3.3.4.1 Pure maize starch

Proton peak assignments for the internal standard is shown in Figure 3.10 (DSS-1 = 0.0 ppm; DSS-2 = 0.62 ppm; DSS-3 = 1.75 ppm; DSS-4 = 2.91 ppm). The peaks related to $H_{2,3,4,5,6}$ on the ringbone of the AGU is detected between 2.9 and 3.9 ppm. The anomeric H_1 splits into 2 peaks, which relate to the α and β anomers of the anhydrous glucose produced by hydrolysis. $H_{1,\alpha}$ is detected at about 5.2 ppm and $H_{1,\beta}$ at 4.7 ppm. The area ratio of $H_{1,\alpha}/H_{1,\beta}$ is about 0.57 indicating that the β anomer is favourable for the unsubstituted AGU. The solvent signal (HOD) is normally detected at 4.8 ppm in a neutral solvent system, but fortunately it shifts to a lower field (ca. 5.5 ppm) and the shifting gap depends on the pH (i.e. the DCl concentration), which makes it completely distinguishable with peaks of the anomeric H_1 peaks.

It should also be noted that the area ratio of $A_{H2,3,4,5,6}/A_{H1}$ is 6.1, which agrees well with the theoretical value of 6 (the number of hydrogen atoms in an AGU).

3.3.4.2 Carboxymethyl starch

In Figure 3.11 it is observed that both H_1 anomers split into 2 peaks, and this is a result due to carboxymethyl substitution at the C_2 position[15]. Therefore H_1 will split into α-C_2-

unsubstituted, H(1α,u), α-C$_2$-substituted, H(1α,s), β-C$_2$-unsubstituted, H(1β,u), and β-C$_2$-substituted, H(1β,s), peaks.
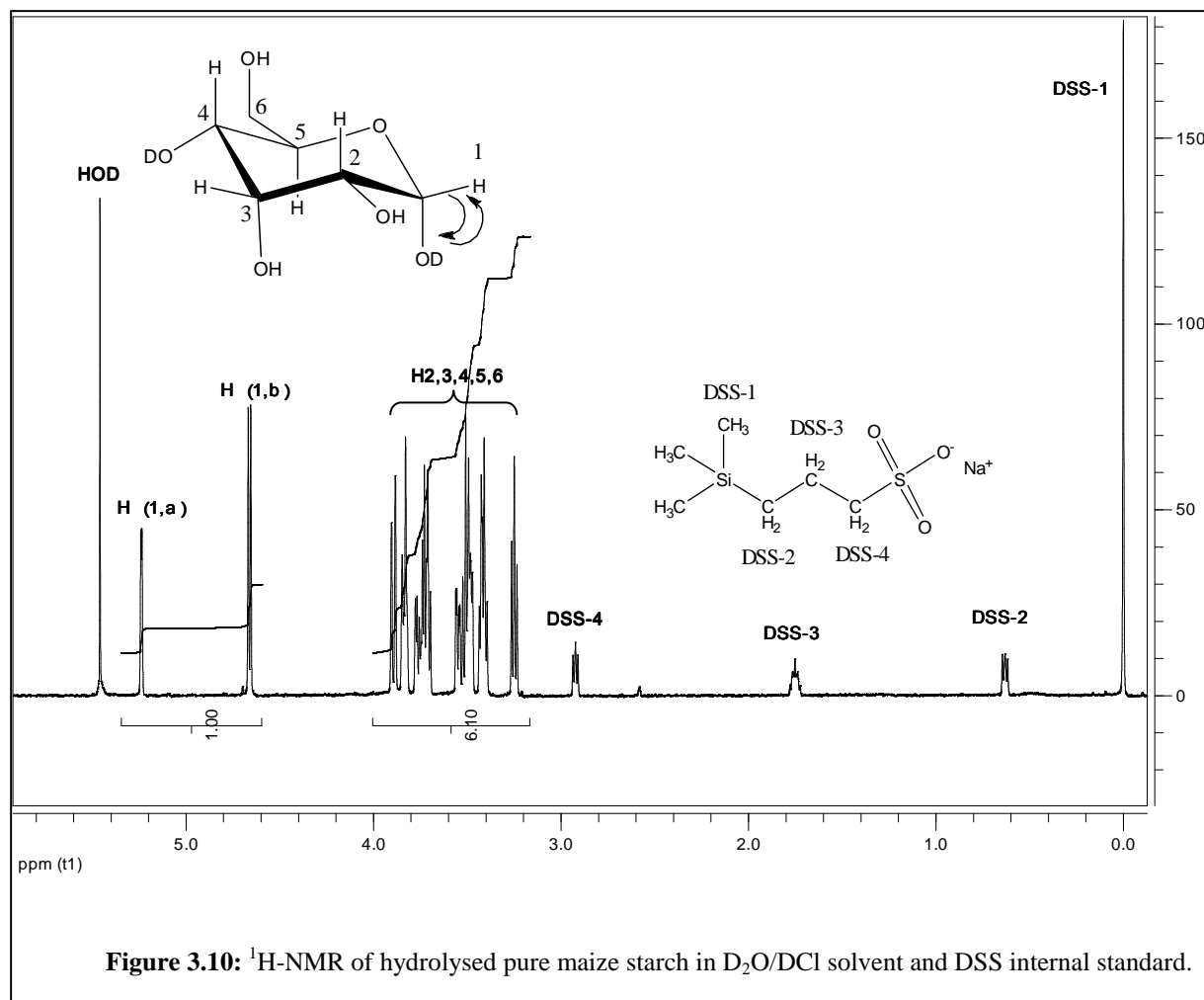
Figure 3.10: ^{1}H-NMR of hydrolysed pure maize starch in D$_2$O/DCl solvent and DSS internal standard.

The carboxymethyl substituted groups (H$_a$) is detected between 4.25 ppm and 4.50 ppm. As shown in the figure H$_a$ splits into four main peaks, which relates to the substitution at positions C$_2$, C$_3$, and C$_6$ on the AGU backbone, where C$_2$ splits into two peaks due to the α- and β-anomers at position C$_1$.

The experimental degree of substitution (DS) can be calculated by integrating the areas (A$_i$) of the individual position (i=1,2,3,6) peaks and using the following equation:

$$DS_{anionic} = [\frac{A_{Ha-2a} + A_{Ha-2b} + A_{Ha-3} + A_{Ha-6}}{2(A_{H-(1a,s)} + A_{H-(1a,u)} + A_{H-(1b,s)} + A_{H-(1b,u)})}] \qquad \text{equation 3.3}$$

63

The DS calculated by NMR using the technique above will be compared to conventional back titration techniques in the following chapter.

Figure 3.11: ^{1}H-NMR of hydrolysed carboxymethyl starch (DS = 0.4) in D_2O/DCl solvent.
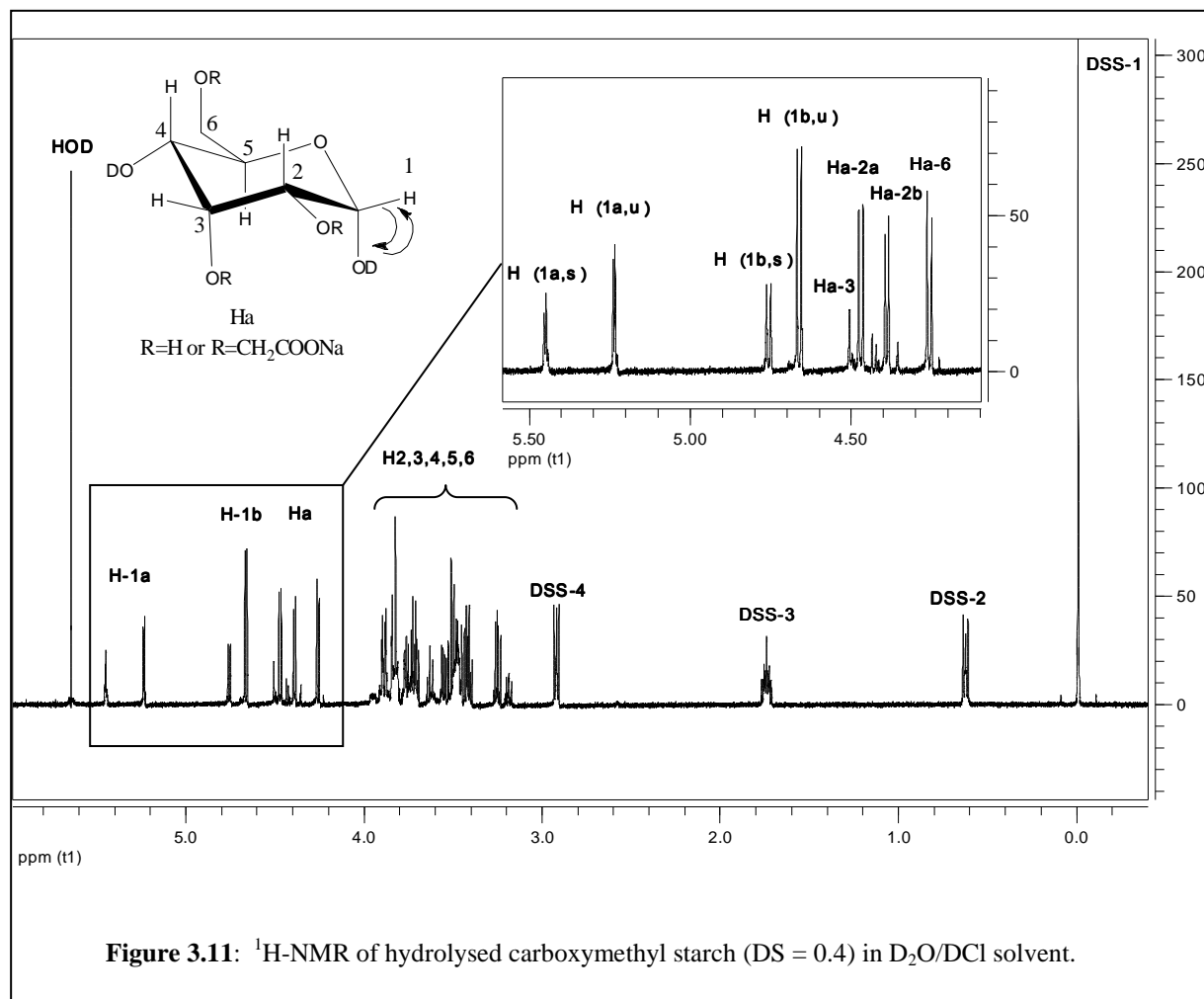
3.3.4.3 Cationic starch

Similar to carboxymethyl starch, the NMR spectra of cationic starch (2-hydroxy-3-trimethylammonium chloride propyl ether) substitution at position C_2 will shift the unsubstituted H_1 peak to a lower field (Figure 3.12), although the signal strength appears to be significantly lower. The CH peak (H_b) at 4.44 ppm as well as the CH_3 peak (H_d) at 3.23 ppm of the cationic substituent group can clearly be distinguished, but overlapping of the CH_2 peaks (H_a and H_c) and $H_{2,3,4,5,6}$ peaks occur (between 3.23 and 3.90 ppm). This complicates calculating the DS using these areas. However, DS can also be calculated from the areas under the splitted H_1 peaks and H_b using the following equation:

$$DS_{cationic} = \frac{A_{Hb}}{A_{H-(1a,s)} + A_{H-(1a,u)} + A_{H-(1b,s)} + A_{H-(1b,u)}}$$

equation 3.4

Figure 3.12: ^{1}H-NMR of hydrolysed cationic modified starch (DS = 0.4) in D_2O/DCl solvent.
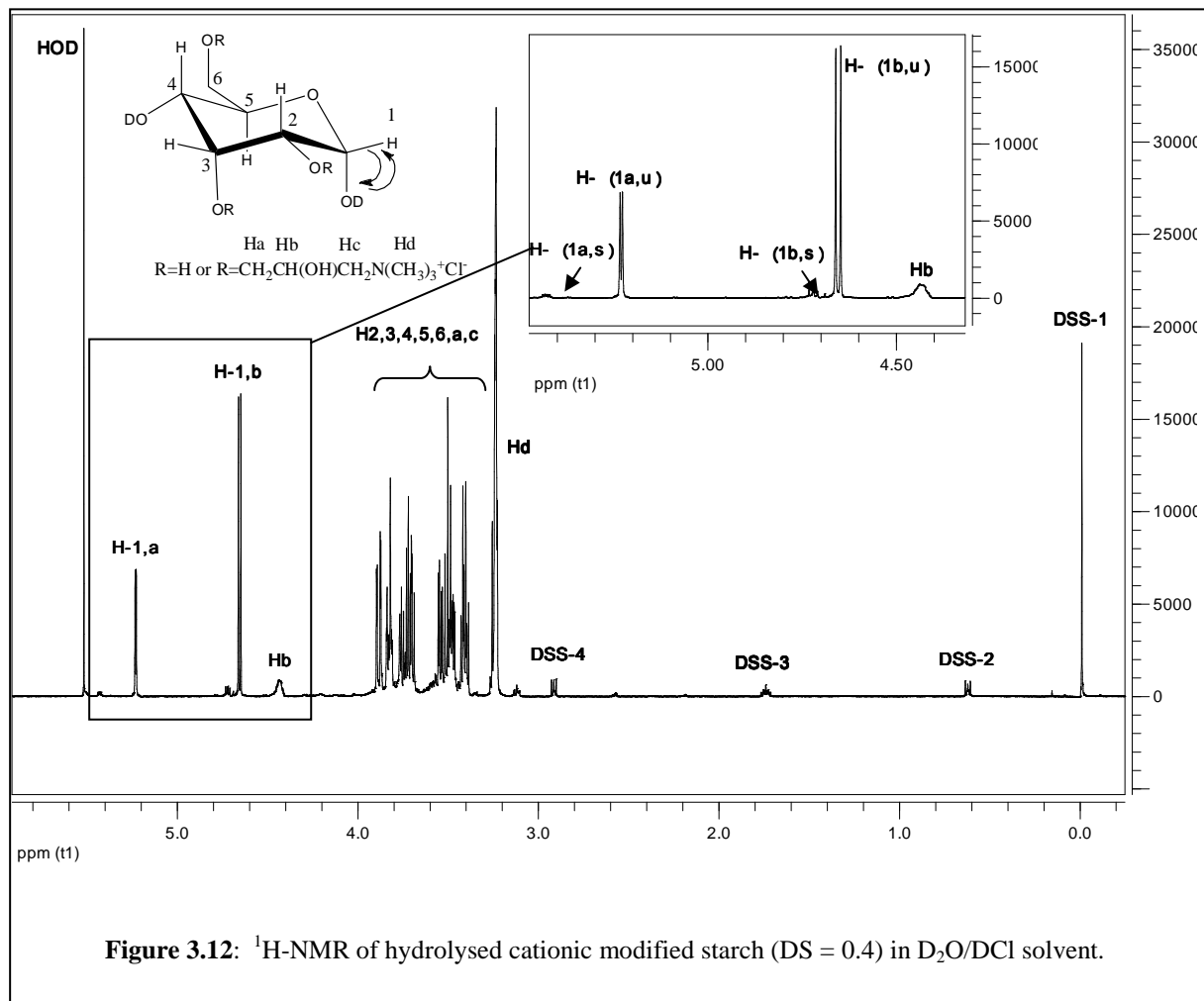
3.3.4.4 Allyl starch

In the allyl starch spectrum (Figure 3.13) the H_1 peaks overlap with the CH_2 peak on the allyl group double bond (H_c) making it difficult to clearly distinguish the separate peaks between 5.29 ppm and 5.64 ppm. Another peak is detected at a lower field (5.98 ppm) and this is assigned to the CH_2 group on the allyl group double bond (H_b). Since the solvent peak (HOD) is normally detected at 5.50 ppm, which will be in the same region as the H_1 and H_c peaks, the amount of DCl added had to be lowered in order to move the peak to a higher field (4.8 ppm). The lower amount of DCl also caused poorer separation of the $H_{2,3,4,5,6}$ peaks as

65

can be seen from the figure (3.40 – 4.30 ppm), although this will not effect DS calculation results. It only indicates that the modified starch probably did not hydrolyse completely. This is also the reason why separate peaks for the H_1 anomers (substituted and unsubstituted) can not be clearly distinguished in the figure. The CH_2 peak of the allyl moiety adjacent to the double bond (H_a) overlaps with the peaks $H_{2,3,4,5,6}$ in the 3.40 – 4.30 ppm region.

Figure 3.13: ^{1}H-NMR of hydrolysed allyl modified starch (DS = 0.4) in D_2O/DCl solvent.
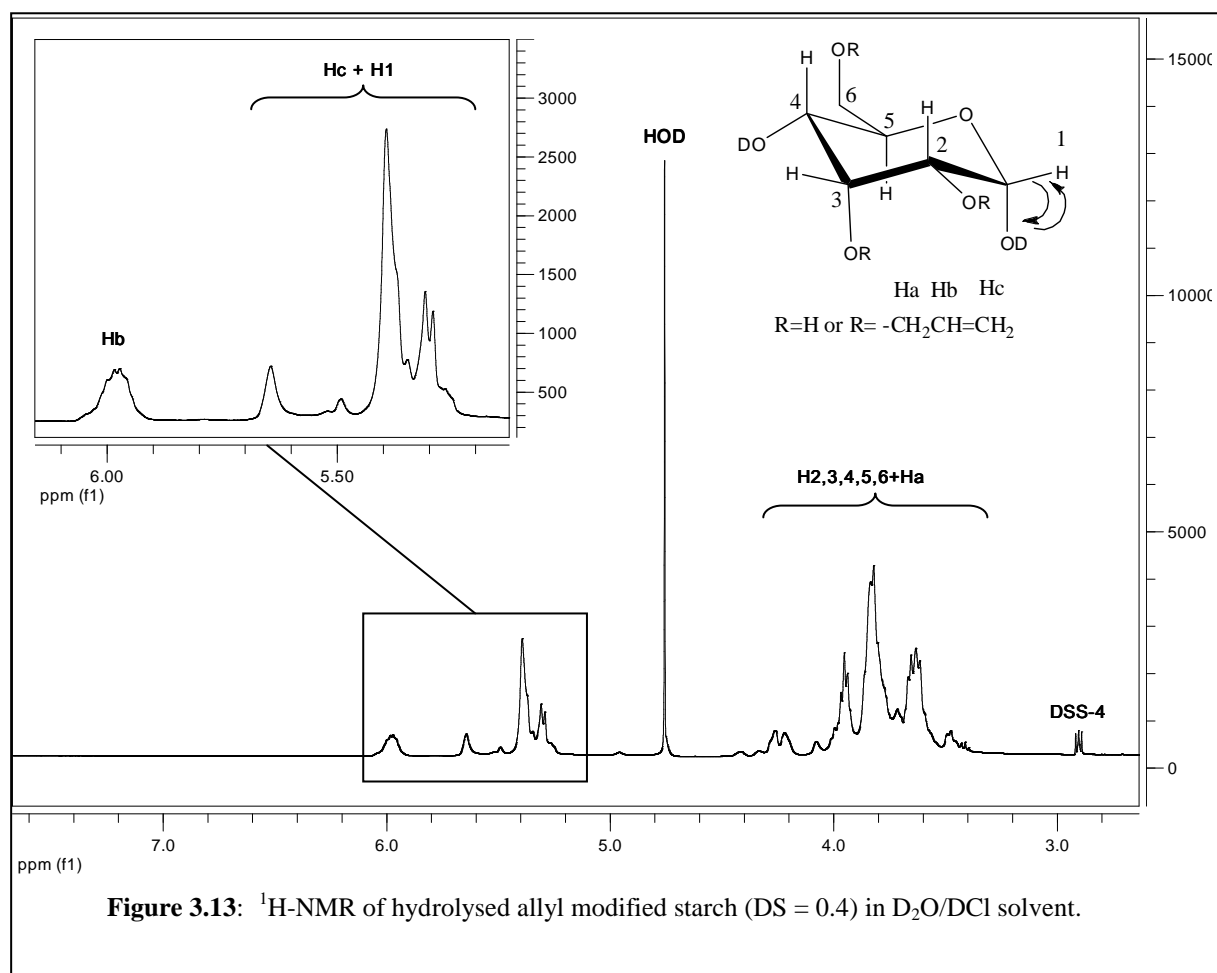
The DS of allyl groups can therefore be calculated using any one of the two following equations:

$$DS_{allyl} = \frac{1}{[(\frac{A_{Hc+H1}}{A_{Hb}}) - 2]}$$

equation 3.5

66

$$OR \quad DS_{allyl} = \frac{6}{[(\frac{A_{H1,2,3,4,5,6+Ha}}{A_{Hb}}) - 2]} \qquad\qquad \text{equation 3.6}$$

Both equations can be used to test if the DS is comparable.

3.3.4.5 Modification over reaction time

A study was done to see how the experimental DS would increase as a function of reaction time. Experiments were conducted where each of the anionic, cationic, as well as allyl modified maize starch with theoretical DS of 0.4 was allowed to react for a total period of 30 hours. Samples were taken every hour for the first 5 hours, after 10 hours, and then again every 10 hours. Each sample was neutralised after extraction to stop the substitution reaction and washed several times in order to purify it. The DS was calculated using ^{1}H-NMR and plotted in Figure 3.14.

Figure 3.14: Degree of substitution and reaction efficiency of anionic, cationic, and allyl modified starch (DS = 0.4) over time.
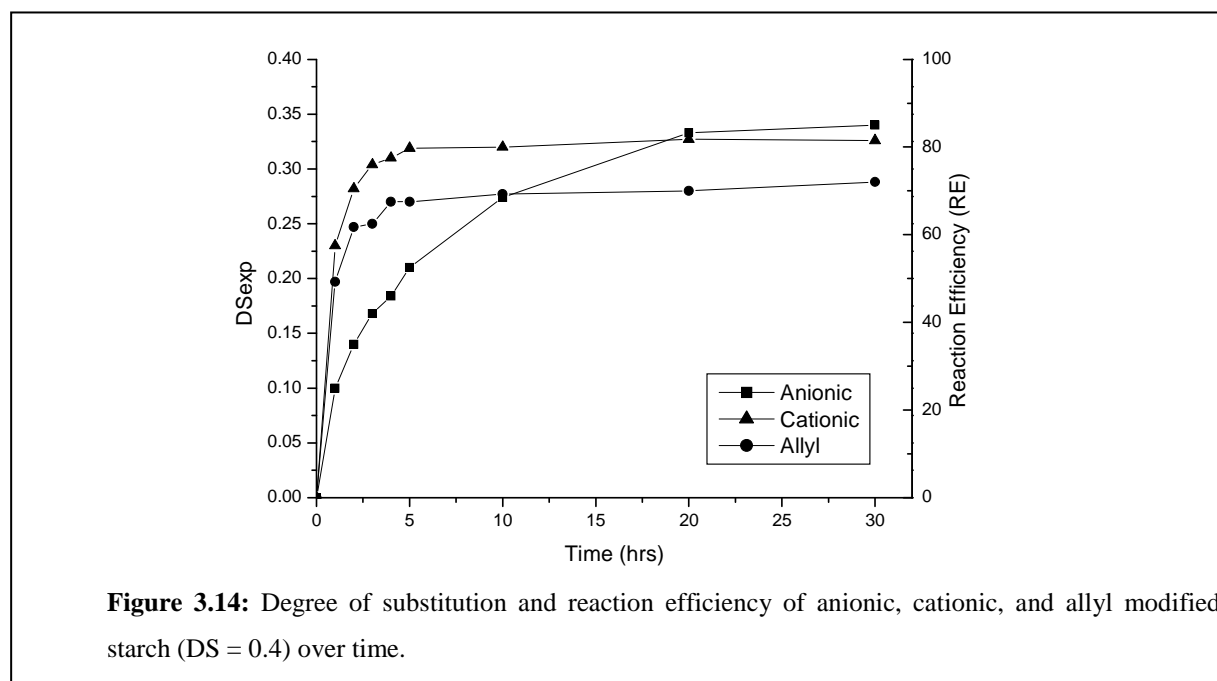
For both the cationic and allyl modified starch, the DS reached its maximum DS within the first 5 hours. The cationic starch achieved the highest DS relatively with a reaction efficiency (RE) of about 80%, whereas allyl starch reached an RE of just above 70%.

The substitution reaction of the anionic starch proceeded significantly slower with only 50% RE achieved after a period of 5 hours. However, after a period of 30 hours a RE of about 82% was reached, which was a little higher than that achieved with the cationic and allyl modified starch. The hydrophilic carboxymethyl groups increases the swellablility of the starch as it is attaches during reaction, causing a much higher viscosity product to form. This restricts the mobility of unreacted carboxymethyl groups to travel through the solution where available sites are for further substitution and this would explain the lower reaction rate[15].

3.4 Interaction of anionic and cationic modified starch with fillers and fibres: a fluorescence study

3.4.1 Introduction

Fluorescence microscopy is a technique for examining fluorescent substances, offering high sensitivity and specificity[16]. Many substances are naturally fluorescent, while others can be made fluorescent. Under the microscope the specimen is illuminated with light of a short wavelength, such as ultraviolet or blue light. Part of this light is absorbed by the sample and re-emitted as fluorescence. The re-emitted light has a longer wavelength than that of the illuminated light. The light used for excitation is filtered out by a barrier filter placed between the specimen and the eye, making only the fluorescent light visible. The fluorescent object is therefore seen and captured as a bright image against a dark background. Introducing fluorescent groups onto both anionic and cationic modified starch, would be very useful in observing where these starches would be present after introducing them to both paper fibres and PCC filler. A benefit of fluorescent markers is that a very low concentration attachment onto polymers, such as starch, is required to allow adequate detection.

Fluorescein is a widely used fluorescence agent, but on its own not able to react with starch. However, fluorescein isothiocyanate (FITC) will react with the hydroxyl groups of starch in methyl sulphoxide solvent at elevated temperatures[17]. Since FITC is very expensive, it was decided to synthesise it from aminofluorescein.

3.4.2 Experimental

3.4.2.1 Materials

5-Aminofluorescein (Fluka, Cat: 07,980) was stored in a cool dark place in order to avoid fluorescent intensity degradation in the presence of heat and light. Acetone (Kimix, AR grade) and pyridine (Merck, Cat: SAAR5124060 LC) were distilled and dried. Thiophosgene (Aldrich, Cat: 115,150), dimethyl sulfoxide (DMSO) (Merck, Cat: SAAR1865000 LP), lithium chloride (LiCl) (Aldrich, Cat: 213,233), *N*,*N*-dimethylacetamide (DMAc) (Aldrich, Cat: 185,884), and dibutyltin dilaurate (DBTD) (Aldrich, Cat: 291,234) was used as received. Anionic and cationic starch (DS = 0.4) was prepared as described in Sections 3.3.2.2 and 3.3.2.3 and oven dried before use. Fibre sheets and PCC filler solutions (22.5 wt%) were supplied by Mondi.

3.4.2.2 Synthesis of fluorescein isothiocyanate

Synthesis of FITC was performed using a modification of the procedure used by Riggs *et al.*[18] and McKinney *et al.*[19] A solution of 7.8 g thiophosgene in dry acetone (80 ml) was prepared in a 250 ml roundbottom flask and placed under continuous magnetic stirring. Another solution of 1.71 g 5-aminofluorescein in dry acetone (60 ml) was prepared and added dropwise to the thiogene solution over a period of 2 hours under a nitrogen atmosphere.
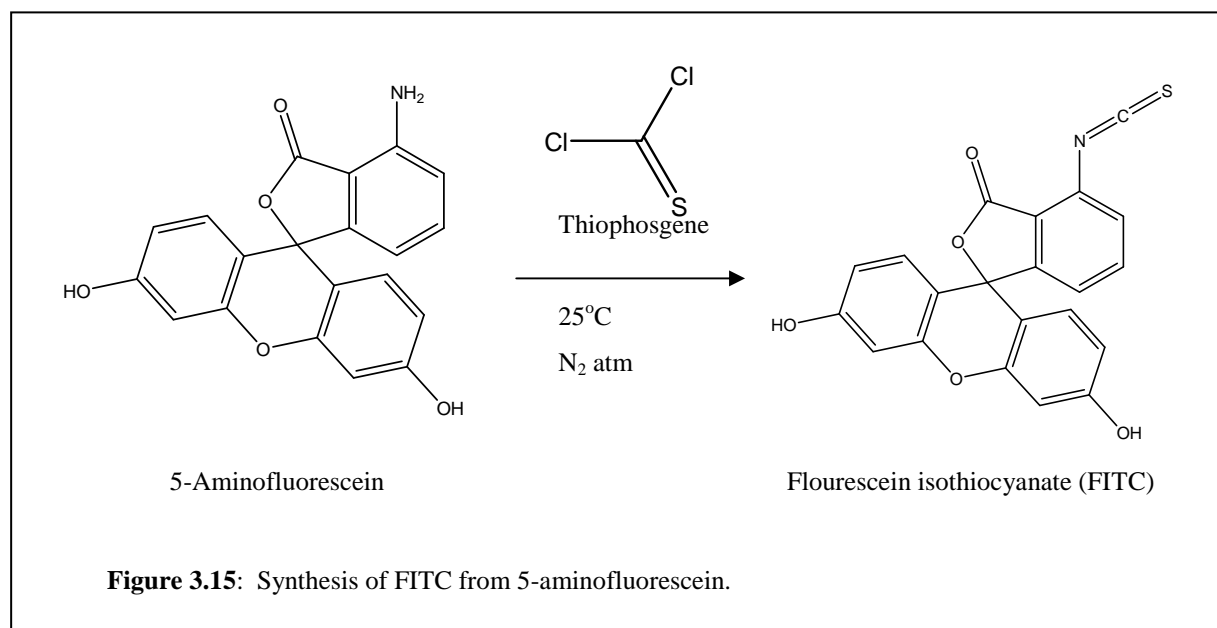
Figure 3.15: Synthesis of FITC from 5-aminofluorescein.

The mixture was stirred for a further 2.5 hours after which the acetone-insoluble reaction mixture was collected on a sintered glass filter and washed with 250 ml dry acetone. The filtered fluorescein isothiocyanate was vacuum dried overnight to fine powder. The reaction mechanism is presented in Figure 3.15.

3.4.2.3 Preparation of FITC-carboxymethyl and FITC-cationic starch

Attachment of FITC to the modified starch was conducted using the method described by De Belder and Granath[17]. Although starch will dissolve in DMSO, it is extremely difficult to dissolve carboxymethyl starch in a hydrophobic solvent, due to the inherent hydrophilic nature of the carboxymethyl groups. A significantly stronger solvent system was therefore used. Dry carboxymethyl starch and cationic starch (1.1 g) were individually added to 50 ml DMAc solvent treated with 0.3 g LiCl and the solutions were heated to 95 $^{\circ}$C under continuous stirring until the starch was completely dissolved. The mixtures were vacuum distilled to remove excess solvent and all traces of water present in the system. Another 50 ml DMAc was added and once again vacuum distilled until the final volume was around 30 ml. About 10 drops pyridine was added followed by 0.8g FITC. This amount corresponds to a DS of about 0.001. The catalyst, dibutyltin dilaurate (DBTD) (40 mg) was added and the reaction mixtures were left stirring for 2 hours at 95 $^{\circ}$C under a nitrogen blanket. Heating was removed and the mixtures left stirring overnight. The reaction mechanism is shown in Figure 3.16.

Figure 3.16: Fluorescein isothiocyanate (FITC) attachment onto anionic/cationic starch.

70
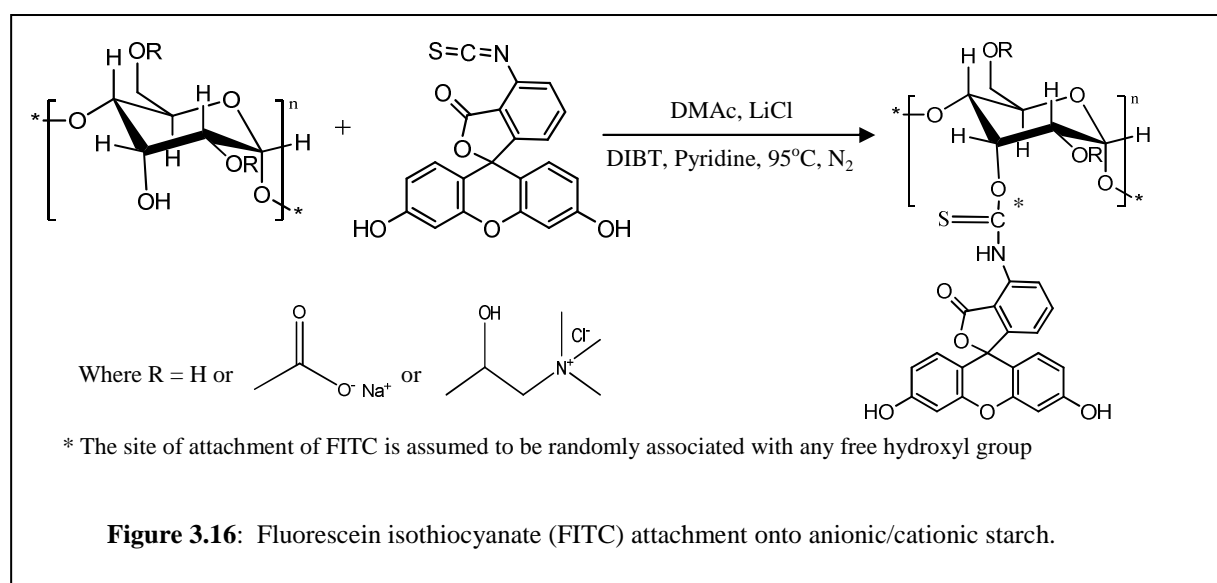
The ionic modified FITC-starches were repeatedly (3 times) precipitated in ethanol and redissolved in DDI water to remove excess reagents and the final precipitate filtered off and dried in a cool vacuum oven overnight. The modified starches were stored at 4 ^{o}C in a dark environment until further use.

3.4.3 Analysis

3.4.3.1 Fourier transform infrared (FTIR) spectroscopy

5-Aminofluorescein and FITC samples were submitted for FTIR analysis and the spectra compared to verify that the isothiocyanate group was present on the FITC. Analysis was conducted using a Perkin Elmer Paragon 1000 FTIR spectrometer equipped with a photoacoustic MTEC 300 cell.

3.4.3.2 Fluorescence spectroscopy

Cationic and anionic modified FITC-starch samples were analysed to verify if the FITC attached onto the starch and if so, what the fluorescence intensity was for each sample. Furthermore it was necessary to determine exactly what the excitation and emission wavelengths for each sample were. Fluorescence spectroscopy was performed using a Perkin Elmer LS 55 Luminescence Spectrometer and samples were prepared by dissolving very diluted samples (ca. 0.01 wt%) of the modified starches in DDI water and placing it in a quartz cuvette.

3.4.3.3 Fluorescence microscopy

Samples were observed on an Olympus Cell^R system attached to an IX-81 inverted fluorescence microscope equipped with an F-view-II cooled CCD camera (Soft Imaging Systems). Using a Xenon-Arc burner (Olympus Biosystems GMBH) as light source, samples can be seen under normal optical light or can be excited using 360 nm, 472 nm, and/or 572 nm excitation filter (Chroma). Emissions were collected using an UBG triple-bandpass emission filter cube (Chroma).

Image quality was found to be significantly better if the samples were wet. Dried samples were highly condensed making it difficult to observe the exact location of the modified starch on the fibre and filler surfaces. The following samples were prepared:

1. Pure PCC filler (control sample)
2. Pure fibre (control sample)
3. Anionic FITC-starch + PCC

    - 1 ml of a 0.5 wt% aqueous anionic FITC-starch solution was added to 2.5 ml of PCC (22.5 wt%) and thoroughly mixed for 5 min. DDI water (50 ml) was added and the sample centrifuged. This was done 3 times to ensure all excess or unabsorbed starch was removed from the system.

4. Anionic FITC-starch + Fibre

    - 1 ml of a 0.5 wt% aqueous anionic FITC-starch solution was added to 10 g of a 2 wt% fibre solution and mixed for 5 min. The sample washed 3 times with 50 ml DDI water and centrifuged.

5. Anionic FITC-starch + Fibre + PCC

    - 5g fibre solution (2 wt%), 0.4g PCC solution (22.5 wt%), and 0.5g anionic FITC-starch solution (0.5 wt%) were thoroughly mixed for 5 min, after which it was washed and centrifuged three times with 50 ml DDI water.

6. Cationic FITC-starch + PCC

    - prepared as in 3.

7. Cationic FITC-starch + Fibre

    - prepared as in 4.

8. Cationic FITC-starch + Fibre + PCC

    - prepared as in 5.

3.4.4 Results and discussion

Figure 3.17 shows an FTIR comparison between 5-aminofluorescein and the synthesised FITC and the latter clearly shows a strong isothiocyanate absorption peak between 1900 to 2200 cm^{-1}. This is in agreement to reported literature[19] and shows that FITC was successfully synthesised.

72
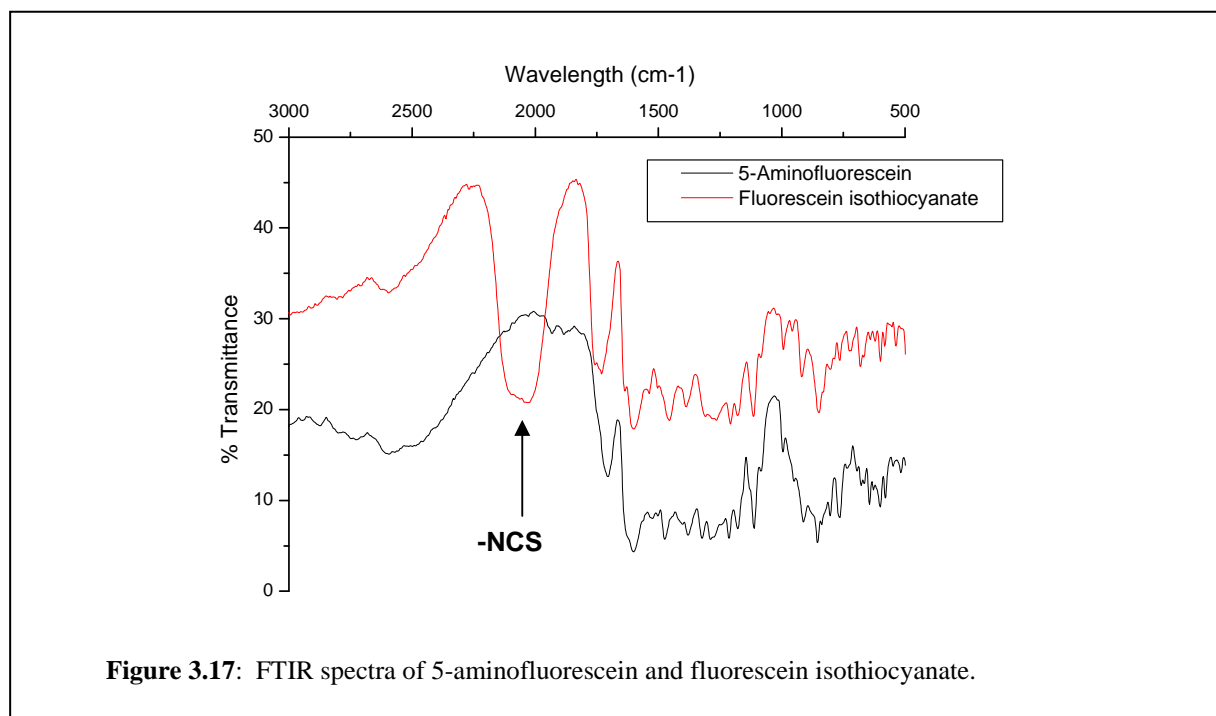
Figure 3.17: FTIR spectra of 5-aminofluorescein and fluorescein isothiocyanate.

Figures 3.18 and 3.19 show fluorescence spectra of the anionic and cationic FITC-starches, respectively. Each spectrum has a bimodal intensity distribution over the wavelength range and the first peak presents the excitation spectrum, in other words the wavelength of light used for exciting the fluorescent moiety. The second peak, the emission spectrum, presents the wavelength at which the excitation light is emitted or fluoresces. The excitation wavelength was varied from 200 – 800 nm to determine where fluorescence occurs and at which wavelength maximum fluorescence is detected.

The most intense fluorescence for the anionic and cationic FITC-starch was detected at excitation wavelengths of 490 nm and 500 nm respectively as can be seen from the excitation peaks in the graphs. This corresponds very well with the excitation wavelength of pure fluorescein which is 490 nm according to literature[20]. Maximum fluorescence for both samples occurs between 500 nm and 520 nm which fall within the green spectral area. The spectra further indicate that the cationic FITC-starch fluoresces with a much higher intensity relative to the anionic FITC-starch. This is most probably due to a lower FITC substitution degree due to the poor solubility of the anionic starch in solvent (DMAc) during FITC-starch synthesis.

73
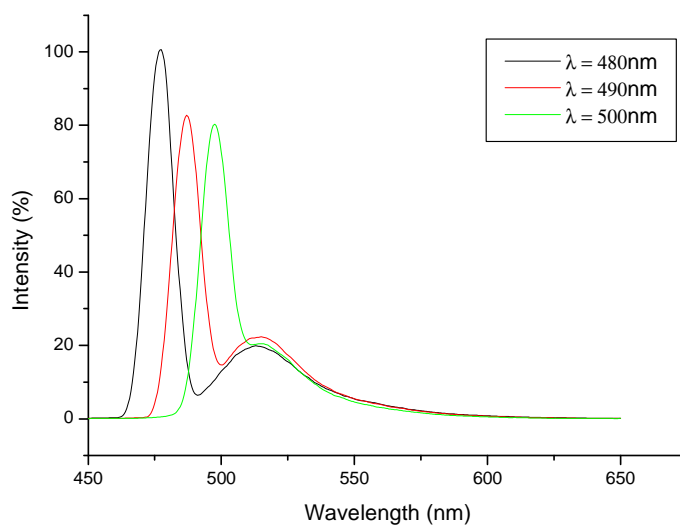
Figure 3.18: Fluorescence spectra of anionic FITC-starch showing excitation and emission intensity at different excitation wavelengths.
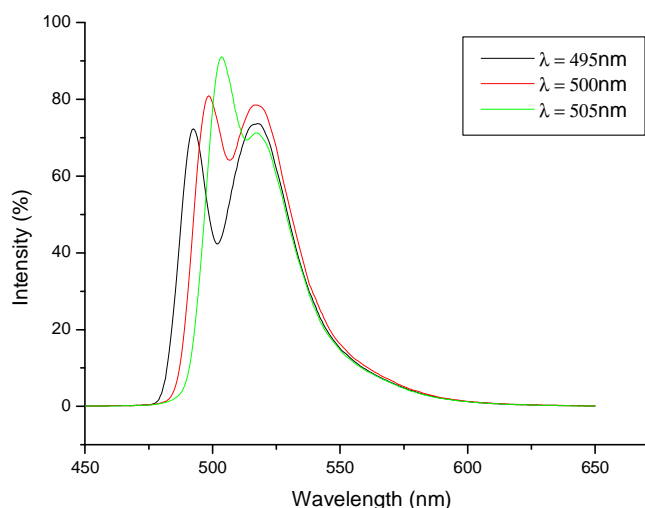
Figure 3.19: Fluorescence spectra of cationic FITC-starch showing excitation and emission intensity at different excitation wavelengths.

Figure 3.20 presents the fluorescence microscope images of PCC treated with the anionic and cationic FITC-starches and the presence of the starch can clearly be observed on the surfaces of the crystals. The reference sample of pure PCC (without starch) was completely black, abandoning the possibility that the filler might auto-fluoresce. Since the overall surface charge of PCC is positive, it was surprising to find that cationic starch also attaches to its surface, but since the potential determining ions (PDI) of calcium carbonate is a calco-

carbonic equilibration system[21] consisting of Ca^{2+} as well as CO_3^{2-} ions, cationic starch will also interact with the CO_3^{2-} ions.

Figure 3.20: Fluorescence microscope images of PCC treated with anionic FITC-starch (**A**) and cationic FITC-starch (**B**).

Figure 3.21: Microscope images of fibres treated with cationic FITC-starch (**A**) and anionic FITC-starch (**B**) [1 - optical microscope images, 2 – fluorescence images, 3 – overlay images].
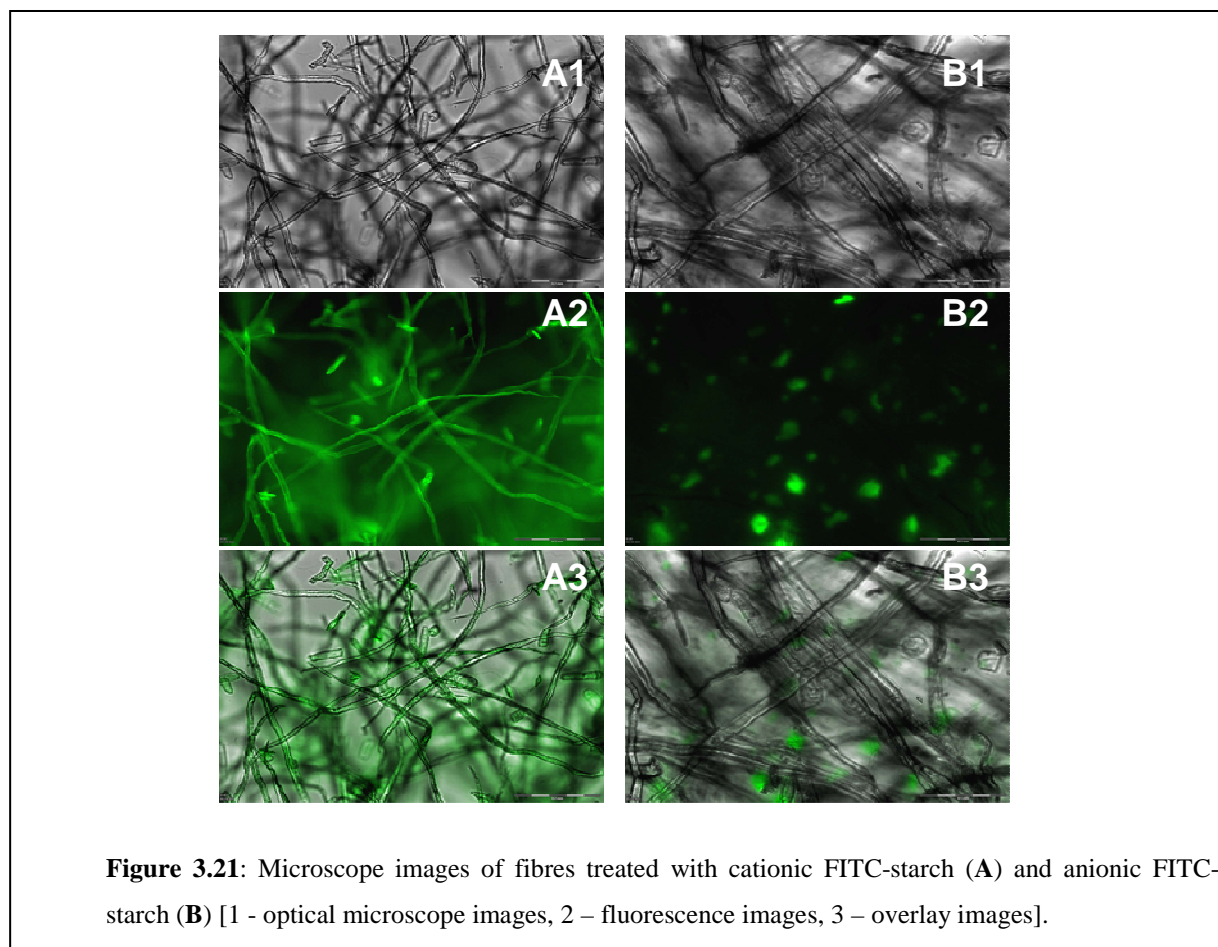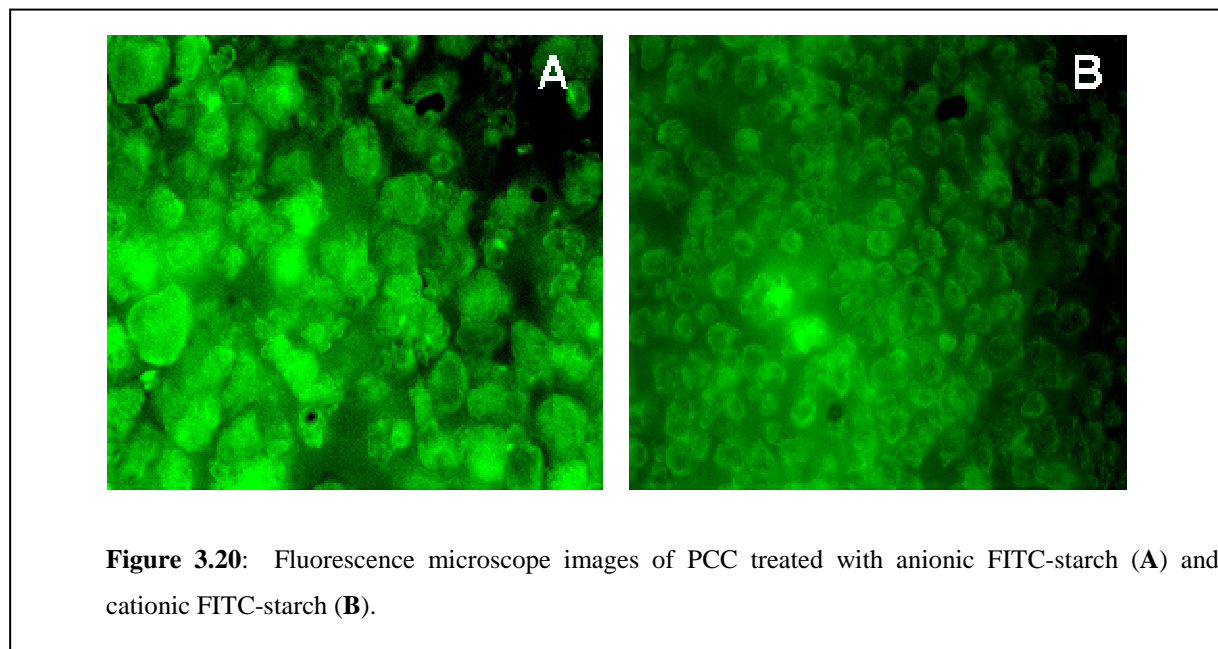
In Figure 3.21 images are shown of fibres treated with both modified starches. Optical microscope images were first taken of the fibres, followed by fluorescence microscope images of the same area. These images were then overlayed to see exactly where fluorescence is located. In Figure 3.21 (A2 and A3) fluorescence of cationic FITC-starch is clearly visible on the surface of the fibres verifying ionic interaction of cationic starch with the anionic fibres. In the case of the anionic FITC-starch some fluorescence can be detected, but looking at the overlay image (Figure 3.21 B3) it is evident that it is not present on the surface of the fibres. This could be as a result of interactions with ionic contaminants that were present in the system.

Figure 3.22: High magnification microscope images of two fibres (**A** and **B**) treated with cationic FITC starch [1-optical microscope images, 2 – fluorescence images, 3 – overlay images].
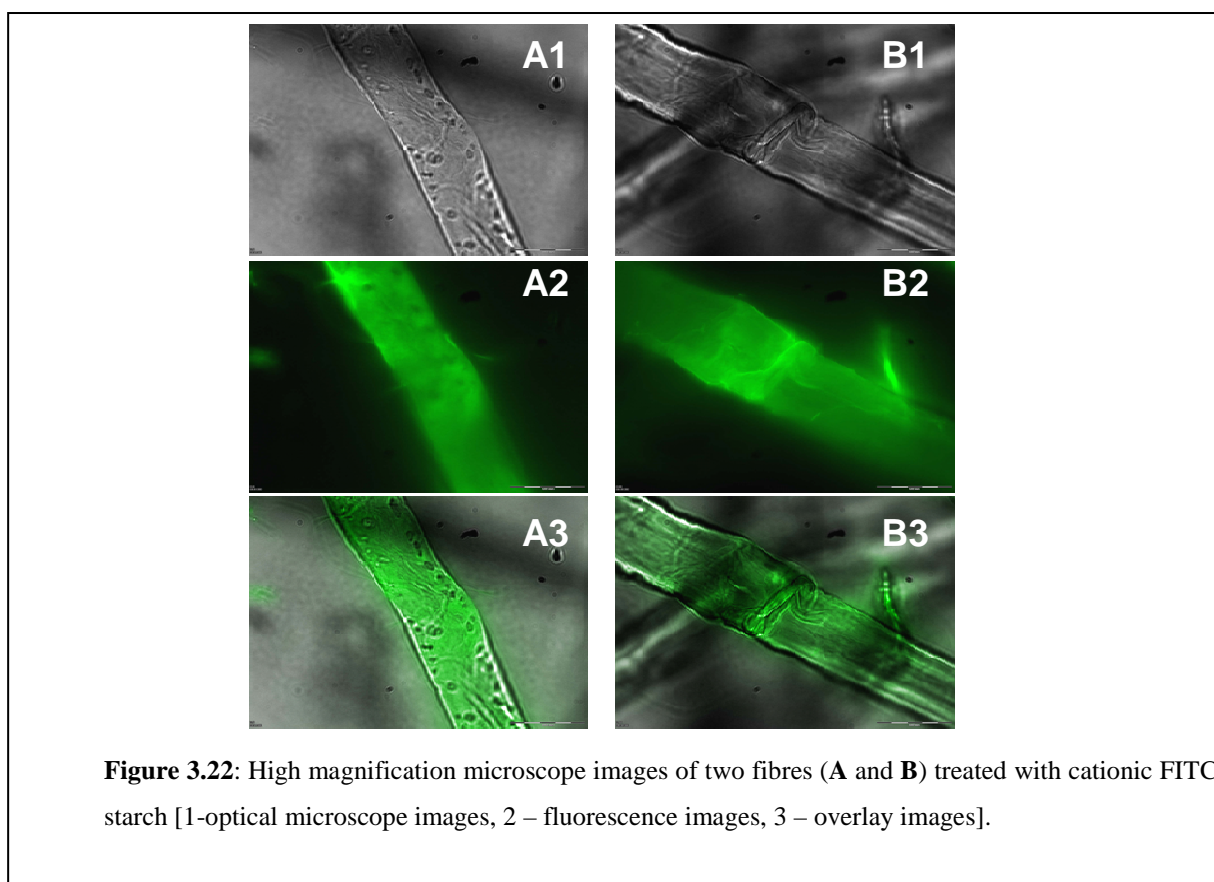
Figure 3.22 presents higher magnification images of fibres treated with the cationic FITC-starch and it is interesting to observe the change in fluorescence intensity along the fibre surface. Brighter areas indicate concentrated areas of adsorbed starch and correspond to areas where the fibre is damaged or beaten. This implies that anionic moieties are more prevalent within the inner cell walls of the fibres. It can therefore be concluded that increased

disintegration of paper fibres will expose more anionic moieties, allowing higher cationic starch retention, which should be beneficial in improving the mechanical properties of paper.

Figure 3.23 shows images where the two modified starches were combined with both the PCC and fibre. Once again the anionic starch is only detected on the PCC surface and not on the fibre. It is also observed that the anionic starch severely flocculated the PCC (Figure 3.23 A2). Cationic starch is once again observed on both surfaces (Figure 3.23 B).

Figure 3.23: Microscope images of anionic FITC-starch, PCC, and fibre (**A**), and cationic FITC-starch, PPC, and fibre (**B**) [1 – optical microscope images, 2 – fluorescence images, 3 – overlay images].
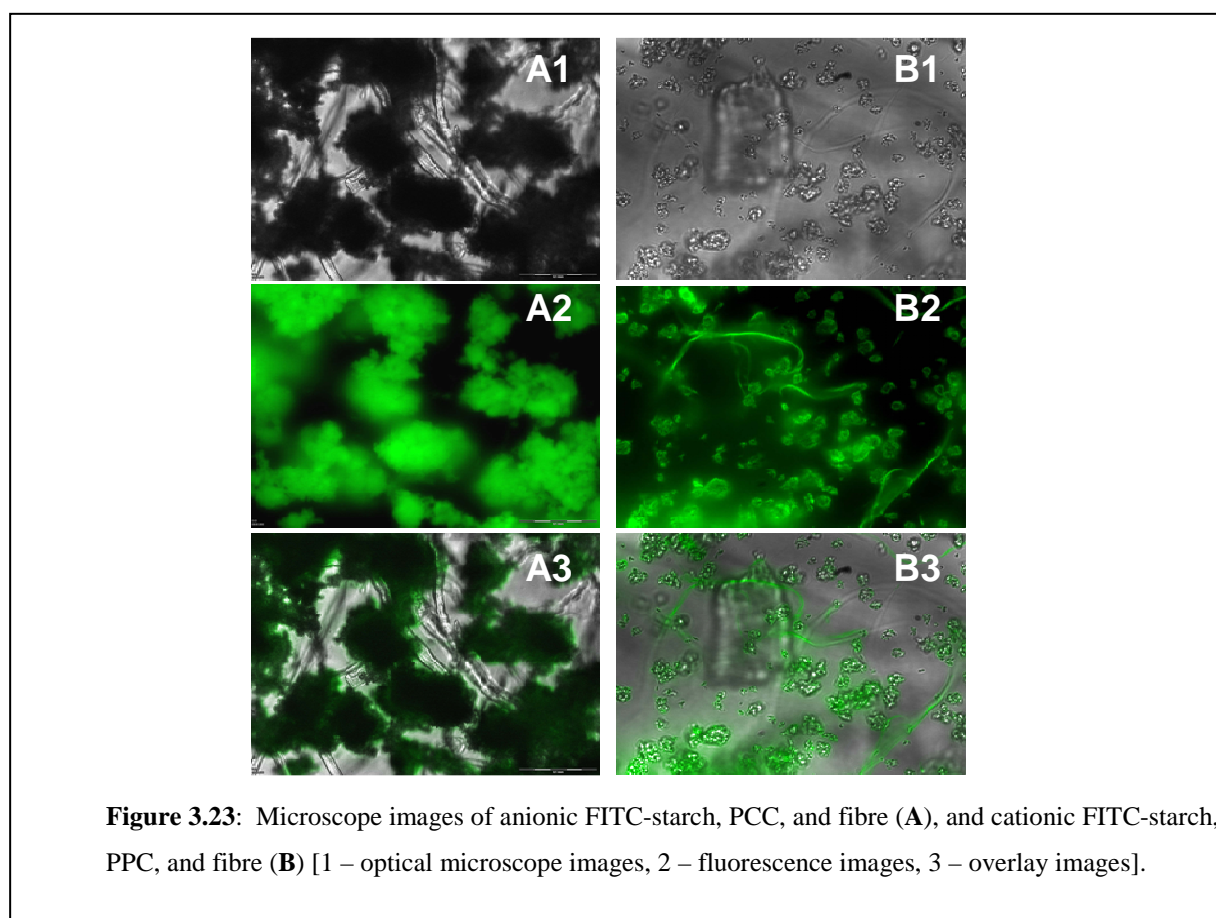
3.5 Conclusions

The concept of introducing ionic modified particles to paper was initially studied using polyester granules. Strong interaction between cationic modified particles and filler was observed while the anionic particles were shown to flocculate PCC. Samples were also submitted for testing in paper hand sheets.

The modification of maize starch was conducted based on the Williamson ether synthesis where sodium monochloroacetate, 3-chloro-2-hydroxypropyltrimethylammonium chloride, and allyl bromide was attached onto the starch backbone under alkali conditions to produce anionic, cationic, and unsaturated starch, respectively. The modified starch was characterised using ^{1}H-NMR and the applications of these for preparing polysaccharide particles will be discussed in following chapters.

The interaction of the ionic modified starch with paper fibres and PCC was studied using fluorescence microscopy. Fluorescein isothiocyanate was synthesised and attached to the individual starches. Imaging showed adsorption of cationic starch on both fibre and PCC, while anionic starch interaction with fibres was exclusive.

3.6 References

1. M. Laleg, Swollen Starch-Latex Compositions for use in Papermaking, Patent: US 7,074,845 B2, **2006**.

2. J. B. Calkin, *Modern Pulp and Paper Making*. 3rd ed.; Reinhold Publishing Corporation: New York, **1957**.

3. J. C. Terblanche. The Development of Vesiculated Beads. M.Sc (Eng.) Thesis, University of Stellenbosch, Stellenbosch, **2003**.

4. R. H. Gunning; B. C. Henshaw; F. J. Lubbock, Polyester Granules and Process, Patent: US 4,137,380, **1979**.

5. M. Karickhoff, Vesiculated Beads, Patent: US 4,489,174, **1984**.

6. H. Horvath, *Journal of Quantitative Spectroscopy & Radiative Transfer*, **2009**, 110, 787-799.

7. O. B. Wurzburg, *Modified Starches: Properties and Uses*. CRC Press, Inc.: **1986**.

8. Z. Stojanovic; K. Jeremic; S. Jovanovic, et al., *Starch-Starke*, **2005**, 57, 79-83.

9. C. J. Tijsen; R. M. Voncken; A. Beenackers, *Chemical Engineering Science*, **2001**, 56, 411-418.

10. O. S. Lawal; M. D. Lechner; B. Hartmann, et al., *Starch-Starke*, **2007**, 59, 224-233.

11. J. S. Lee; R. N. Kumar; H. D. Rozman, et al., *Carbohydrate Polymers*, **2004**, 56, 347-354.

12. Z. Stojanovic; K. Jeremic; S. Jovanovic, *Starch-Starke*, **2000**, 52, 413-419.

13. A. Lehmann; B. Volkert; S. Fischer, et al., *Colloids and Surfaces A-Physicochemical and Engineering Aspects*, **2008**, 331, 150-154.

14. O. S. Lawal; M. D. Lechner; W. M. Kulicke, *Polymer Degradation and Stability*, **2008**, 93, 1520-1528.

15. B. Volkert; F. Loth; W. Lazik, et al., *Starch-Starke*, **2004**, 56, 307-314.

16. F. W. D. Frost, *Fluorescence Microscopy*. Cambridge University Press: Cambridge, **1992**; Vol. 1.

17. A. N. De Belder; K. Granath, *Carbohydrate Research*, **1973**, 30, 375-378.

18. J. L. Riggs; R. J. Seiwald; R. H. Burkhalter, et al., *American Journal of Pathology*, **1958**, 34, 1081-1097.

19. R. M. McKinney; J. T. Spillane; G. W. Pearce, *Analytical Biochemistry*, **1964**, 7, 74-86.

20. S. S. Twining, *Analytical Biochemistry*, **1984**, 143, 30-34.

21. S. Knez, *Chemical Engineering Science*, **2006**, 61, 5867-5880.

Chapter 4: Polysaccharide particle processing: conventional techniques

4.1 Introduction

The preparation of polysaccharide particles has been widely investigated and reported in the open literature and patents due to their broad range of applications, mostly in the drug delivery industry and as carrier system in foods. Water-in-oil emulsification is the most commonly used method for preparing spherical polysaccharide particles. Generally, a polysaccharide solution is emulsified in an oil phase, such as heptane, cyclohexane, or even vegetable oil with the assistance of a lipophilic emulsifier such as sorbitan mono-oleate (Span 80). Particles are usually cross-linked by reactions of the hydroxyl group with polyfunctional reagents (e.g. epichlorohydrin[1-4], phosphorus oxychlorides[5-7], dialdehydes[8, 9]) or by radical polymerization of unsaturated groups created on the starch (e.g. acrylate[10, 11], methacrylate[12, 13], allyl, maleate[14], acrylamide[15-17]). The role that these particles play is often limited to their ability to be used as a non-toxic transport vehicle and therefore research has been more focused around techniques for making polysaccharides cross-linkable. It has seldom been reported how they can be modified further to perform as multi-functional additives, and this is even more lacking in the paper industry.

In the previous chapter the interaction of ionic modified maize starch solutions with paper components were demonstrated. However, as reported, the effect of these solutions in enhancing the stiffness and mechanical properties of paper is limited to the net charge that can be neutralised. In this chapter different techniques for preparing ionic modified cross-linked polysaccharide particles are discussed, with the aim to add it in paper to improve bulk and ultimately sheet strength properties at higher filler loadings. The techniques involved the application of conventional processes such as batch system emulsification, dispersion, high shear homogenisation, and ultrasonication. Depending on the performance of the dual additive system in hand sheets, this allows the potential to scale-up processes to pilot and/or production scale without justifying excessive expenditure on new processing equipment. Preparation of functional polysaccharide particles might even be tested using existing batch

reactor systems in order to test their performance on a continuous paper mill. For possible future industrialisation, the ease of production and environmental friendliness was also considered for each processing technique. The degree of ionic modification was also varied in order to determine its effect on paper properties. Since cationic starch solutions are already added during papermaking as a wet end additive, more emphasis was placed on preparing anionic starch particles that can act with the cationic starch as a dual retention aid system.

4.2 Water-in-oil emulsified starch particles

4.2.1 Introduction

Conventional water-in-oil (W/O) emulsification was initially evaluated according to techniques well documented where a hydrophobic solvent is treated with a cross-linking agent and lipophilic emulsifier and combined with an aqueous polysaccharide solution. The fluidity of aqueous maize starch solutions is generally very low even at concentrations of 4 wt%. However, the viscosity can be lowered substantially by the addition of a small amount of NaOH (ca. 1 wt% based on dry starch) which will greatly decrease the gelatinisation temperature of starch, subsequently increasing its fluidity in water. Alternatively the starch can be partially substituted with low molecular weight (M_w between 5,000 and 30,000 g/mol) polyvinyl alcohol (PVA) which will not only improve fluidity, but also enhance the adhesiveness of the particles. Combinations of cross-linked starch and PVA is commonly used in industry as natural biodegradable adhesives, especially in wood[18, 19].

The large interfacial tension between a low density solvent (eg. heptane or cyclohexane) and high molecular weight starch solution calls for intensive mixing principles, such as high shear homogenisation to effectively disperse and stabilise polysaccharide particles.
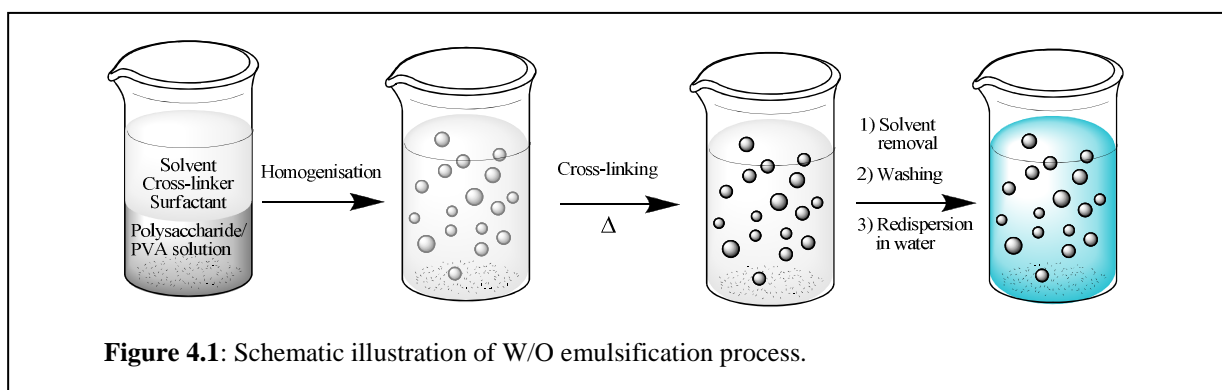
Figure 4.1: Schematic illustration of W/O emulsification process.

Since cross-linking is achieved by the etherification of hydroxyl groups on the starch/PVA backbone, initiation will slowly start to occur upon contact of the cross-linking agent with the starch/PVA solution in an alkali environment. The rate of reaction is slow, but can be increased by applying heat. Once the reaction is essentially complete, the cross-linked gel particles need to be isolated from the solvent and re-dispersed in water. Figure 4.1 demonstrates the processing steps required for preparing W/O emulsified polysaccharide particles.

4.2.2 Experimental

4.2.2.1 Materials

Maize starch (Acros, Cat: 24,073) was dried before use. Polyvinyl alcohol (PVA) (M_w 15,000 g/mol) (Merck, Cat:8438,650), heptane (Kimix, CP grade), epichlorohydrin (ECH) (Merck, Cat: 8032,960), sorbitan mono-oleate (Span 80) (Sigma, Cat: S6760), NaOH (Merck, Cat: SAAR5823160 EM), HCl (32%) (Merck, Cat: SAAR3063040 LP), and silver nitrate (AgNO$_3$) (N.T. Analytical Reagents, Cat: R2810) were used as received.

4.2.2.2 W/O emulsified maize starch particles

Polysaccharide particles consisting of a 6:4 (w/w) ratio maize starch to PVA were prepared by first adding 45 g maize starch and 30 g PVA to 420 g DDI water. The starch/PVA mixture was dissolved in the water by heating it to 90 ^{o}C. NaOH (5 g) was added and the solution mixed for 40 minutes after which heating was removed and the homogenous solution allowed to cool to room temperature.

A solvent phase was prepared by dissolving 4 g Span 80 and 2.5 g ECH in 60 g heptane. A total of 40 g of the 15 wt% starch/PVA solution was weighed off and added to the solvent phase. Immediately after addition emulsification was performed with a Silverson (Model L4R) homogeniser at a speed of 5,600 rpm for 5 minutes, after which the emulsion was transferred to a 250 ml round bottom flask and placed in a 60 ^{o}C oil bath under low shear magnetic stirring for 24 hours to allow for cross-linking to complete (Figure 4.2).

Ethanol was added to the emulsion until a white starch particle precipitate formed at the bottom of the vessel. The precipitate was separated from the heptane/ethanol solvent by

centrifugation and re-dispersed in 25 ml DDI water. The pH was adjusted to pH 7-8 by adding HCl and the particles once again precipitated by adding 25 ml ethanol. Washing in DDI water and precipitation was repeated until no chloride ions could be detected as a precipitate of AgCl after treating with $AgNO_3$ added to a sample of the aqueous emulsion. The total solids content of the final aqueous emulsion was adjusted to 2.5 wt%.

Figure 4.2: Cross-linking of maize starch using epichlorohydrin.
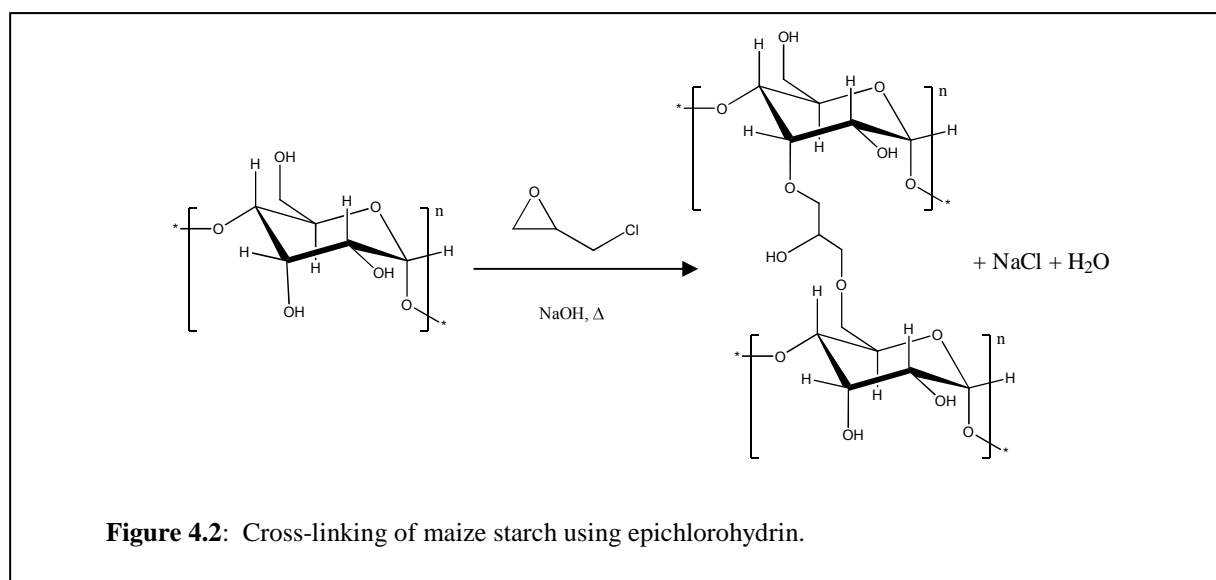
4.2.3 Analysis

4.2.3.1 Optical microscopy

Optical microscopy of wet samples was performed as described in Section 2.3.2.3.

4.2.3.2 Scanning electron microscopy

An aqueous emulsion sample was freeze dried at -60 ^{o}C and 0.01 mbar overnight to remove all water and to minimise deformation of the gel particles. The dry powder was placed onto carbon tape and imaging was performed using a Leo 1430VP Scanning Electron microscope fitted with a variable pressure detector.

4.2.4 Results and discussion

Figure 4.3A shows an optical microscope image of the starch/PVA particles in heptane immediately after emulsification with the homogeniser and the average particle size was

roughly about 6μm. After cross-linking (Figure 4.3B) the particles appear larger indicating that coalescence occurred over time.
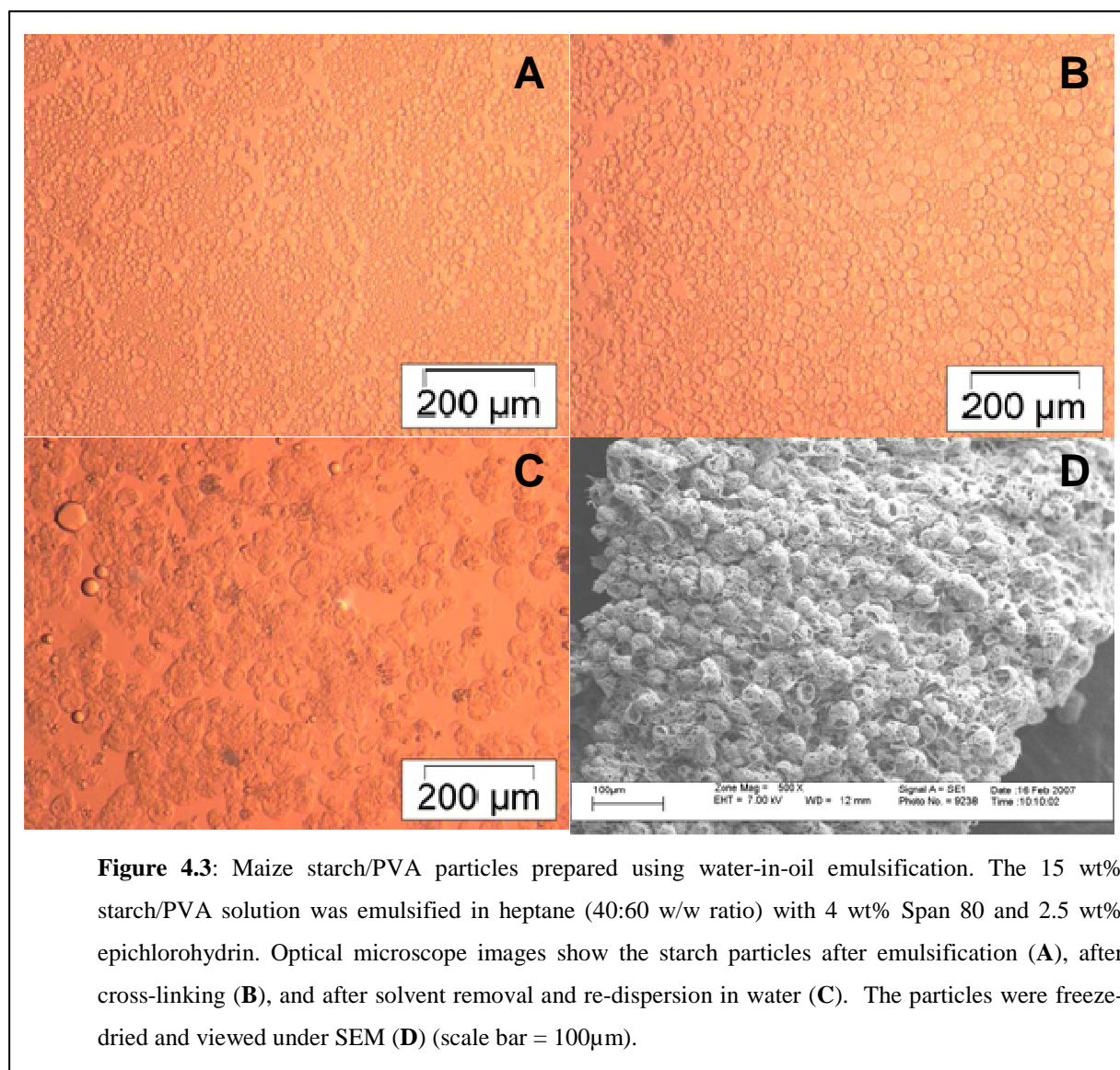
Figure 4.3: Maize starch/PVA particles prepared using water-in-oil emulsification. The 15 wt% starch/PVA solution was emulsified in heptane (40:60 w/w ratio) with 4 wt% Span 80 and 2.5 wt% epichlorohydrin. Optical microscope images show the starch particles after emulsification (**A**), after cross-linking (**B**), and after solvent removal and re-dispersion in water (**C**). The particles were freeze-dried and viewed under SEM (**D**) (scale bar = 100μm).

There are a limited amount of commercially available water-in-oil emulsifiers available. This is because ionic emulsifiers will not work in the case of water-in-oil emulsions and since a low hydrophilic-lipophilic balance (HLB) is required (between 3 and 6), variations using ethylene oxides are not possible[20]. Therefore oleates (such as sorbitan mono-oleate) are generally the most widely used, although not very effective where a large surface tension between the two phases exists, as in this case. This can be attributed to the low molecular weight of the emulsifier and an alternative higher molecular weight emulsifier should improve stabilisation of the starch particles. This is discussed further in the following chapter.

After removing the particles from heptane and redispersing them in water, the particles swelled significantly to an average particle size of about 50μm (Figure 4.3C). Upon drying these particles they completely deformed and collapsed. However, freeze drying did preserve the overall integrity of the particles, although they became porous as water was removed during the drying process (Figure 4.3D). Ionic modification of polysaccharide-based particles prepared by W/O emulsification was studied further using microfluidics and will be discussed further in Chapter 5.

4.3 Preparation of macrogel starch particles

4.3.1 Introduction

Although conventional techniques, such as water-in-oil emulsification, can offer advantages such as easy particle size and distribution control as well as surface functionalisation, the so-formed polysaccharide particles need to be separated and purified to remove all traces of solvents that were used as continuous phase. Therefore, a simple economical and environmentally friendly technique for preparing modified starch particles was investigated. Macrogel starch particles were prepared where anionic modified starch solutions were first cross-linked to form a stiff gel, after which the gel was added to water and subjected to high shear homogenisation, washed, and ultrasonicated to break up the gel to smaller particles (Figure 4.4). Although the so-formed particles were non-uniform, processing was simple and no subsequent solvent removal was required.
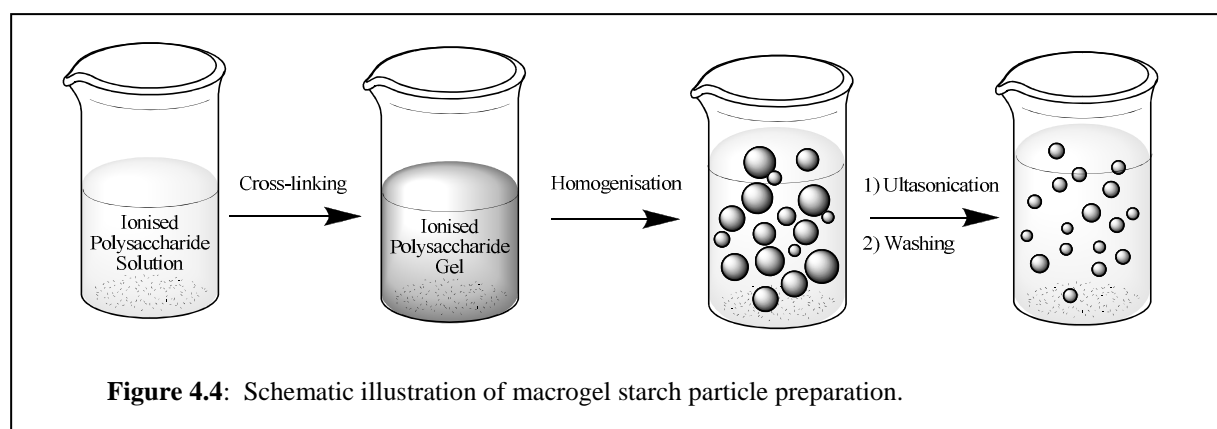
Figure 4.4: Schematic illustration of macrogel starch particle preparation.

4.3.2 Experimental

4.3.2.1 Materials

Carboxymethyl starch (CMS) with DS = 0.15, 0.3, and 0.6 was synthesised following the method described in Section 3.3.2.2 and using formulations appearing in Table A1, Appendix A. Epichlorohydrin (ECH) (Merck, Cat: 8032,960), HCl (32%) (Merck, Cat: SAAR3063040 LP), and NaOH (Merck, Cat: SAAR5823160 EM) were used as received.

4.3.2.2 Synthesis of starch macrogel

Dry CMS powder (15 g) was first dispersed in 83 g DDI water in a 250 ml 3-neck round bottom flask using an overhead mechanical stirrer. The slurry was heated to 95 $^{\circ}$C and mixed until the starch was completely dissolved and the solution clear, whereupon heating was removed. NaOH (2 g) was dissolved in 10 g DDI water and added to the solution followed by addition of 2 g ECH. After 5 min stirring, the reaction mixture was removed, poured into a sealed container and placed overnight in a 50 $^{\circ}$C laboratory oven to allow the starch to fully cross-link into a stiff macrogel.

4.3.2.3 Macrogel starch particle preparation

The total solids content of the macrogel was adjusted to 5 wt% by adding DDI water and the macrogel refined to smaller particles using a Silverson (Model L4R) homogeniser at 5,000 rpm for 5 min. In order to reduce the particle size further, the particle suspension was subjected to ultrasonication using a Sonics Vibra cell VCX 750 Watt ultrasonic processor with a ½ " tip. Samples were ultrasonicated for 2 min and the typical energy input was about 12 kJ/20 ml sample. The pH of the solution was neutralised (pH 7) using HCl and the sample centrifuged and washed 3 times with 50 ml DDI water to remove NaCl formed during neutralisation and the final solution's solids content was adjusted to 4 wt%.

4.3.3 Analysis

4.3.3.1 Optical microscopy

Optical microscopy was performed as described in Section 4.2.3.1.

4.3.3.2 Particle size analysis

A robust technique of determining particle size and distribution was employed using Scion Image Alpha 4.0.3.2 image processing and analysis program. Images captured using optical microscopy can be loaded and user-defined measurements of area, mean, centroid, perimeter, etc. conducted. Since particles obtained using the macrogel processing technique are non-spherical and highly polydisperse, this measurement only allows a rough indication of particle size with a limited degree of certainty.

4.3.3.3 Degree of substitution

In order to determine the amount of carboxylate groups present on the starch, the sodium carboxylate (-COO$^-$ Na$^+$) groups were converted to carboxylic acid (-COOH) by first dissolving an oven dried (50°C) sample of CMS in DDI water and adjusting the pH to 4 by addition of 6 M HCl followed by stirring for 30 min. The starch was precipitated in acetone and filtered to remove the excess HCl and the precipitate washed with a 90:10 (v/v) acetone-water solution until the pH was neutral (pH 7). The precipitate was once again dispersed in pure acetone, filtered, dried under vacuum at 50°C, and ground. The obtained protonated carboxymethyl starch (H-CMS) was used to determine the DS$_{anionic}$ by back titration.

About 0.5g of the dry H-CMS was weighed off and dissolved in 20 cm^3 of a 0.2 M NaOH aqueous solution and transferred to a 100 cm^3 volumetric flask and filled to the mark with DDI water. Exactly 25 cm^3 of the solution was transferred to an Erlenmeyer flask and diluted with 50 cm^3 DDI water. The excess NaOH was back titrated with a standard 0.05 M oxalic acid solution using phenolphthalein as indicator. Titration was repeated 3 times and the average volume oxalic acid determined. The DS$_{anionic}$ was calculated as follows[21]:

$$DS_{anionic} = \frac{162 \times n_{COOH}}{m_{ds} - 58 \times n_{COOH}}$$

equation 4.1

where 162 g/mol is the molar mass of an anhydroglucose unit (AGU), m_{ds} (in g) is the dry weight of H-CMS used, 58 g/mol is the net increase in mass of an AGU for each carboxymethyl group substituted, and n_{COOH} (in mol) is the amount of carboxymethyl groups calculated from the following equation:

$$n_{COOH} = 4 \times (V_b - V) \times c_{ox}$$

equation 4.2

where 4 is the ratio of the total solution volume (100 cm^3) and the volume used for titration (25 cm^3), V_b (in cm^3) is the volume of oxalic acid used for titration of the blank, V (in cm^3) is the volume oxalic acid used for titration of the sample and c_{ox} (in mol/dm^3) is the concentration of the oxalic acid.

4.3.4 Results and discussion

In Figure 4.5 optical microscope imaging shows the coursely dispersed anionic macrogel particles (DS$_{th}$ = 0.3) after homogenisation and ultrasonication. Even over extended homogenisation periods and mixing intensities, the high shear was not able to break particles down to below an average size of roughly 200 - 500 µm. However, ultrasonication can be used to actually break down and degrade polysaccharide chemical bonds and is reportedly also used to extract polysaccharides from the outer layer (or skin) of fleshy fruit[22]. Therefore this technique can be effectively used to reduce the average particle size even further as an alternative to using ultra-high shear dispersion techniques, such as ball milling or rotor-stator mixers.

Particle size analysis of the macrogel samples with DS$_{th}$ of 0.15, 0.30, and 0.60 showed that ultrasonication produced poly-disperse particles of up to 55 µm with the majority of particles found within 5 to 20 µm and the average particle size ranging between 10 and 20 µm (Figure 4.6).

Figure 4.5: Optical microscope images of anionic macrogel particles (DS_{th}=0.3) after homogenisation (**A**) and after ultrasonication (**B**).

Figure 4.6: Particle size distribution of ultrasonicated anionic macrogel starch particles with different degrees of substitution.
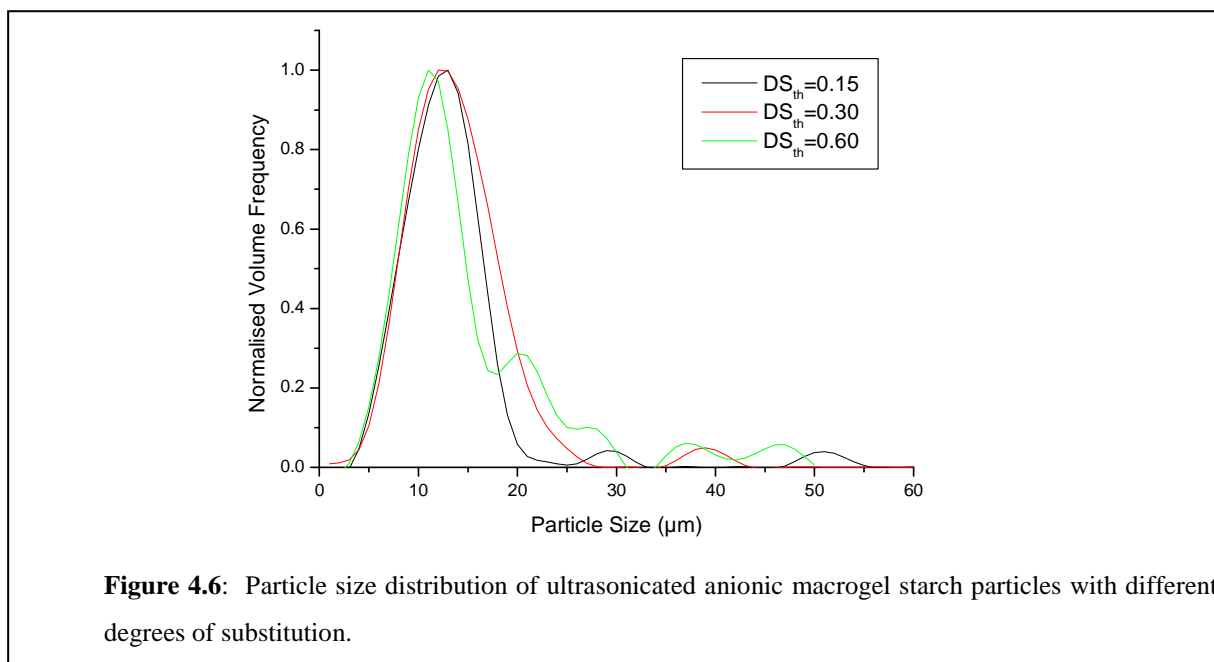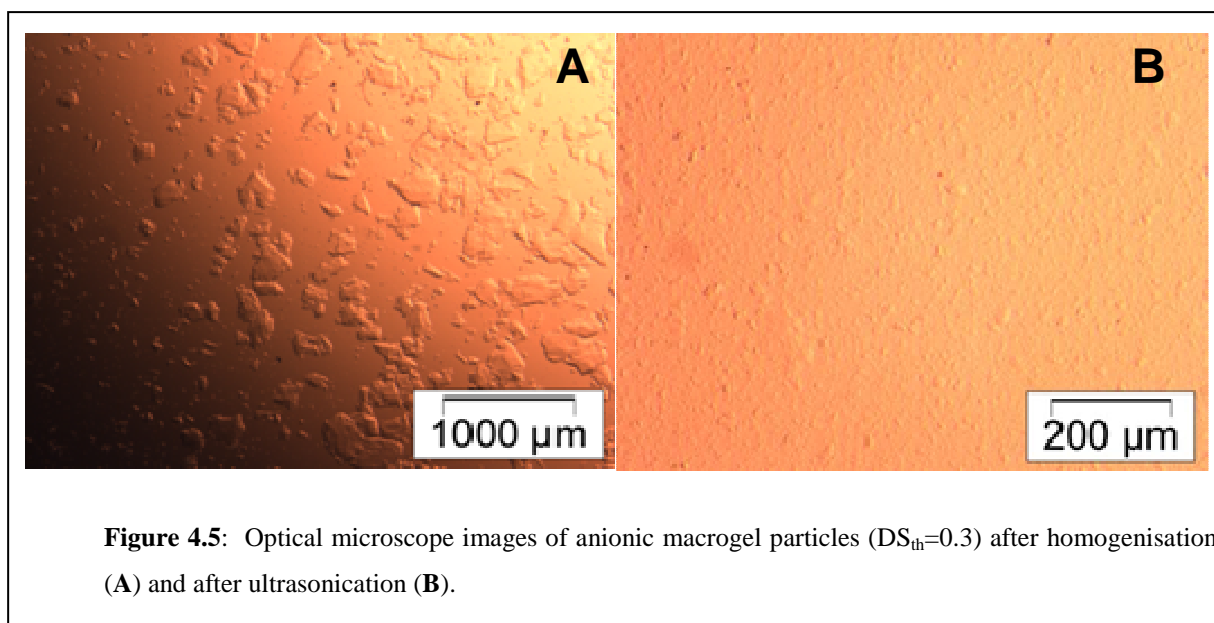
Table 4.1 presents the average particle size and DS obtained for the ionic macrogel samples. The carboxymethylation of starch determined by back titration indicated low reaction efficiency especially for the lower substitution degree samples, which can once again be attributed to the poor mobility of SMCA through the highly swollen hydrophilic carboxymethylated starch structure during reaction. However, these samples were submitted for testing in paper hand sheets to investigate if and how the difference in DS will affect filler retention and mechanical properties. Furthermore, additional macrogel samples were

prepared with a wider DS range as well as different cross-linking degrees (different concentrations ECH used) and submitted for hand sheet testing. Details of these samples as well as hand sheet properties obtained will be presented in Chapter 6.

Table 4.1. Properties of anionic macrogel starch particles with different DS.

Sample	Average Particle Size (μm)	DS_{th}	DS_{exp}	Reaction efficiency (RE) (%)
MG 015	13.0	0.15	0.042	28.0
MG 030	17.6	0.30	0.099	33.0
MG 060	14.6	0.60	0.19	31.7

4.4 Preparation of water-in-water emulsified polysaccharide particles (designer particles)

4.4.1 Introduction

Water-in-water emulsification is an attractive method for preparing polymeric microspheres since it involves an all-aqueous system, avoiding the use of organic solvents. Aqueous polymer immiscibility occurs with many combinations of water-soluble polymers, such as combinations of dextran, poly(ethylene glycol) (PEG), poly(vinyl alcohol), poly(vinylpyrrolidone), gelatine, soluble starch, or ficoll[23]. The polymers will stay in solution, but will separate above a certain concentration. After emulsification, the dispersed polymer can be cross-linked to form microparticles.

For the purpose of this study maize starch and dextrin solutions were emulsified in a PEG solution continuous phase (Figure 4.7). SMCA used for anionic modification and ECH used for cross-linking are both water-soluble and introducing these to the all-aqueous system will cause these agents to migrate in between the phases, causing poor reaction efficiency as these agents will not be specifically available to react with the starch. Therefore, prior to emulsification, the starch itself was modified with carboxymethyl as well as allyl groups in order to make a cross-linkable anionic starch. After emulsification, the starch globules were polymerised by the addition *N,N,N',N'*-tetramethylethylenediamine (TEMED) and potassium persulfate (KPS). Although the particles have to be removed from the PEG solution and re-

dispersed in water, no salt (NaCl) is generated as by-product of the Williamson ether synthesis, making it easier to recycle the PEG solution.

Figure 4.7: Schematic illustration of polysaccharide particles prepared by water-in-water emulsification.
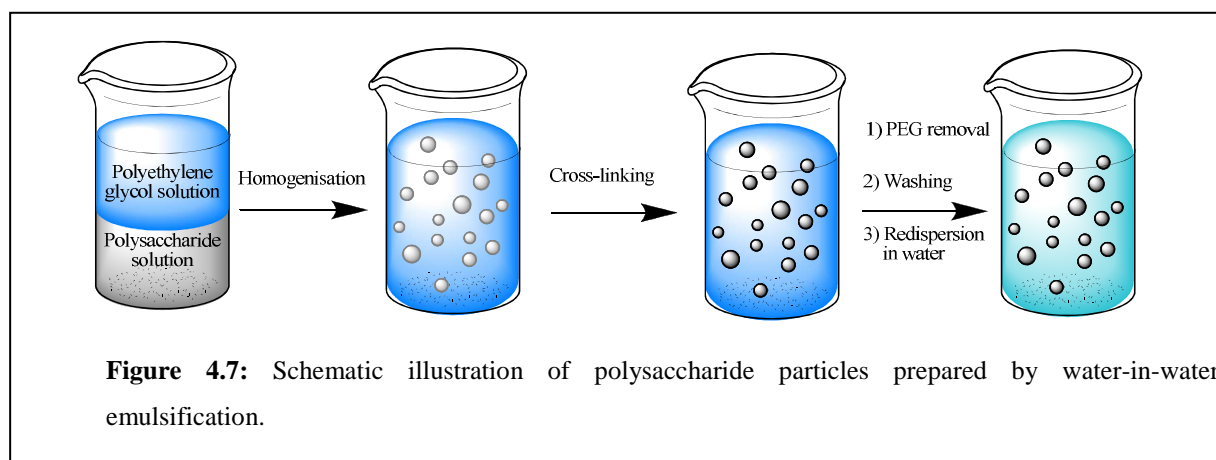
4.4.2 Experimental

4.4.2.1 Materials

Maize starch (Acros, Cat: 24,073) was dried before use. Allyl bromide (Aldrich, Cat: A29,585) was stored at 4 $^{\circ}$C. SMCA (Fluka, Cat: 24,610), poly(ethylene glycol) (PEG) (M_w 20,000 g/mol) (Merck, Cat: S4624297-715), NaOH (Merck, Cat: SAAR5823160 EM), HCl (32%) (Merck, Cat: SAAR3063040 LP), and $AgNO_3$ (N.T. Analytical Reagents, Cat: R2810) were used as received. Potassium persulfate (KPS) (Merck, Cat: 1.05091) was dissolved in DDI water to concentration of 5 wt% and *N,N,N',N'*-tetramethylethylenediamine (TEMED) (Fluka, Cat: 87,687) was diluted to 20 vol% and neutralised to pH 7 using 4 M HCl. Both KPS and TEMED were stored at 4 $^{\circ}$C.

4.4.2.2 Preparation of anionic allyl maize starch

Maize starch (20 g) was slurried in 25 ml acetone in a 250 ml round bottom flask, followed by the addition of 75 ml 5 wt% NaOH solution and the mixture heated to 40 $^{\circ}$C under a nitrogen blanket. Allyl bromide (14.9 g, DS = 1) was added drop-wise to the solution over a period of 15 min and heated further to 55°C for a period of 2 hours. SMCA (3.35 g, DS = 0.4) was added to the solution and mixed for a further 2 hours. The sample was neutralised (pH 7) with HCl, removed, and precipitated in 500 ml acetone. Alternate washing and precipitation

was repeated until no chloride could be detected (by AgNO$_3$ addition). The aqueous solution was vacuum distilled at 56 ^{o}C to remove residual acetone and the final total solids content adjusted to 15 wt%.

4.4.2.3 Preparation of microspheres

An anionic allyl starch solution (14 g, 15 wt%) was added to 233 g 24 wt% PEG solution. Two immiscible starch/PEG layers were clearly visible. The solution was subjected to high shear homogenisation (5,600 rpm) for 5 min using a Silverson (Model L4R) homogeniser. The resulting emulsion was allowed to stabilise for 15 min before 4.7 g KPS (5 wt%) and 8.4 g TEMED (20 vol%) was added under slow stirring to initiate cross-linking. After 5 hours at ambient temperature, the emulsion was centrifuged to remove the starch from the PEG and the particles re-dispersed in DDI water. The final total solids content (TSC) was adjusted to 2 wt%.

4.4.3 Analysis

4.4.3.1 Optical microscopy

Optical microscopy was performed as described in Section 4.2.3.1.

4.4.3.2 Degree of substitution

The DS of allyl groups attached onto the starch (DS$_{allyl}$) was determined by ^{1}H-NMR and using equation 3.5 or equation 3.6 as described in Section 3.3.3.1. During synthesis of anionic allyl starch, a sample was taken immediately before addition of SMCA. The sample was thoroughly washed, precipitated in acetone, and dried before submitting it for NMR analysis.

The DS of the anionic groups (DS$_{anionic}$) were determined using back titration as described in Section 4.3.3.3. However, equation 4.1 was adjusted in order to compensate for the mass increase of an AGU unit for the allyl groups substituted. The equation is therefore given as:

$$DS_{anionic} = \frac{162 \times n_{COOH}}{m_{ds} - 40 \times DS_{allyl}(\frac{m_{ds} - 58 \times n_{COOH}}{162}) - 58 \times n_{COOH}}$$
equation 4.3

where DS_{allyl} is the degree of allyl group substitution as determined by ^{1}H-NMR and 40 g/mol is the nett increase per AGU for each allyl group substituted.

4.4.4 Results and discussion

Initial experimentation was conducted where modification of the maize starch was done only with allyl groups (DS = 1) in order to test the cross-linking efficiency of the starch particles in the all-aqueous system. By omitting addition of SMCA, cross-linking was initiated with KPS and TEMED and after 5 hours reaction time the emulsion was removed and studied under optical microscopy (Figure 4.8A). To confirm cross-linking the emulsion was also studied after removing the PEG solution, washing, re-dispersing the particles in DDI water to a TSC of 2 wt% followed by mixing for 24 hours (Figure 4.8B).

Figure 4.8: Optical microscope images of cross-linked allyl (DS = 1) maize starch particles in PEG solution after homogenisation and cross-linking (**A**) and after centrifugation, washing, and re-dispersion in water for 24 hours (TSC= 2 wt%) (**B**).
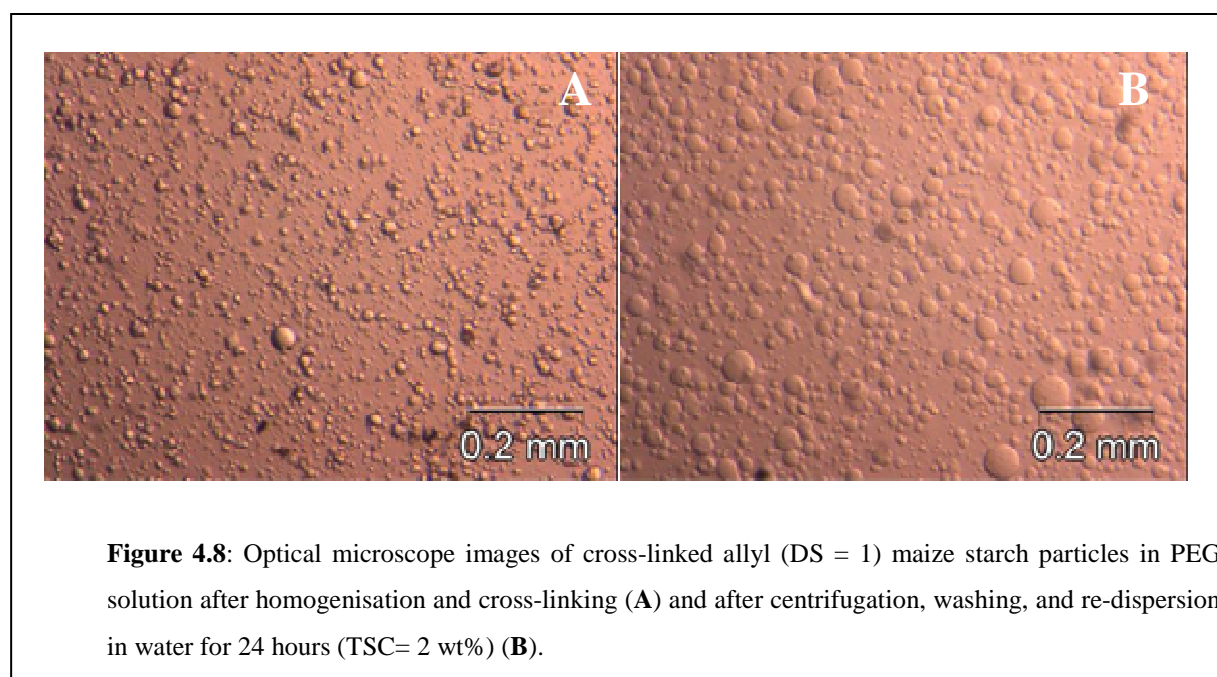
Imaging shows discrete particle formation, with some swelling of the particles occurring after re-dispersion in water. To further verify that the particles formed were starch-based, the solution was treated with a few drops of iodine (I$_2$/KI) solution. Iodine stained starch to a

blue/purple colour due to complex formation with the hollow helical structure of linear amylose chains[24]. The solution was left for 24 hours in a vial placed in a dark area for the colour to develop and a clear blueish coloured particle suspension could be observed settled at the bottom of the vial, whilst the top layer was clear, confirming that the particles were indeed starch-based.

Following successful synthesis of cross-linked starch particles, the allyl maize starch was anionic modified with SMCA and the same procedure followed as above. However, a completely different phenomenon was observed (Figure 4.9).

Figure 4.9: Optical microscope images of cross-linked anionic (DS=0.4) allyl (DS=1) maize starch particles in PEG solution (**A**) and after centrifugation, washing, and re-dispersion in water (**B**) (TSC=2 wt%). Particles prepared using the same starch that was hydrolysed prior to emulsification are shown in PEG solution (**C**) and after washing and re-dispersion in water (TSC=2 wt%) (**D**).
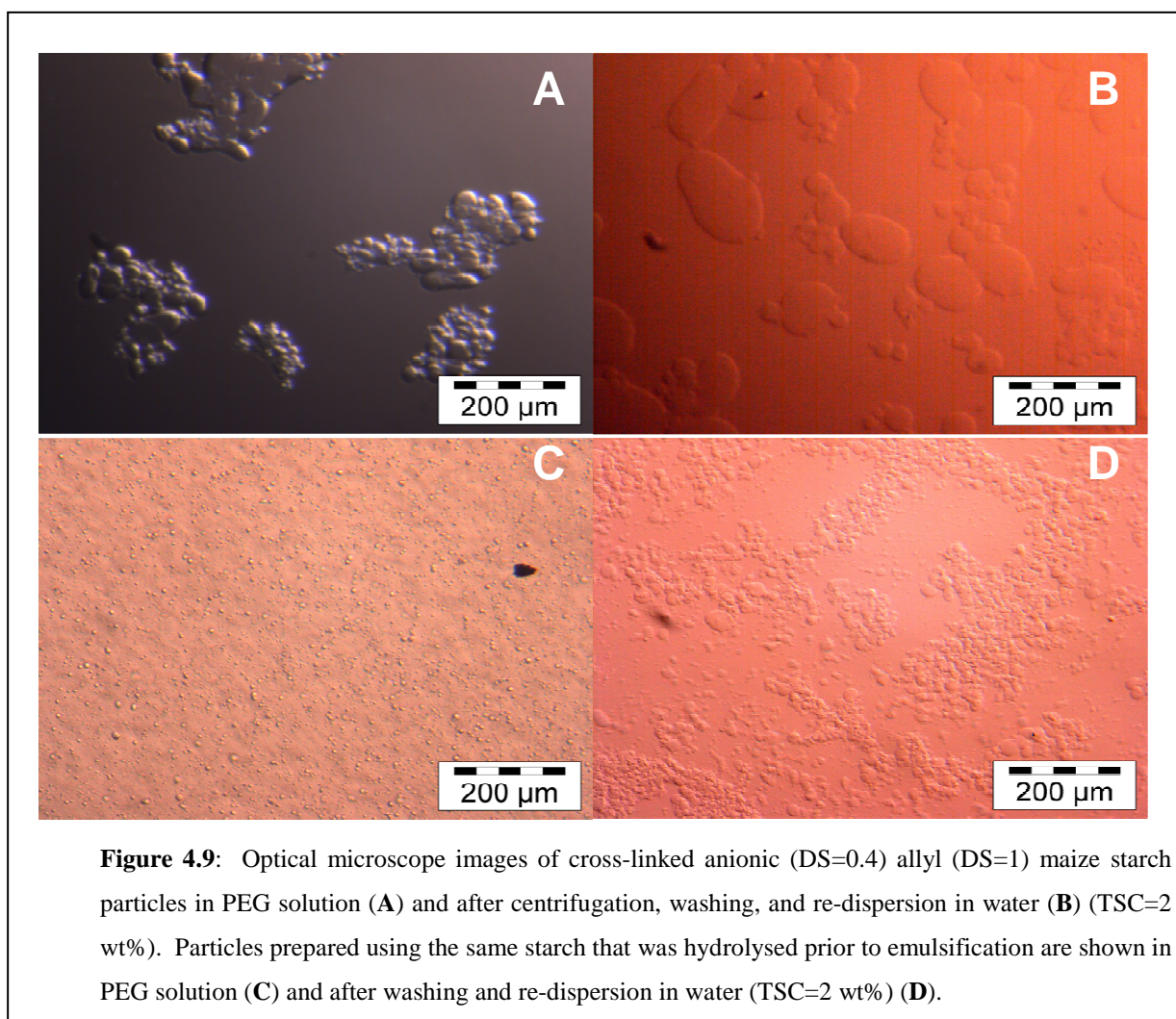
The anionic particles appeared to be severely non-uniform, poly-dispersed, and adhered to each other. This was also observed during the emulsification stage. The higher viscosity, almost glue-like, anionic starch solution was difficult to disperse in PEG and a significant

amount settled into a separate layer during the 15 min stabilisation time after emulsification. After washing and re-dispersion in water, severe swelling occurred and this is once again attributed to the enhanced hydrophilic character of the carboxymethyl groups on the starch. The particles remained non-uniform with the majority being oblong in shape.

In order to improve the poor emulsification behaviour without reducing the DS, it was decided to investigate lowering the molecular weight of the modified maize starch in an attempt to lower the viscosity of the starch solution. The anionic allyl maize starch was hydrolysed by subjecting it to microwave radiation for 2 min in the presence of 0.5 M HCl[25]. The starch was once again purified by repeated precipitation (in acetone) and washing in DDI water followed by oven drying. This was used to prepare another sample of particles in PEG solution and evaluated under optical microscopy. Ease of emulsification improved significantly and in Figure 4.9C a major improvement in particle uniformity can be seen together with a large decrease in particle size. Separation and re-dispersion in water still showed substantial swelling with particles still exhibiting some degree of adhesive behaviour, but the overall shape of the particles were more spherical.

Since particle size and morphology was affected by the molecular weight of the starch, other techniques of hydrolysis were investigated such as enzymatic hydrolysis using a commercially available enzyme treatment, Aquazyme 120L (Novozymes), but since it is difficult to accurately control the molecular weight by hydrolysis in the laboratory, it was decided to rather use a commercially available, lower molecular weight polysaccharide, such as dextrin. Dextrin is similar in structure to starch, also consisting of AGU repeating units bonded by α-D-(1$\rightarrow$4) glucosidic bonds, but with the presence of some α-D-(1$\rightarrow$6) bonds amongst the bulk of the glucan bonds[26]. Dextrin is usually produced by depolymerisation of unmodified starch using dry heating, acid-catalysed hydrolysis, or enzymatic hydrolysis with α-amylase (an enzyme that breaks starch down into sugar). A range of commercially available dextrin grades were evaluated. The molecular weight of these was not specified, but generally will vary between 800 to 70,000 g/mol. Available grades include:

1. Dextrin Type II, from maize starch, 15% water-soluble (Sigma, Cat: D2131).
2. Dextrin Type III, from maize starch, 75% water-soluble (Sigma, Cat: D2256).

3. Dextrin Type IV, from potato starch, 40% water-soluble (Sigma, Cat: D4894).

The procedure for preparing cross-linked allyl starch particles was repeated, substituting the maize starch with the same amount of dried dextrin. Only Dextrin Type II yielded clearly visible cross-linked particles after re-dispersion in water, whilst with the other grades no particles could be detected. This can be attributed to the molecular weight of these grades being too low (indicated by their higher water-solubility) to form a densely cross-linked macromolecular structure. Anionic allyl dextrin Type II particles prepared showed discreet spherical particles after re-dispersion in water with very little inter-particle attachment (Figure 4.10A). To investigate the anionic character of these particles, a 10 ml sample was treated with 0.5 ml PCC solution (TSC = 22.5 wt%). Immediate flocculation of the PCC was observed, which settled at the bottom of the vial. Optical microscope imaging confirmed the presence of the PCC on the particles as can be seen in Figure 4.10B (PCC shown as small black particles).

Figure 4.10: Optical microscope images of cross-linked anionic (DS = 0.4) allyl (DS = 1) dextrin Type II particles (TSC = 1.6 wt%) after washing and re-dispersion in water (**A**) and after treatment of 10ml particle solution with 0.5 ml PCC (TSC = 22.5 wt%).
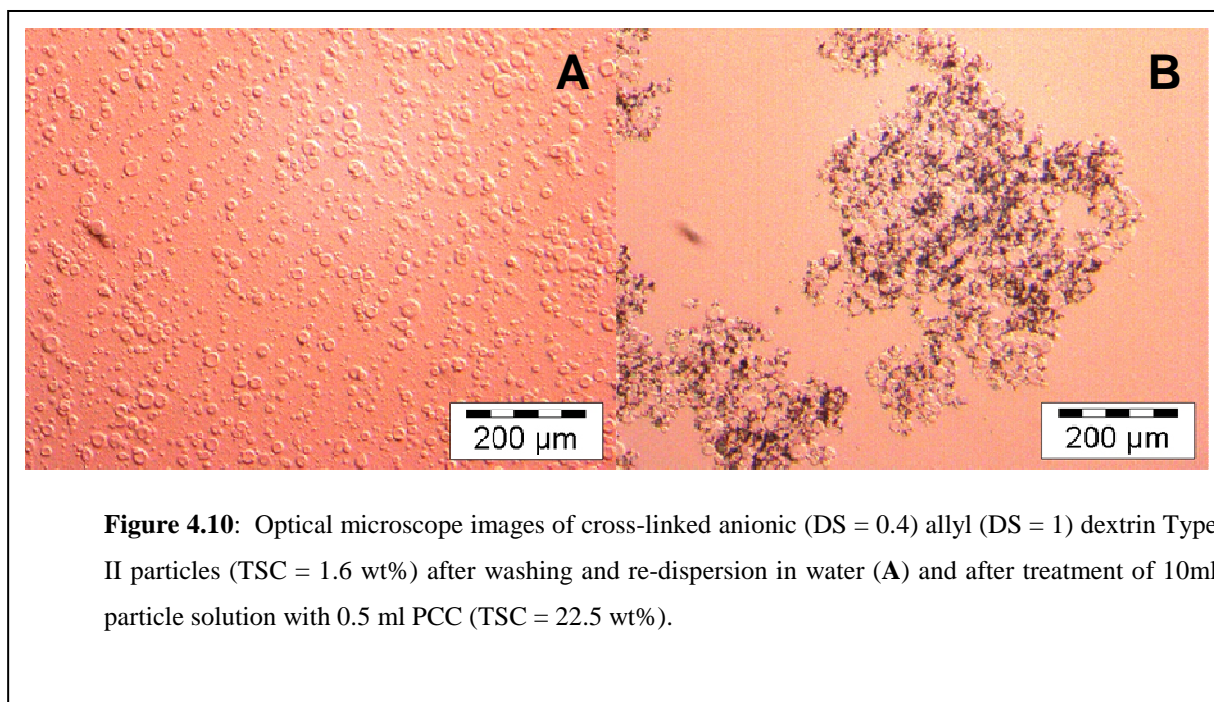
Table 4.2 presents the properties of the anionic dextrin particles as well as the DS of the modified dextrin used for synthesis. The RE_{allyl} compared well to values obtained in Figure 3.11. However, the $RE_{anionic}$ was comparatively lower than the values obtained for pure carboxymethyl maize starch, which can be attributed to the reduced concentration of free

hydroxyl groups present after the allyl substitution reaction. To investigate the performance of these particles in paper and its effect on paper stiffness and other mechanical properties, a sample was submitted for hand sheet trials and results will be discussed in Chapter 6.

Table 4.2: Properties of anionic (DS=0.4) allyl (DS=1) dextrin Type II particles prepared by water-in-water emulsification.

Sample	Average Particle Size (μm)	Total Solids Content (wt%)	$DS_{anionic}$	$RE_{anionic}$ (%)	DS_{allyl}	RE_{allyl} (%)
DP1	14.8	1.6	0.09	23	0.59	59

4.5 Encapsulation of PCC with starch using layer-by-layer (LbL) assembly

4.5.1 Introduction

A novel approach of introducing starch composites to paper making was investigated where, instead of preparing separate ionic modified polysaccharide particles, PCC filler particles themselves were encapsulated in starch layers, using a technique known as layer-by-layer assembly (LbL). Similar techniques have found application in diverse areas, which range from medicine and biotechnology to catalysis, electronics and synthetic chemistry[27]. Ultrathin polyelectrolyte films can be self assembled onto colloidal surfaces and these films can comprise, for example, of synthetic polyelectolytes, biopolymers (proteins and nucleic acid), lipids , and inorganic particles[28]. Multiple layers can be engineered onto composites using alternate and consecutive adsorption of oppositely charged macro-ions. This technology has successfully been transferred to surface nano-engineering of micron to submicron sized core colloidal particles and furthermore, these cores can be eliminated (by dissolution, oxidation, or decomposition) by suitable means to yield stable multilayer polyelectrolyte hollow spheres. This allows encapsulation of reactive polymers or enzymes, which promotes the formation of microreactors where small solutes can penetrate and enter the hollow particle, while macromolecules remain on the outside[29-34]. The permeability of these molecules can also be tuned by varying the amount of polyelectrolyte layers (eg. less

layers imply higher penetrability). A study conducted by Sukhorukov *et al.*[29] used calcium carbonate as a core and successively added anionic and cationic modified dextran solutions to it in order to build up a polysaccharide shell around it. The calcium carbonate was easily dissolved and removed by lowering the pH with HCl, leaving behind a hollow polysaccharide shell.

Figure 4.11: Schematic illustration of layer-by-layer assembly of anionic/cationic starch on PCC.
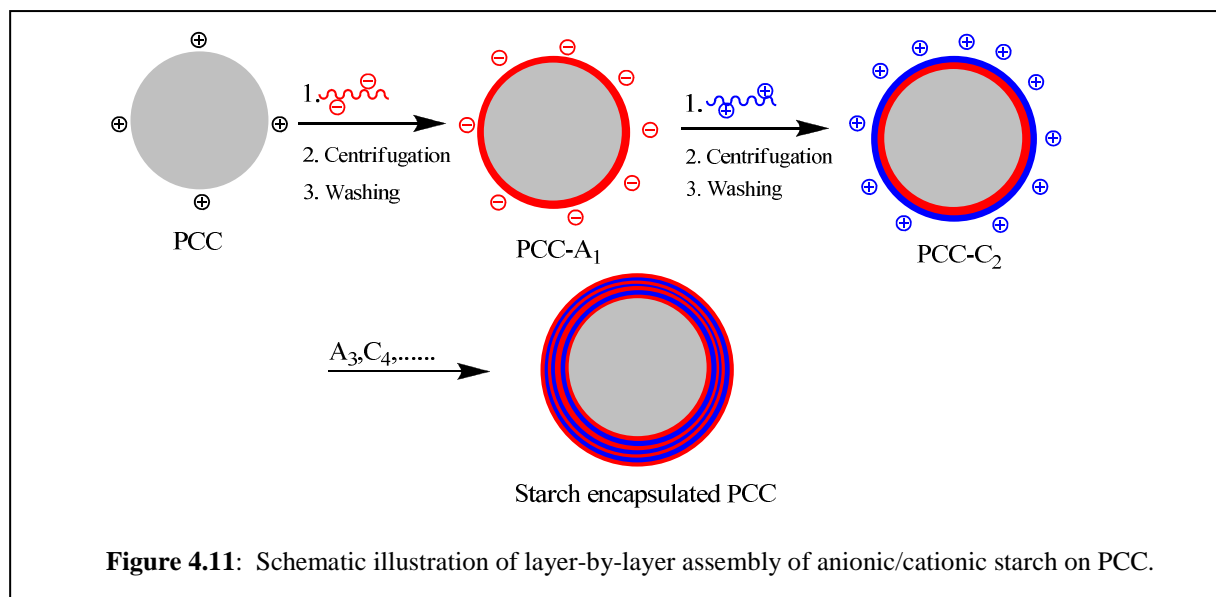
A similar approach was taken in this study to encapsulate PCC in multiple ionic modified starch layers, but excluding dissolution (Figure 4.11). In Chapter 3 fluorescence microscopy showed that both cationic as well as anionic modified starch will adsorb onto the PCC surface, but since the overall charge of the filler surface is slightly more positive, the first layer consisted of anionic modified starch. After each treatment, the PCC had to be separated and washed several times to remove excess un-adsorbed starch from the solution, since this can interfere and react with the subsequent oppositely charged treatment.

Verification of layer formation on the surface of PCC was performed by once again employing fluorescence imaging methodology. However, in order to differentiate between the two oppositely charged polyelectrolytes, two different fluorescence agents emitting at widely separated wavelengths of the colour spectrum were utilised. Fluorescein, emitting in the green colour range of the spectrum was selected for the one species, while in the other, Rhodamine B, which emits in the red colour range was selected. The presence of these fluorescence agents can be clearly distinguished due to their colour contrast.

The effect of using different ionic degrees of substitution on the layering behaviour was also studied using SEM, zeta potential, and thermogravimetric analysis (TGA).

4.5.2 Experimental

4.5.2.1 Materials

Carboxymethyl maize starch (CMS) as well as cationic maize starch with 2 different degrees of substitution (DS_{th} = 0.05 and 0.4) were synthesised as described in Section 3.3.2.2 (using formulations in Table A1, Appendix A) and Section 3.3.2.3 (using formulations appearing in Table A2, Appendix A), respectively. Fluorescein isothiocyanate (FITC) was synthesised as described in Section 3.4.2.2 and stored in a cool (4°C) dark place. Rhodamine B isothiocyanate (RITC) (Aldrich, Cat: 283,924) was kindly supplied by Mondi, Austria and stored as above. Precipitated calcium carbonate (TSC = 22.4 wt%) was obtained from Mondi, South Africa and used as received.

4.5.2.2 Layer by layer (LbL) assembly of ionic starch onto PCC

Due to the retrogradation (lower water affinity) of amylose at low concentrations in water, all starch samples were diluted in DDI water to a 10 wt% concentration and heated to 90°C in order to completely dissolve the starch. After a period of 1 hour the samples were cooled and filtered in order to remove any particulate undissolved or precipitated starch that may be present and that may interfere with the layering process. Oppositely charged starch solutions were paired off according to their theoretical degree of substitution and diluted further to 1 wt% concentration.

Three PCC filler samples (40 ml) were slurried in a 50 ml centrifugation tube to completely separate and disperse the precipitated particles. To each of these a 1 ml CMS solution (each possessing different DS) was added and thoroughly slurried for 2 minutes after which it was left static for 5minutes to allow sufficient time for colloidal interaction to occur and for the slurry to stabilise.

Samples were centrifuged to separate the PCC from the solution and washed with DDI water to remove any excess un-adsorbed starch from the system. The separation and washing steps were repeated 3 times before zeta potential measurements were taken. Another 1 ml CMS

was added and the process repeated with subsequent additions until the zeta potential stabilised.

The stable washed PCC samples were subsequently treated with 1 ml cationic starch solutions (DS_{th} coinciding with the previous CMS used) and the procedure once again followed whereby cationic starch treatment was repeated until the zeta potential remained essentially unchanged.

A total of three layers were adsorbed onto the surface of each PCC sample (2 anionic layers and 1 intermediate cationic layer).

4.5.2.3 Preparation of RITC-cationic starch

Examining the chemical structure of Rhodamine B isothiocyanate (RITC) (Figure 4.12B), a cationic charge is observed on one of the amine groups attached to the fluorescence agent backbone. Although this charge theoretically should have minor impact on the colloidal interaction between the modified starch and PCC due to the low fluorescence DS used ($DS_{th} = 0.001$), it was decided to completely separate ionic species and using this agent for attachment onto cationic maize starch, while utilising FITC for attachment onto CMS.

Preparation of FITC-CMS starch ($DS_{anionic} = 0.4$) and RITC-cationic starch ($DS_{cationic} = 0.4$) was synthesised as described in Section 3.4.2.3, where FITC was simply replaced with RIBC in the latter sample.

Figure 4.12: Chemical structures of (**A**) Fluorescein isothiocyanate, and (**B**) Rhodamine B isothiocyanate.
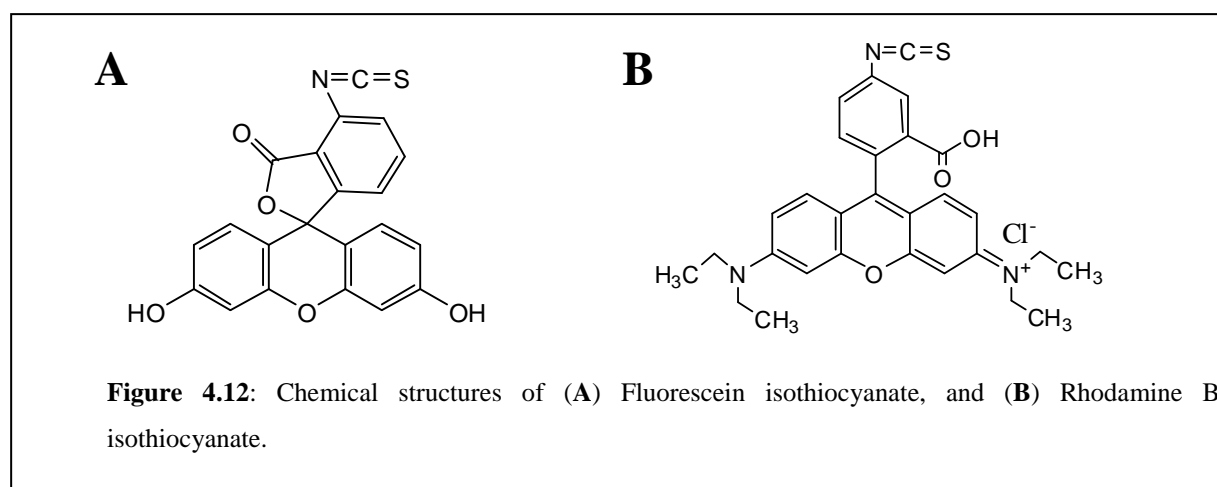
4.5.3 Analysis

4.5.3.1 Degree of substitution

Degree of substitution was determined using ^{1}H-NMR analysis according to the procedure described in Section 3.3.3.1.

4.5.3.2 Fluorescence spectroscopy

The presence of the RITC group on the backbone of cationic modified starch was verified using a Perkin Elmer LS 55 Luminescence Spectrometer. The optimum excitation and emission wavelengths were also determined.

4.5.3.3 Fluorescence microscopy

In order to observe the oppositely charged layer formation on PCC, samples were prepared where FITC-anionic starch was first attached onto the filler followed by RITC-cationic starch. The PCC was centrifuged and washed 3 times with DDI water after each treatment and wet samples observed using the fluorescence microscope specified in Section 3.4.3.3.

4.5.3.4 Thermogravimetric analysis (TGA)

Thermogravimetric analysis was performed on layered PCC samples using a Perkin Elmer TGA 7. The temperature was ramped from 20 ^{o}C to 920 ^{o}C at a rate of 20 ^{o}C/min in an inert atmosphere.

4.5.3.5 Zeta potential

Most solid particles dispersed in an aqueous phase will acquire a surface charge, either by ionization of surface groups or adsorption of charged species. These surface charges change the distribution of surrounding ions, causing the formation of a layer around the particle that is different to the overall charge of the bulk solution[35, 36]. This is known as the interfacial double layer consisting of a Stern layer and a Guoy-Chapman layer. The Stern layer is the

dense layer of ions, opposite in charge to the particle surface, located around the particle (Figure 4.13).

Figure 4.13: Electric double layer surrounding solid colloidal particles in an aqueous phase.
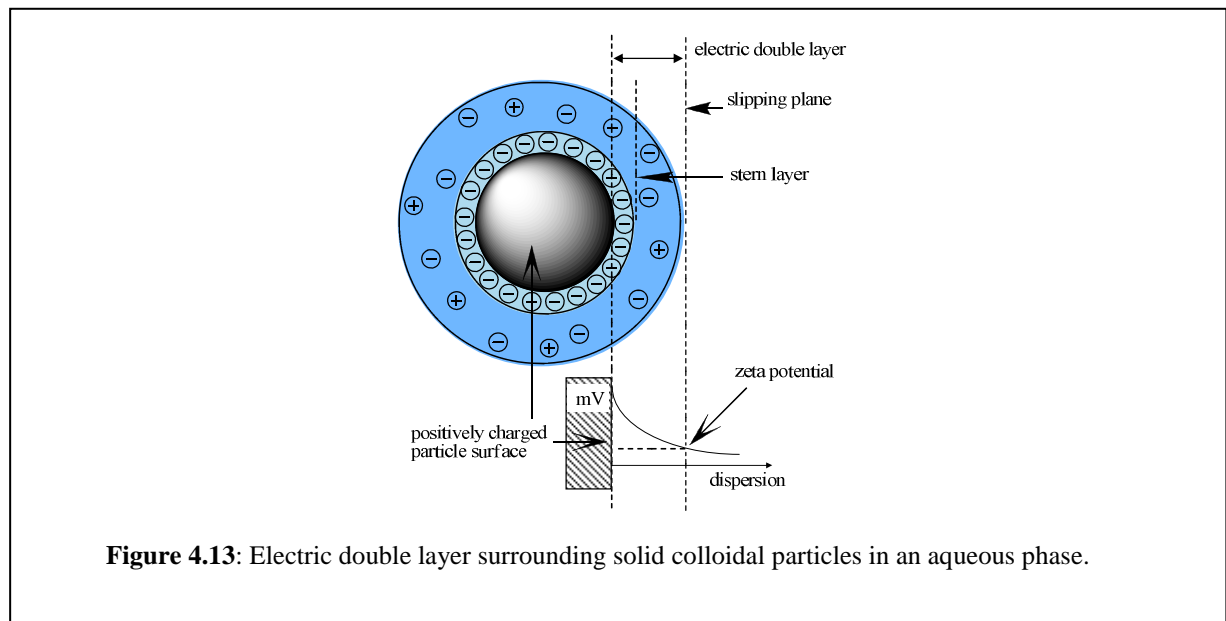
This layer is surrounded by another layer, more diffused than the first, possessing an electrical charge of its own. The slipping plane is found at the point where the charge on this layer moves past that of the bulk solution. This is also referred to as the hydrodynamic shear plane[37] and if the particles move, under Brownian motion, for example, this plane moves as part of the particle.

Zeta potential is the electrical potential in the interfacial double layer at the location of the slipping plane versus a point in the bulk fluid away from the interface. In other words it is the potential difference between the dispersion medium and the stationary layer of fluid attached to the particle. Electrophoretic mobilities of colloidal PCC particles were measured using a Malvern Zetasizer Nano-ZS90 where an electrical field is applied across a dispersion and the rate of migration (usually in m/s) per unit electrical field strength (usually V/s) was measured and converted to zeta potential using the Smoluchowski relation:

$$\zeta = \frac{\mu \eta}{\varepsilon}$$
equation 4.4

where ξ is the zeta potential (in V), μ is the electrophoretic mobility ($m^2V^{-1}s^{-1}$) and η (Nsm^{-2}) and ε (F/m) are the viscosity and permittivity of the solution, respectively.

4.5.3.6 Particle size analysis

Average particle size of PCC particles was measured using a Saturn DigiSizer 5200 as described in Section 3.2.3.1.

4.5.3.7 Scanning electron microscopy (SEM)

Washed and oven dried (50 ^{o}C) layered PCC samples were submitted for SEM analysis using a Leica/Leo Stereoscan S440 electron microscope unit.

4.5.4 Results and discussion

The experimental DS for each modified maize starch sample determined by ^{1}H-NMR are presented in Table 4.3, showing that the RE for the anionic starch to be lower than the cationic modified starch with values corresponding well with typical values obtained after 2 hours reaction time (Figure 3.14).

Table 4.3: Degree of substitution of modified starches used for LbL determined by ^{1}H-NMR

Sample Code	Modification	DS_{th}	DS_{exp}	RE (%)
LBL0.05A	Anionic	0.05	0.013	26
LBL0.40A	Anionic	0.40	0.14	35
LBL0.05C	Cationic	0.05	0.037	74
LBL0.40C	Cationic	0.40	0.25	63

By using the samples LBL0.40A and LBL0.40C to prepare anionic FITC-starch and cationic RITC-starch, the optimum excitation wavelength for maximum fluorescence for each sample was determined by fluorescence spectroscopy and the bimodal peaks observed in Figure 4.14 show both the excitation (first peak) and emission peaks for the modified starches (second peak).

Figure 4.14: Fluorescence spectra of cationic-RITC starch ($DS_{cationic} = 0.4$) and anionic FITC-starch ($DS_{anionic} = 0.4$).
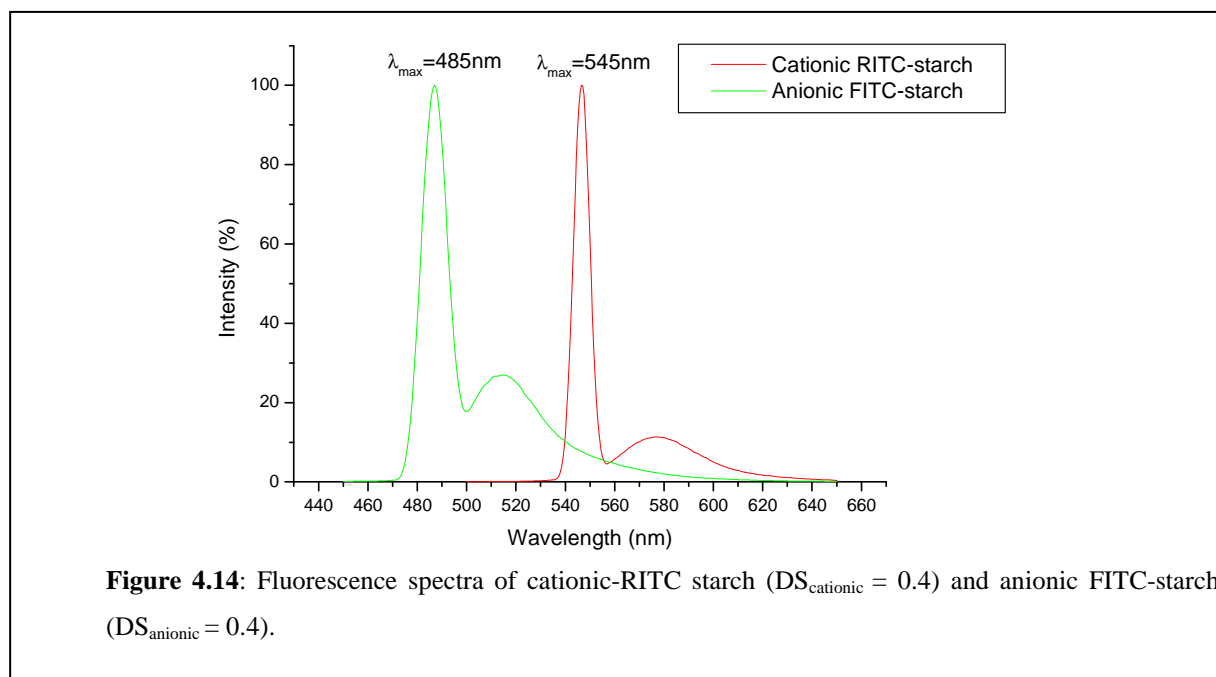
Maximum emission for the anionic FITC-starch was observed with a maximum excitation wavelength (λ_{max}) of 485 nm and emission occurring within the green range of the colour spectrum. Emission of cationic RITC-starch occurred at a higher wavelength (red range) with maximum fluorescence detected at an excitation wavelength of 545 nm. These spectra correspond well with those obtained in literature where similar fluorescence dyes were used[38,][39]. The large difference in emission wavelengths is ideal for simultaneous detection of the individual species on a fluorescence microscope using the adjustable excitation filter and overlaying the images captured to show the location of each of the modified starches.

As an addition to this study, the newly synthesised cationic RITC-starch (1 ml of a 0.5 wt% aqueous solution) was first treated to an aqueous fibre solution (10 g, 2 wt% TSC) to determine ionic interaction and visibility of the modified starch on the fibre surface. Figure 4.15 presents optical, fluorescence, and overlay images of a treated fibre surface.

The imaging compared well with the results obtained with cationic FITC-starch (Figure 3.22) with clear presence of the polymer visible on the fibre surface. Once again a higher concentration starch is detected at a point of fibrillation, indicated by the brighter areas.
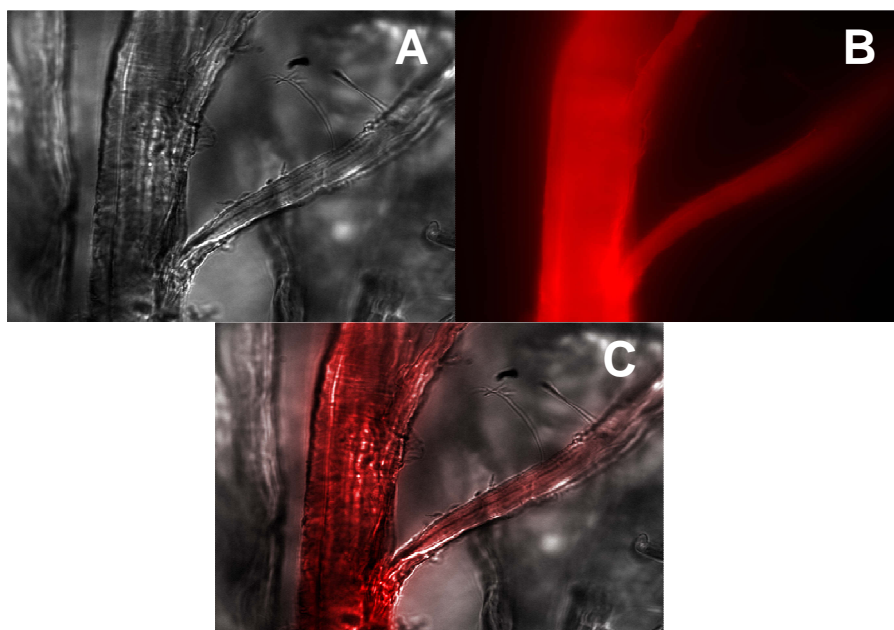
Figure 4.15: Microscope images of fibres treated with cationic RITC-starch [**A**-optical microscope, **B**-fluorescence microscope, **C**-overlay image].

By performing LbL assembly onto PCC using the fluorescent ionic modified starches, imaging was conducted after each layer. Starting with the anionic FITC-starch, the first layer is shown as green on the filler surface (Figure 4.16A). The fluorescence changes to an orange-red hue after the second layer (Figure 4.16B), indicating adsorption of the cationic starch on the first layer. After the third layer anionic starch, the colour returns to a green colour (Figure 4.16C), with the second layer still visible as reddish-yellow areas.

The presence of starch on the PCC surface was also validated by treating the layered PCC with an I_2/KI solution. The white filler surface turned from light blue to a dark violet colour as more layers was added.

In order to compare the effect of the DS on the amount of starch adsorbed on the filler surface, cleaned dry samples of PCC-LBL0.05 (encapsulated in 2 layers LBL0.05A and 1 intermediate LBL0.05C layer) and PCC-LBL0.40 (encapsulated in 2 layers LBL0.40A and 1 intermediate LBL0.40C layer) was submitted for thermogravimetric analysis (TGA).
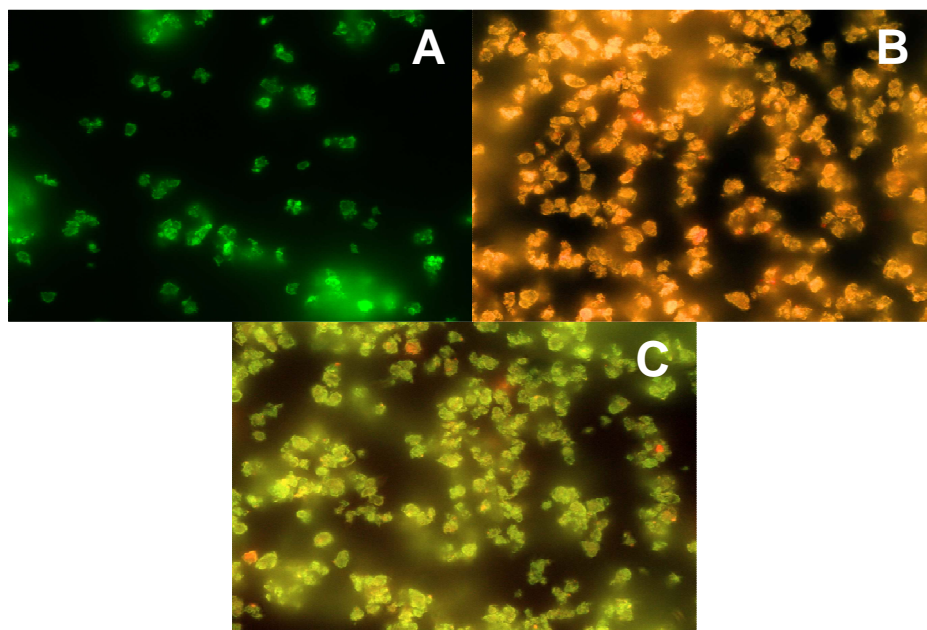
Figure 4.16: Fluorescence imaging showing PCC after treatment with a layer anionic FITC-starch (**A**), followed by another cationic RITC-starch layer (**B**), and a third layer anionic FITC-starch (**C**).

Pure PCC (standard) showed thermolysis starting at 600°C, corresponding well with literature where a heating rate of 20 $^{\circ}$C/min was utilised[40] (Figure 4.17). By comparing this with the layered PCC samples, a small weight loss was already noticed from 50-100°C with a more significant thermal decomposition observed starting at 300°C, corresponding to the decomposition temperature of starch[41].
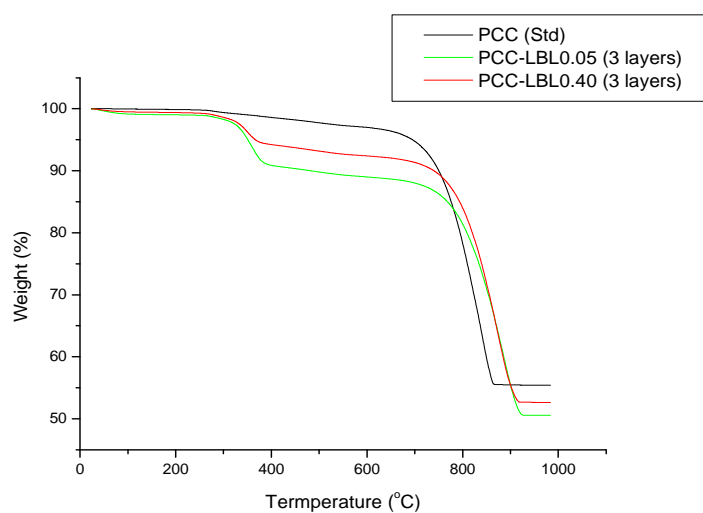
Figure 4.17: TGA of pure PCC and PCC encapsulated in 3 layers of modified maize starch. The DS_{th} of starches used for PCC-LBL0.05 and PCC-LBL0.04 was 0.05 and 0.4, respectively.

The small initial weight loss could therefore be ascribed to evaporation of water, due to the hygroscopicity of the starch. The TGA curve for sample PCC-LBL0.05 showed a higher percentage weight loss of starch compared to PCC-LBL0.40, suggesting a higher percentage starch on the surface of the filler. This can be ascribed to the difference in DS. A lower DS denotes a lower concentration charge on the starch backbone, requiring a larger amount of starch to neutralise the surface charge of the PCC.

Figure 4.18: Schematic illustration suggesting a greater degree of starch adsorption and molecular extension in the case of a low-charge anionic starch on a positively charged PCC surface.
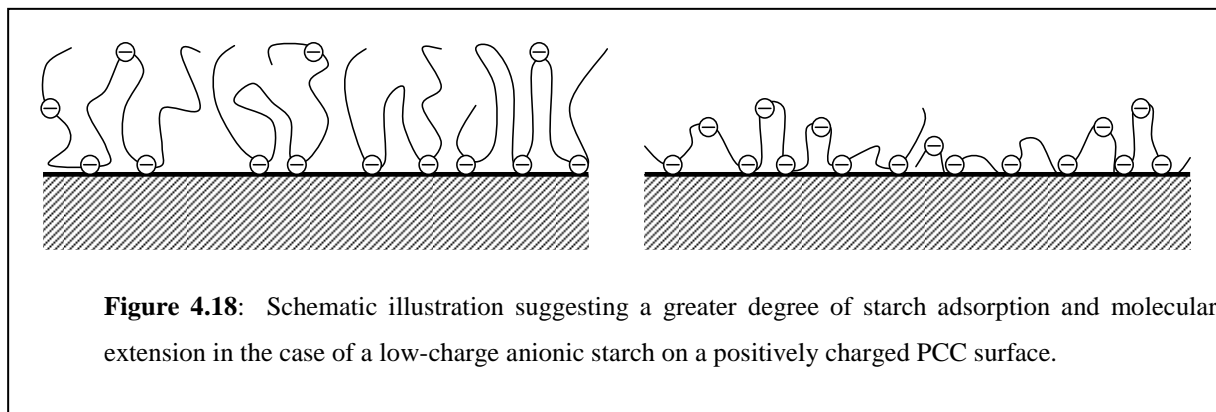
As depicted in Figure 4.18 higher levels of charge tend to reduce the amount of adsorbed polymer and provides a higher driving force for it to lie down flat on the positively charged filler surface.

From the TGA spectra another interesting phenomenon was observed. The starch encapsulated PCC samples appeared to shift the thermal decomposition of the filler to a higher temperature. This is easier observed by differentiating the TGA curves with respect to temperature (Figure 4.19). The polymer shell surrounding the PCC appears to protect the filler by improving its thermal stability, increasing the decomposition temperature with at least 50°C.

Change in the PCC surface charge as a function of starch addition for the first two layers was studied using zeta potential in order to determine the charge saturation points for each ionic additive. The zeta potential of pure PCC, having an overall weak cationic charge of about 6mV, rapidly started dropping to 0 mV as anionic starch (2 wt% solution) was added, and it is at this isoelectric point of negligible net repulsive surface charge that severe flocculation of PCC was observed (Figure 4.20).

107
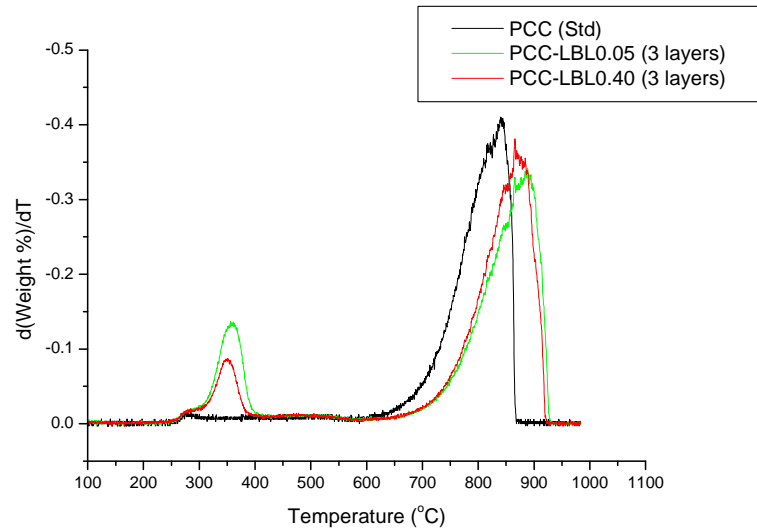
Figure 4.19: Differentiated TGA curves of pure PCC and PCC encapsulated in 3 layers of modified maize starch. The DS_{th} of starches used for PCC-LBL0.05 and PCC-LBL0.04 is 0.05 and 0.4, respectively.

The zeta potential dropped further, getting increasingly negative to a saturation point where further polymer addition had negligible effect on the values.
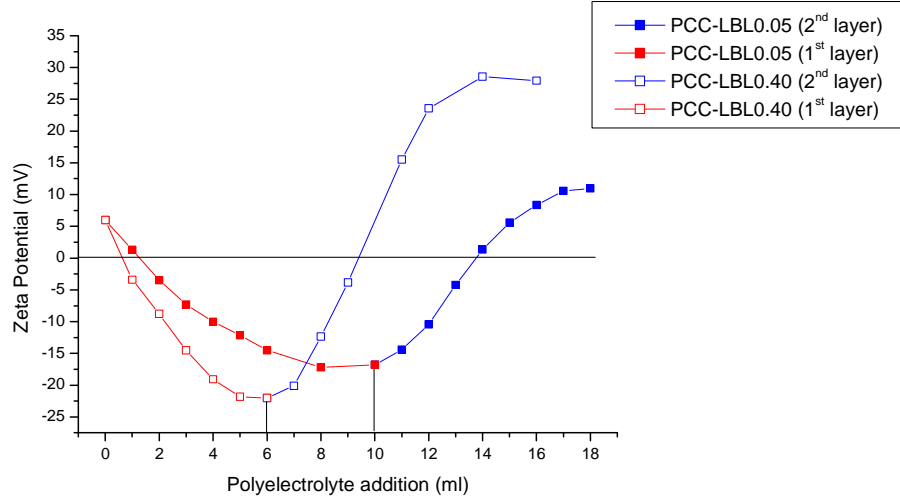
Figure 4.20: Zeta potential change as a function of polyelectrolyte addition during consecutive 2 wt% anionic and cationic solution additions, indicating saturation points after each layer formation.

Compared to LBL0.05A, the higher charge density of LBL0.40A caused a lower polymer demand to neutralise the filler surface, whilst providing a higher concentration negatively charged ions within the particle's slipping plane, hence the lower zeta potential. After 3 washing cycles (to remove any excess polyelectrolytes) cationic starch solution was added. A similar observation was made where the zeta potential increased rapidly for PCC-LBL0.40, becoming saturated at a much higher positive value, compared to PCC-LBL0.05.

By continuing the layering process, a total of 5 layers were added onto the surface of PCC and Figure 4.21 presents the saturation points after each layer. Upon reaching the saturation point, re-dispersion after centrifugation and washing became increasingly difficult as more and more layers were formed. Polyelectrolyte-induced bridging may produce particle aggregates predominantly caused by the centrifugation cycles. This process forces starch layers of adjacent particles together, and due to the adhesive nature of starch, resulted in filler particle aggregation. This does not necessarily pose a detrimental effect in the paper making process, since filler flocculation is one of the mechanisms used for achieving higher filler retention during the wet end of the sheet forming process.

Figure 4.21: Zeta potential saturation points after consecutive 2 wt% anionic and cationic solution additions, indicating saturation points after each layer formation.
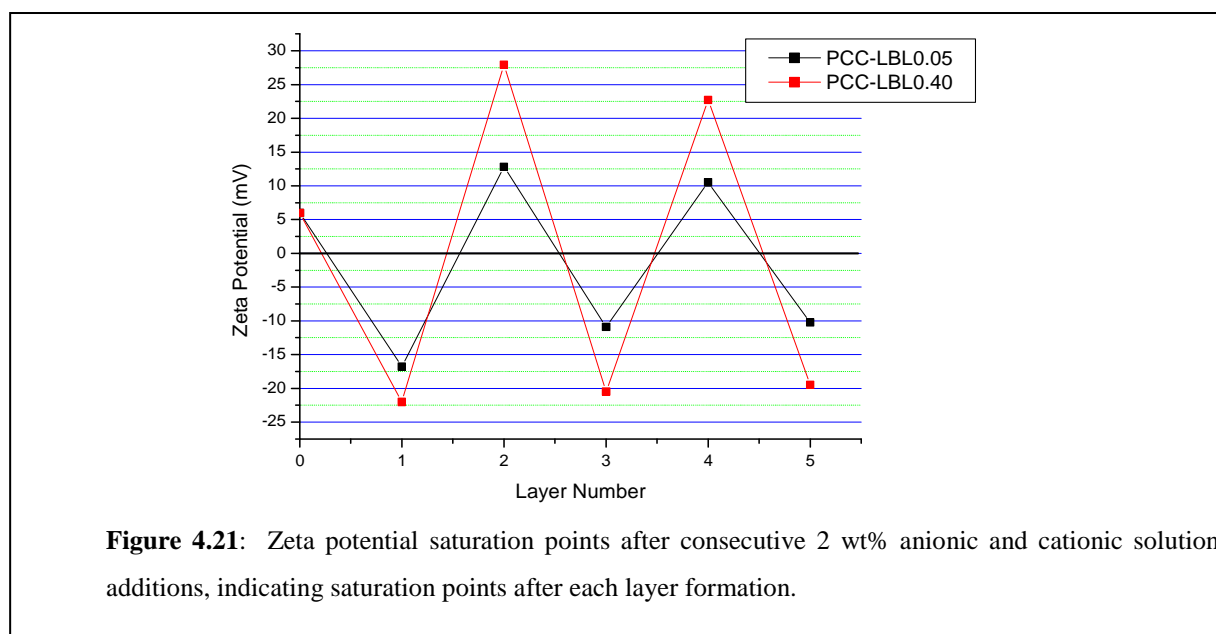
Figure 4.22 shows the particle size distribution of the filler for samples PCC-LBL0.05 and PCC-LBL0.40 after adsorption of three layers. Already a significant amount of aggregation

was observed if compared to pure PCC, and in the case of PCC-LBL0.05 the distribution was significantly wider than PCC-LBL0.40, affirming the higher concentration starch on the filler surface, which caused the particles to become increasingly adhesive, and hence more aggregated.

Figure 4.22: Particle size distribution of starch layered (3 layers) PCC (using LBL0.05 and LBL0.40) compared to pure PCC.
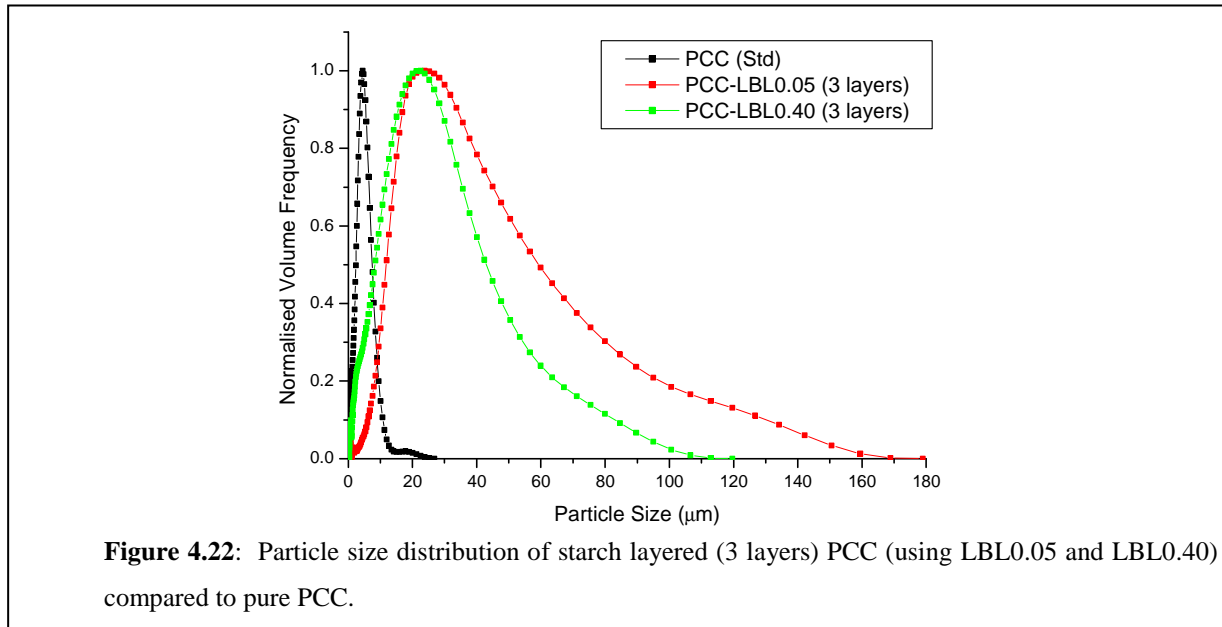
It is difficult to determine layer thickness using light scattering techniques, not only due to the aggregation, but also because the polymer layers adsorbed onto the 3µm (average particle size) filler particles are normally only a few nanometers thick[28], making the increase in particle size negligible.

Scanning electron microscopy of PCC-LBL0.05 and PCC-LBL0.40 (3 layers) presented filler particles with a smoothed surface, compared to pure PCC (Figure 4.23) and more noticeably it is observed how these filler particles are bonded together by starch as aggregates, with PCC-LBL0.05 exhibiting significantly enhanced particle fusion due to its higher starch content.

The interaction of the two 3-layered PCC samples with fibres was also investigated. The fibre (2 wt% dispersion in DDI water) was first treated with a 5 wt% cationic starch solution (0.8 wt% based on dry pulp) after which PCC-LBL0.05 and PCC-LBL0.40 (anionic outer layer) was added (25 wt% based on dry pulp). After 5 min mixing a sample of each was dried and submitted for SEM. Imaging indicates enhanced filler-fibre interaction for sample PCC-

LBL0.40 compared to PCC-LBL0.05 (Figure 4.24A and B). Although the latter sample had a higher starch concentration on the filler surface, the overall charge available for interaction with the cationic starch attached to the fibre was lower, resulting in lower retention.

Figure 4.23: SEM images showing (**A**) PCC filler particles (standard) (scale bar = 300 nm), (**B**) PCC-LBL0.05 (3 layers) (scale bar = 1 µm), and (**C**) PCC-LBL0.40 (3 layers) (scale bar = 1 µm).
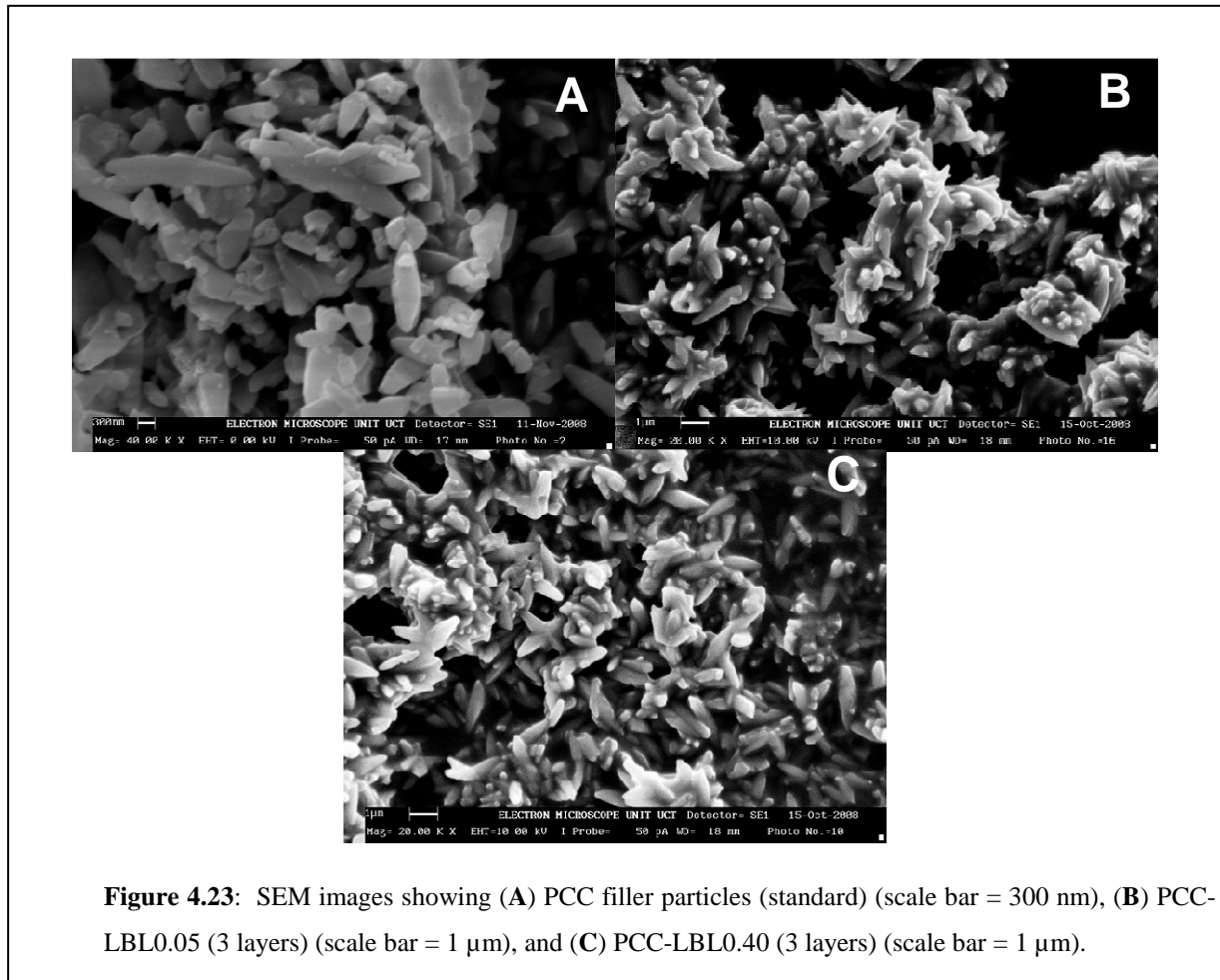
A closer magnification of PCC-LBL0.40 on the fibre surface (Figure 4.24C) showed the presence of starch 'strings' bonding the PCC to the fibre, indicating the effective use of multiple layers ionic modified starch to, not only bond filler particles to each other for easier entrapment in the porous filler matrix during web formation, but has also acted as an adhesive for bonding PCC to fibres. Ultimately the true effectiveness of incorporating layered PCC into the paper making process is in its capability to improve the mechanical properties of paper. Therefore a sample of PCC-LBL0.40 (3 layers) was submitted to Mondi, Austria for testing in paper hand sheets and results will be discussed in Chapter 6.
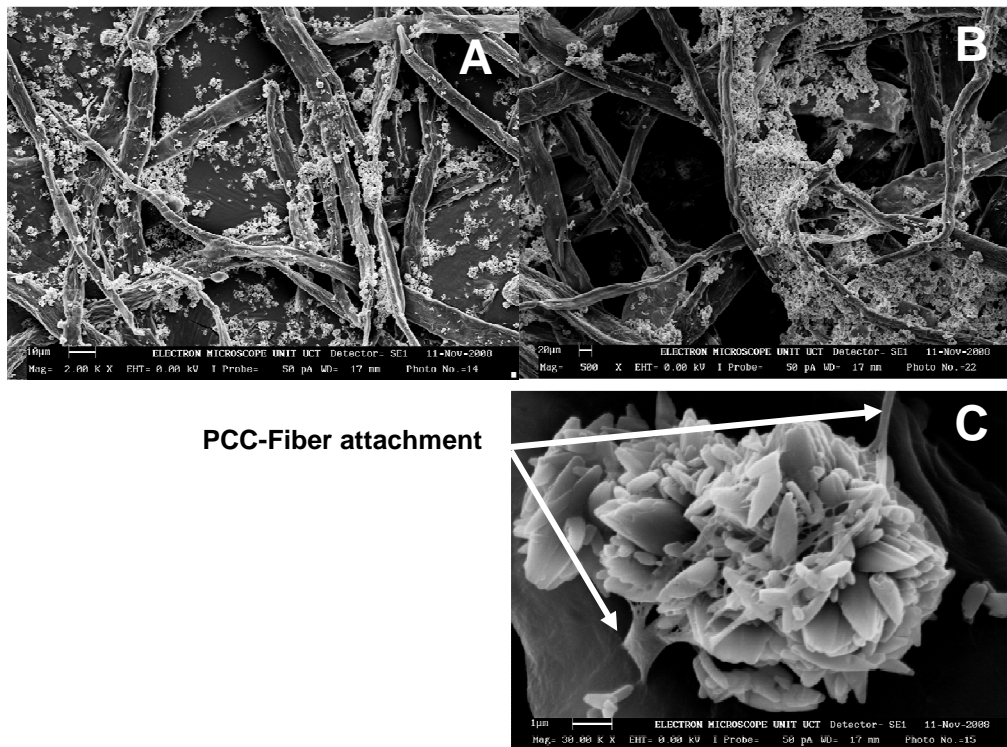
Figure 4.24: SEM imaging showing interaction of fibres (pretreated with 0.8 wt% cationic starch) with 25 wt% PCC-LBL0.05 (**A**) (scale bar = 10 µm), PCC-LBL0.40 (**B**) (scale bar = 20 µm), and a higher magnification of PCC-LBL0.40 (**C**) (scale bar = 1 µm) showing filler-fibre attachment.

From a processing point of view, the LbL technique is difficult to commercialise due to the extensive centrifugation and washing steps required after each starch layer was adsorbed. However, by determining the exact saturation point for each layer, deposition can be made using polyelectrolyte concentrations just beyond the onset of zeta potential saturation[28], whilst having control over filler particle aggregation.

A single batch reactor system or even a continuous plug flow system (Figure 4.25) would therefore be sufficient to continuously add consecutive polyelectrolytes of opposite charge to the PCC slurry prior to addition at the wet end of the paper making process. The concept requires that adequate adsorption efficiency can be achieved and the main decisions to be made involve the order of addition and the amount of material that is added in each step. Too little polyelectrolyte would be considered undesirable, since a strong reversal of net surface charge is required at each step in order to render the surface attractive to the subsequent

oppositely charged layer. Addition of too much polyelectrolyte, on the other hand, would allow an excess of un-adsorbed polyelectrolyte to be present in the system and this would be subject to uncontrolled complexation with the next oppositely charged treatment, before having the chance to reach the PCC surface.

Figure 4.25: Concept of how self-assembly of multi-layers onto PCC can be applied in a continuous process, with on-line control of dosage levels and optimization of streaming potential.
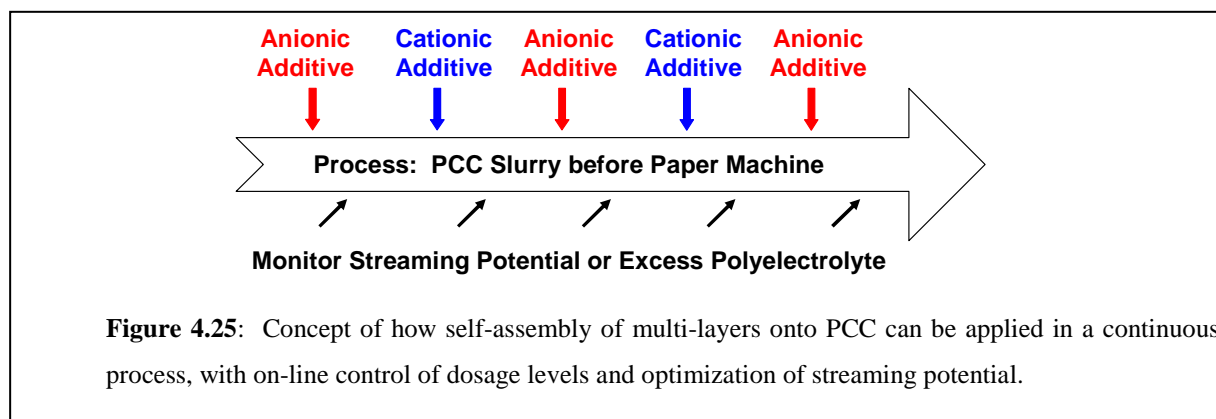
In order to demonstrate the effect of polyelectrolyte over-charge a sample of PCC-LBL0.40 was prepared where polyelectrolyte additions were made with at least a 20 vol% additional polyelectrolyte treatment past the onset of each zeta-potential saturation point and without intermediate centrifugation and washing. Figure 4.26 presents SEM images of starch-based particles that formed as a result of complexation of excess polyelectrolytes in the system. Notice from an enlarged image of one such particle (Figure 4.26B) the protrusion of some encapsulated filler particles.

Figure 4.26: SEM imaging showing starch complex particle formation (**A**) (scale bar = 1µm) and close-up (**B**) (scale bar = 1µm) after polyelectrolyte over-charge in preparing PCC-LBL0.40 (3 layers) without centrifugation and washing.
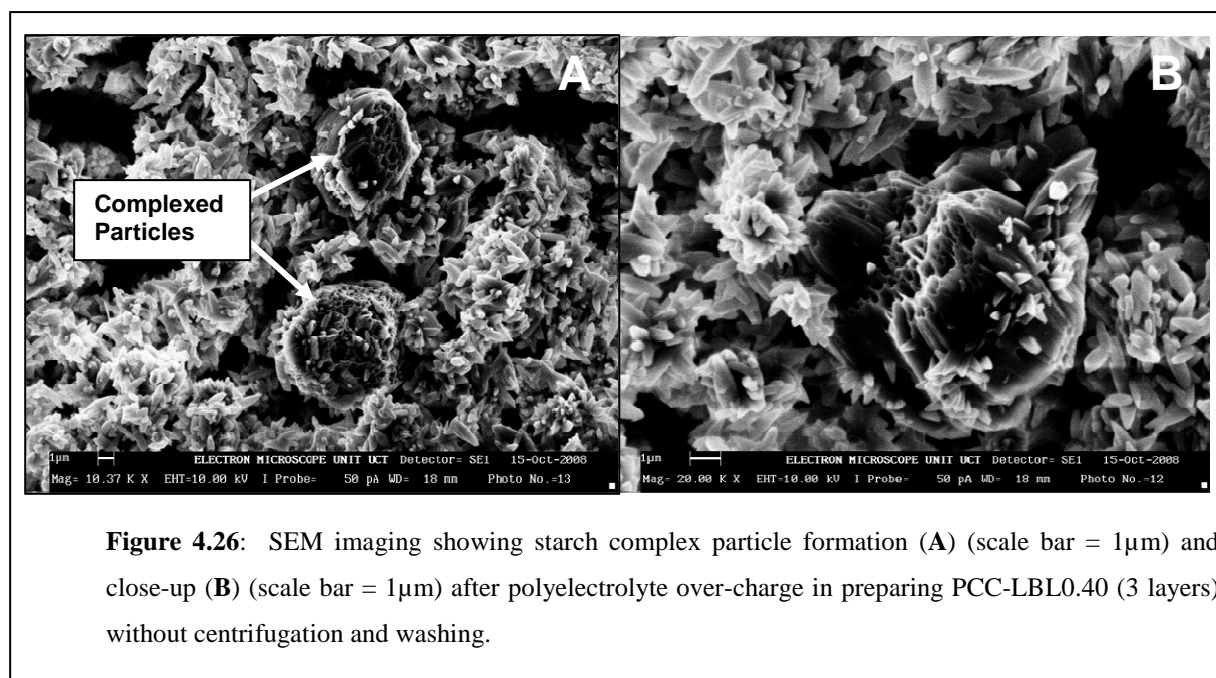
The presence of these complex particles might not adversely affect the mechanical performance of paper and might even improve it further, but it is best to avoid its formation, since there is little control over particle size and distribution as it increases in size after each layer deposition. Furthermore, such interactions would defeat the goal of achieving multilayer self-assembly.

Fortunately, electrokinetic methods are available for monitoring and controlling levels of polyelectrolyte addition during preparation. One such method involves the titration with a highly charged polyelectrolyte in order to determine the net colloidal charge of the bulk solution, after a given treatment step. Automated systems are available for such tests, using streaming current measurements as an indication of the titration endpoint[42, 43]. This enables one to control the added amount of polyelectrolyte, in each step, so that a very small controlled excess of that polymer remains in solution after mixing with PCC.

4.6 In-situ cross-linking and anionic modification of granular maize starch

4.6.1 Introduction

In all the previous sections, synthesis of polysaccharide particles and multi-layered filler particles required preparation of gelatinised polysaccharide solutions for anionic, cationic, and allyl modifications. From a processing point it is extremely difficult to handle these high viscosity solutions especially during carboxymethylation. Although the use of more diluted starch solutions may assist in lowering viscosity, it may also cause retrogradation, prompting polysaccharide precipitation and particle agglomeration. Furthermore the viscosity of CMS is already difficult to blend at a concentration of 10 wt% in water due to its hydrophilic character, which increases even further with higher substitution degrees, resulting in lower modified starch yields per batch. The precipitation and washing steps following modification pose an even greater challenge for industry due to its great demand for cleaning solvents and handling of the highly adhesive precipitated pastes.

Since starch (eg. maize starch) is already in granular form, it makes little sense to gelatinise it in order to prepare just another particle again. Ionic modification would however be difficult to achieve if the starch is in a solid granular form, where reaction would occur exclusively at the particle surface. However, partial swelling of the granules in water below its gelatinisation point would allow mobility of reactants through the granule without destroying its overall structure. For CMS it is not possible to achieve substitution degrees beyond 0.07 whilst retaining granular integrity due to the increase in water solubility of starch at higher DS values. Significantly higher DS values can however be achieved if a starch swelling retardant such as sodium sulphate or sodium citrate[44] is added to the media, although very high concentrations is required to achieve this. Using an essentially non-aqueous dispersion media overall allows enhanced control over swelling even for producing CMS beyond a DS of 1[45]. Suitable solvents include ethanol, methanol, 1-propanol, 2-propanol, or any lower alkyl alcohols as well as acetone[46]. These solvents are compatible with water, but will not dissolve starch. Studies show that the optimum solvent to water ratio for achieving the highest reaction efficiency is between 90:10 and 80:20 (v/v)[47, 48].

A novel approach was taken in this study whereby the partially swollen granules were cross-linked with a bi-functional cross-linker, such as ECH, prior to ionic modification. This would ensure the final product remains in particulate form after preparing aqueous dispersions. Once the reaction was complete, the excess reagents and by-products could easily be removed by filtration and rinsing the particles in an 80:20 (v/v) solution of alkyl alcohol (or acetone) and water. Additionally, the particle size of swollen granules could be reduced using ultrasonication, homogenisation, or any other high shear agitation.

4.6.2 Experimental

4.6.2.1 Materials

Maize starch (Acros, Cat: 24,073) was dried before use. Acetone (Kimix, CP grade), SMCA (Fluka, Cat: 24,610), ECH (Merck, Cat: 8032,960), NaOH (Merck, Cat: SAAR5823160 EM), HCl (Merck, Cat: SAAR3063040 LP), and $AgNO_3$ (N.T. Analytical Reagents, Cat: R2810) were used as received.

4.6.2.2 Preparation of swollen cross-linked CMS granules

In preparing in-situ cross-linked (ISXL) particles having a $DS_{anionic} = 0.4$ and cross-linked with 3 wt% (based on dry starch) ECH, 20 g maize starch was loaded to a 500 ml round-bottom flask followed by the addition of 91 ml acetone. The starch was slurried in an enclosed system, while 1.26 g NaOH was dissolved in 9 ml DDI water [solvent to water ratio of 90:10 (v/v)]. The NaOH solution was added dropwise over 10 min to ensure gradual swelling of starch, thereby avoiding gelatinisation. The flask was fitted with a condenser and the mixture heated to 56 ^{o}C after which 0.60 g ECH was added. After 1 hour reaction time, a further 8.31 g NaOH was added followed by 5.75 g SMCA. After 2 hours the mixture was neutralised (pH 7) using 26.55 g HCl and heating removed. The modified starch granules were allowed to cool overnight under continuous stirring.

The modified starch slurry was filtered in a glass sinter filter to remove the dispersion media, after which continuous loadings of an 80:20 (v/v) blend of acetone and water were filtered off to remove by-products and excess reagents until no excess chloride could be detected in the filtrate, identified as AgCl precipitate following treatments of $AgNO_3$. A final addition of pure acetone was made to remove excess water still present in the granules.

After drying the filtrand in an oven at 50°C, a white powder was collected, resembling the native maize starch powder used for modification. Formulations for preparing swollen ISXL maize starch particles with various DS and percentage ECH appear in Table A4, Appendix A.

4.6.3 Analysis

4.6.3.1 Degree of substitution

Both ^{1}H-NMR (Section 3.3.4.2) and back titration (Section 4.3.3.3) techniques were used and compared in determining the reaction efficiency of the anionic modification.

4.6.3.2 Optical microscopy

Optical microscopy was performed as described in Section 4.2.3.1.

4.6.3.3 Scanning electron microscopy (SEM)

Washed and oven dried (50 ^{o}C) samples were submitted for SEM analysis using either a Leica/Leo Stereoscan S440 or Leo 1430VP Scanning Electron microscope unit.

4.6.3.4 Particle size analysis and flocculation

Average particle size (APS) of swollen starch granules as well as flocculated PCC particles were performed using a Saturn DigiSizer 5200 as described in Section 3.2.3.1. Measurements of starch and PCC were performed using two separate models, which were based on the refractive indices of starch and $CaCO_3$.

To determine if the Digisizer instrument was reliable for measuring a starch particle system, a comparison was made by applying conventional robust techniques, such as Scion Image Alpha 4.0.3.2 (Section 4.3.3.2) or AnalySIS 5.0 (Olympus) software image processing and analysis programs for determining APS and distribution of pure maize starch granules.

In Figure 4.27A a SEM image of dry starch was used for determining size using AnalySIS 5.0 processing and counting a total of 230 particles as indicated. The APS of 14.4 µm estimated using this technique compared very well with the 15.1 µm determined using the Digisizer, with less than 5% deviation. The particle size distribution was also in reasonable agreement (Figure 4.27B), although image processing for accurately determining the size of finer particles is difficult from a SEM image (poor visibility). The slightly wider distribution of particles measured using the Digisizer could be attributed to the fact that these particles are measured in an aqueous solution, as opposed to SEM imagery which was performed under vacuum. Although native starch is essentially cold water insoluble, it does possess some hygroscopic character which would allow it to swell slightly when exposed to moisture. It could ultimately be concluded that the light scattering techniques used by the Digisizer were sufficiently accurate in determining APS and distribution for this system and was used exclusively for further analysis.

All ISXL starch samples were prepared by first mixing 2 wt% dried sample in DDI water and heating the solutions to 90°C for 2 hours, which allowed sufficient time for particles to

become fully swollen. The solutions were mixed at ambient temperature for a further 48 hours before particle size analysis on the Digisizer was performed.

These solutions were also used for flocculation studies, where 1.12 wt% solutions of PCC filler were prepared followed by the addition of 2 wt% (based on dry PCC) modified starch. This was mixed for a further 48 hours to allow sufficient time for flocculation to occur.

Figure 4.27: Determination of average partice size (APS) of pure maize starch particles using SEM imaging and AnalySIS 5.0 software (**A**) and comparison of particle size distribution as determined by AnalySIS 5.0 software and Saturn Digisizer (**B**).
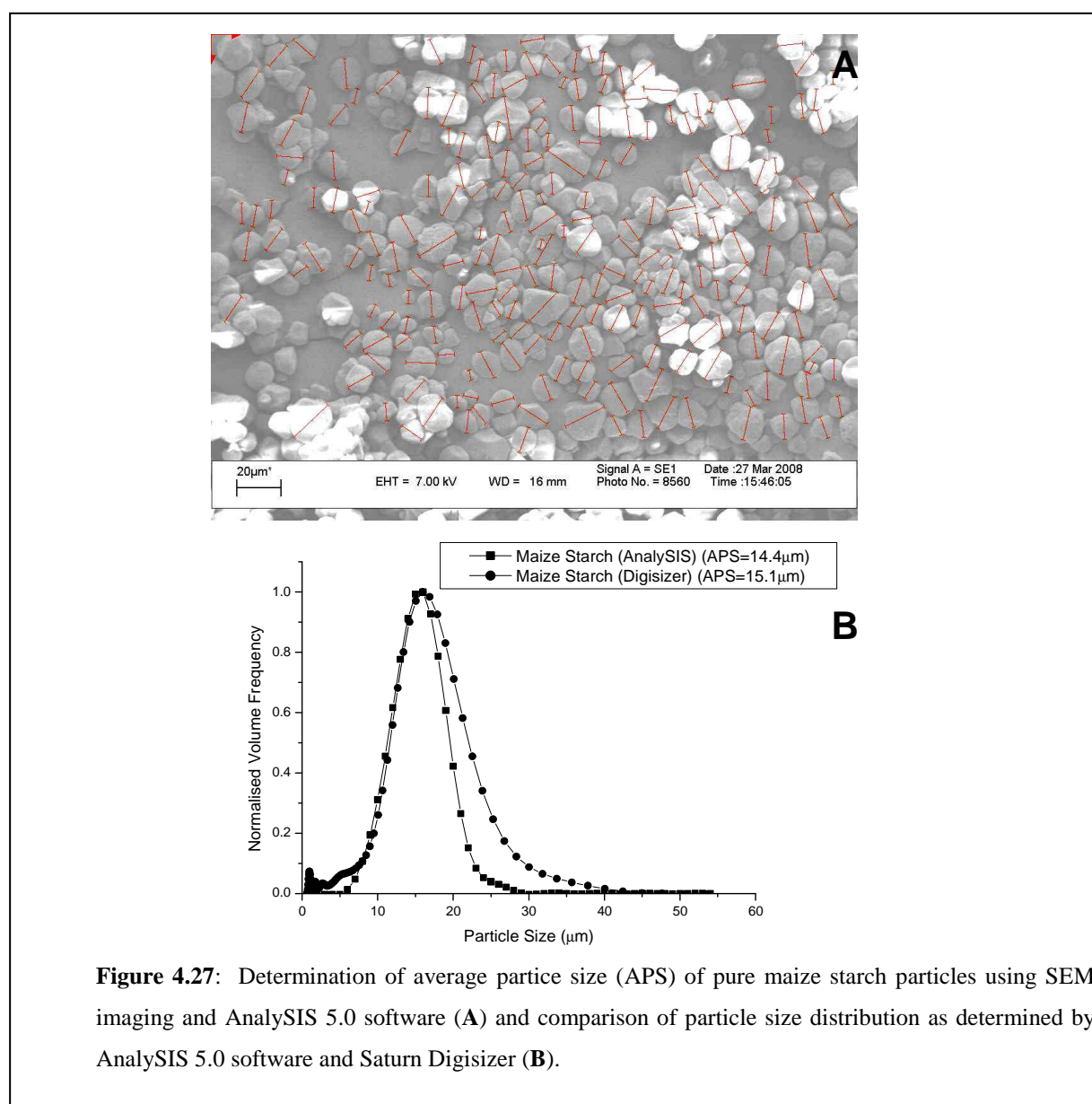
4.6.3.5 X-ray diffraction

Native starch granules inherently contain amorphous and crystalline regions, where the latter is due to structured areas around the hilum where amylopectin chains are more radially

orientated. The crystalline region typically comprises 20 – 25% of the volume of the starch granule as determined by X-ray diffraction techniques[49, 50]. Crystallinity is essentially destroyed once granules gelatinise and only partially recovered over a long period of time during retrogradation[51].

The effect of partial swelling and modification of starch granules on crystallinity was investigated to determine if any changes can be related to its performance in paper hand sheet mechanical properties. Dry powder samples were analysed using a wide angle Bruker D8 ADVANCE powder diffractometer with a Bragg-Brentano geometry and radiating samples with a Nickel filtered Cu k_{α} ($\lambda = 0.15406$nm) emission source at room temperature with a 2θ range of $5 – 50^{\circ}$ and measurement time of 5 s per 2θ intervals.

4.6.3.6 Gel point

The degree of swelling of ISXL particles was compared to native maize starch by measuring the increase in viscosity as a function of temperature. This was done using an Anton Paar MCR-501 rheometer (Paar Physica) fitted with a C-ETD160/ST starch cell with ST24/2D-2V-2V starch cell stirrer and the temperature of 10 wt% particle dispersions in DDI water was increased at a rate of 3 $^{\circ}$C/min from 20 – 95 $^{\circ}$C.

4.6.3.7 Swelling power

The swelling power of ISXL starch particles was expressed as the percentage increase in the average particle size of swollen granules compared to the dry starch particle size, as determined by particle size analysis. The equation used was as follows:

$$Swelling(\%) = (\frac{APS_{ss} - APS_{ds}}{APS_{ds}}) \times 100 \qquad\qquad \text{equation 4.5}$$

where APS_{ss} is the average particle size of the swollen starch granules and APS_{ds} is the average particle size of the dry native maize starch.

4.6.4 Results and discussion

Similar to Section 3.3.4.4 a study was conducted to compare how the experimental DS of carboxymethylation changed as a function of time using the technique of in-situ cross-linking versus preparing gelatinised CMS solutions. Following cross-linking of the starch particles with ECH, samples were taken periodically after addition of SMCA. Neutralised, washed, and dried samples were submitted for DS analysis using ^{1}H-NMR. Figure 4.28 presents DS values over time for both gelatinised and ISXL (cross-linked with 3 wt% ECH based on dry starch) CMS solutions with theoretical DS of 0.4.

Figure 4.28: Experimental degree of substitution and reaction efficiency of ISXL-CMS starch (with $DS_{th} = 0.4$ and cross-linked with 3 wt% ECH) and gelatinized CMS solution ($DS_{th} = 0.4$) over time.
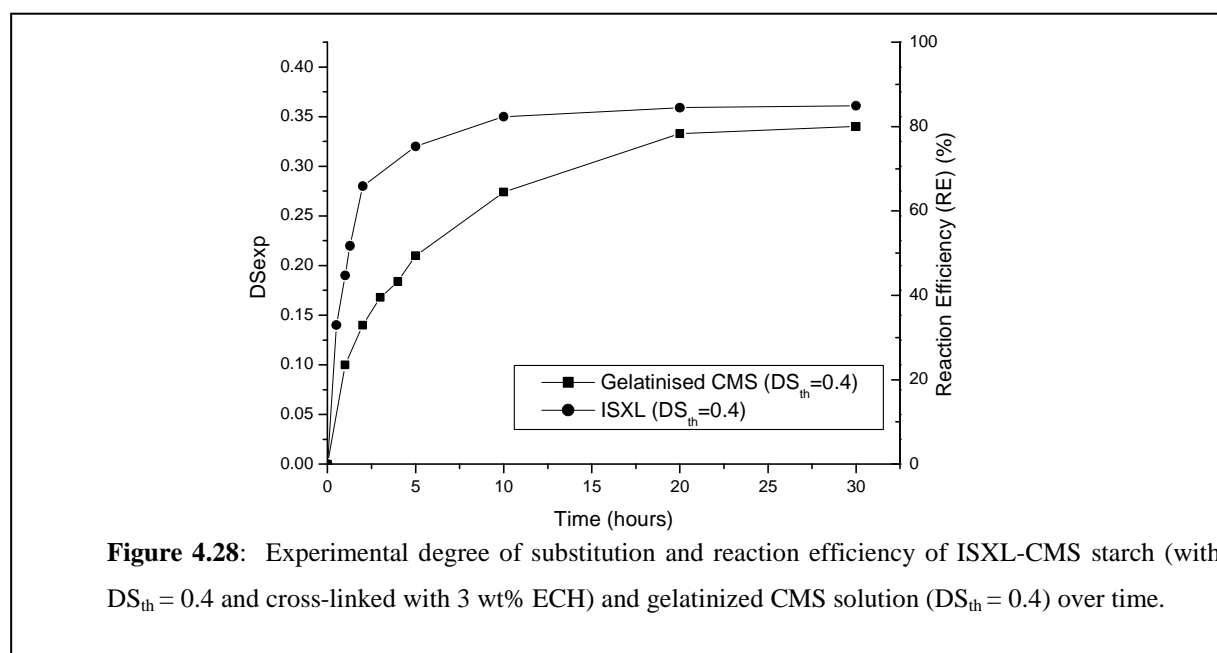
The rate of substitution for ISXL starch particle was significantly higher than gelatinised starch with almost 70% reaction efficiency achieved after 2 hours reaction time. After 10 hours maximum RE was achieved above 80%, which was higher than values achieved for gelatinised CMS. The reason for the higher reaction rate and RE can be contributed to two factors. The first is that the SMCA, which dissolves in water, acetone, and alkyl alcohols, had more mobility to react with hydroxyl groups on starch since excessive increase in swelling (and therefore viscosity) was retarded by the solvent system. Secondly, the NaOH dissolved in the small amount of water used for partially swelling the starch granules was present at a significantly higher concentration inside the swollen composite, since NaOH has only limited solubility in acetone and other alkyl alcohols. This caused the starch to become highly

activated as a starch alkoxide (first step of starch carboxymethylation) for reaction with SMCA[47, 52].

The experimental DS (DS_{exp}) of various ISXL starch samples prepared using different cross-linking degrees and DS_{th} values were determined by back titration with oxalic acid. The results in Table 4.4 indicate that the degree of cross-linking did not appear to influence the RE and percentages typically ranged between 60 and 80%. These values were also comparable to values obtained for other samples (Samples ISXL1 – ISXL8, Table A3, Appendix A), where DS_{exp} was determined using ^{1}H-NMR analysis, indicating that both methods used were comparable.

Table 4.4: DS values and reaction efficiency of various ISXL starch samples determined using back titration with oxalic acid.

Sample	ECH (based on starch) (%)	DS_{th}	DS_{exp}	Reaction efficiency (RE) (%)
ISXL9	1	0.20	0.15	76
ISXL5	1	0.50	0.31	62
ISXL10	1	0.80	0.51	63
ISXL2	3	0.20	0.14	71
ISXL6	3	0.50	0.36	72
ISXL3	3	0.80	0.53	67
ISXL4	3	1.00	0.68	68
ISXL11	6	0.20	0.15	74
ISXL12	6	0.50	0.35	70
ISXL13	6	0.80	0.51	64

Figure 4.29 presents optical microscopy images of native starch granules compared to ISXL particles. Cross-linking of the granules using 3 wt% ECH (no anionic modification) showed swelling of particles after heating to 95°C without indication of granule rupture or gelatinisation.

After anionisation the particles appear to be significantly more swollen due to the hydrophilic character of CMS (Figure 4.29C). However, sonication (20kJ/20ml sample for 4 minutes) could be used to break down these particles to a lower particle size (Figure 4.29D).

Figure 4.29: Optical microscope images of dry maize starch granules (**A**), swollen (at 95°C for 2 hours) starch particles cross-linked with 3 wt% (based on dry starch) ECH (DS = 0) (**B**), swollen anionic ISXL starch particles (6 wt% ECH, DS = 1) (**C**), and anionic ISXL starch particles (6 wt% ECH, DS = 1) after 4 min sonication (12kJ/20 ml sample) (**D**).
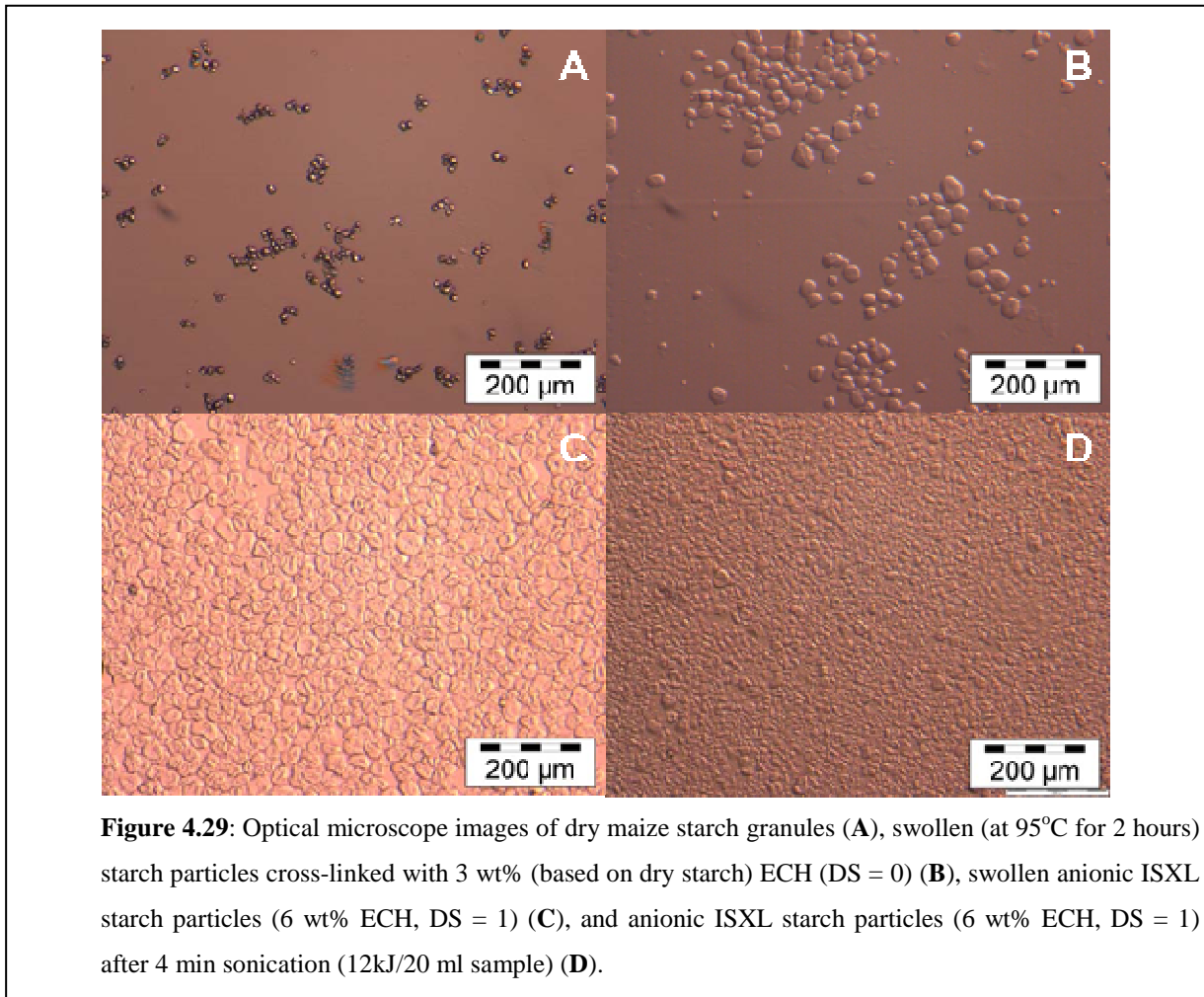
Scanning electron microscopy showed pure maize starch particles to be predominantly polyhedral in shape, with a smooth surface, visible thickness, and a wide size distribution (Figure 4.30A). Cross-linking these particles with 3 wt% ECH using the ISXL technique indicated that the overall integrity of the partially swollen granules remained intact after drying with granules retaining a smooth surface with polyhedral to almost oval shaped granules. The process of anionisation however resulted in increased swelling and, although the particles essentially remained intact, the highly swollen granules deformed during drying with particle walls shown to have collapsed.

The effect of anionisation on the crystallinity of ISXL granules was investigated using XRD analysis of samples (ISXL1 – ISXL4, Table A3, Appendix A) modified with similar percentage cross-linker (3 wt% ECH based on dry starch) and different anionic DS values.
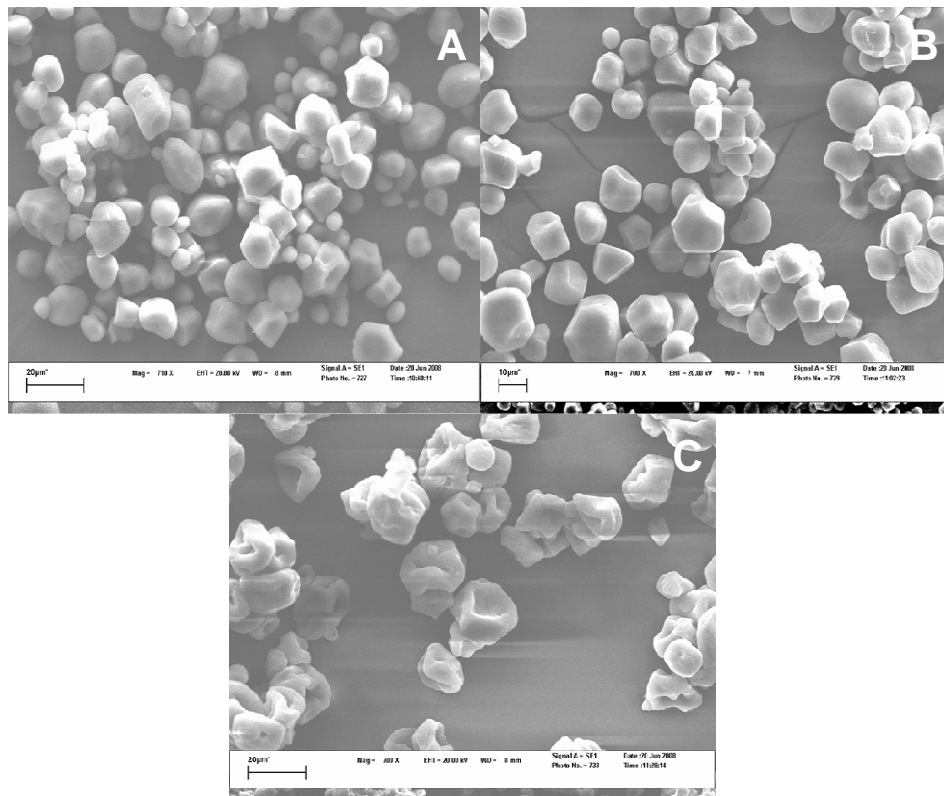
Figure 4.30: SEM images showing native maize starch granules (**A**) (scale bar = 20µm), ISXL starch granules cross-linked (DS = 0) using 3 wt% ECH (based on dry starch) (**B**) (scale bar = 20µm), and anionic ISXL granules with 3 wt% ECH and DS=0.20 (**C**) (scale bar = 20µm).

Figure 4.31 shows 3 strong reflections at 15, 18, and 23° of refraction angle 2θ for native maize starch. These values are in agreement with values reported in literature and indicates that maize starch, like most other cereal starches, have an A-type crystal pattern[53, 54]. Cross-linking of the granules caused a slight decrease in intensity of reflection peaks, although some degree of crystallinity was preserved. Subsequent anionisation drastically diminished all crystalline peaks as the DS was increased and at DS = 0.8 no peaks were present indicating that these particles remained essentially amorphous after modification. The X-ray diffractograms correlated well with SEM results, showing how the morphological change in granules after anionisation caused complete collapse of particles upon drying.

The effect of cross-linking degree and anionic DS on swollen ISXL starch granules' particle size were also studied and Table 4.5 presents the APS and percentage swelling of a selection of these samples.
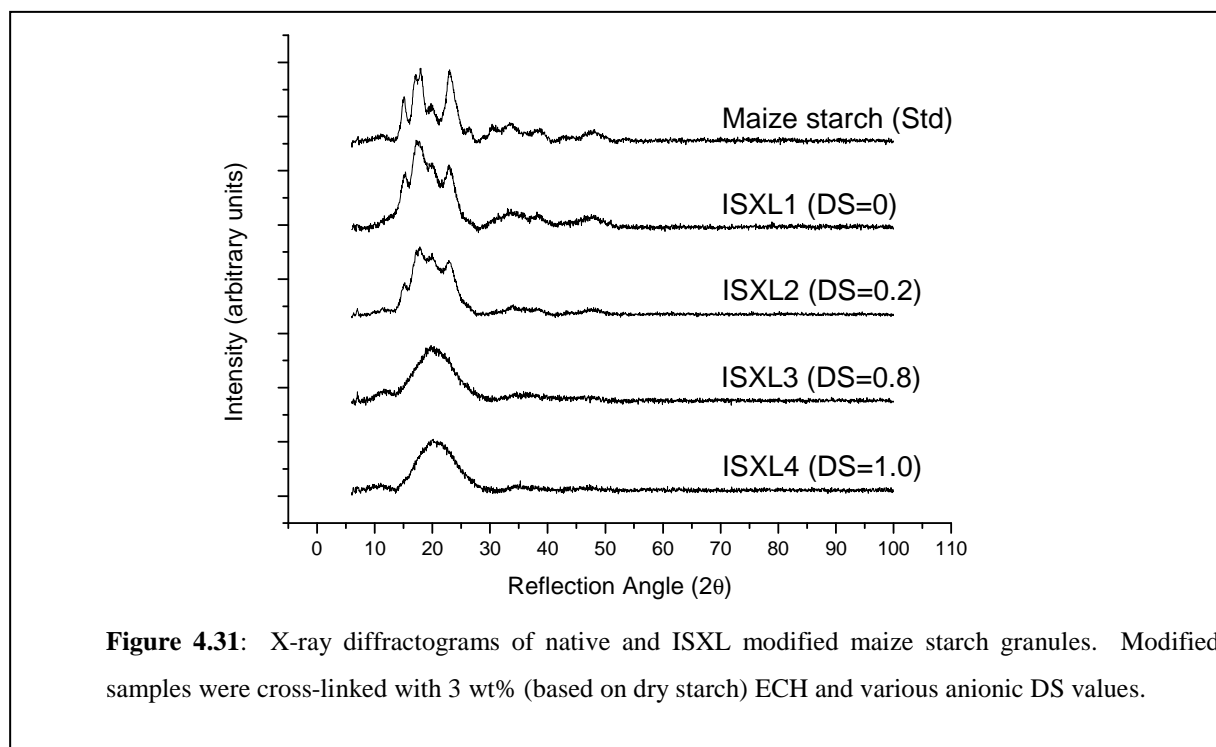
Figure 4.31: X-ray diffractograms of native and ISXL modified maize starch granules. Modified samples were cross-linked with 3 wt% (based on dry starch) ECH and various anionic DS values.

Table 4.5: Effect of percentage cross-linking and anionic DS on particle size and swelling.

Sample	Theoretic Degree of Substitution (DS_{th})	Epichlorohydrin (ECH) (%)	Average Particle Size (APS) (µm)	Swelling (%)
ISXL5	0.5	1	68.4	353
ISXL6	0.5	3	39.2	160
ISXL7	0.5	5	34.7	130
ISXL8	0.5	10	25.1	66
ISXL1	0	3	19.0	26
ISXL2	0.2	3	45.7	203
ISXL3	0.8	3	33.2	120
ISXL4	1.0	3	33.3	121

In samples prepared with DS_{th} values constant ($DS_{th} = 0.50$) and various percentages ECH (between 1 and 10 wt%), a very broad bimodal distribution was recorded where only 1 wt% ECH was used, with swelling averaging up to 353% compared to normal maize starch (Figure 4.32). The bimodality is most probably due to bridging of swollen particles. The swelling reduced significantly as the percentage was increased to 3 wt% with a much narrower

distribution. Further increases in ECH concentrations up to 10 wt% resulted in a further decrease in average particle size and distribution.

Figure 4.32: Particle size distribution of swollen ISXL starch particles with DS = 0.5 and various percentage cross-linking.

Figure 4.33: Particle size distribution of swollen ISXL starch particles cross-linked with 3 wt% (based on dry starch) ECH and various anionic DS values.
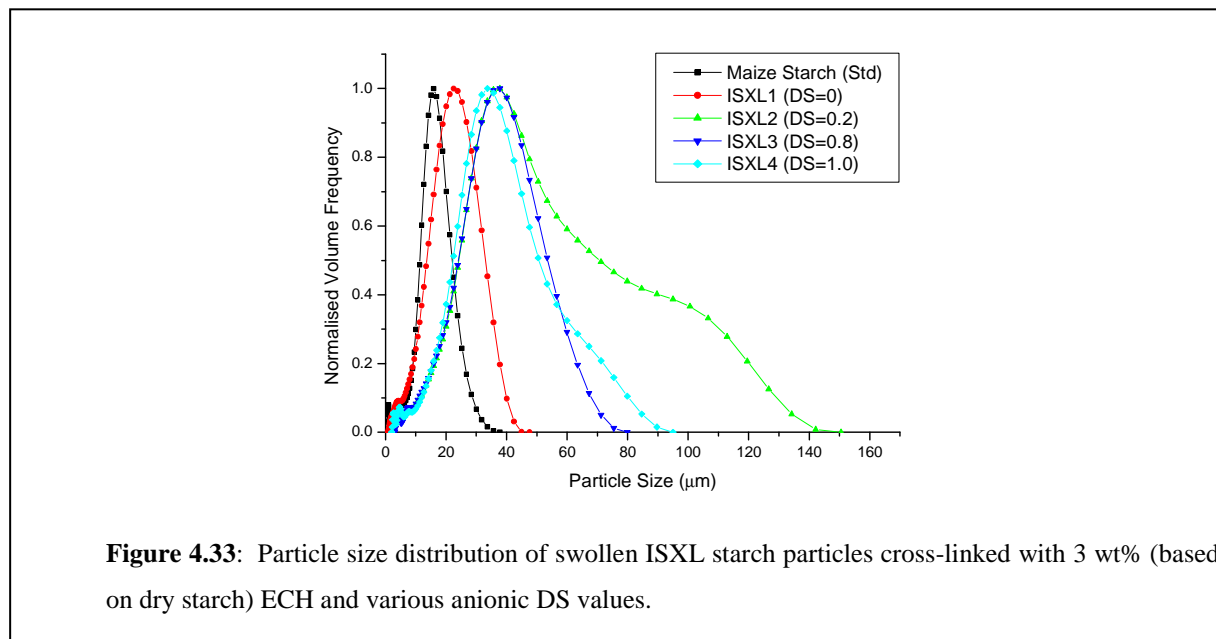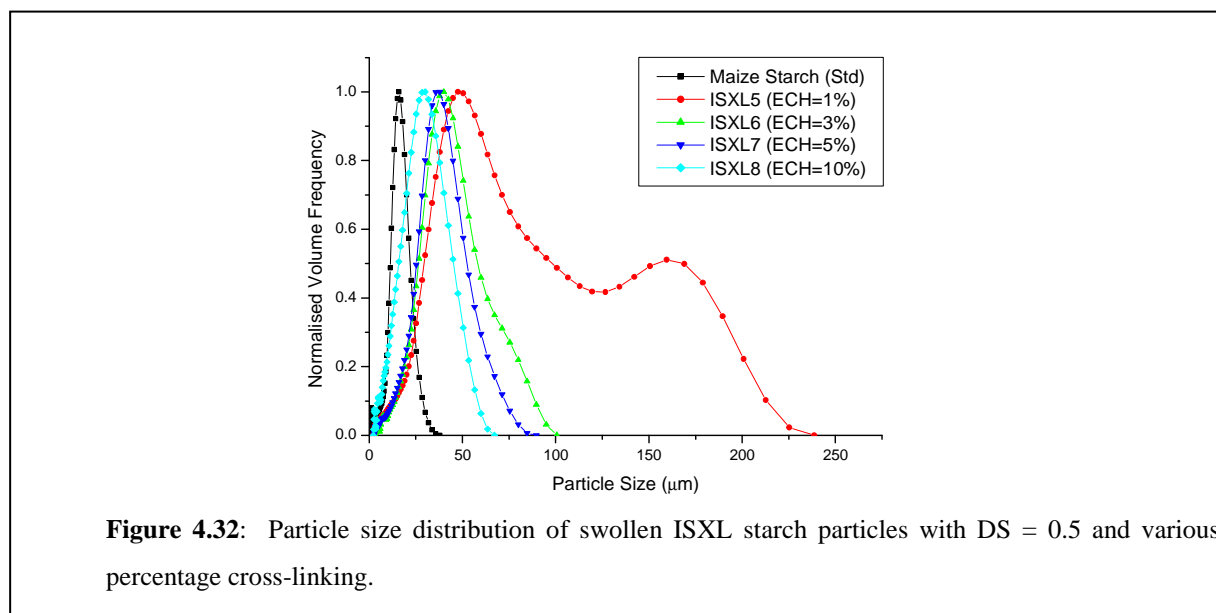
In samples where the percentage ECH was maintained at 3 wt% and increasing the anionic DS from 0 to 1, slight swelling occurred in the sample with DS = 0, which can be related back to the slight deterioration of crystallinity that occurred during cross-linking. A significant increase in particle size was observed from DS of 0 to 0.2, with particles swelling by more than 170%. These particles were also highly poly-disperse as seen in Figure 4.33 with significant peak broadening observed. Although it is expected that a further increase in DS

would cause the granules to swell even further, the opposite phenomenon was observed. The average particle size decreased with a narrower distribution as the DS increased from 0.2 to 1.0.

A filler interaction study was conducted where flocculation was measured by means of particle size analysis for PCC samples treated with ISXL samples (ISXL1 – 4) of various DS_{th} values (Figure 4.34). For the sample where particles contained no charge (DS = 0), the position of peaks remained essentially unchanged, but the distribution to higher particle size shifted considerably, indicating that some degree of flocculation occurred even where no charge was present. This may well be attributed to the adhesive characteristic of starch combined with van der Waals forces causing filler particles to adhere as flocs on the starch particle surface. The anionic modified starch particles shifted the distribution further to a higher peak and increasing the DS from 0.2 to 1.0 primarily resulted in further peak broadening.

Figure 4.34: PCC flocculation using 2 wt% ISXL starch particles cross-linked with 3 wt% (based on dry starch) ECH with various anionic DS values.
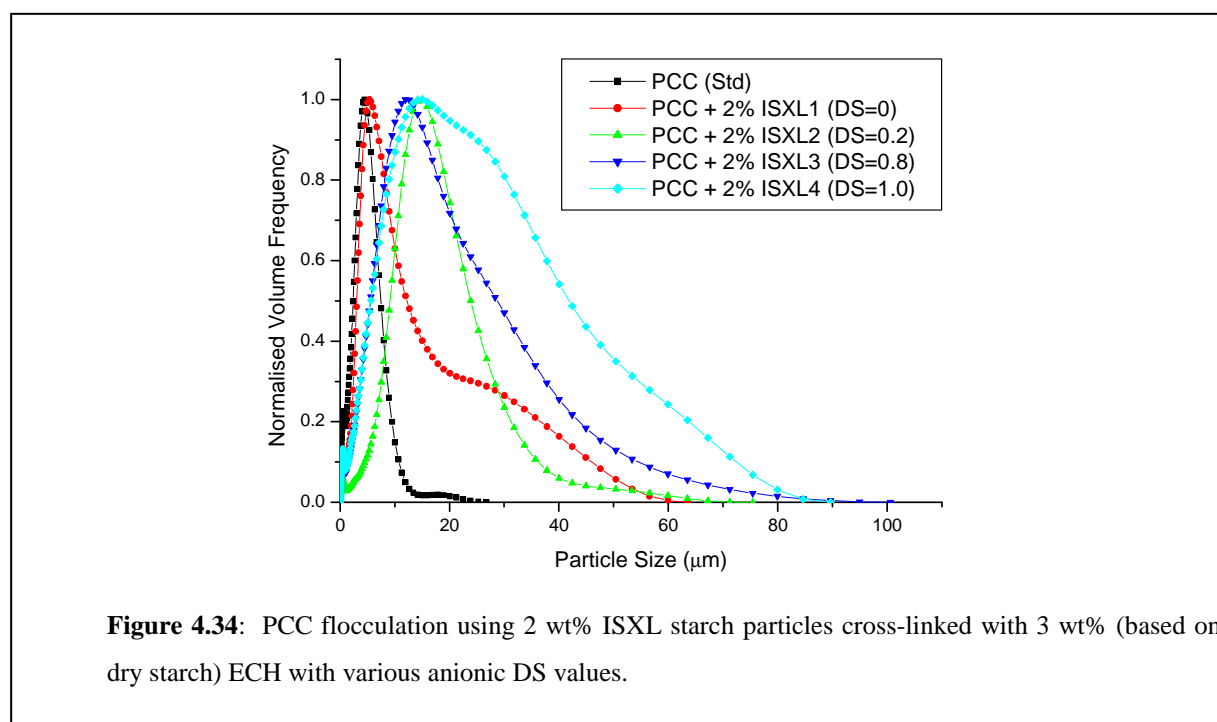
The effect of treating different concentrations of ISXL2 (DS = 0.2, ECH = 3 wt%) to PCC was also investigated. In Figure 4.35 gradual peak shifting occurred to larger floc sizes as the

particle concentration was increased from 1 to 5 wt% (based on dry PCC). It is important to take into account that although PCC flocculation indicates that the starch particles are active towards PCC, it does not necessarily follow that better flocculation denotes improved filler retention and/or mechanical properties of paper. Therefore it is required to incorporate these particles in the paper making process to verify performance. Samples of ISXL1 to 8 with different anionic DS and cross-linking degrees were subsequently sent to Mondi, Austria for testing in hand sheets (refer to Chapter 6 for results).

Figure 4.35: PCC flocculation using various concentrations (based on dry PCC) ISXL2 (DS_{th} = 0.2 and cross-linked with 3 wt% ECH).
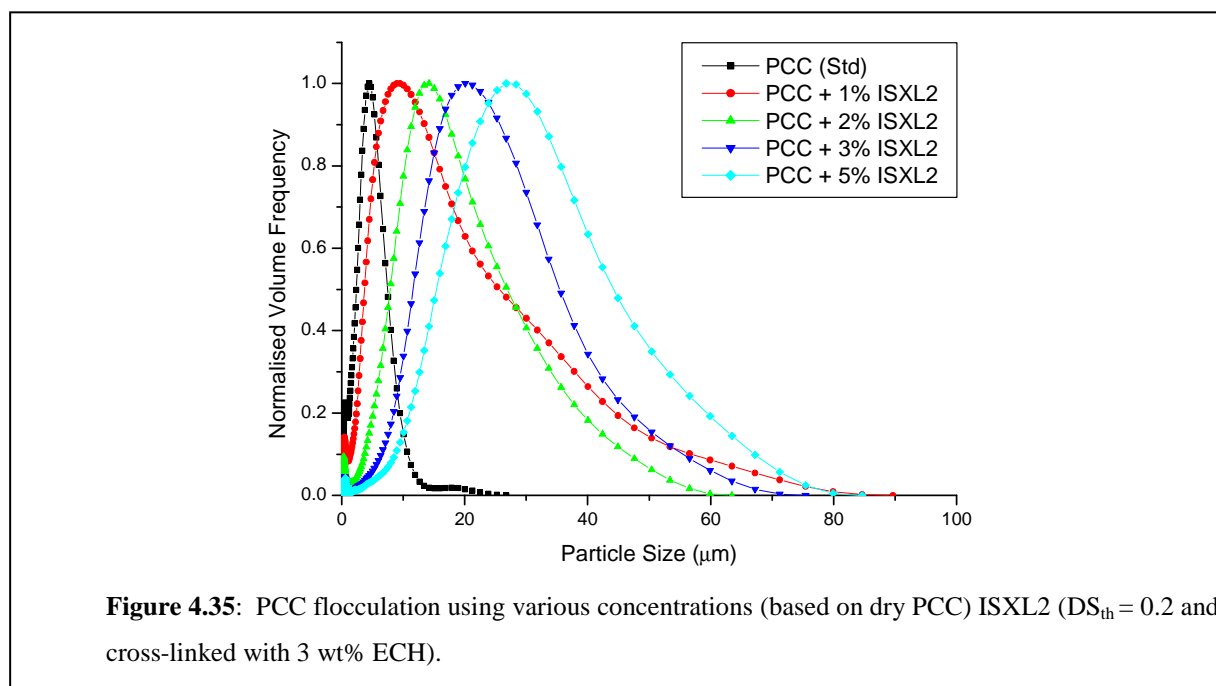
4.6.4.1 "Self cross-linked" in-situ modified maize starch particles

Fully protonated carboxylic acids generally have high melting and boiling points since both the carbonyl and hydroxyl groups are polar. These acids readily form hydrogen bonding with water which contributes to water solubility. Polyacrylic acid is also highly water-soluble and widely used as superabsorbent. However, for the polymer to be hydrophilic, the presence of carboxylic acid groups in their salt form is essential since a strong repulsive ionic force reduces the osmotic pressure of the polymer and attracts water into the network structure[55]. In the absence of water, carboxylic acids are also unique in that it forms strong intermolecular attractive forces, contributed by a very strong type of hydrogen bonding existing between two adjacent carboxylic acids[56]. A given acid forms two hydrogen bonds with another acid,

producing a "complex", which is also known as a dimer (Figure 4.36). Since dimers have twice the amount of hydrogen bonding than carboxylic acid with water, higher temperatures are required to dissolve solids containing carboxylic acid groups in water. Carboxylic acid salts are significantly more soluble in water and often carboxylic acids are converted to its salt form in order to make it more water-soluble.

Figure 4.36: Dimer formation of carboxylic acids.
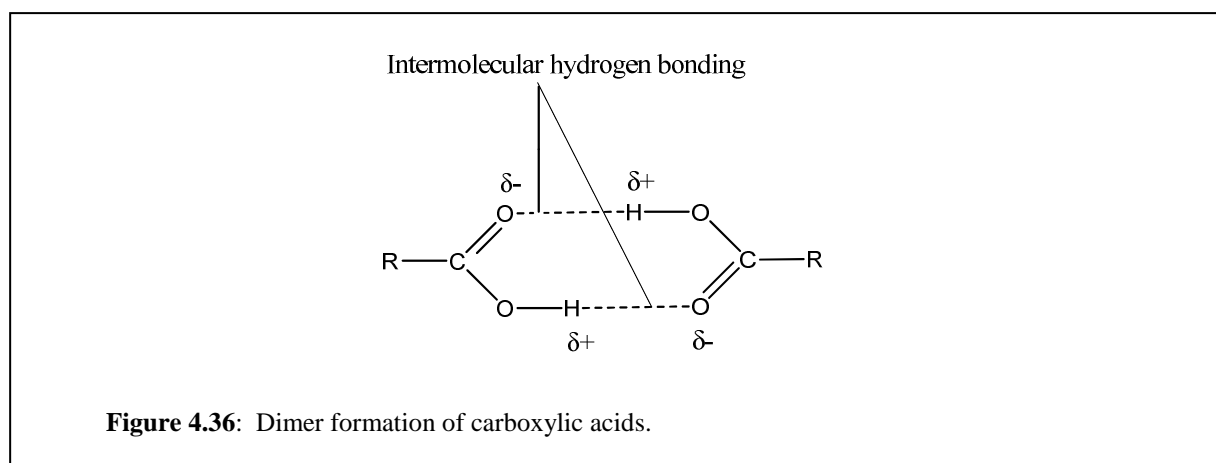
Polymers containing protonated carboxylic acid groups become increasingly water-insoluble as the molecular weight of the polymer is increased[57, 58]. The longer hydrocarbon "tail" will come between water molecules and break the hydrogen bonds. These broken hydrogen bonds are only replaced with much weaker Van der Waals dispersion forces[59]. Shieh *et al.*[60] reported on the carboxymethylation of carbon nanotubes. The untreated tubes are inherently non-polar and thus insoluble in solvents such as water. After carboxymethylation the tubes dissolved in water under alkali conditions. However, full protonation of the acid groups (by lowering pH below 6) rendered the tubes water-insoluble and carboxylic complexation was reported to be the reason.

It has been shown that the addition of sodium carboxylate groups onto the starch backbone significantly enhances its solubility in water. However, it was also found during the course of this study that if HCl neutralisation of anionic starch solutions after modification proceeded below a pH of 6, the dried starch remained essentially insoluble in water. Alkalinisation of these dispersions with NaOH immediately swelled and dissolved the anionic modified starch. Carboxylic acid dimer formation together with the high molecular weight of starch serves as explanation why the acidic carboxymethyl starch remained insoluble in water even at

temperatures up to 95 ^{o}C. The strong hydrogen bonding between carboxylic acid groups together with hydrogen bonding between hydroxyl groups on the starch backbone caused the gelatinisation point to shift to a higher temperature beyond 100 ^{o}C. By converting the acid to sodium carboxylate, the hydrogen bonding was removed and replaced by repulsive anionic charged moieties, resulting in immediate dissociation in water.

A method for preparing "self-cross-linked" anionic starch granules without the use of ECH cross-linking agents was investigated. A similar approach for making ISXL starch particles was taken, but omitting ECH addition and adjusting the pH of the final solution to 5 prior to washing and drying. Samples prepared included using an anionic DS of 0.2 and 0.4 and formulations appear in Table A4, Appendix A. Since the HCl used was 32 wt% solutions in water and the neutralisation reaction also formed water, the HCl was first dissolved in acetone (10:90 w/w) before addition in order to prevent possible granule gelatinisation.

Dried "self cross-linked" granules with anionic DS_{th} of 0.2 was used to prepare a 5 wt% solution in DDI water and mixed at 95 ^{o}C for 2 hours. The starch was filtered off and precipitated in acetone before drying (50 ^{o}C). In Figure 4.37 SEM images of these particles are shown and compared to a similar sample prepared where alkalinisation of the granules to pH 9 was done using NaOH, before drying.
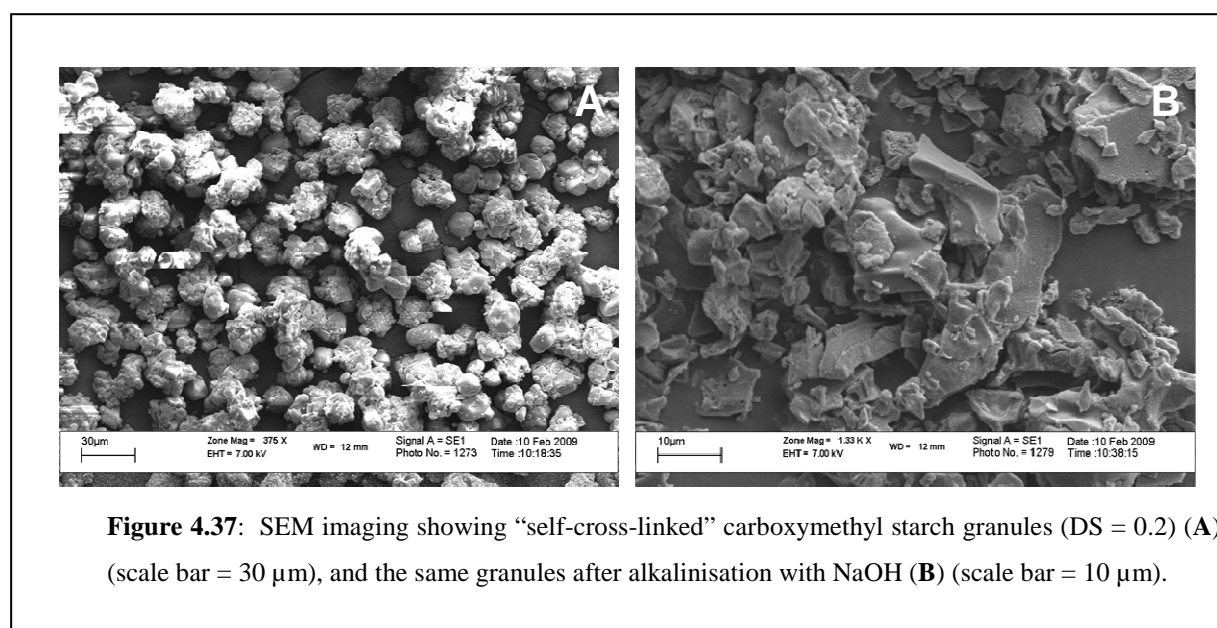
Figure 4.37: SEM imaging showing "self-cross-linked" carboxymethyl starch granules (DS = 0.2) (**A**) (scale bar = 30 µm), and the same granules after alkalinisation with NaOH (**B**) (scale bar = 10 µm).

The images show that the granules essentially remained intact although smaller unfamiliar particles are visible on the granules. These are most possibly retrograded amylose aggregates, formed as amylose leached out of the granules during anionisation and attached to larger granules as a result of complex formation between individual particles during drying. The solubilisation and leaching of amorphous low molecular weight amylose from starch granules during swelling have been reported[61].

Subsequently, alkalinisation resulted in complete rupture of granules as the ionic carboxymethylate groups dissociated, attracted water into the granules and gelled.

Figure 4.38: Gel point curves for ISXL and "self-cross-linked" starch granules with anionic DS_{th} = 0.20 (**A**), as well as "self-cross-linked" granules with DS_{th} = 0.2 and 0.4 at pH 5 and 9 (**B**).
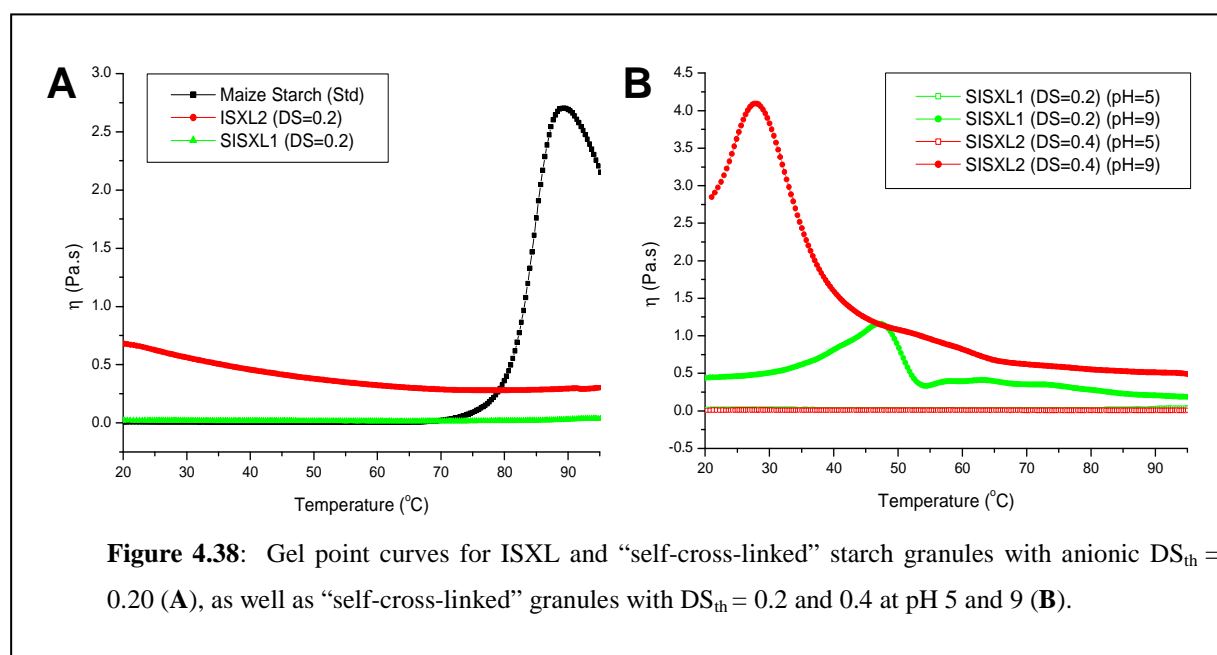
Gel point curves for the particles shown in Figure 4.37A were compared to ISXL starch granules with a similar DS_{th} as well as native starch granules (Figure 4.38A). Gelatinisation of native granules started to occur at about 70 °C. As these particles swelled the viscosity gradually increased to a maximum hydration point of about 90 °C where the particles irreversibly started to rupture, collapse, and fragment, releasing the polymeric molecules which in turn caused the viscosity to drop. The presence of hydrophilic sodium carboxylate groups in the ISXL starch granules rendered these particles cold water soluble as can be seen from the relatively higher viscosity at 20 °C. The ECH cross-linked particles did not swell further as the temperature increased, suggesting that particles essentially remained intact. Similar to native starch the "self-cross-linked" particles (sample SISXL1) remained insoluble

and even up to 95 ^{o}C no indication of gelatinisation could be observed (as an increase in viscosity), validating the high intermolecular hydrogen bonding strength of carboxylic acid dimers.

Gel point curves of SISXL1 was also compared to the sample prepared with anionic DS_{th} = 0.40 (SISXL2) at pH of 5 and 9 (Figure 4.38B). The viscosity of both these samples at pH 5 was similar and did not change over the temperature range. However, as the pH was adjusted to 9 the solutions immediately thickened at around 20 ^{o}C and gradually increased until a granule rupture point was reached with subsequent decrease in viscosity. The higher DS of SISXL2 showed a significantly higher initial viscosity attributed to the higher hydrophilic sodium carboxylate content and particle rupture occurred at a much lower temperature than SISXL1.

Figure 4.30: Particle size distribution of SISXL1 (DS_{th}=0.20) and SISXL2 (DS_{th}=0.40) compared to pure maize starch and ISXL2 (DS_{th}=0.2).
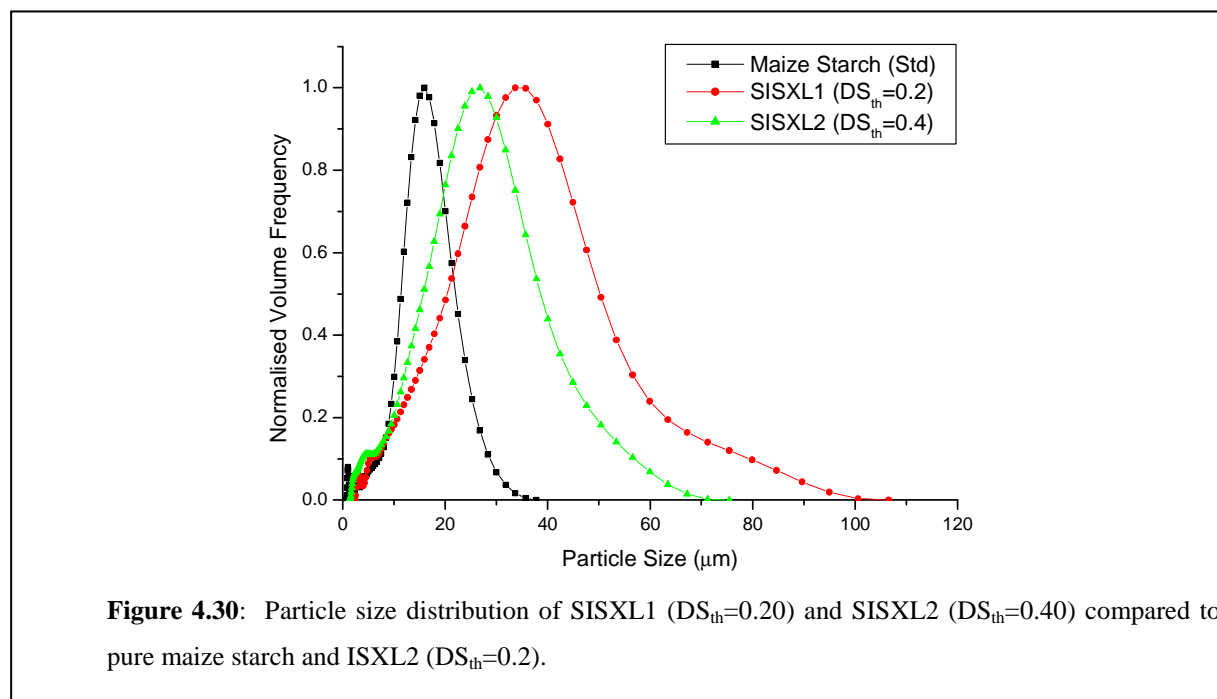
Although small aggregates were observed on the surface of "self cross-linked" granules, particle size analysis was performed on swollen granules as a comparison of the distribution between SISXL1 and SISXL2. Analysis showed that the higher concentration hydrogen bonds (from carboxylic acid dimers) in SISXL2 resulted in granules being less swollen than SISXL1. The formation of dimers could also be used as explanation for the decrease in

particle size and distribution observed for the ISXL granules as the DS was increased (Figure 4.25). During neutralisation of these particles, the addition of HCl will not only react with NaOH, but inevitably protonate sodium carboxylate groups attached on the starch, providing opportunity for carboxylic acid complex formation to occur that restricts swelling. Another reason could also be that the bulky sodium carboxylate groups restricted and interfered with the inherent affinity of hydroxyl groups to form hydrogen bonding with water as the temperature was increased. Higher DS values would therefore result in the starch particles absorbing less water and becoming less swollen.

Even though carboxylic acids are weak acids, it will readily dissociate in an alkali environment such as PCC (pH 8.5 – 9)[62]. Subsequently, the carboxylic acid modified starch should also be able to interact and flocculate the filler. This was confirmed by particle size analysis where SISXL1 and SISXL2 were used to flocculate PCC. In Figure 4.31 a slight shift in particle size distribution was observed where ISXL1 was used and, as expected, the ISXL2 containing a higher concentration carboxylic acid groups shifted the particle size even further to a larger floc size. The flocculation efficiency for both these samples was, however, not as good if compared to ISXL2 ($DS_{th} = 0.2$, 3 wt% ECH). Apart from the dissociation of free acid groups that is necessary for flocculation, complex formation between acid groups signifies that even less active groups are available to interact with PCC.
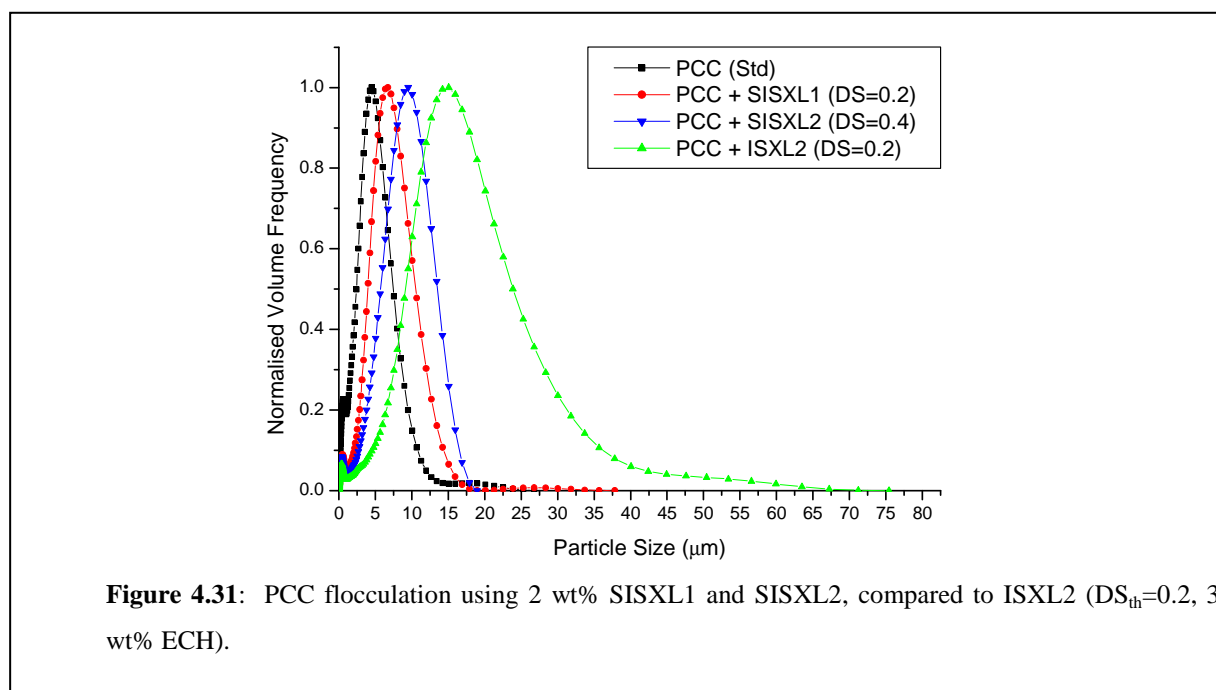
Figure 4.31: PCC flocculation using 2 wt% SISXL1 and SISXL2, compared to ISXL2 (DS_{th}=0.2, 3 wt% ECH).

Even though the "self cross-linking" of anionic modified starch granules omits the requirement for cross-linking agents prior to anionisation, it remains sensitive to pH fluctuations which might pose a problem in a processing environment. Furthermore, the performance of these particles as flocculation aid was found not to be as good as ISXL particles, which provide a wide range of floc size and distribution that can be used for evaluation in papermaking.

4.7 Summary

In summary, the contributions made of the study discussed in this chapter are:

- Carboxymethylation of granular starch have been documented in literature as a process to produce anionic polysaccharides as an intermediate product for subsequent gelatinisation and application in industry. However, this study showed that the granules can essentially be made insoluble by adding an additional cross-linking step prior to anionisation and that granule size, crystallinity, and filler flocculating ability can be controlled by the degree of chemical modification made.

- Sequential layering of ionic modified starch solutions (as polyelectrolyte) onto PCC is a unique and attractive technique to increase the starch retention in paper. The attachment of individual fluorescent markers onto the polyelectrolyte backbones was effective in showing the sequential layers deposited on the filler surface. Layer thickness was also shown to be dependent on degree of ionic substitution.

- Water-in-water emulsification of methacrylated dextrans have been reported, but in this study unsaturated allyl groups together with carboxymethyl groups were successfully attached onto dextrin prior to emulsification and the interaction of these particles with PCC was shown.

- Homogenisation and ultrasonication of cross-linked CMS was found to be a simple, yet effective technique to prepare poly-disperse particles without the use of an additional solvent system.

4.8 Conclusions

Water-in-oil emulsification is the most widely reported process providing reasonable control over particle size, although it calls for separation (eg. centrifugation) from an organic solvent as additional processing step after cross-linking with, for example, epichlorohydrin. A suitable lipophilic emulsifier is also required to sufficiently stabilise the formed emulsions, which will be discussed further in the following chapter.

Macrogel maize starch particles with different degrees of anionic modification were prepared by cross-linking anionic starch solutions to a gel with subsequent re-dispersion in water using a high shear dispersion to break down particles to a suitable size. Although the so-formed particles were highly poly-disperse and non-uniform in shape and required high energy dispersion input, processing was simple with no need for additional emulsifier or organic solvent system.

So-called "designer particles" were prepared using a W/W emulsification technique where a dextrin solution, containing both carboxymethyl and unsaturated allyl groups, were dispersed in an aqueous PEG solution and cross-linked using a redox initiation system. The particles formed still required separation from the PEG solution (which can be recycled), but the system was essentially organic solvent free and together with the absence of salt formation during polymerisation, allowed easier particle purification.

Alternate and subsequent layering of oppositely charged starch layers onto PCC using an LbL technique was employed in order for the filler to effectively, by itself, act as a polysaccharide particle. Intermediate washing of PCC was performed after each layer deposition cycle, which proved to be tedious. However, addition of polyelectrolyte concentrations just beyond the onset of zeta potential saturation would imply that these intermediate cycles can be omitted, which would make the process much more attractive in a production environment.

The in-situ ionic modification and cross-linking technique allowed particles to be prepared from the granules themselves, without any prior gelatinisation steps. This is of great advantage from a processing point of view. Partially swollen granules acted as mini reactors and enhanced reaction efficiencies (for carboxymethyl substitution) were achieved within

shorter periods. Although the system employed a solvent system, the particles could be isolated and purified simply using conventional filtration techniques.

The "self cross-linking" ability of carboxylic acid modified starch (no additional cross-linker added), allowed granules to essentially remain non-gelatinised upon heating in aqueous solutions. This was attributed to carboxylic acid dimer formation. Avoiding the requirement of additional cross-linking agents simplified the process even further, but the interaction with PCC obtained was lower compared to carboxymethylated granules.

Various samples described were submitted for evaluating their effect on paper stiffness and other mechanical properties. This is discussed in Chapter 6.

4.9 References

1. Y. Dziechciarek; J. J. G. van Soest; A. P. Philipse, *Journal of Colloid and Interface Science*, **2002**, 246, 48-59.

2. I. Simkovic; J. A. Laszlo; A. R. Thompson, *Carbohydrate Polymers*, **1996**, 30, 25-30.

3. G. Hamdi; G. Ponchel; D. Duchene, *Journal of Microencapsulation*, **2001**, 18, 373-383.

4. Y. X. Chen; G. Y. Wang, *Journal of Applied Polymer Science*, **2006**, 102, 1539-1546.

5. S. Y. Xiao; C. Y. Tong; X. M. Liu, et al., *Chinese Science Bulletin*, **2006**, 51, 1693-1697.

6. T. Yoneya; K. Ishibashi; K. Hironaka, et al., *Carbohydrate Polymers*, **2003**, 53, 447-457.

7. T. Kasemsuwan; J. Jane, *Cereal Chemistry*, **1994**, 71, 282-287.

8. H. Selek; S. Sahin; H. S. Kas, et al., *Drug Development and Industrial Pharmacy*, **2007**, 33, 147-154.

9. A. R. Kulkarni; K. S. Soppimath; T. M. Aminabhavi, et al., *Journal of Applied Polymer Science*, **1999**, 73, 2437-2446.

10. S. H. Kim; C. Y. Won; C. C. Chu, *Carbohydrate Polymers*, **1999**, 40, 183-190.

11. E. Marsano; E. Bianchi; S. Gagliardi, et al., *Polymer*, **2000**, 41, 533-538.

12. K. Osth; L. Strindelius; A. Larhed, et al., *Journal of Drug Targeting*, **2003**, 11, 75-82.

13. A. Larhed; L. Stertman; E. Edvardsson, et al., *Journal of Drug Targeting*, **2004**, 12, 289-296.

14. A. Biswas; R. L. Shogren; S. Kim, et al., *Carbohydrate Polymers*, **2006**, 64, 484-487.

15. A. Hebeish; A. Higazy, *American Dyestuff Reporter*, **1990**, 79, 43-52.

16. F. Verbanac, Starch Acrylamides and the Method for Preparing the Same, Patent: US 4060506, **1977**.

17. S. L. Maher, Method for Treating and/or Coating Nonwoven Cellulosic Substrates with Acrylamide-substituted Starch Derivatives, Patent: W/O/1988/008757, **1988**.

18. S. H. Imam; S. H. Gordon; L. Mao, et al., *Polymer Degradation and Stability*, **2001**, 73, 529-533.

19. J. H. Kim; R. E. Robertson, *Advanced Cement-Based Materials*, **1998**, 8, 66-76.

20. D. F. Williams, *Chemistry and Technology of the Cosmetics and Toiletries Industry*. 2nd ed.; Chapman & Hall: London, **1992**.

21. Z. Stojanovic; K. Jeremic; S. Jovanovic, et al., *Starch-Starke*, **2005**, 57, 79-83.

22. B. Yang; Y. Jiang; M. Zhao, et al., *Polymer Degradation and Stability*, **2008**, 93, 268-272.

23. O. Franssen; W. E. Hennink, *International Journal of Pharmaceutics*, **1998**, 168, 1-7.

24. S. Santacruz; R. Andersson; P. Aman, *Carbohydrate Polymers*, **2005**, 59, 397-400.

25. L. Kunlan; X. Lixin; L. Jun, et al., *Carbohydrate Research*, **2001**, 331, 9-12.

26. K. Alvani; X. Qi; R. Tester, *Carbohydrate Polymers*, **2009**, 78, 997-998.

27. A. P. R. Johnston; C. Cortez; A. S. Angelatos, et al., *Current Opinion in Colloid and Interface Science*, **2006**, 11, 203-209.

28. G. B. Sukhorukov; E. Donath; H. Lichtenfeld, et al., *Colloids and Surfaces*, **1998**, 137, 253-266.

29. G. B. Sukhorukov; D. V. Volodkin; A. M. Gunther, et al., *Journal of Materials Chemistry*, **2004**, 14, 2073-2081.

30. B. G. De Geest; C. Dejugnat; E. Verhoeven, et al., *Journal of Controlled Release*, **2006**, 116, 159-169.

31. S. Ye; C. Wang; X. Lui, et al., *Journal of Controlled Release*, **2006**, 112, 79-87.

32. A. A. Antipov; G. B. Sukhorukov, *Advances in Colloid and Interface Science*, **2004**, 111, 49-61.

33. X. Shi; M. Shen; H. Mohwald, *Progress in Polymer Science*, **2004**, 29, 987-1019.

34.   S. Sukhishvili, *Current Opinion in Colloid & Interface Science*, **2005**, 10, 37-44.

35.   Y. Lin; S. Mao, *Biomass and Bioenergy*, **2001**, 20, 217-222.

36.   M. T. Sejersen; T. Salomonsen; R. Ipsen, et al., *International Dairy Journal*, **2007**, 17, 302-307.

37.   H. Ohshima; T. Kondo, *Colloid & Polymer Science*, **1986**, 264, 1080-1084.

38.   S. S. Twining, *Analytical Biochemistry*, **1984**, 143, 30-34.

39.   S. N. Smith; R. P. Steer, *Journal of Photochemistry and Photobiology A: Chemistry*, **2001**, 139, 151-156.

40.   P. K. Gallagher; D. W. Johnson, *Thermochimica Acta.*, **1973**, 6, 67-83.

41.   X. Liu; L. Yu; H. Liu, et al., *Polymer Degradation and Stability*, **2008**, 93, 260-262.

42.   L. Bley, *Pulp & Paper Canada*, **1998**, 99, 51-55.

43.   M. A. Hubbe; J. Chen, *Paper Technology Journal*, **2004**, 45, 17-23.

44.   V. K. Villwock; J. N. BeMiller, *Strarch - Starke*, **2005**, 57, 281-290.

45.   B. Volkert; F. Loth; W. Lazik, et al., *Starch-Starke*, **2004**, 56, 307-314.

46.   O. S. Kittipongpatana; J. Sirithunyalug; R. Laenger, *Carbohydrate Polymers*, **2006**, 63, 105-112.

47.   Z. Stojanovic; K. Jeremic; S. Jovanovic, *Starch-Starke*, **2000**, 52, 413-419.

48.   C. J. Tijsen; H. J. Kolk; E. J. Stamhuis, et al., *Carbohydrate Polymers*, **2001**, 45, 219-226.

49.   A. A. Aly, *Starch-Starke*, **2006**, 58, 391-400.

50.   D. Sievert; Z. Czuchajowska; Y. Pomeranz, *Cereal Chemistry*, **1991**, 68, 86-91.

51.   C. Primo-Martin; N. H. van Nieuwenhuijzen; R. J. Hamer, et al., *Journal of Cereal Science*, **2007**, 45, 219-226.

52.   K. Sangseethong; S. Ketsilp; K. Sriroth, *Starch-Starke*, **2005**, 57, 84-93.

53.   P. Chen; L. Yu; L. Chen, et al., *Starch-Starke*, **2006**, 58, 611-615.

54.   P. Chinachoti; M. P. Steinberg, *Journal of Food Science*, **1986**, 51, 997-1000.

55.   C. M. Garner; M. Nething; P. Nguyen, *Journal of Chemical Education*, **1997**, 74, 95-96.

56.   B. L. Rivas; I. Moreno-Villoslada, *Macromolecular Chemistry and Physics*, **1998**, 199, 1153-1160.

57.   K. J. Shahinpoor; K. J. Kim; M. Mojarrad, *Artificial muscles: applications of advanced polymeric nanocomposites*. CRC Press: Florida, **2007**.

58.   H. R. Kricheldorf, *Handbook of Polymer Synthesis, Part 1*. Marcel Dekker, Inc.: New York, **1992**.

59.   H. S. Stoker, *General, Organic, and Biological Chemistry*. 2nd ed.; Houghton Miffin Harcourt (HMH): Belmont, **2000**.

60.   Y. Shieh; G. Lui; H. Wu, et al., *Carbon*, **2007**, 45, 1880-1890.

61.   A. Hermansson; K. Svegmark, *Trends in Food Science & Technology*, **1996**, 7, 345-353.

62.   H. Liimatainen; S. Kokko; P. Rouso, et al., *Tappi*, **2002**, 5, 11-17.

Chapter 5: Polysaccharide particle processing: microfluidics

5.1 Introduction

In the previous chapter the preparation of multi-functional polysaccharide particles was performed using processing techniques that could potentially be scaled-up for testing in larger continuous pilot plant paper mills without excessive capitalisation on new processing equipment. However, it would be improvident to ignore new technology that may offer significant process solutions for the future. Microfluidics was recognised as a process that could benefit the paper industry in the future and therefore it was chosen to study it as a novel approach for preparing modified starch-based particles that can be used to strengthen paper.

Using microfluidic systems to perform emulsification has several advantages, which include[1, 2]:

- The size of the produced droplets can be controlled easily by changing the flow rates of both phases.
- It is compact.
- It is resistant to organic solvents.
- It has no moving parts; therefore there is no abrasion that can contaminate the product.
- In comparison with rotor stator mixers, similar size particles can be obtained with much less energy input.
- Scale-up can easily be achieved using several reactors in parallel (numbering up), reducing the uncertainty about product reproducibility which is normally associated with process transfer to larger vessels.

Over the past 10 years, micro-structured devices have received considerable interest as a novel process for chemical processing, from lab-scale to pilot plant scale to production scale. Apart from being used for performing emulsifications, these systems can also be used for reactions, blending, gas-absorption, and foaming[3]. One of the main features of microfluidic

reactors is its very high surface area to volume ratio. While traditional systems typically have ratios averaging about 100 m^2/m^3, microfluidic reactors can be engineered to possess ratios of up to 50,000 m^2/m^3 [4]. This offers high heat transfer rates allowing highly exothermic reactions to be conducted at almost isothermal conditions. Hot spots are eliminated that may not only result in the formation of undesired and often dangerous by-products, but also pose danger to the operator. An example of such a process is the fluorination of aromatics which has been characterised by formation of explosive by-products caused by a large heat release[5,6]. Suppressing by-product formation with sufficient heat transfer leads to better product quality and higher yields.

The high surface to volume ratio also allows enhanced mass transfer in liquid/liquid, gas/gas and liquid/gas reactions, significantly reducing diffusion times. Coating channel walls with catalyst enriched films can drastically improve reaction efficiency in some catalytic reactions. Process intensification using compact microfluidic reactors for reforming hydrogen from hydrocarbons (including methanol, ethanol, diesel, and gasoline) for energy conversion in fuel cells is an example and part of extensive research conducted by Prof. Volker Hessel and his group at the Institut für Mikrotechnik Mainz GmbH (IMM)[7-12].

Classic emulsion polymerisation techniques are widely used to create mono-dispersed microspheres of up to 1 µm. Suspension polymerisation of two immiscible fluids using mechanical stirring in a conventional batch reactor is used to produce particles with diameters in the micron range (typically 10 – 100 µm) and the so-formed droplets generally have a wide size distribution. Fractionation can be used to tighten the distribution, but this technique is tedious and often only mildly effective[13]. Well controllable and narrow size distributions are difficult to obtain using bulk mixing since it depends on chaotic turbulent flow patterns for disruption of fluid interfaces to form droplets. Reproducibility and predictability of micron sized emulsion particle size and distribution are often a necessity in industries such as food, coatings, drug delivery, and cosmetics[14]. In recent years membrane emulsification techniques, in which a discontinuous phase is forced through a continuous phase, have been reported to be effective for producing mono-dispersed particles[15]. Micro-structured mixers have also been proven efficient in processes involving homogeneous mixing, offering the advantage of fast, reproducible, and efficient mixing as shown by the work of Prof. Hessel[16].

Two principals for inducing mixing at a micro-scale have been identified, namely active and passive mixing[3]. In active mixing external energy sources are used and these include, amongst others, ultrasonics, small impellers, and integrated micro-pumps. In passive mixing pumping action (or hydrostatic potential) is used for restructuring flow in such a way that enhanced mixing can be attained.

This study follows from the simple W/O emulsion chemistry that was introduced in the previous chapter (Section 4.2) and the development of a formulation for producing anionic polysaccharide-based particles using passive mixing through micro-mixers. Finally the effect of flow conditions and emulsifier levels on particle size and distribution were modelled using response surface methodology with the ultimate aim of determining if size influences paper properties and how.

5.2 Microfluidic set-up and devices

Initial investigation by the writer into the performance of microfluidic devices was conducted at IMM and the Department of Chemical Engineering and Chemistry, Eindhoven University of Technology (TU/e). A process flow diagram of the set-up used appears in Figure B1, Appendix B. The set-up consisted of 2 pressurised (ca. 4 bar) stainless steel (SS) vessels. Feed lines (1/8 inch ID, SS) running from the bottom of these tanks were connected to Cori-flow digital mass flow meters, which were used for flow control from a computer using LabVIEW instrument control software (National Instruments) that was connected to the instruments via a RS-232 interface. The feed lines were reduced to 1/16 inch diameter SS and combined in the micro-mixer. The emulsion outlet line (1/8 inch tubing) was subsequently fed through a catalysis loop section in a temperature bath with an extra feed line joined for optional catalyst treatment. Temperature regulation of the feed lines to the micro-mixer could also be performed with the feed as well as the mixer located in a separate temperature bath.

Two different types of microfluidic devices were evaluated for conducting W/O emulsification, the first based on a split-and-recombine (SAR) concept and the other on interdigital multi-lamellae arrangement. Initial concerns were that the high molecular weight and solution viscosity associated with starch may cause poor flow due to the relatively low

pressure available for pressurising the feed vessels, and this was confirmed during experimentation. Pure maize starch gel solutions with concentrations even down to 2 wt% exhibited poor flow through the system along with deficient control over stable flow rates. Subsequently, preliminary W/O emulsification was performed using poly(vinyl alcohol) (PVA) (M_w 14,000 g/mol) (Merck, Cat:8438,650), dissolved in DDI water to a concentration of 6 wt%, as aqueous phase. The oil phase consisted of heptane (Aldrich, Cat: 246,654) containing 6.7 wt% sorbitan mono-oleate (Span 80) (Sigma, Cat: S6760) as emulsifier.

5.2.1 Caterpillar split-recombine micro-mixer

The caterpillar micro-mixer (supplied by IMM) consists of a single channel (dimension of 300 µm × 300 µm) with a ramp-like shape (Figure 5.1A). The laminated flow of two inlet feeds is joined together in the channel and proceeds to where the combined streams are forced to split in two, with the one stream folding simultaneously over the other (Figure 5.1C)[17]. These streams are subsequently recombined into four vertically laminated streams, after which they are once again split and folded over each other to yield a total number of eight lamellae. This implies that after a total number of eight split and recombination units, there would theoretically be 512 fine laminated streams. In the emulsification of two immiscible fluids droplet rapture from the continuous oil phase occurs in the shear field generated in the aqueous phase as a result of a convective velocity field (recirculation flows).
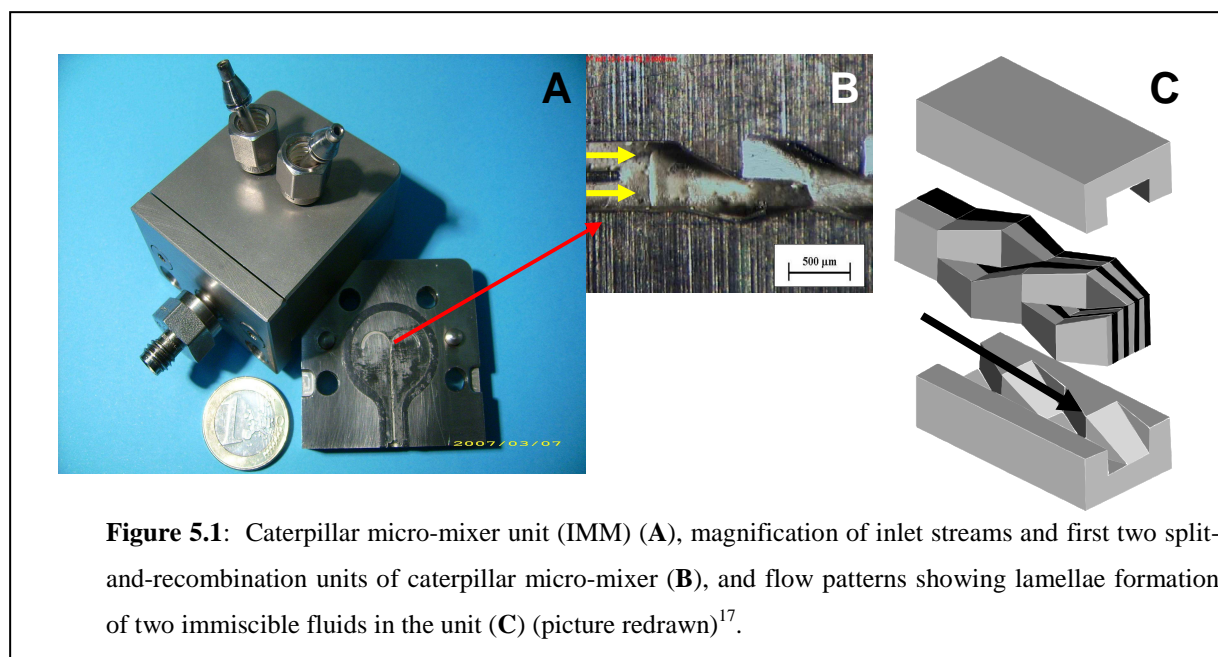
Figure 5.1: Caterpillar micro-mixer unit (IMM) (**A**), magnification of inlet streams and first two split-and-recombination units of caterpillar micro-mixer (**B**), and flow patterns showing lamellae formation of two immiscible fluids in the unit (**C**) (picture redrawn)[17].

Caterpillar micro-mixers are particularly suitable in cases where higher throughputs are required, since the channel diameter and length can be increased and tailored to meet the dispersion demand. This differs from interdigital mixers where channel enlargement means increasing diffusion distances and thus decrease of mixing performance. These devices are generally considered for pilot and production plant applications where output volumes varying from 1 l/hr up to hundreds of litres per hour are required.

Figure 5.2: Optical microscope images showing droplet size, distribution, and stability of a 6 wt% aqueous PVA solution emulsified in a heptane (containing 6.7 wt% Span 80) oil phase using a caterpillar micro-mixer at various flow rates (**A**) and flow ratios (**B**) (scale bar = 150µm).
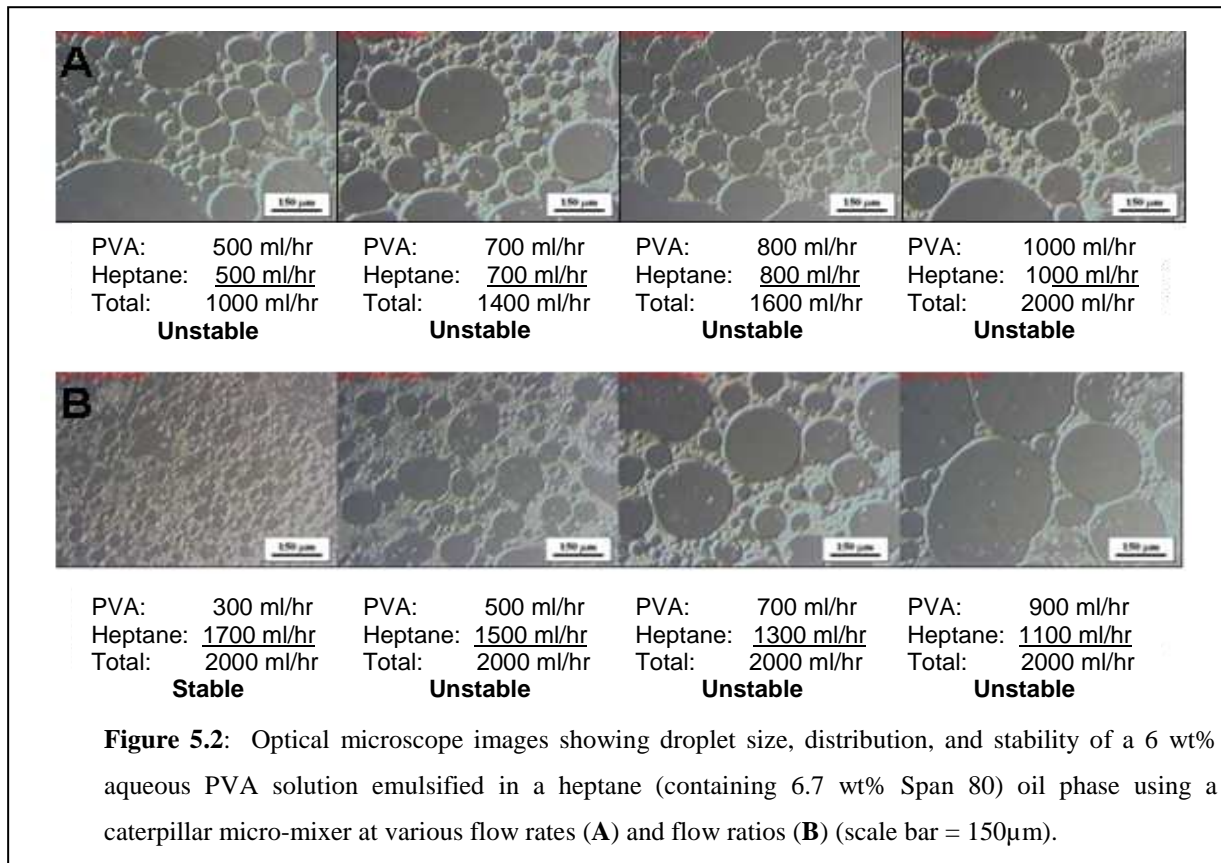
In Figure 5.2 optical microscope images show PVA droplets emulsified in heptane where increases in the individual flow rates (constant flow ratio) as well as the flow rate ratios (total flow rate constant) were studied. An emulsion was rated stable if after 24 hours, no separation of a clear PVA layer could be detected at the bottom of the sample vial. The images indicate that PVA globules were large, highly poly-dispersed and unstable irrespective of higher flow rates used at similar flow ratios. However, where the PVA flow rates were lower compared to the oil phase, PVA droplet size was reduced, with a corresponding improvement in stability probably through better conditions in jet formation. Lower PVA flow rates corresponded to the formation of thinner aqueous phase lamellae within the micro-

mixer, resulting in smaller globules being formed. Higher heptane flow rates also denote more turbulent PVA droplet flow and less residence time for droplets to coalesce again within the micro-mixer.

5.2.2 Interdigital micro-mixers

In interdigital micro-mixers the fluids are fed separately into 2 inlets within an SS housing, consisting of a top and bottom plate. Within the bottom part of the housing interchangeable inlays are secured, these bearing an array of channels etched into a metallic substratum (such as SS, nickel, or silver based on copper) using, for example, laser-ablation techniques[2]. Inlets are forced by counter-current flow through an array of micro-channels that are alternately accessible to the two fluids and forced through a slit located in the top housing, which bears a slit above the middle of the array[16]. Inlays developed by IMM (Figure 5.3A-C) can consist of 3 channels, where the 2 outer channels are reserved for the continuous phase and the inner channel for the dispersed phase, or a multiple-channel feed system containing more than 3 liquid supply channels with corrugated walls.

Figure 5.3: Interdigital micro-mixer set-up (IMM) showing the SS housing (**A**) with interchangeable three-channel (**B**) and multi-channel (**C**) array feed systems[16]. The counter-current fluid flows forms lamellae and combined at the outlet slit where droplet formation occurs (**D**) (picture redrawn)[18].
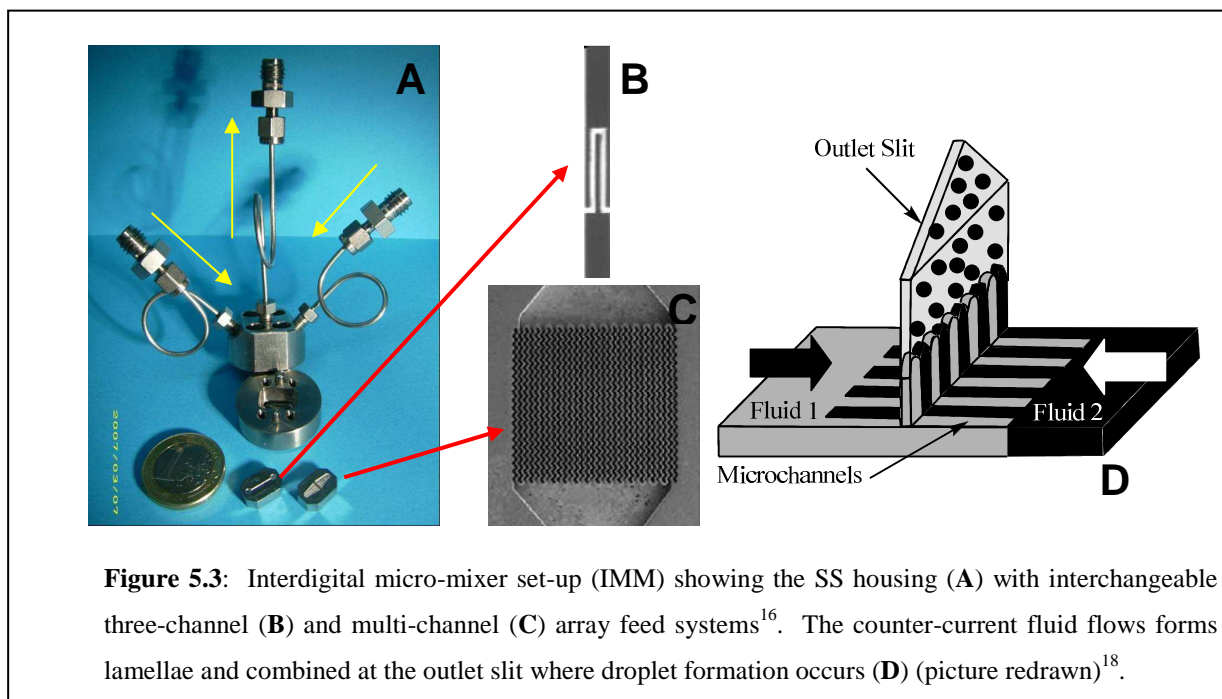
The flow pattern results in the formation of alternate fluid lamellae travelling through the slit and out through the top part of the housing, disintegrating into dispersed droplets in the

continuous phase (Figure 5.3D)[2]. The inlays are tightly screw-fastened into the housing and, together with a FKM (Viton) O-ring surrounding the inlay in the housing, can withstand operating pressures of up to 100 bar.

A multiple-channel inlay system with 15 channels available for both the dispersed and continuous phase supply was used for experimentation. Each channel had a width of 45 µm and depth of 200 µm. In performing a preliminary W/O emulsification study using PVA and heptane similar as in Section 5.2.1, but using the multiple channel inlay interdigital micro-mixer, overall flow rates achieved was not as high as in the caterpillar micro-mixer, since the pressure drop over the narrow channels were much higher. However, PVA droplets formed were generally smaller and remained more stable as seen in Figure 5.4. An increase in the overall flow rate (constant flow ratio) caused droplets to become increasingly smaller, since the higher pressure drops at higher flow rates denoted higher energy input at the interface of the fluids at the slit and the decay mechanism at this point were mainly determined by shear forces and vortex flows[16].

PVA: 275 ml/hr	PVA: 300 ml/hr	PVA: 350 ml/hr	PVA: 400 ml/hr
Heptane: 275 ml/hr	Heptane: 300 ml/hr	Heptane: 350 ml/hr	Heptane: 400 ml/hr
Total: 550 ml/hr	Total: 600 ml/hr	Total: 700 ml/hr	Total: 800 ml/hr
Unstable	**Unstable**	**Unstable**	**Stable**

PVA: 50 ml/hr	PVA: 100 ml/hr	PVA: 200 ml/hr	PVA: 300 ml/hr
Heptane: 650 ml/hr	Heptane: 600 ml/hr	Heptane: 500 ml/hr	Heptane: 400 ml/hr
Total: 700 ml/hr	Total: 700 ml/hr	Total: 700 ml/hr	Total: 700 ml/hr
Stable	**Stable**	**Stable**	**Stable**

Figure 5.4: Optical microscope images showing droplet size, distribution, and stability of a 6 wt% aqueous PVA solution emulsified in a heptane (containing 6.7 wt% Span 80) oil phase using a multiple-channel inlay interdigital micro-mixer at various flow rates (**A**) and flow ratios (**B**) (scale bar = 150 µm).

Further control over droplet size was achieved by manipulation of the feed ratios. Droplet size analysis of samples prepared with various ratios were performed using a Beckman Coulter laser diffraction particle size analyser (at IMM) and in Figure 5.5 it is observed how particle distribution widened as PVA/heptane ratios were increased.

Equipped with better knowledge of the different types of passive micro-mixers and its application in performing W/O emulsification, it was decided to continue further studies focussing on the use of the multiple-channel inlay micro-mixer. The versatility of this device in tailoring droplet size and distribution by manipulating flow rates showed interesting prospects for further investigation.

Figure 5.5: Droplet size analysis of 6 wt% PVA solutions emulsified in heptane (containing 6.7 wt% Span 80) using a multiple-channel inlay interdigital micro-mixer at various flow ratios.
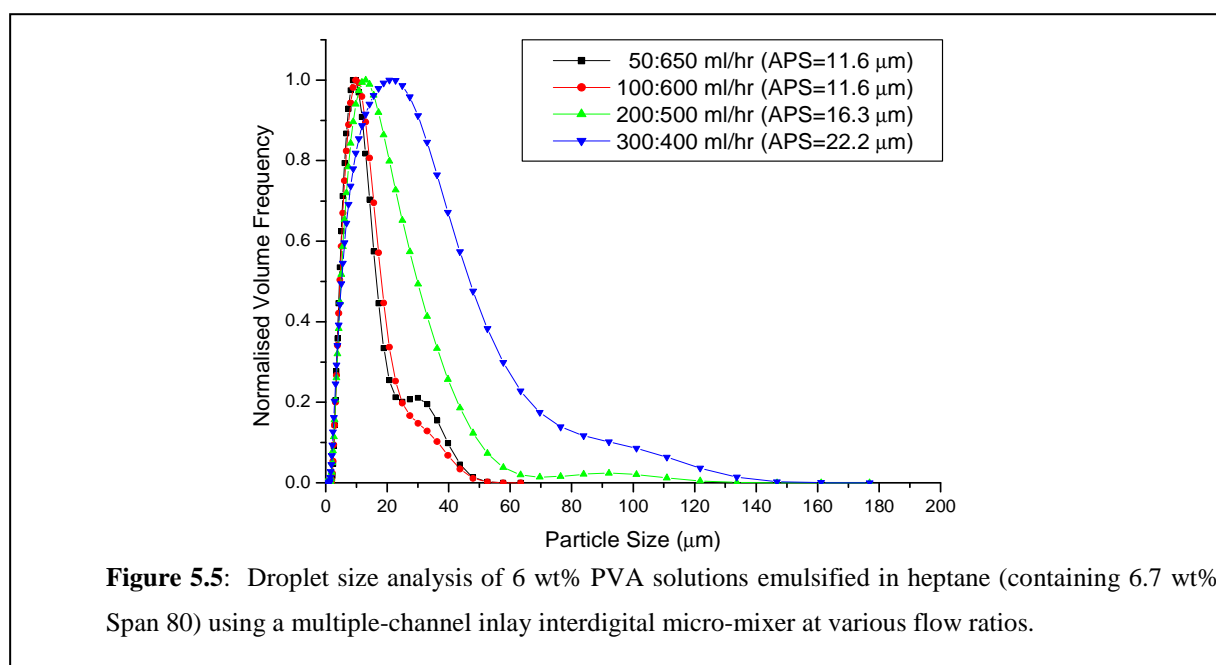
5.3 Process for preparing polysaccharide particles using microfluidics

5.3.1 Introduction

The high viscosity of maize starch solutions was initially a concern in this processing approach since difficulty in maintaining accurate control over the flow rates was encountered previously. Additionally, the carboxymethylation of this starch was shown in the previous

chapter to cause even further solution viscosity increases. Excessive dilution of the solutions would ultimately adversely affect the cross-linking efficiency of the particles causing the polymers to dissolve back in water during purification. Subsequently an alternative polysaccharide system had to be developed and the operating pressure of the experimental set-up needed to be high enough to accurately control the flow rates.

In Section 4.2 it was further shown that coalescence of the W/O emulsions occurred, which indicated that Span 80 was maybe not be the best emulsifier for this particular system. A suitable surfactant was required together with a technique to anionise the gel particles prior to commencing an investigation on flow conditions and the effect it has on the particle size and distribution.

5.3.2 Experimental set-up
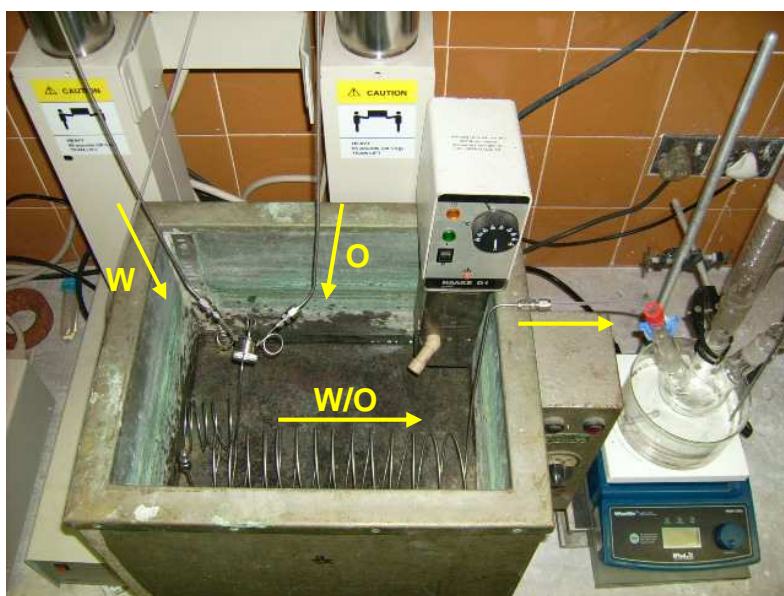
Figure 5.6: Microfluidic set-up consisting of high pressure syringe pumps, micro-mixer unit, heating coils and heated round bottom flask for sample collection.

Another microfluidic set-up was assembled at the Department of Process Engineering, Universtiy of Stellenbosch as shown in Figure 5.6. The primary requirement for the system was to ensure continuous flow through the micro-mixer with precision control over the individual feed rates. Pulsating flow would imply disruption of flow patterns, which in turn

would result in poly-disperse emulsion droplet formation. Two high pressure syringe pumps (Teledyne Isco, Model 1000D) were obtained for delivering each phase with the capability of supplying constant flow rates from 0.001 ml/min to 400 ml/min at pressures up to 2,000 psi (about 138 bar) and an accuracy of 0.5% of setpoint.

After emulsification in the interdigital micro-mixer, the emulsion was passed through a set of coils located in a temperature controlled water bath, which provided segmentation for thermal initiation to occur. Samples were collected in a 250 ml glass round bottom flask fitted with a condenser and immersed in an oil bath, which allowed for further heating/cooling.

5.3.3 Methods

5.3.3.1 Materials

Dextrin (Type II) (Sigma, Cat: D2131) was oven dried before use. Allyl Bromide (Aldrich, Cat: A29,58599%), sodium acrylate (Aldrich, Cat: 408,220), and *N,N'*-methylene bisacrylamide (MBA) (Fluka, Cat: 666,667) were stored at 4 $^{\circ}$C. Potassium persulfate (KPS) (Merck, Cat: 1.05091) was dissolved in DDI water to concentration of 5 wt% and stored at the same temperature. HCl (32%) (Merck, Cat: SAAR3063040 LP), NaOH (Merck, Cat: SAAR5823160 EM), heptane (Kimix, CP grade), and sorbitan mono-oleate (Span 80) (Sigma, Cat: S6760) was used as received. Hypermer B247 was kindly supplied by Croda Chemicals.

5.3.3.2 Polysaccharide selection

Due to the poor flow of aqueous maize starch solutions through the micro-mixer, which was attributed to its high molecular weight, it was decided to further investigation using a lower molecular weight polysaccharide. Following the successful synthesis of W/W emulsified anionic particles using dextrin (Type II) (Section 4.4), it was selected for testing in this investigation as well. The concentration of the polysaccharide in water plays a significant role in the preparation of emulsions. If the concentration is too low, the aqueous starch droplets will not have enough hydroxyl groups to sufficiently cross-link in order to form stable gel particles. If the concentration of the starch is too high, the viscosity of the aqueous phase increases causing an increase in the pump pressure demand to pass it through the

narrow microfluidic channels. Several aqueous concentration dextrin solutions were prepared to find the lowest concentration required to ensure sufficient cross-linking.

A 20 wt% dextrin solution was first prepared by dissolving it in DDI water and heating the solution to 90 ^{o}C for 1 hour under continuous stirring. After cooling, samples containing between 1 and 20 wt% dextrin was prepared by additions of DDI water (see formulations in Table A5, Appendix A) after which NaOH was dissolved in each sample (1% based on total solution weight).

Figure 5.7: Epichlorohydrin cross-linked (3 wt% based on total solution) dextrin particles in water, prepared using W/O emulsification with 10 wt% (**A**), 15 wt% (**B**), and 20 wt% (**C**) dextrin (Type II) homogenised in heptane containing 6.7 wt% (based on solvent) Span 80.
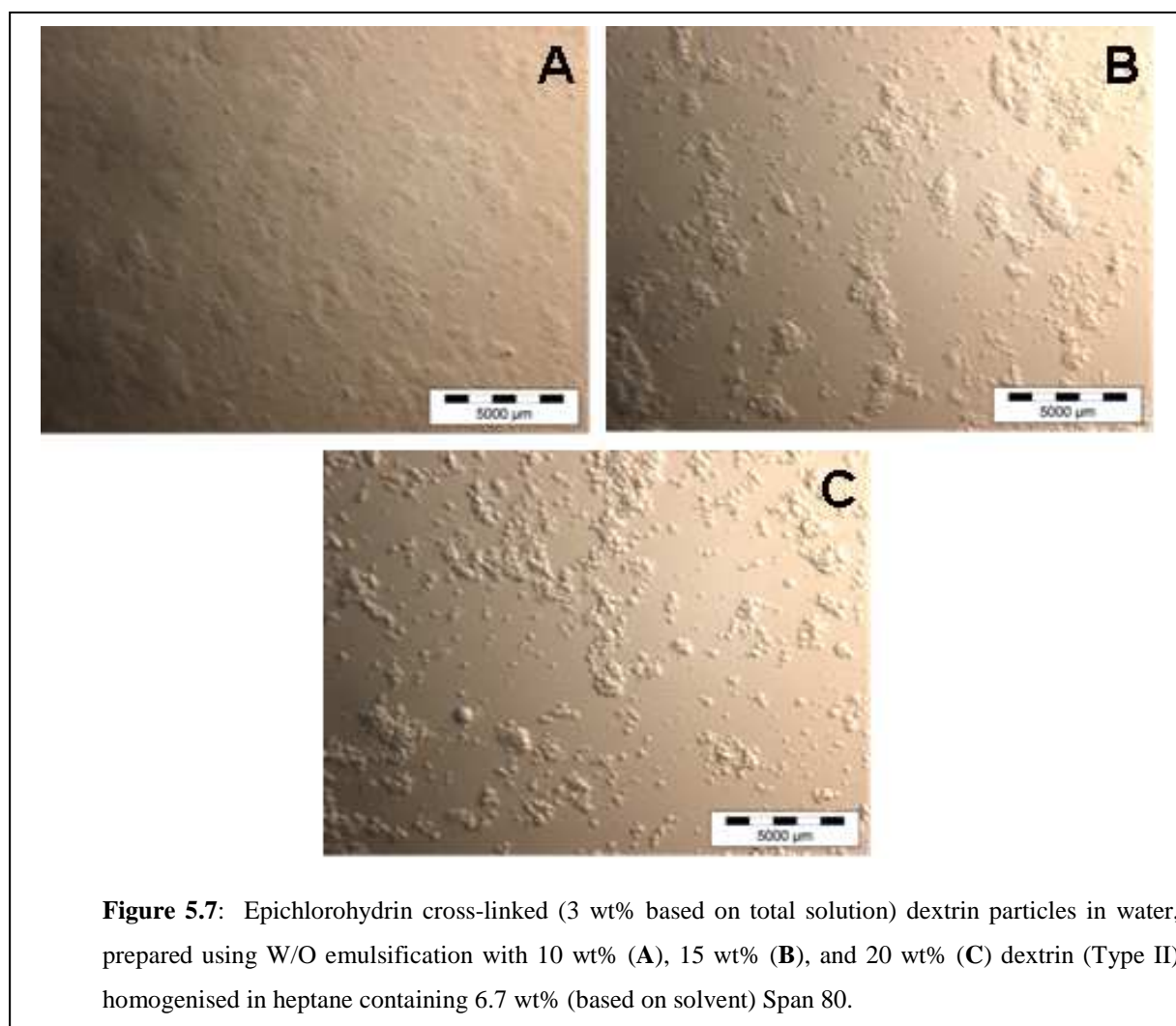
A solvent phase was prepared by dissolving the emulsifier Span 80 (6.7 wt% based on solvent) and the cross-linking agent ECH (3% based on total solution weight) in heptane. The aqueous and solvent phases were combined in a 2:3 (w/w) ratio and homogenised using a Silverson (Model L4R) homogeniser for 2 minutes at 5,500 rpm. The samples were removed

and placed under low shear magnetic stirring for 24 hours to allow cross-linking to complete. The pH of the final solution was adjusted to pH 7 by addition of HCl. Samples were centrifuged to separate the cross-linked dextrin particles (if formed) from the solvent, washed 3 times with DDI water with intermediate centrifugation cycles, and finally re-dispersed in DDI water to make up a total sample weight of 50 ml.

The samples prepared using dextrin concentrations below 10 wt% formed clear solutions during washing cycles and no particles were detected during further inspection under an optical microscope, denoting insufficient cross-linking due to the low dextrin concentrations. From 10 wt% dextrin particles developed with increased discreteness and, although some agglomeration was detected throughout, it can be concluded that the minimum dextrin concentrations would preferably be between 15 and 20 wt% for adequate cross-linking and particle formation (Figure 5.7).

5.3.3.3 Emulsifier selection

Span 80 (sorbitan mono-oleate), which is a non-ionic lipophilic emulsifier with a molecular weight of 428 g/mol and HLB (hydrophilic/lipophilic balance) of 4.3, is a carrier of water molecules, and as a result causes swelling of the discontinuous phase of W/O emulsions, resulting in destabilisation of emulsion droplets[19]. Span 80 is biodegradable, making it very attractive for application as non-toxic emulsifier for food, textile, and cosmetic industries, but together with its water-carrier ability renders it prone to undergo microbial degradation. Furthermore it exhibits poor chemical stability, and quickly undergoes hydrolysis, especially when NaOH is incorporated into the internal phase[20], which is the case in this particular system.

An aqueous phase containing 15 wt% dextrin and 2.5 wt% NaOH was prepared and loaded to one of the high pressure syringe pumps. A solvent phase consisting of 6.7 wt% Span 80 and 5 wt% ECH dissolved in heptane was loaded to the other pump. Emulsification using the interdigital micro-mixer was conducted and two samples collected, prepared using aqueous phase to solvent phase flow rates of 5 ml/min: 10 ml/min and 10ml/min: 20 ml/min, respectively. Samples were left for 24 hours in order for cross-linking to complete. Optical

microscopy performed on these samples showed that particles obtained were fairly poly-disperse, especially those obtained with lower flow rates (Figure 5.8 A and B). It is evident that coalescence occurred after emulsification as clear aqueous layers formed at the bottom of the sample vials.

As opposed to Span 80, consisting of one hydrophilic unit with a hydrophobic hydrocarbon chain, higher molecular weight emulsifiers, consisting of repeating hydrophobic and hydrophilic units, have been found to produce W/O emulsions of high stability and controllable droplet size[21]. These emulsifiers occupy a stable position at the interface with the hydrophilic portion of the molecule, which can consist of a polyethylene glycol group, acting as an anchor group embedded in the aqueous phase. The hydrophobic portions, such as poly-12-hydroxy stearic acid, penetrate into the solvent phase, providing superior colloidal stability against coalescence. Hypermer B246, a commercial emulsifier, is a polymeric surfactant consisting of an A-B-A block copolymer of polyhydroxystearic acid-polyethylene glycol-polyhydroxystearic acid with an HLB value of approximately 4.6 and a molecular weight between 400 and 5,000 g/mol. It is widely used in mining applications for preparing stable high interface W/O dispersions, which include oil-based drilling fluids and has been used to emulsify polar organic materials such as methanol or ethanol in automotive fuel blends.

Experimentation using the micro-mixer was repeated where Span 80 was replaced with 1 wt% (based on solvent phase) Hypermer B246, using aqueous phase to solvent phase ratios of 10 ml/hr: 40 ml/hr as well as 15 ml/hr: 30 ml/hr. Emulsions showed improved stability with no phase separation detected in the 24 hours after emulsification. Optical microscope images (Figure 5.8 C) displayed droplet particles of significantly lower poly-dispersity, validating the superior performance of this emulsifier. Subsequently this emulsifier was used for all further experimentation.

5.3.3.4 Preparation of anionic modified dextrin particles

Superabsorbents are hydrogels consisting of cross-linked three dimensional hydrophilic networks that can absorb and retain significant amounts of water[22]. It is mainly used as absorbents in healthcare (such as diapers) and agricultural industries and commonly based on acrylic monomers such as acrylamide, acrylic acid, as well as salts of the acid[23].
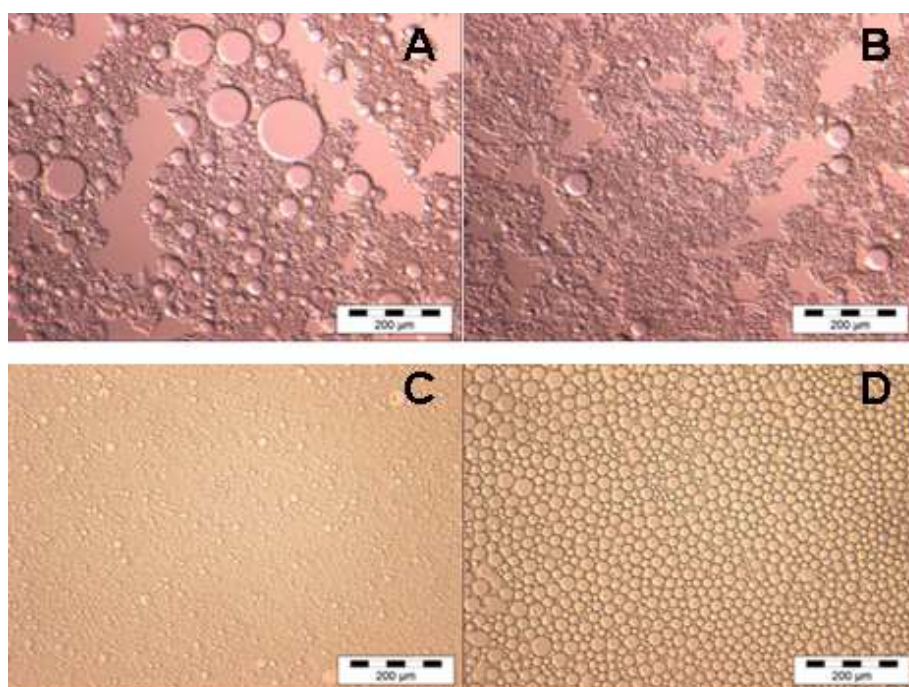
Figure 5.8: Dextrin particles prepared by W/O emulsification in heptane using the microfluidic device Span 80 surfactant (6.7 wt% based on solvent) at aqueous phase to solvent phase flow rates of 5 ml/min: 10 ml/min (**A**) and 10ml/min: 20 ml/min (**B**), as well using Hypermer B246 as surfactant (1 wt% based on solvent) at 10ml/min: 40 ml/min (**C**) and 15 ml/min: 30 ml/min (**D**).

Lately, the majority of superabsorbents are manufactured using synthetic polymers such as acrylics, but "greener" alternatives, such as polysaccharide-based superabsorbents are gaining renewed interest due to increased environmental protection demand.

Generally, reactions for preparing these mostly involve grafting acrylic monomers (acrylic acid[24], acrylonitrile[25], and acrylamide[26-28]) onto starch in the presence of a suitable cross-linking agent. Copolymerisation of reactive allyl maize starch with acrylic monomers have also been reported[29]. These monomers can be polymerised by solution as well as inverse suspension/emulsion techniques though inverse emulsion polymerisation is preferred due to its simplicity and ability to reach high molecular weights, as well as high reaction rates during polymerisation. By using a water-soluble initiator system, solution polymerisation was realised with reaction rates enhanced even further, as opposed to using an oil-soluble initiator where the micellar model is sometimes valid. Another disadvantage of using an oil-soluble cross-linker during emulsification in a microfluidic device is that the cross-linker

concentration varies proportionately to the aqueous starch phase with variation in feed flow ratios, resulting in vagaries in the degree of cross-linking.

The bifunctional compound *N,N'*-methylene bisacrylamide (MBA) is most often used as a water-soluble cross-linking agents in graft and copolymerisation reactions of hydrogels, and usually used in combination with potassium persulphate (KPS) or ammonium persulphate water-soluble thermal initiators where solution and inverse-suspension methods of polymerisation is applied and polymerisation is initiated by heating reaction mixtures to 50 – 70 °C[22, 30, 31].

Allyl dextrin (DS = 0.4) was prepared following the procedure described in Section 3.3.2.4, with maize starch replaced with similar quantities of oven dried dextrin. Following purification, the solids content of the allyl dextrin was adjusted to 20 wt% with DDI water. In order to eliminate variability in composition, a bulk solution was prepared by combining about 15 samples. Sodium acrylate, an anionic monomer, was selected for copolymerisation with allyl dextrin (Figure 5.9) due to its solubility in water, whilst remaining essentially insoluble in non-polar solvents such as heptane.

Figure 5.9: Synthesis of anionic cross-linked dextrin hydrogel.
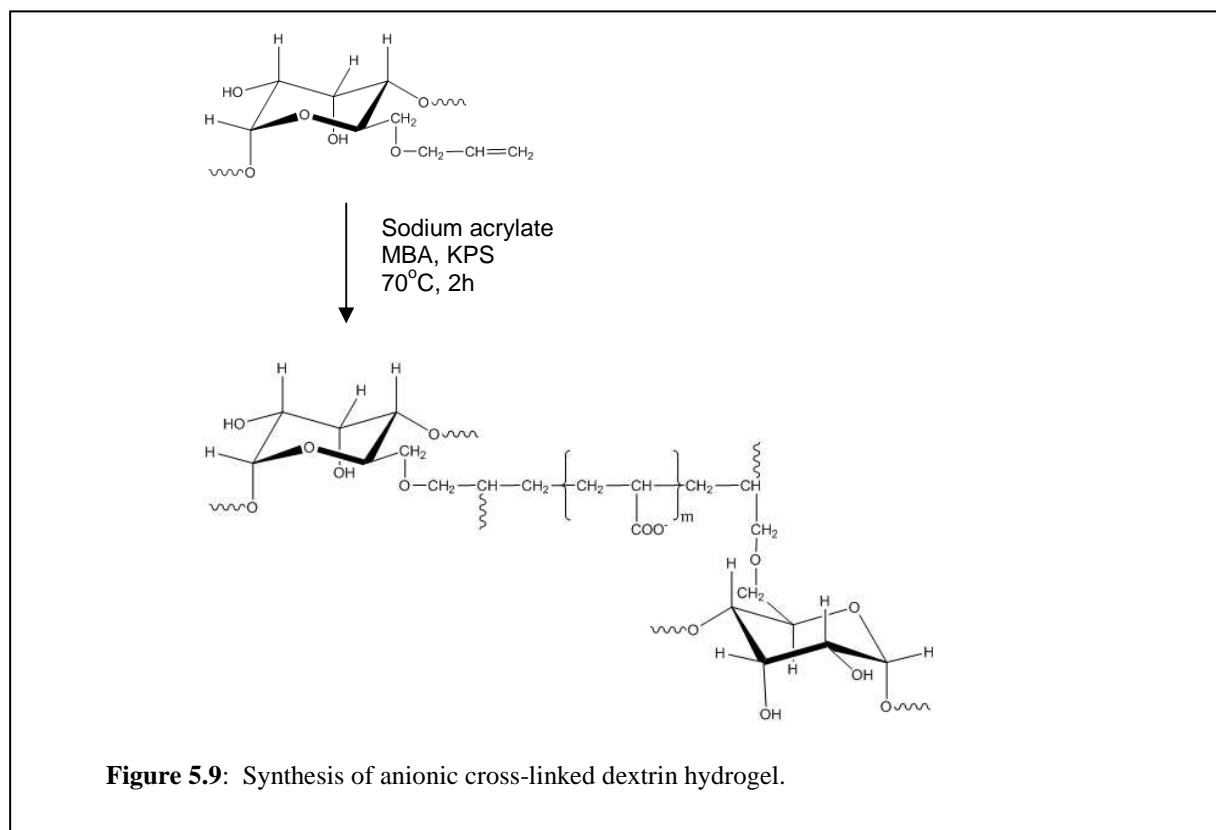
An aqueous phase was prepared consisting of 89.6 wt% of a 20 wt% allyl dextrin solution, 2.4 wt% sodium acrylate, 0.9 wt% MBA, and 7.2 wt% of a 2.5 wt% KPS solution. The oil phase used consisted of heptane in which 1 wt% Hypermer B246 was dissolved. Both phases were filtered through a glass sinter filter to remove any impurities that might block the system before being loaded to the individual syringe pumps. After emulsification in the micro-mixer, polymerisation was initiated using the temperature baths, which was heated to 70 ^{o}C. Samples collected were allowed to react further for a period of 2 hours and cooled. The cross-linked particles were separated from the solvent by centrifugation, followed by repetitive precipitation in acetone and washing with DDI water in order to purify particles and remove any polyacrylate homopolymer that may have formed. The solids content of the final aqueous particle suspension was adjusted to 2 wt%.

5.3.4 Analysis

5.3.4.1 Fourier transform infrared (FTIR) spectroscopy

In order to confirm presence of the carboxylate group in the cross-linked hydrogel, purified dextrin particles were precipitated in acetone, isolated, and dried in a vacuum oven at 50 ^{o}C and submitted for FTIR (Perkin Elmer Paragon 1000 PC FTIR Spectrometer equipped with a Photoacoustic MTEC 300 cell and fitted with a PAS attachment).

5.3.4.2 Optical microscopy

Optical microscopy of wet samples was performed as described in Section 2.3.2.3.

5.3.4.3 Scanning electron microscopy (SEM)

Oven dried (50°C) samples were submitted for SEM analysis using a Leica/Leo Stereoscan S440 electron microscope unit.

5.3.4.4 Particle size analysis

Washed W/W starch particles (2 wt%) were mixed at ambient temperature for 48 hours before submitting it for particle size analysis using a Saturn DigiSizer 5200.

5.3.5 Results and discussion

The FTIR spectrum of pure dextrin (Figure 5.10) shows a typical starch-like profile with a broad band between 3600 and 3000 cm^{-1}, which was assigned to the O-H stretching mode and is due to hydrogen bonding involving the hydroxyl groups on the dextrin molecules. The intense band at 1653 cm^{-1} was assigned to the first overtone of the O-H bending vibration, whilst the bands at 2920 and 1140 cm^{-1} were assigned to symmetrical stretching vibrations of C-H and C-O, respectively. The strong bands at 1070 and 994 cm^{-1} were attributed to CH_2-O-CH_2 stretching vibrations[32-34]. The hydrogel consisting of allyl dextrin copolymerised with sodium acrylate shows a very strong additional band at 1700 cm^{-1}, which is characteristic of carbonyl (C=O) stretching vibration of carboxylic acid groups and confirms presence of the sodium carboxylate in the polymer[35]. The much smaller increase in peak intensity at 1220 cm^{-1} was assigned to the C-O stretching vibration of the additional ether groups formed during attachment of the allyl groups on the dextrin backbone. The peak at 1524 cm^{-1} was assigned N-H bending vibrations from the amine groups present on the cross-linker used during the polymerisation reaction.
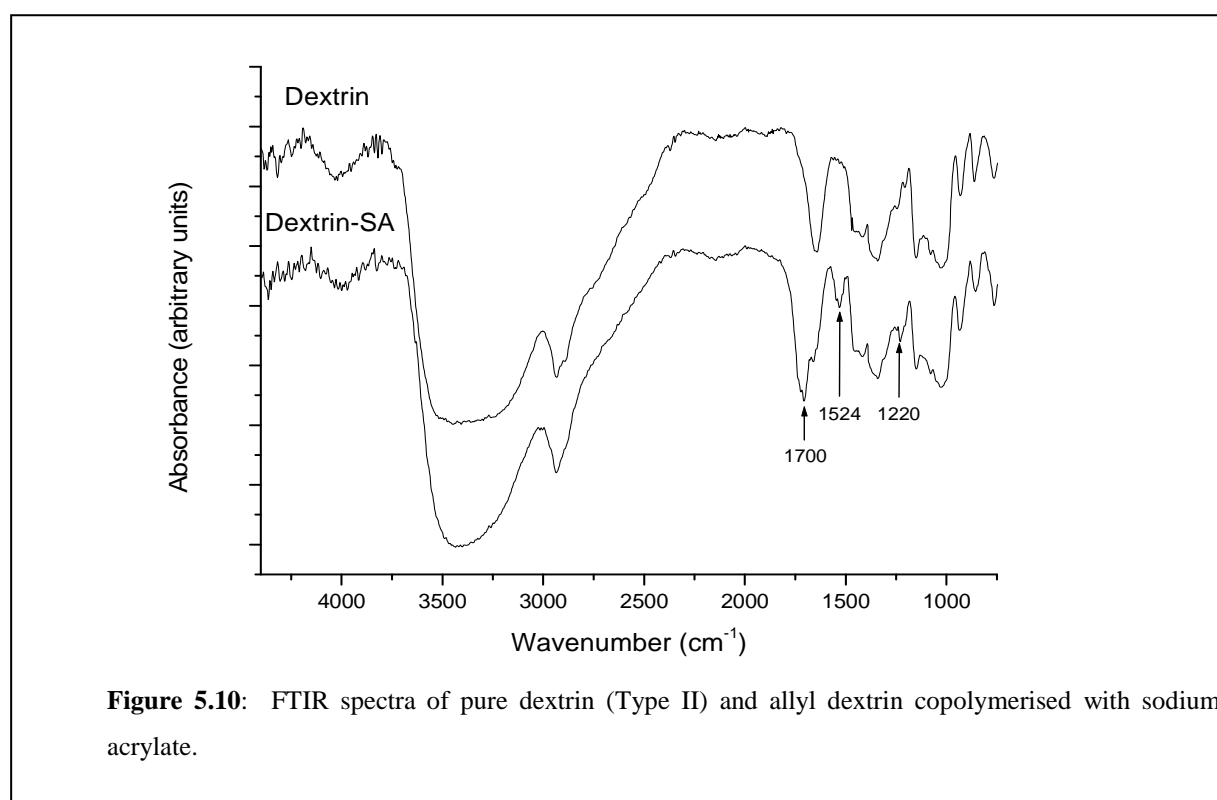
Figure 5.10: FTIR spectra of pure dextrin (Type II) and allyl dextrin copolymerised with sodium acrylate.

Optical microscope images of cross-linked dextrin particles prepared in the microfluidic device using an aqueous flow rate of 5 ml/min and a solvent flow rate of 20ml/min appear in Figure 5.11. Particles are shown in solvent as well as after removal of solvent, purification, and re-dispersion in DDI water. In order to evaluate its interaction with filler, these particles were subsequently treated to a 1.12 wt% solution of PCC and imaging shows clear flocculation of PCC in the presence of the anionic particles (Figure 5.11C). These flocs were isolated and treated with acetone in order to precipitate the dextrin particles. After drying, a sample was submitted for SEM imaging and Figure 5.10D shows some dextrin particles protruding from the flocculated filler particles.

Figure 5.11: Optical microscope images showing cross-linked anionic dextrin particles in heptane (**A**) and after purification and redispersing in DDI water (**B**). Particles were prepared using an aqueous flow rate of 5 ml/min and solvent flow rate of 20 ml/min and subsequently tested for interaction with PCC (2 wt% dry particles based on dry PCC) (**C**). Following precipitation in acetone, the PCC/particle blend was submitted for SEM imaging (**D**) (scale bar = 2µm).

The interaction of particles with both fibre and filler were also investigated using SEM imaging. A 0.5 wt% fibre solution was first treated with a 0.8 wt% (dry starch/ dry fibre) cationic starch (Mondi) solution, before adding 20 wt% (based on dry fibre) PCC solution treated with 2 wt% (dry particles/ dry filler) anionic dextrin particles. The slurry was mixed on a magnetic stirrer for a period of 1 hour, before a sample was taken and dried in a vacuum oven. Figure 5.12 clearly shows strong attachment of particles onto the surface of the fibre along with the filler.
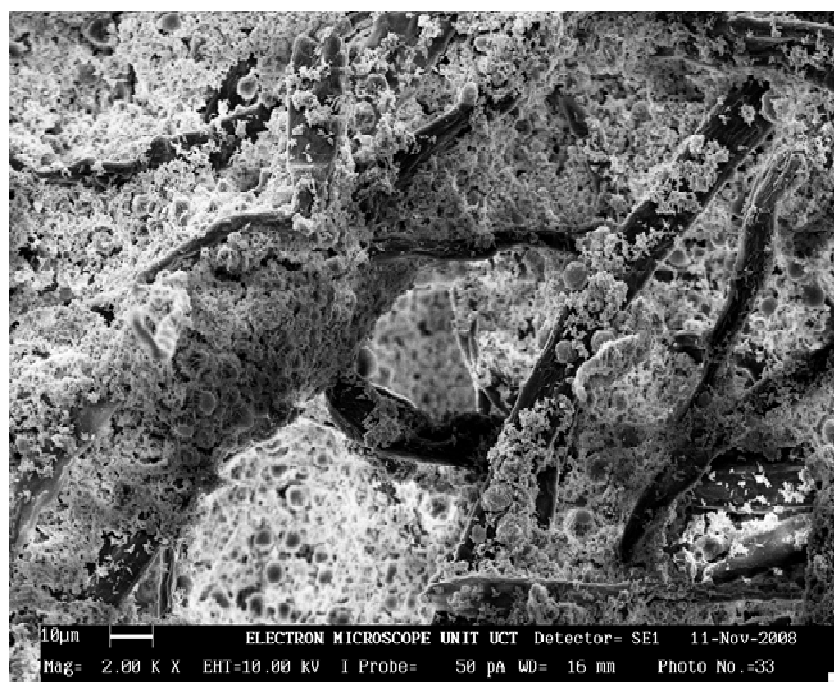
Figure 5.12: SEM image showing interaction of anionic modified dextrin particles with PCC and fibre. (scale bar = 10µm).

The effect of the individual feed rates on particle size and distribution of water dispersed cross-linked dextrin emulsions was studied further. A series of anionic cross-linked particles were prepared where the aqueous feed rate was increased (solvent phase constant) as well as the solvent phase (aqueous phase constant). Figure 5.13 presents particle size distribution curves where the aqueous flow rate was increased from 5 to 15 ml/min (solvent phase flow rate kept at 20 ml/min) and where the solvent phase flow rate was increased from 10 to 40 ml/min (aqueous phase flow rate maintained at 10 ml/min). In the former a marginal increase in distribution was observed at higher aqueous phase flow rates, whilst increasing the solvent flow significantly caused reduction in size and poly-dispersity. A more comprehensive study

was conducted on modelling particle size and standard deviation using response surface methodology (RSM).

Figure 5.13: Particle size distribution of anionic cross-linked dextrin particles prepared using the microfluidic device using different aqueous flow rates (solvent phase flow rate constant) (**A**), and different solvent phase flow rates (aqueous phase flow rate constant) (**B**) (APS = average particle size).
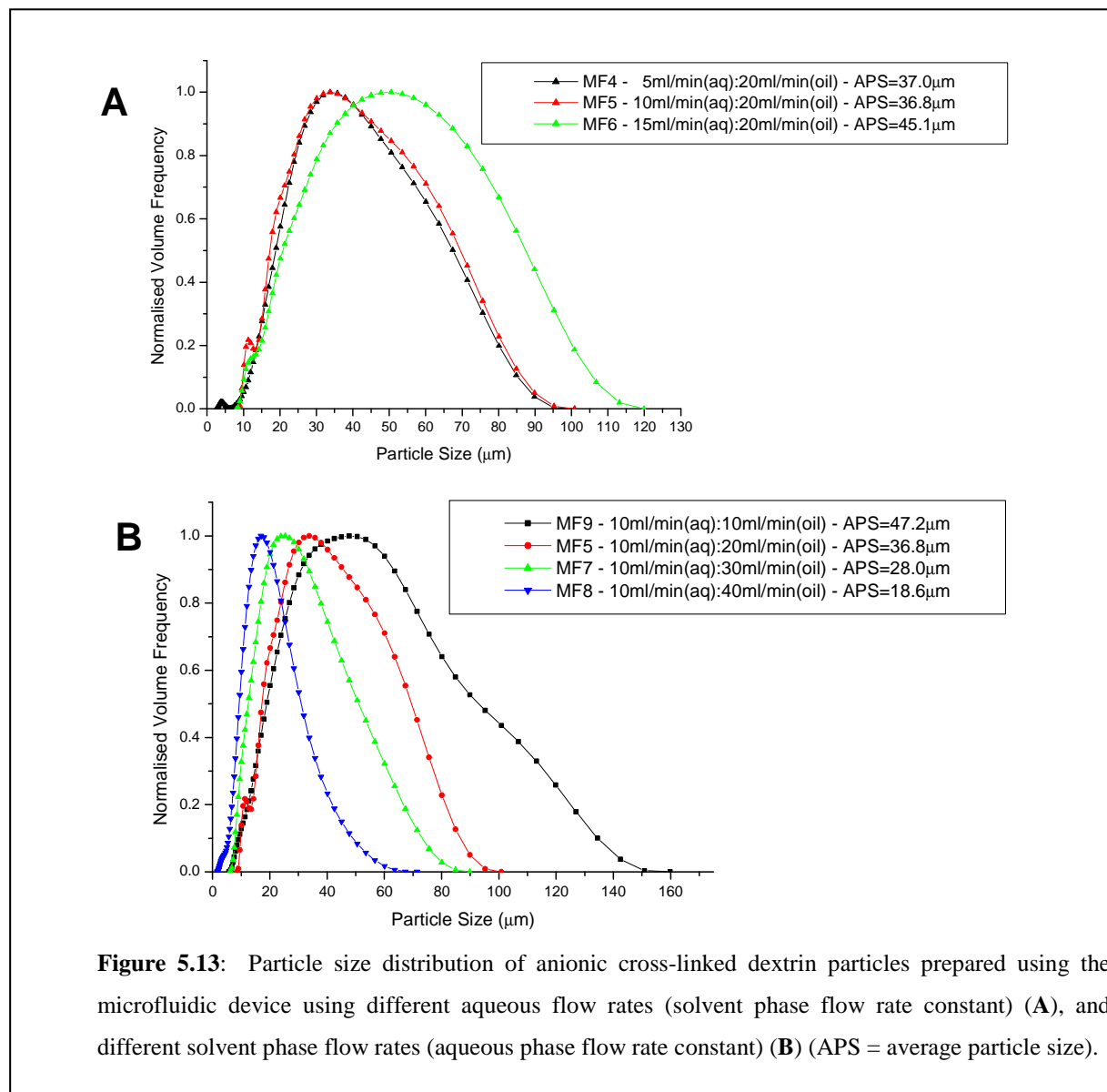
RSM is a combination of statistical and mathematical techniques that are used for optimising, improving, and developing processes and applied for evaluating the effect of multiple factors on a response, even in the event of complex interactions between factors[36, 37]. It usually consists of planning an experimental design followed by conducting of experiments, response surface modelling through regression, and optimisation. The main objective of RSM is to determine the required or optimal operational conditions for satisfying operating

specifications. For this study a three-factor D-optimal experimental design was conducted using Design-Expert® version 7.1.5 software. The D-optimal criterion can be used to select points in a design space in a constrained region and point selection from a candidate point set that are spread throughout the design region.

The main key is that designs are built algorithmically (stepwise approach in a finite number of runs) in order to ensure most accurate estimates of the model coefficients. Unlike Central Composite and Box-Behnken designs, where there is a specific pattern to design points, the points in this type of design are chosen mathematically to satisfy statistical criteria, which are known as D-optimality[38]. Independent variables selected include aqueous phase flow rate, organic phase flow rate, and percentage emulsifier to model its effect on average particle size (APS) and standard deviation (STDev) (dependent variables). The independent variables were coded with high and low levels as indicated in Table 5.1 and the design constrained in order for the discontinuous phase flow rate not to exceed the flow rate of the continuous phase.

Table 5.1 Experimental design of anionic dextrin particle preparation using microfluidics.

Factor name	Units	Low actual value	High actual value	Low coded value	High coded value
Starch flow rate	ml/min	1	20	-1	1
Solvent flow rate	ml/min	2	40	-1	1
Emulsifier conc.	wt % (based on solvent phase)	1	3	-1	1

The D-optimal design required 10 model points and was further augmented to include 5 more model points to calculate the lack-of-fit with another 3 replications to evaluate the pure error. Experiments were carried out in randomised order as required in many design procedures. In the optimisation process, the responses can be related to the factors by linear or quadratic models. In this design a quadratic model was selected, which includes the linear model, and is given as:

$$\eta = \beta_0 + \sum_{j=1}^{k} \beta_j x_j + \sum_{j=1}^{k} \beta_{jj} x_j^2 + \sum_{i} \sum_{<j=2}^{k} \beta_{ij} x_i x_j + e_i \qquad \text{equation 5.1}$$

where η is the response, x_i and x_j are variables, k is the number of independent variables (factors), β_0 is the constant coefficient, β_j, β_{jj}, and β_{ij} are interaction coefficients of linear, quadratic, and second order terms, respectively, while e_i is the error. Analysis of variance (ANOVA) was used to obtain the interaction between process variables and the response. In experimental design the coefficient of determination, R^2, is often used as a measure of the amount of variability between the actual response and the model and higher values (approaching 1) are usually associated with low variability and hence a good fit. This is not always the case, as adding more and more variables to the model, whether they are statistically significant or not, usually result in an increase in R^2 even though the actual regression is poor. Therefore ANOVA is carried out by comparing these values with the adjusted R^2 (R_{adj}^2), which is a measure of the amount of variation around the mean explained in the model and usually decreases as more and more insignificant model terms are added. If a significant difference between R^2 and R_{adj}^2 exists, there is a good chance that insignificant terms were included in the model. Another coefficient used is the predicted R^2 (R_{pred}^2), which is another measure of the amount of variance in new data, as explained by the model. In other words, it is an indication of how good the model predicts each response value. Ideally R_{pred}^2 and R_{adj}^2 should be in agreement with each other. The R^2, R_{adj}^2, and R_{pred}^2 values were calculated using equations 5.2, 5.3, and 5.4, respectively.

$$R^2 = 1 - \frac{SS_{residual}}{SS_{model} + SS_{residual}} \qquad \text{equation 5.2}$$

$$R_{adj}^2 = 1 - \frac{SS_{residual}/DF_{residual}}{(SS_{model} + SS_{residual})/(DF_{model} + DF_{residual})} \qquad \text{equation 5.3}$$

$$R_{pred}^2 = 1 - \frac{PRESS}{SS_{model} + SS_{residual}} \qquad \text{equation 5.4}$$

In equations 5.2 and 5.3, SS is the sum of squares and DF the degrees of freedom. The predicted residual sum of squares (PRESS) is a measure of how the model fits each point in the design and determined by setting aside an individual observation from the dataset and

refitting the regression model to the remaining n-1 data[39]. The error in predicting this point is squared and repeated for all remaining points. The PRESS is the sum of these errors.

The design matrix tabling the experimental conditions (actual and coded values) as well as the response record is shown in Table C1, Appendix C. Multiple regression coefficients were estimated, employing the method of least squares, in order to realise quadratic polynomials that can accurately approximate response predictions. Analysis of fitted surfaces is considered accurate if it is approximately equivalent to the true response and in most cases a second-order model is found to be adequate[38]. In equations 5.5 and 5.6 the average particle size ($\hat{y}_{APS}$) and standard deviation ($\hat{y}_{STDev}$) responses are shown (in terms of coded and actual factors), respectively, with x_1, x_2, and x_3 corresponding to the independent variables of starch flow rate, solvent flow rate, and emulsifier percentage, respectively.

$$\hat{y}_{APS}(coded) = 34.39 + 4.47x_1 - 13.60x_2 - 6.31x_3 + 7.39x_1x_2 \\ - 8.68x_1x_3$$

equation 5.5A

$$\hat{y}_{APS}(actual) = 46.94 + 1.44x_1 - 1.15x_2 + 3.28x_3 + 0.04x_1x_2 \\ - 0.91x_1x_3$$

equation 5.5B

$$\hat{y}_{STDev}(coded) = 37.06 + 2.09x_1 - 10.95x_2 - 5.90x_3 + 7.99x_1x_2 \\ - 10.75x_1x_3 - 10.53x_2x_3$$

equation 5.6A

$$\hat{y}_{STDev}(actual) = 21.38 + 1.55x_1 + 0.07x_2 + 17.61x_3 + 0.04x_1x_2 \\ - 1.13x_1x_3 - 0.55x_2x_3$$

equation 5.6B

Adequacy and fitness of the models were evaluated by ANOVA and presented in Tables 5.2 and 5.3 for $\hat{y}_{APS}$ and $\hat{y}_{STDev}$, respectively. . The statistical significance of the model was also checked by the F-test in the Design-Expert® software program[40, 41]. In both tables, the model F-values of 72.79 and 31.14 was higher than the critical F-values, implying that both models were significant. From the low p-values, which is the probability of seeing the observed F-value if there is no factor effect (Prob>F), there is less than 0.01% chance that the model F-values could be this large due to noise.

Table 5.2: ANOVA results of the second order model for estimating average particle size.

Source	Sum of squares (SSE)	Degrees of freedom (DF)	Mean square (MS)	F-value	P-value
Model	4870.08	6	811.68	72.79	< 0.0001
X_1 -Aqueous flowrate (ml/min)	156.33	1	156.33	14.02	0.0032
X_2-Solvent flowrate (ml/min)	960.69	1	960.69	86.15	< 0.0001
X_3-Surfactant level (%)	368.05	1	368.05	33.01	0.0001
X_1X_2	269.46	1	269.46	24.16	0.0005
X_1X_3	683.33	1	683.33	61.28	< 0.0001
X_2X_3	46.51	1	46.51	4.17	0.0658
Residual	122.66	11	11.15		
Lack of Fit	104.35	7	14.91	3.26	0.1354
Pure Error	18.31	4	4.58		

R^2=0.975; R_{adj}^2=0.962; R_{pred}^2=0.955; adequate precision=22.44 (>4)

Table 5.3: ANOVA results of the second order model for estimating standard deviation.

Source	Sum of squares (SSE)	Degrees of freedom (DF)	Mean square (MS)	F-value	P-value
Model	6270.48	6	1045.08	31.14	< 0.0001
X_1 -Aqueous flowrate (ml/min)	34.14	1	34.14	1.02	0.3348
X_2-Solvent flowrate (ml/min)	623.30	1	623.30	18.57	0.0012
X_3-Surfactant level (%)	390.70	1	390.70	11.64	0.0058
X_1X_2	314.98	1	314.98	9.38	0.0108
X_1X_3	1200.15	1	1200.15	35.76	< 0.0001
X_2X_3	1000.80	1	1000.80	29.82	0.0002
Residual	369.19	11	33.56		
Lack of Fit	326.38	7	46.63	4.36	0.0867
Pure Error	42.81	4	10.70		

R^2=0.944; R_{adj}^2=0.914; R_{pred}^2=0.773; adequate precision=16.68 (>4)

The "Lack of Fit" p-value of 0.0867 for the STDev model was slightly lower than 0.10, which is the minimum preferred value. However, values above 0.05 can still be considered to be an indication that the data fits the model reasonably well. The R_{pred}^2 value of 0.773 was in reasonable agreement with the R_{adj}^2 value of 0.914 (values should be within 0.2 to be considered as in reasonable agreement). Coefficients for the APS model varied between 0.96 – 0.98, indicating very good correlation. Adequate precision values, which is an indication of the signal to noise ratio, should ideally be higher than 4. For both models these values were above 10, suggesting that the models were significant and could be used to explore the design space[41].

It should be noted that the effect of each variable on the response is a combination of the coefficients and variable values as well as the contribution of joint effects (or interactions) of

variables. Often this can not be easily observed by traditional experimental design procedures[42]. By looking at the p-values of individual factor coefficients as well as the model coefficients of the coded models (equations 5.5A and 5.6A) the significance of each variable can be distinguished. For significant terms, the p-value should be below 0.05. Where p>0.05 model terms can usually be regarded as insignificant. In the present case ANOVA indicated the combined second order interaction term of solvent flow rate and emulsifier percentage (x_2x_3) in the APS model is not a significant term (p-value = 0.0658) and was subsequently excluded from regression analysis. In the case of the STDev model, the aqueous flow rate term (x_1), where p > 0.05, became an insignificant variable. However, this factor can not be excluded from the model as this will render the model "hierarchically unstable" due to significant second order terms that include this variable.

The normal (%) probability plot of studentised residuals is an important diagnostic tool in the detection and explanation of systematic departures from assumptions that errors are normally distributed and independent of each other. Errors should not be dependent on when the observation occurred, the size of the prediction, or even the factor settings involved in making the prediction.

Figure 5.14: Diagnostic plots of the ANOVA showing the normal (%) probability plot of the internally studentised residuals for APS (**A**) and STDev (**B**) models shown in Equation 5.5 and 5.6, respectively.
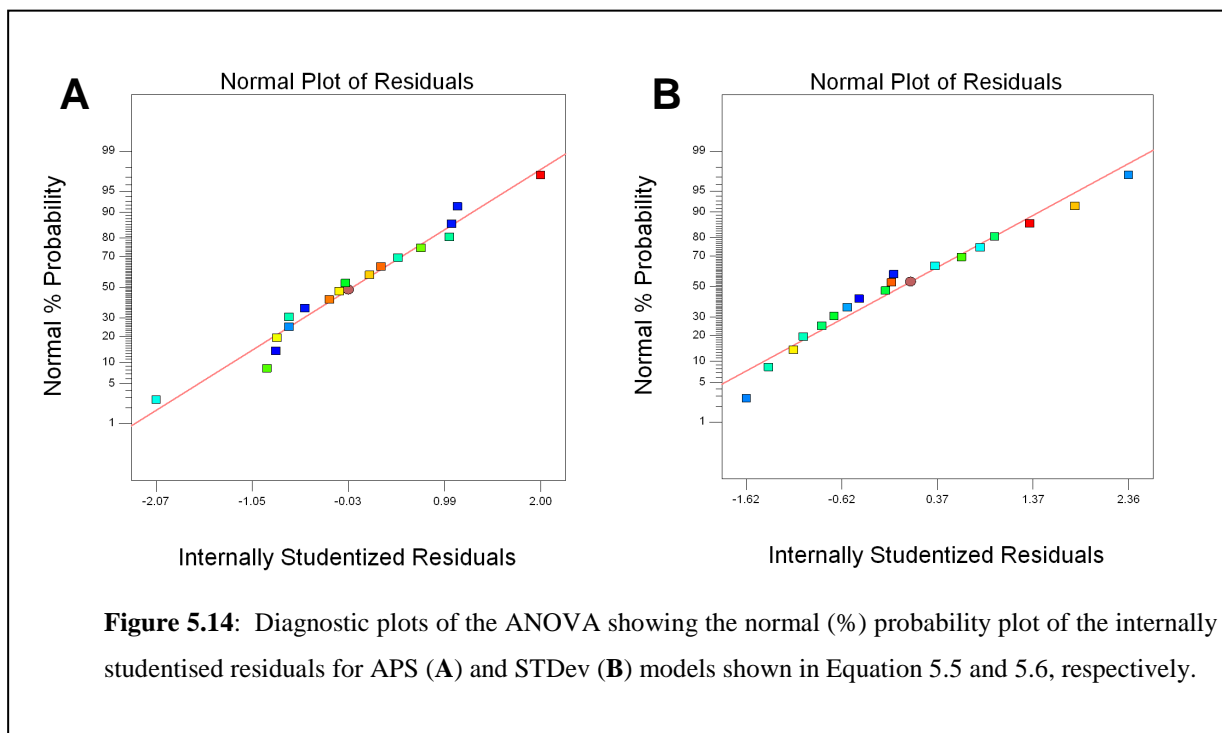
Departures from assumptions usually indicate that the residuals contain "structure", which was not accounted for by the model and that model transformation (such as power or logarithmic transformation) may be required. In Figure 5.14 residuals for both models occur randomly along a straight line, which is indicative of normal residual distribution. A prominent S-shaped distribution for example, would have implied transformation was necessary.

A plot of predicted versus actual response values for APS and STDev is shown in Figure 5.15 (also see Table C1, Appendix C). The actual values are the measured response for a given run, and the predicted value was evaluated from the model and generated using the approximating function. In both models these predicted values are overall in good agreement with actual responses of data points evenly distributed along the straight line. From the diagnostics tool no outlier data points was detected and all response values were therefore considered significant.

Figure 5.15: Diagnostic plots of the ANOVA showing the observed versus predicted data points for APS (**A**) and STDev (**B**) models shown in equations 5.5 and 5.6, respectively.
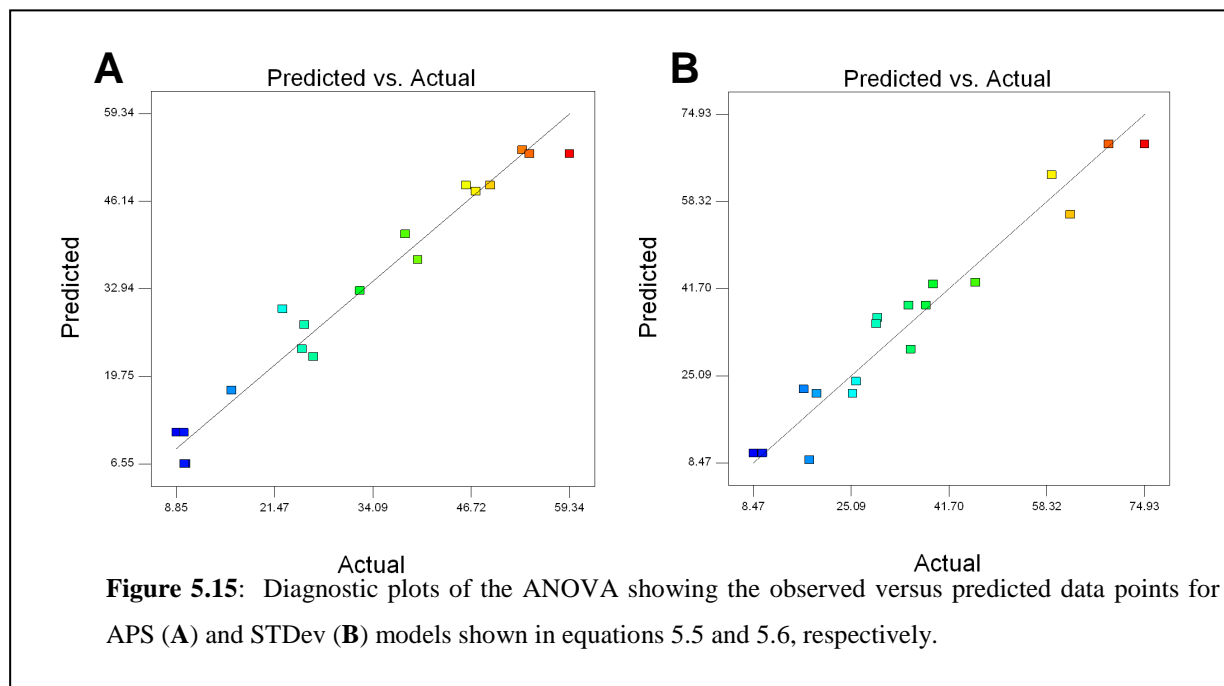
Response surface plots of the APS and STDev models are presented in Figure 5.16 and 5.17, respectively, indicating change in response as a function of aqueous and solvent flow rates. Plots are shown with emulsifier concentration at 1 wt% (min) and 3 wt% (max).

164

Figure 5.16: Response surface plots of APS showing the effect of aqueous and solvent flow rates at 1 wt% (min) (**A**) and 3 wt% (max) (**B**) emulsifier concentration.

Figure 5.17: Response surface plots of STDev showing the effect of aqueous and solvent flow rates at 1 wt% (min) (**A**) and 3 wt% (max) (**B**) emulsifier concentration.
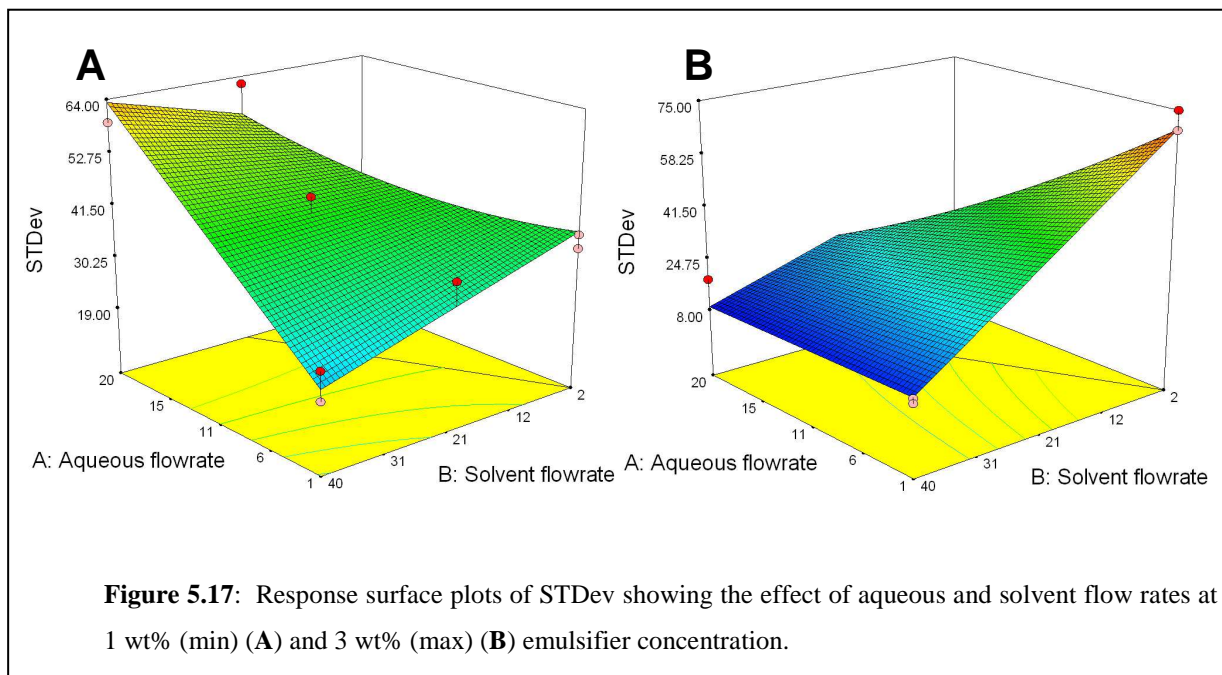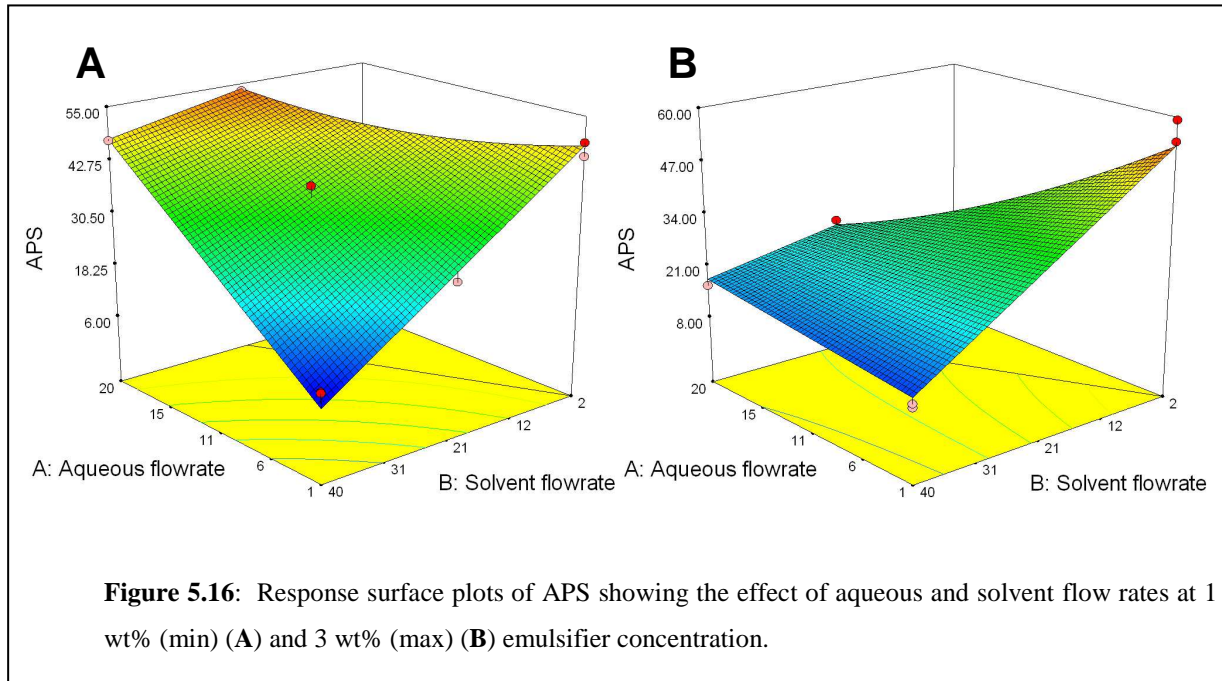
In both models APS and STDev values decreased sharply as the aqueous flow rate was decreased and solvent flow increased at the lower emulsifier level. As emulsifier level increased, dependence of response values on the aqueous flow rate decreased with increasing solvent flow rate levels, with APS as well as STDev values remaining at a close minimum as the solvent flow reached its maximum. At low solvent flow rate levels, the interaction of the

165

emulsifier (in the solvent phase) with the aqueous phase is poor, causing an increase in particle size and standard deviation. The interaction can significantly be improved if higher levels of emulsifier are used, allowing smaller, less poly-dispersed particle formation at higher aqueous flow rates. At lower emulsifier levels, the aqueous phase to solvent phase ratio must be maintained at a minimum in order to achieve similar results.

The interaction of factors can be visualised more clearly by looking at a 3-dimensional cube plot of predicted responses (Figure 5.18) at minimum and maximum levels of all 3 variables. The APS model indicates that lower aqueous as well as solvent flow rates produced larger particles at lower emulsifier levels. Increasing the emulsifier level at these flow conditions did not show any significant effect. However, at higher flow rates the interaction of the emulsifier with the aqueous phase increased, resulting in smaller particle formation at relatively higher aqueous flow rates. A similar observation is seen in the STDev model, although particles prepared at higher flow rates and emulsifier levels appear to be less poly-dispersed.

Figure 5.18: Cube plots for the APS (**A**) and STDev (**B**) models indicating modeled response values at each maximum and minimum factor design points.
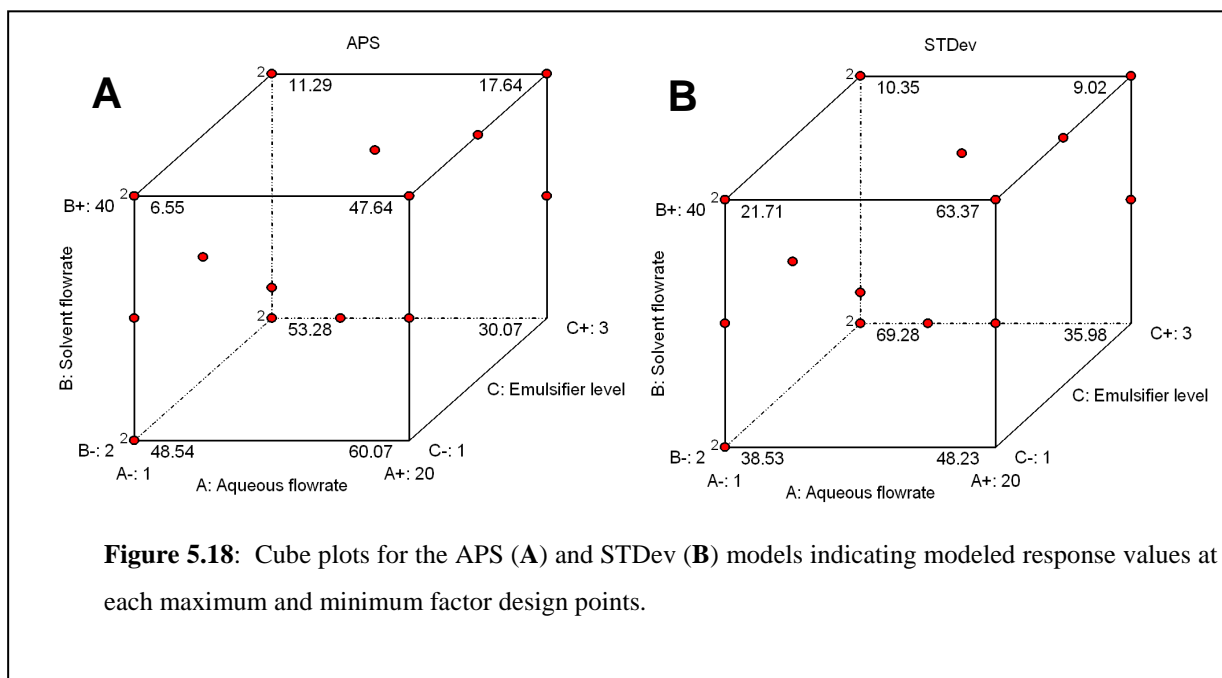
In order to investigate the performance of these anionic modified dextrin particles and its size in paper, three samples from the experimental design study were selected for testing in paper

hand sheets. These samples vary in average particle size and distribution and include (from Table C1, Appendix C) Run 16 (APS = 8.9 µm, STDev = 10.0), Run 11 (APS = 25.0 µm, STDev = 17.0), and Run 10 (APS = 49.1 µm, STDev = 37.8). Results are presented and discussed in Chapter 6.

Micro-structured devices for pilot and even production sized plants have already been developed by IMM and include the Star Laminator (or StarLam) series[3]. These devices consist of plates containing star-shaped openings that are stacked together within a housing. The large internal openings, together with high feed rates, allow eddy formation, resulting in emulsification. Several hundred (low cost) plates can be stacked together which allows extremely high throughputs of up to 5 m^3/hr. A further study on the performance of these devices for process industrialisation purposes would prove to be very interesting.

5.4 Conclusions

The ultimate aim of this part of the study was to explore an opportunity to introduce new processing technology that could potentially benefit the papermaking industry in the future. The most widely reported processes for preparing polysaccharide-based particles today consist of traditional W/O emulsification procedures and this study would have offered limited contribution if merely similar processes were followed. Subsequently microfluidic devices were identified as a novel technique for performing W/O emulsification, offering a number of benefits such as reduced energy demand, control over particle size and reproducibility. Environmentally friendly superabsorbent chemistry was used as basis for developing a system for preparing anionic modified dextrin particles using these devices.

Since it was shown early on in the investigation that emulsion particle size was influenced by changes in flow conditions, a more comprehensive experimental design was used to determine its effect on both size and distribution. A superior W/O emulsifier to the commonly used sorbitan mono-oleate was also obtained and the effect of addition levels was included in the design.

Dextrin was selected as preferred polysaccharide due to its lower molecular weight and solution viscosity and modified with unsaturated allyl groups. Copolymerisation with sodium acrylate was conducted after emulsification in heptane, containing Hypermer B246 as the preferred emulsifier using a multi-channel interdigital micro-mixer.

The response surface methodology used indicated that both size and distribution were the most significantly effected by both the solvent and aqueous flow rates and, in general, increasingly smaller particles were formed when the solvent to aqueous flow rate ratio was increased. However, by increasing the emulsifier concentration in the solvent phase, the aqueous phase flow rate could essentially be increased together with the solvent flow rate without causing an increase in the particle size and/or distribution.

While various size particles were prepared during this investigation, the composition of each remained essentially unchanged. Therefore the opportunity was presented to establish what the effect of gel particle size would be on the strength of paper. Additionally, its functionality could then be compared to the hand sheets made using the polymers prepared by conventional techniques as described in the previous chapter. From all the different approaches undertook during the course of this study, it would subsequently follow that insightful conclusions be drawn at the end of this study, both from a chemical and processing perspective.

5.5 References

1.   C. Wischke; D. Lorenzen; J. Zimmermann, et al., *European Journal of Pharmaceutics and Biopharmaceutics*, **2006**, 62, 247-253.

2.   S. Freitas; A. Walz; H. P. Merkle, et al., *Journal of Microencapsulation*, **2003**, 20, 67-85.

3.   V. Hessel; H. Lowe; F. Schonfeld, *Chemical Engineering Science*, **2005**, 60, 2479-2501.

4.   O. de la Iglesia; V. Sebastian; R. Mallada, et al., *Catalysis Today*, **2007**, 125, 2-10.

5.   K. Jahnisch; M. Baerns; V. Hessel, et al., *Journal of Fluorine Chemistry*, **2000**, 105, 117-128.

6.   P. Lob; H. Lowe; V. Hessel, *Journal of Fluorine Chemistry*, **2004**, 125, 1677-1694.

7. Y. Men; G. Kolb; R. Zapf, et al., *Chemical Engineering Research and Design*, **2009**, 87, 91-96.

8. M. O'Connell; G. Kolb; R. Zapf, et al., *Catalysis Today*, **2009**, 144, 306-311.

9. Y. Men; G. Kolb; R. Zapf, et al., *International Journal of Hydrogen Energy*, **2008**, 33, 1374-1382.

10. G. Kolb; R. Zapf; V. Hessel, et al., *Applied Catalysis A: General*, **2004**, 277, 155-166.

11. G. Kolb; J. Schurer; D. Tiemann, et al., *Journal of Power Sources*, **2007**, 171, 198-204.

12. Y. Men; G. Kolb; R. Zapf, et al., *Trans IChemE*, **2007**, 85, 413-418.

13. T. Nisisako; T. Torii; T. Higuchi, *Chemical Engineering Journal*, **2004**, 101, 23-29.

14. A. S. Utada; E. Lorenceau; D. R. Link, *Science*, **2005**, 308, 537-541.

15. T. Nakashima; M. Shimizu; M. Kukizaki, *Advanced Drug Delivery Reviews*, **2000**, 45, 47-56.

16. P. Löb; H. Pennemann; V. Hessel, et al., *Chemical Engineering Sciences*, **2006**, 61, 2959-2967.

17. V. Hessel; H. Löwe; A. Muller, et al., *Chemical Microprocessing Engineering: Processing and Plants*. Wiley-VCH: Weinheim, **2005**.

18. P. Löb; H. Pennemann; V. Hessel, *Chemical Engineering Journal*, **2004**, 101, 75-85.

19. N. N. Dutta, *History and Trends in Bioprocessing and Biotransformation*. Springer-Verlag: Heidelberg, **2002**.

20. A. Kargari; T. Kaghazchi; M. Soleimani, *Desalination*, **2004**, 162, 237-247.

21. K. E. Cawiezel; R. Hodge, High Internal Phase Ratio Water-in-oil Emulsion Fracturing Fluid, Patent: US 5,633,220, **1997**.

22. M. J. Zohuriaan-Mehr; K. Kabiri, *Iranian Polymer Journal*, **2008**, 17, 451-477.

23. Q. Tang; J. Wu; H. Sun, et al., *Carbohydrate Polymers*, **2008**, 73, 473-481.

24. V. D. Athawale; V. Lele, *Carbohydrate Polymers*, **1998**, 35, 21-27.

25. R. Mehrotra; B. Ranby, *Journal of Applied Polymer Science*, **2003**, 21, 3407-3415.

26. I. K. Varma; O. P. Singh; N. K. Sandle, *Macromolecular Materials and Engineering*, **2003**, 119, 183-192.

27. O. P. Singh; N. K. Sandle; I. K. Varma, *Macromolecular Materials and Engineering*, **2003**, 121, 187-193.

28.   P. Lanthong; R. Nuisin; S. Kiatkamjornwong, *Carbohydrate Polymers*, **2006**, 62, 229-245.

29.   S. P. Bhuniya; M. S. Rahman; A. J. Satyanand, et al., *Journal of Polymer Science: Part A: Polymer Chemistry*, **2003**, 41, 1650-1658.

30.   I. Neamtu; L. E. Nita; A. P. Chiriac, et al., *Journal of Optoelectronics and Advanced Materials*, **2006**, 8, 201-204.

31.   K. Kratz; A. Lapp; W. Eimer, et al., *Colloids and Surfaces A-Physicochemical and Engineering Aspects*, **2002**, 197, 55-67.

32.   S. Pal; D. Mal; R. P. Singh, *Carbohydrate Polymers*, **2005**, 59, 417-423.

33.   H. Garcia; A. S. Barros; C. Goncalves, et al., *European Polymer Journal*, **2008**, 44, 2318-2329.

34.   K. S. Parvathy; N. S. Susheelamma; R. N. Tharanathan, et al., *Carbohydrate Polymers*, **2005**, 62, 137-141.

35.   D. Pavia; G. Lampman; G. Kriz, *Introduction to Spectroscopy*. 3rd ed.; Brooks/Cole Thomson Learning: Washington, **2001**.

36.   E. R. Gunawan; M. Basri; M. B. A. Rahman, et al., *Enzyme and Microbial Technology*, **2005**, 37, 739-744.

37.   U. K. Garg; M. P. Kaur; V. K. Garg, et al., *Bioresource Technology*, **2008**, 99, 1325-1331.

38.   B. K. Korbahti; M. A. Rauf, *Journal of Hazardous Materials*, **2009**, 161, 281-286.

39.   M. J. Anderson; P. J. Whitcomb, *RSM simplified: Optimizing Processes using Response Surface Methods for Design of Experiments*. Productivity Press: New York, **2005**.

40.   B. K. Korbahti; N. Aktas; A. Tanyolac, *Journal of Hazardous Materials*, **2007**, 148, 83-90.

41.   *Design-Expert® Software, Version 7*, User's Guide, 2007.

42.   S. J. Romeu; J. M. C. Chanfrau; Y. P. Vila, et al., *Biochemical Engineering Journal*, **2008**, 38, 1-8.

Chapter 6: Hand sheet testing trials

6.1 Introduction

Inter-fibre bonding is a crucial force that determines the strength and/or stiffness of a sheet of paper and two mechanisms for these forces have been reported[1-3]. Over decades it has been assumed that dry strength was achieved due to hydrogen bonding between overlapping fibres, but other studies indicate that the inter-fibril entanglement (hooking) may also play a significant role in determining the physical properties of paper. Ultimately an increase in fibre-fibre bonding is associated with an increase in sheet strength and factors including fibre length, fibre width, fibre collapsibility, degree of fibrillation, fines and hemicellulose content have been shown to be key parameters in correlating technical performance of paper[4]. The incorporation of fillers during the wet-end of the paper making process ultimately reduces fibre-fibre bonding, causing weakening of the matrix, resulting in deterioration of the paper's mechanical properties.

The main objective of this study was to improve fibre-fibre, fibre-filler, as well as filler-filler bonding by addition of ionic modified polymer particles in order to negate (to a certain extent) the loss in paper strength, especially stiffness, as the filler level is increased. Even though the properties of individual components may be known, it is only possible to evaluate the true interactions between additives through evaluation in a sheet of paper.

The ability to make samples of paper manually using a hand sheet mould is integral in the analysis of any type of papermaking process, and the most convenient method to study the suitability of materials if the amount of additives is limited. It should however be noted that the protocol followed serves as comparative tool. This is because hand sheet properties do not necessarily relate to the actual specifications of paper made on industrial scale since the processes differ. Even the properties of hand sheets prepared from different stock solutions (even though it was prepared identically) may differ. Subsequently, for each series of tests, standard sheets were first prepared from the particular stock solution prior to adding anionic additives. The strength of sheets treated with these additives was then compared to those of

the standard sheets. Any changes are normally considered by the papermaker to be an indication of what will happen to the paper made on a mill if the same additions were to be made.

Furthermore, filler loadings used in the printing paper industry is typically not more than 18 wt%. In order to study the effect of increased filler loadings on sheet strength, hand sheets prepared in this study contained between 20 and 30 wt% PCC.

In Chapter 3 (Section 3.2) the preparation of ionic modified polyester particles was described. This was done in order to illustrate the concept of introducing modified particulate substances into paper as a strengthening aid and results will be presented at the start of this discussion. This is followed by an evaluation of ionic modified polysaccharide particles prepared by conventional methods as described in Chapter 4. These include samples prepared by macrogel ultrasonication (Section 4.3), W/W emulsification (designer particles) (Section 4.4), layer-by-layer (LbL) polyelectrolyte encapsulated PCC (Section 4.5), and in-situ cross-linked and anionic modified starch granules (Section 4.6). Apart from processing technique, test samples also differed in degrees of modification (refer to Appendix D for sample details). Hand sheet properties are also shown and compared for selected anionic dextrin particle samples prepared using the microfluidic W/O emulsification approach, presented in Chapter 5. These particles were similar in chemical composition, but differ in average particle size and distribution.

The percentage improvement in paper strength using the various modified polysaccharide additives are also summarised and compared.

6.2 Hand sheets preparation

Hand sheets were prepared at Mondi (Ulmerfeld-Hausmening Mill), Austria (Figure 6.1)[5] according to ISO 5269:2005 standards. Exactly 21g dry pulp was added to 250 ml water and placed in a beating vessel after which it was milled for 30 minutes in order to form a well-dispersed pulp slurry. The suspension was subsequently diluted further with approximately 1.5 L water and disintegrated (600 rpm/2 minutes) in order to sufficiently separate any

intertwined fibres that may have remained free in the pulp stock. This was done without significantly changing the structural properties of the fibres.

Figure 6.1: Flow chart of hand sheet preparation[5].
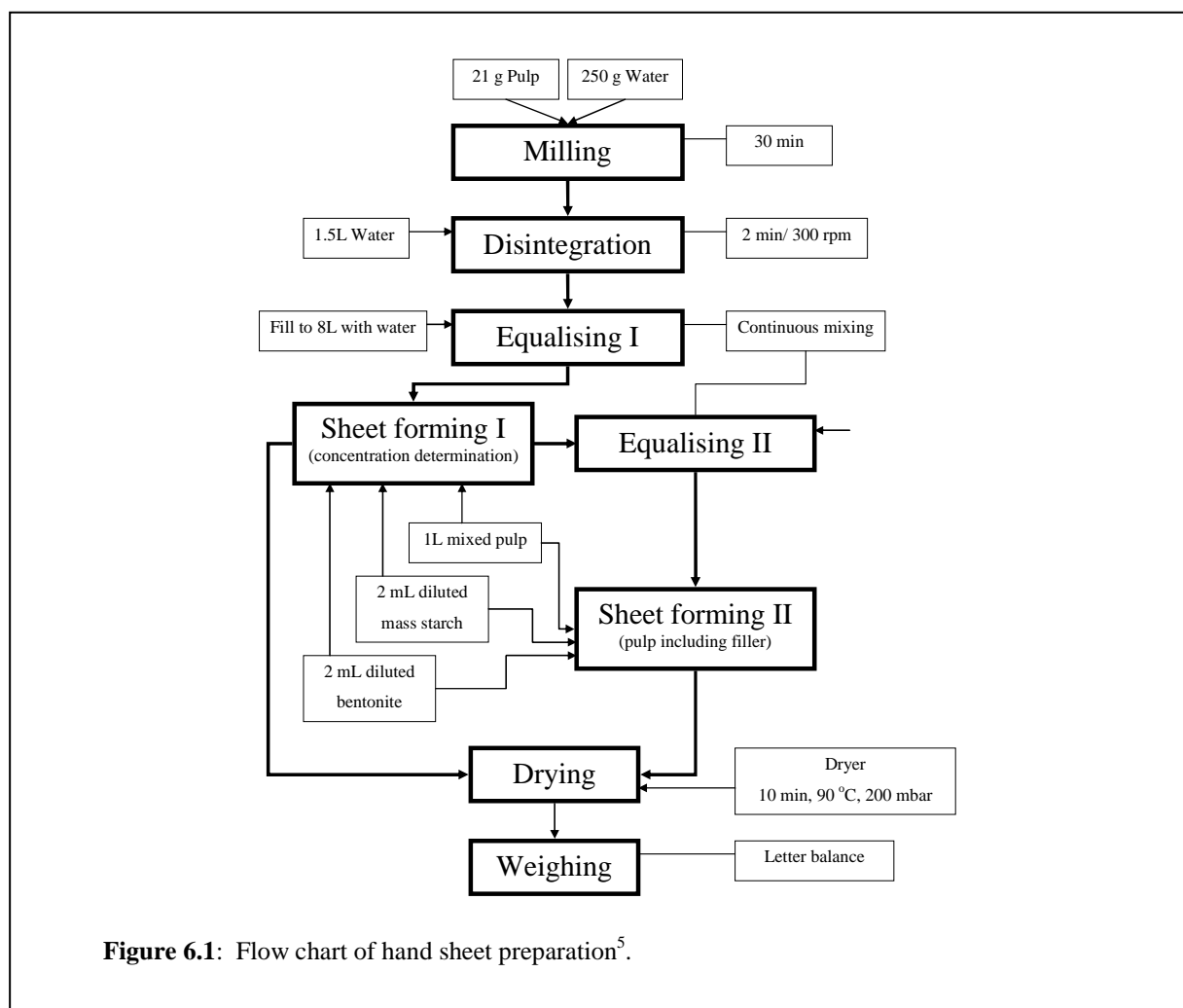
The disintegrated pulp was loaded into an equaliser and once again diluted further to a total volume of 8 L. An equaliser is essentially a mixing vessel that continuously stirs (or aerates) the pulp to ensure uniform pulp distribution within the slurry. Two 1 L samples were taken from the equaliser and placed on a magnetic stirrer and extensively mixed. To each sample, including the standards (unless indicated otherwise), a 0.8 wt% solution of cationic starch, was added followed by 0.1 wt% bentonite. Bentonite is a clay additive used predominantly to absorb wood resins that may obstruct the drainage mesh[6]. It is therefore added to improve water drainage and paper quality. The sequence of additions was done at exactly the same time intervals in order to simulate industrial papermaking processes.

173

The pulp suspensions were subsequently transferred to a continuously stirring stock container on top of a sheet former. The water was drained through a grid plate on which the sheets were formed and subsequently pressed (200 mbar) and dried in a press drier for 10 minutes at 90 $^{\circ}$C.

Dry sheets were weighed and the average calculated. The required grammage (determined by ISO 536:1997 standards) of sheets was 80 g/m^2 and from the average sheet weight obtained during the first sheet forming process, the pulp concentration in the equaliser was adjusted. The filler was also added to the equaliser, at a concentration depending on the percentage pulp being replaced (between 20 and 30 wt%). The sheet forming process (sheet forming II, Figure 6.1) was repeated once again with the same quantity (1 L) samples taken from the equaliser. The average mass of sheets needed to be within 2% of the required sheet grammage, if not, the volume of furnish taken from the equaliser had to be adjusted and repeated once again.

Standard hand sheets were subsequently prepared followed by sheets where anionic polymer additives were added to the filler at a concentration of 2 wt% (based on dry PCC), prior to addition to the pulp stock.

6.3 Hand sheet tests

Paper properties measured include[7]:

- *Bending stiffness* (mN): is the bending moment required to deflect the free end of a clamped piece of paper with specified dimensions. Testing was conducted according to ISO 2493:1992 standards.
- *Breaking length* (m): the length of a paper strip that would be just self-supporting, in other words, the length of a strip paper which has a weight equivalent to the force that would break it. Testing was conducted according to ISO 1924-2:1994 standards.
- *Tear resistance* (mN): is the average force required to continue the tearing of paper from an initial cut in a single sheet. Testing was conducted according to ISO 1974:1990 standards.

- *Folding endurance, or resistance to folding* (dimensionless): is the ability of a strip of paper to resist breaking when folded under a certain load, and expressed as the 10-based logarithm of the number of double folds before rupturing.   Testing was conducted according to ISO 5626:1993 standards.

6.4 Results and discussion

6.4.1 Modified polyester particles

Figure 6.2: Hand sheet testing results of cationic and anionic modified polyester particles (Polpar). Anionic Polpar additions were 2 wt% (dry particles/dry PCC) treated to filler and cationic Polpar additions were 2 wt% (dry particles/dry fibre). The figure shows hand sheet stiffness (**A**), breaking length (**B**), tear resistance (**C**), and folding endurance (**D**) of sheets prepared with different filler contents.

Hand sheet testing conducted with anionic and cationic polyester particles (Polpar), discussed in Section 3.2. The particles were first tested individually, where 2 wt% (dry particles/dry PCC) anionic particles were combined with PCC prior to addition to the pulp suspension in the equaliser, while in another test 2 wt% (dry particles/dry pulp) was added to the pulp ahead to the milling stage. The cationic particle modified pulp and anionic particle modified filler were subsequently combined in another set of hand sheets. Nominal filler levels were varied between 20 and 30% and results are presented in Figure 6.2 (results also shown in Table D1, Appendix D).

As expected, the stiffness, breaking length, and tear resistance significantly deteriorated in standard hand sheets as the filler level was increased. Introducing the anionic particles, resulted in significant improvement in the initial stiffness, but performance was poorer as the filler was increased to 30%. Significant improvement in breaking length and tear resistance were achieved, although the folding endurance (only tested at 20% filler level) was somewhat lower than the standard. The cationic particles, showed some improvement in stiffness, though other mechanical properties had little or no improvement overall.

The combination of anionic and cationic particles illustrated a promising effect on stiffness at higher filler levels, while a significant improvement of breaking length, tear resistance, and especially folding endurance was observed, the latter being more than 3 times higher than the standard.

These results successfully illustrate the potential benefit of using ionic modified particulates as strength enhancing additives for paper. Polyester-based particulates containing multiple micro-voids have been shown in the past to be of potential use in the paper industry[8, 9]. However, its application was exclusively reported to be as an alternative, synthetic opacifier for the partial replacement of organic fillers, such as PCC. The average particle size of the cationic and anionic polyester granules (2.3 µm and 6.0 µm, respectively) synthesised in this study, as well as the distribution, is in a similar range than PCC (1 – 10 µm) if Figure 3.3 (Section 3.2) and Figure 4.22 (Section 4.5) are compared. The claim that these particles can be used as filler replacement is therefore plausible. However, nowhere in literature does it state that it can be modified further to serve as multi-functional additives. The new objective

of this study was achieved by replacing the conventionally used styrene co-monomer with anionic or cationic monomers during the process.

Since it is claimed that opacifying polyester granules can serve as paper fillers, it would have been expected that addition of these polymers to hand sheets would caused further deterioration in paper strength (since it contributes to additional filler loading). This highlights the importance and extreme benefit of ionic modification and the role it can play as an additive system capable of reinforcing fibre and filler bonding.

Although it was not in the scope of this project, it would be very interesting to look at optimising optical properties as well as ionic character of opacifying polyester granules for the paper industry. Not only is there a potential cost benefit to be gained from increasing filler loadings further, but also by replacing the organic fillers itself with an even lower cost synthetic product.

6.4.2 Macrogel starch particles

Various macrogel maize starch particles with anionic DS_{th} of 0.2, 0.5, and 0.8 and each cross-linked with 1, 3, and 6 wt% ECH (based on total solution) were prepared as described in Section 4.3 and submitted for hand sheet testing. The samples were screened using only a filler content of 25%, whilst 0.8 wt% cationic starch solution was added to the pulp according to the standard procedure. Results appear in Table D2, Appendix D and hand sheet test results presented in Figure 6.3.

The graphs show some improvement in stiffness were obtained especially where the DS_{th} were low ($DS_{th} = 0.2$) with the highest value achieved with ECH = 6 wt%. Overall no trend could be highlighted to distinguish the effect of DS_{th} and cross-linking degree on this property. A substantial improvement in breaking length was observed (if compared to the standard) for all macrogel particle samples, but most notably in the case where the cross-linking degree remained low. The tear resistance also showed good improvement with most samples used, although the sample prepared with lower DS_{th} and percentage cross-linker performed somewhat poorer than the standard. However, the same sample offered

exceptionally superior improvement in the folding endurance even though most of the samples also presented some degree of improvement.

Figure 6.3: Hand sheet testing results of anionic modified macrogel maize starch particles prepared with various degrees of substitution and ECH cross-linking degrees. Sample screening was performed using 25% filler loading, treated with 2 wt% particles (dry particles/dry PCC) and the figure shows sheet stiffness (**A**), breaking length (**B**), tear resistance (**C**), and folding endurance (**D**).

By looking at results holistically, it appears that the lower percentage cross-linked particles impart more elasticity to the hand sheets (probably due to a lower starch particle density), hence a greater improvement in breaking length and folding endurance. On the other hand, the denser cross-linked particle show a marginal overall improvement in bending stiffness and tear resistance.

Since bending stiffness is one of the most important strength properties of paper, the high value achieved in screening the macrogel sample with $DS_{th} = 0.2$ and cross-linked with 6 wt% ECH prompted further hand sheet trials at different filler loadings. Results are presented in Figure 6.4 (also tabulated in Table D3, Appendix D).

Figure 6.4: Hand sheet testing results of anionic ($DS_{th} = 0.20$) macrogel maize starch particles cross-linked with 6 wt% ECH. Sample screening was performed using different filler loadings, treated with 2 wt% particles (dry particles/dry PCC) and the figure shows sheet stiffness (**A**), breaking length (**B**), tear resistance (**C**), and folding endurance (**D**).
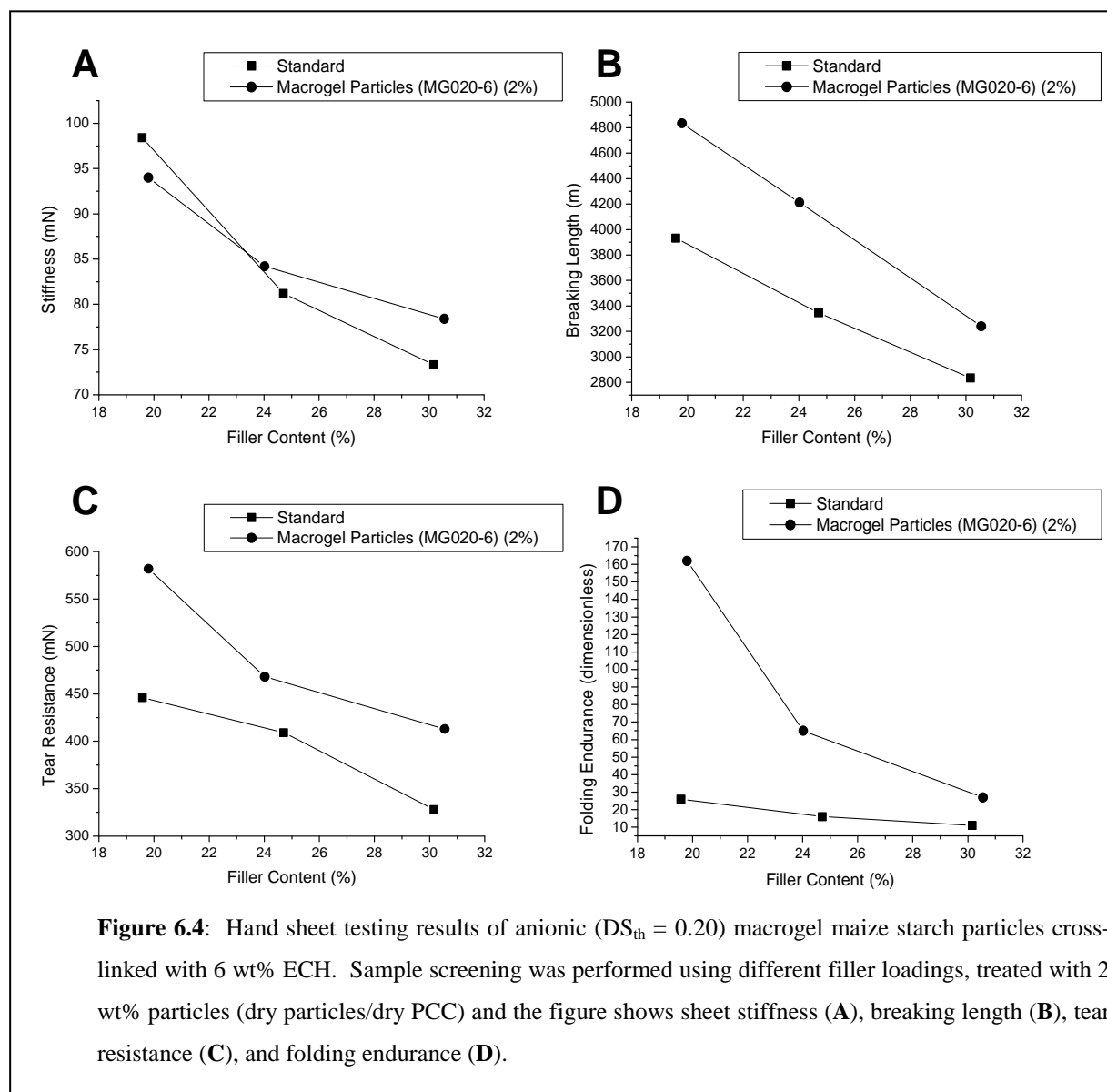
At lower filler loadings, higher fibre-fibre bonding prevailed in the standard with the bending stiffness slightly higher than the sample including macrogel particles. At this stage the particles, contributing to the disruption in inter-fibre bonding had little effect in improving stiffness, but at higher loadings its role in compensating for the loss in interaction became

179

more prevalent, causing some improvement compared to the standard. Other mechanical properties maintained significant improvement across the filler content range, most noticeably at lower filler loadings.

6.4.3 Designer starch particles

Figure 6.5: Hand sheet testing results of anionic designer dextrin particles. Samples were prepared at different filler contents and the figure shows sheet stiffness (**A**), breaking length (**B**), tear resistance (**C**), and folding endurance (**D**).
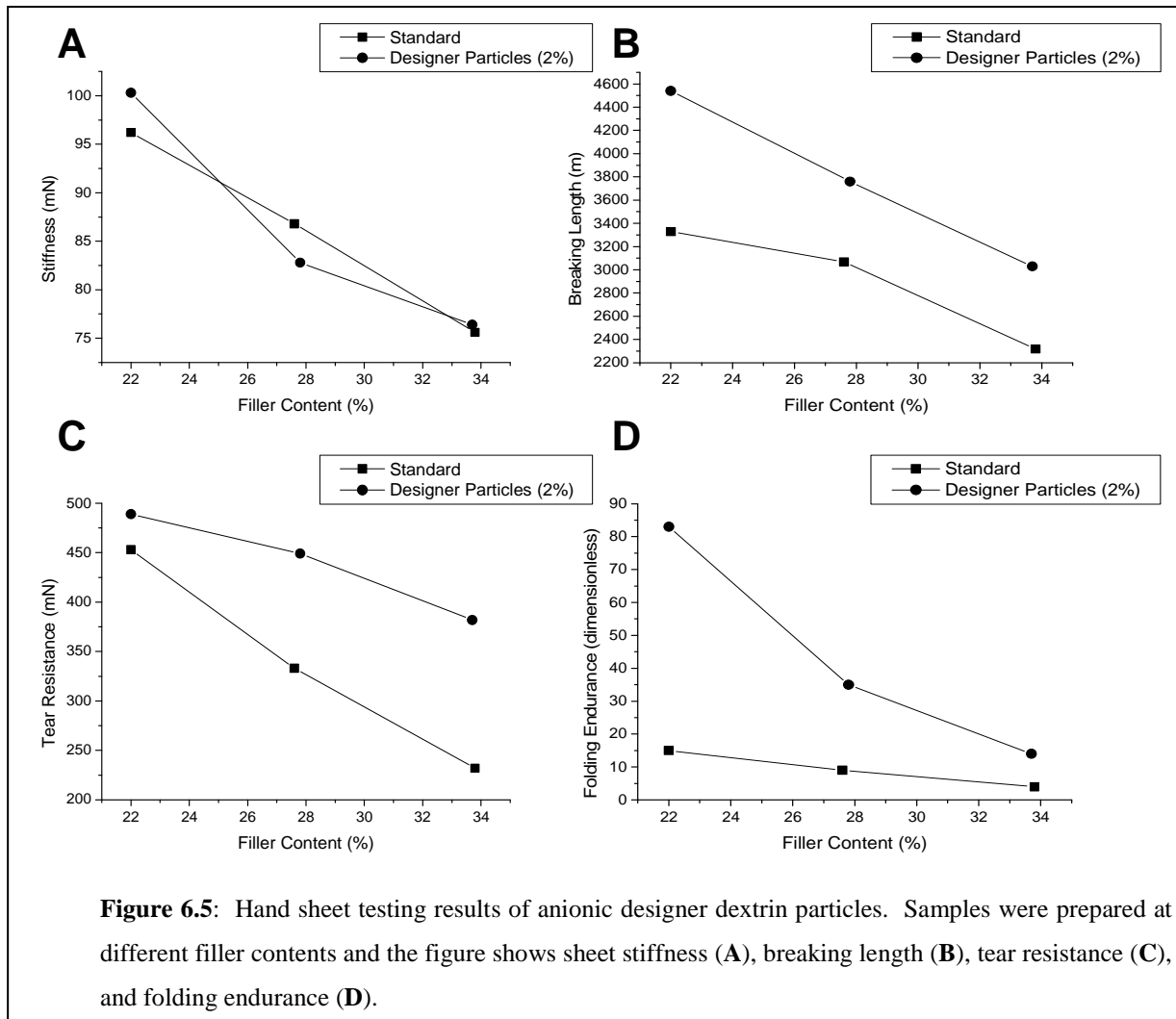
A sample of anionic dextrin ("designer") particles, discussed in Section 4.4, were submitted for hand sheet trials using nominal filler contents of 20, 25, and 30 wt% and results appear in Table D4, Appendix D, and plotted in Figure 6.5. Addition of these particles showed some improvement in stiffness and significant improvement in breaking length and folding endurance, especially at lower filler levels. Tear resistance was also significantly higher with improved performance as the filler level was increased. Apart from the negligible effect on

stiffness at higher loadings, the overall performance of these particles in paper was comparable to those of the combined (anionic and cationic) polyester particles, but not as promising as that of the macrogel starch particles, discussed in the previous sections.

6.4.4 Layer-by-layer (LbL) starch encapsulated PCC

Figure 6.6: Hand sheet testing results of PCC encapsulated in 3 layers maize starch ($DS_{th} = 0.40$) using the LbL technique (PCC-LBL0.40). Samples were prepared at different filler contents and the figure shows sheet stiffness (**A**), breaking length (**B**), tear resistance (**C**), and folding endurance (**D**).
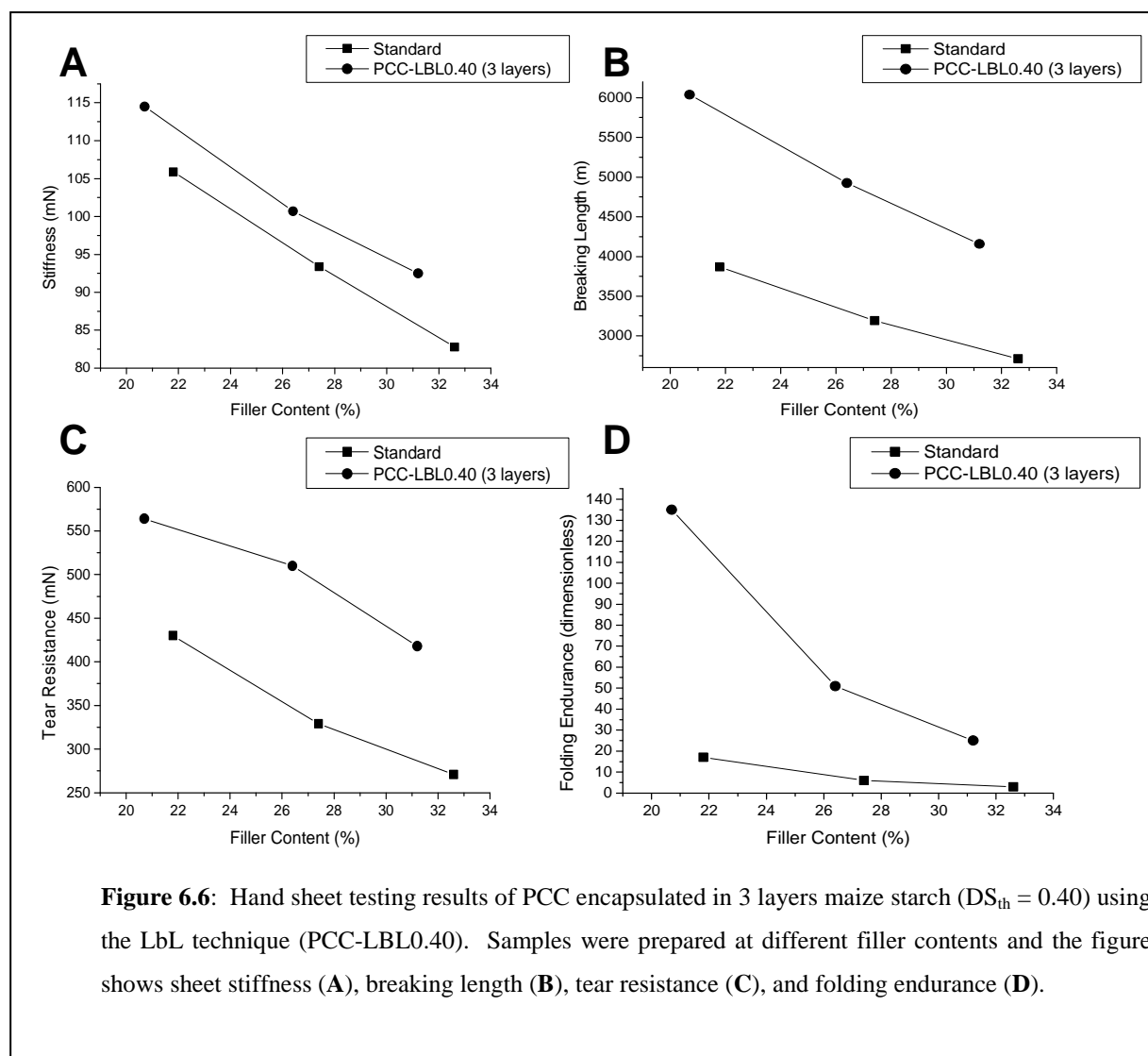
In Section 4.5 a process was described for encapsulating PCC in layers of ionic modified maize starch using an LbL approach. A sample (PCC-LBL0.40) consisting of 3 layers starch (with $DS_{th} = 0.40$) was used for performing hand sheet trials. During preparation, the pure filler was replaced by PCC-LBL0.40, whilst cationic starch solution (0.8 wt% based on dry

pulp) was added to the fibre, as per the standard method. Test results appear in Figure 6.6 (also tabulated in Table D5, Appendix D).

Results indicate a significant improvement in all paper properties, with the most notable an increase in bending stiffness across the filler loading range. This may be attributed to the effective coating of starch layers onto the entire filler surface enabling improved filler-filler as well as filler-fibre adhesion. Where separate polysaccharide particles are used the interaction relies more on selective surface adsorption of filler particles to starch particles to fibres, with the latter also containing a cationic surface layer.

Figure 6.7: Hand sheet testing results of PCC encapsulated in 1 layer anionic maize starch ($DS_{th} = 0.40$) using the LbL technique (PCC-LBL0.40). Samples were prepared at different filler contents and the figure shows sheet stiffness (**A**), breaking length (**B**), tear resistance (**C**), and folding endurance (**D**).
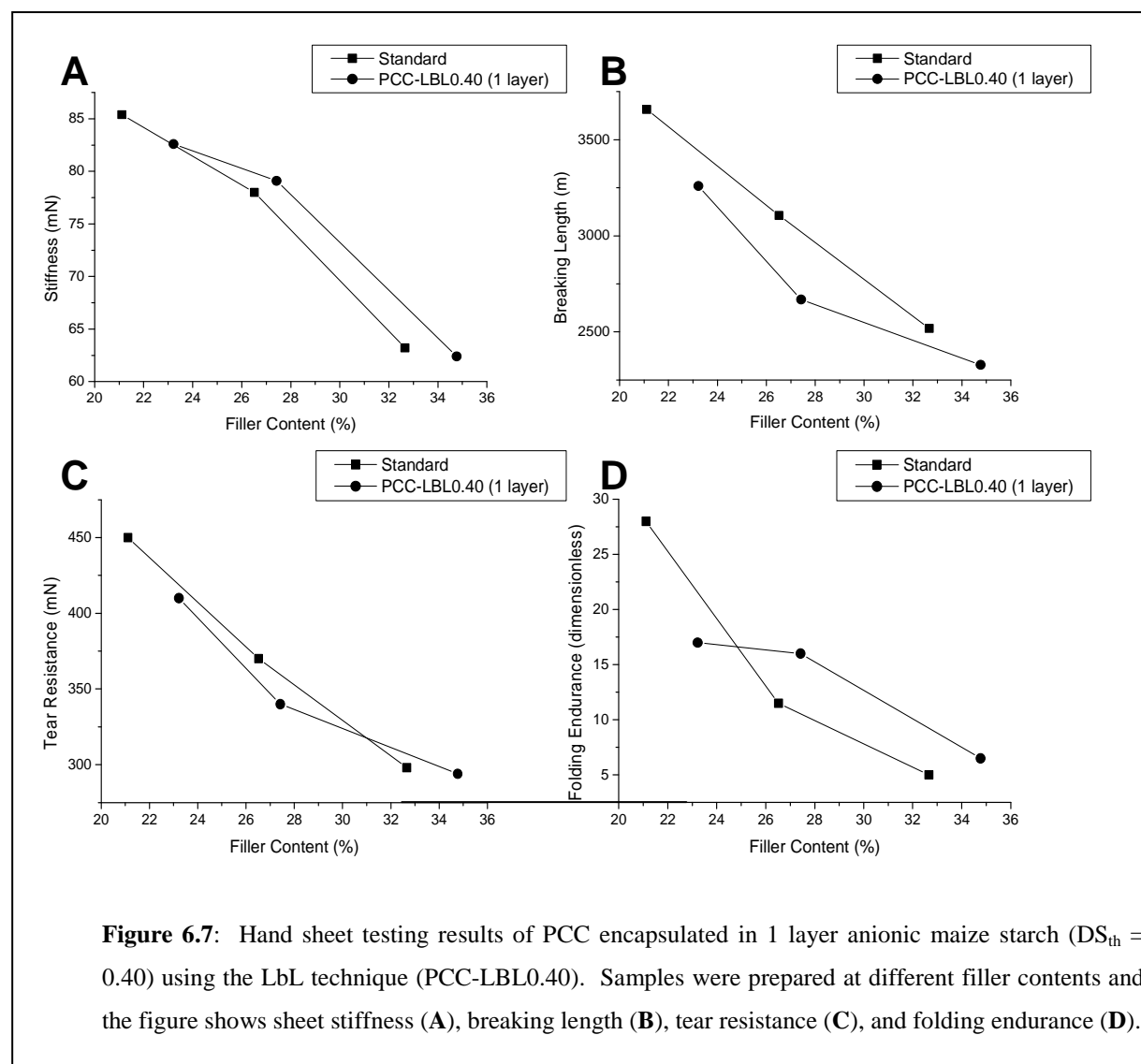
In order to determine if multiple starch layer deposition is indeed effective and that a simple single surface treatment of a modified starch solution (1 layer) onto the filler could also be sufficient to achieve similar results (which would also imply using a simpler modification process), a sample of PCC layered with only an anionic starch solution (DS_{th} = 0.40) was prepared and submitted for trials.

As seen in Figure 6.7 (also refer to Table D6, Appendix D for tables) only a very slight improvement in stiffness as well as folding endurance at higher filler loadings was achieved. Tear resistance as well as breaking length did not show any improvement, in fact a decrease in mechanical properties was observed compared to the standard. The benefits of increasing the overall starch content in the hand sheets is therefore shown and the LbL technique is a method that allows control over how much starch is incorporated into the system (by the number of starch layers deposited on the filler surface). As mentioned in a previous discussion, the mere increase in starch solutions added to the paper process does not necessarily imply a higher final starch content as the amount retained is limited, since excess unabsorbed polymer is lost in the drainage water during web formation.

6.4.5 In-situ cross-linked anionic maize starch particles

The performance of selected in-situ cross-linked (ISXL) anionic maize starch particles synthesised as described in Section 4.6 (also refer to Table 4.5 as well as Table A3, Appendix A) with various anionic DS_{th} values as well as ECH cross-linking percentages was submitted for trials at different filler loadings. Sample screening was performed by only testing stiffness and breaking length and Figure 6.8A shows the effect of DS_{th}, with percentage ECH added a constant at 3 wt%, while Figure 6.8B presents the effect of percentage ECH (DS_{th} = 0.5). Results are also tabulated in Table D7, Appendix D.

Overall improvement in both stiffness and breaking length is shown, especially at lower filler loading levels. Particles prepared without anionic charge (DS_{th} = 0) offered superior performance in stiffness compared to the standard and an increase in breaking length comparable to the performance of charged particles introduced. Even though ionic interaction of these particles with filler and fibre can not be realised, steric interaction can still be

considered to obstruct bulky particles in the paper web, thereby preventing it to escape into the white water during drainage.

Figure 6.8: Hand sheet testing results of ISXL anionic maize starch particles, prepared using various DS_{th} values (ECH constant at 3 wt%) (**A**), and ECH cross-linker percentages (DS_{th} constant at 0.5) (**B**). Sheets were prepared at different filler contents and the figure shows sheet stiffness (**1**), and breaking length (**2**).
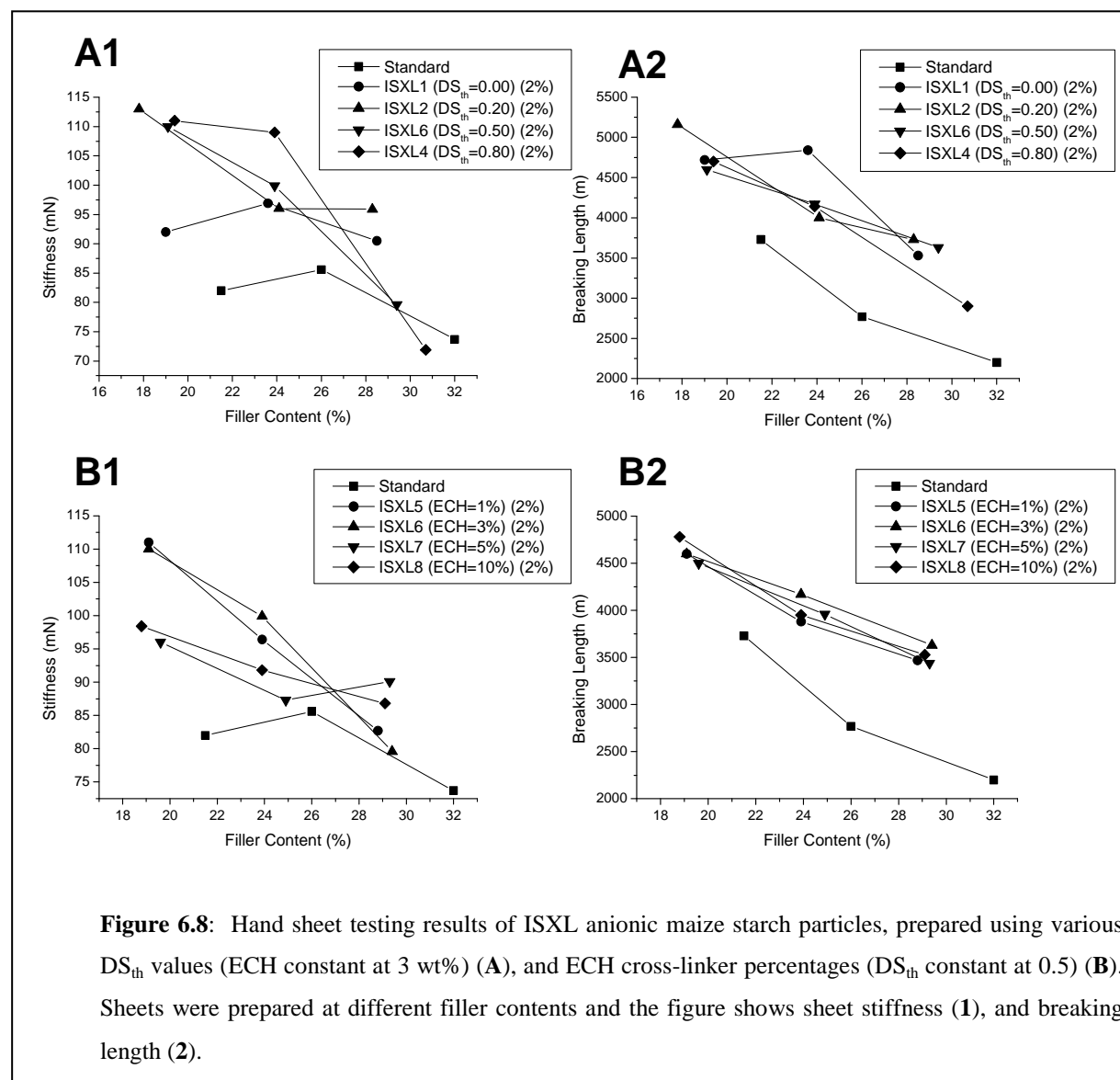
Anionic modified particles showed comparable improvement in stiffness at lower filler contents, but quickly deteriorated as loadings were increased for particles containing higher anionic modifications. The loss in crystallinity, which was shown to increase with higher anionic substitution degrees (Figure 4.31) may be considered to be a contributing factor for this phenomenon, since the crystalline structure of low anionic substituted or even neutral particles in essence compensates for the loss in fibre-fibre bonding at higher PCC levels,

which is considered to adversely affect stiffness. The hypothesis may not be directly related to the breaking length as all samples indicated comparable improvements.

The effect of cross-linker addition indicated that lower percentages tend to favour stiffness improvement at lower filler loadings, though the more densely cross-linked particles caused a lower deterioration gradient over the range, with superior stiffness achieved at higher loadings. The gain in breaking length appears to be independent of the degree of cross-linking.

Figure 6.9: Hand sheet testing results of ISXL anionic maize starch particles, prepared using an anionic DS_{th} of 0.50 and cross-linked with 3 wt% ECH. Samples were prepared at different filler contents and the figure shows sheet stiffness (**A**), breaking length (**B**), tear resistance (**C**), and folding endurance (**D**).
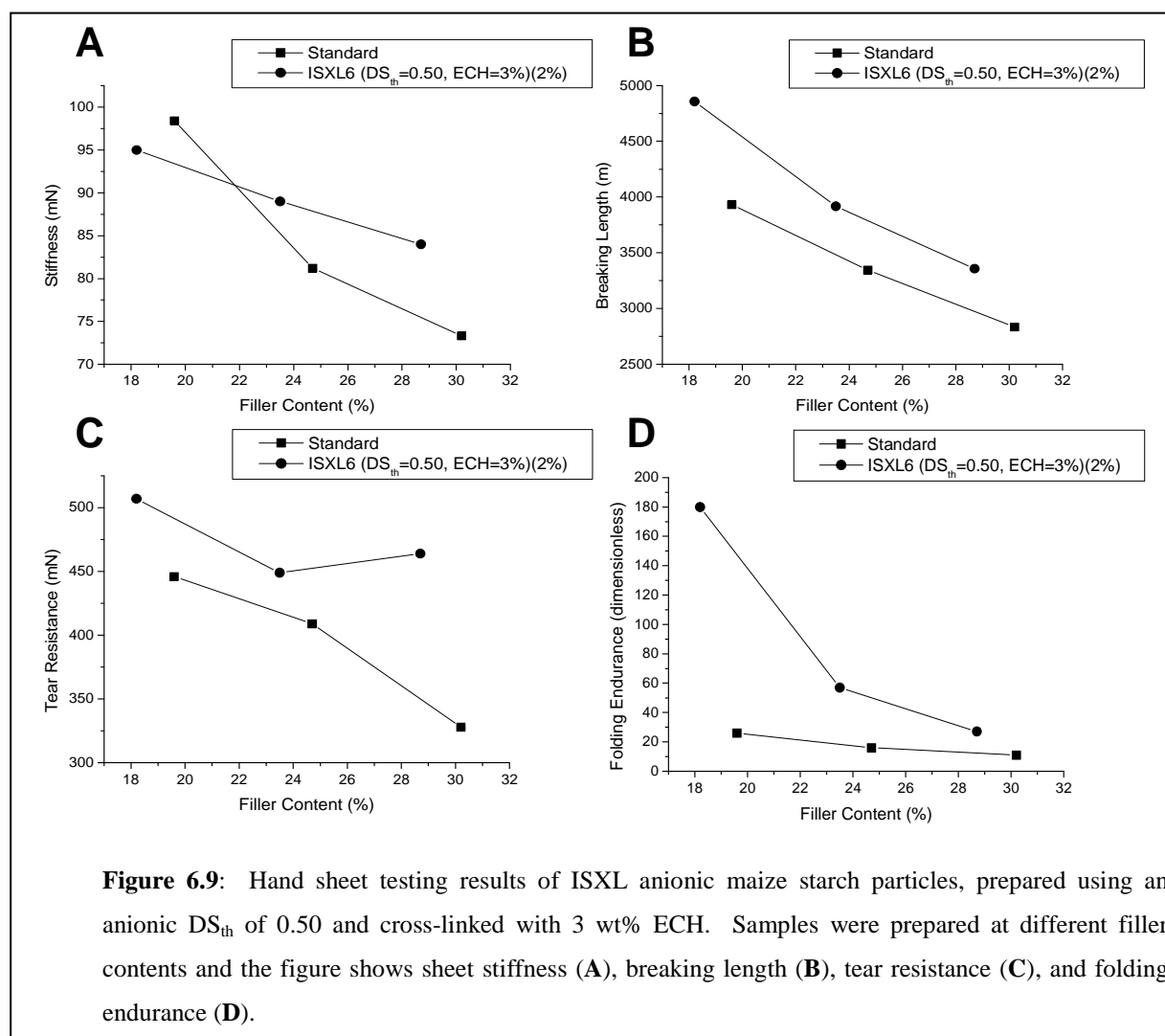
A further, more comprehensive evaluation of hand sheet properties (including tear resistance and folding endurance) were also conducted on another ISXL sample prepared with $DS_{th} =$

0.5 and 3 wt% ECH and are presented in Figure 6.9 (also see Table D8, Appendix D for table).

Results confirms a definite improvement in stiffness at higher filler loading levels with associated improvement in breaking length, tear resistance, as well as folding endurance.

6.4.6 Anionic dextrin particles prepared using microfluidics

Figure 6.10: Hand sheet testing results of various average particle size anionic dextrin particles prepared using microfluidics Samples were prepared at nominal filler contents of 20 and 30 wt% and the figure shows sheet stiffness (**A**), breaking length (**B**), and tear resistance (**C**).
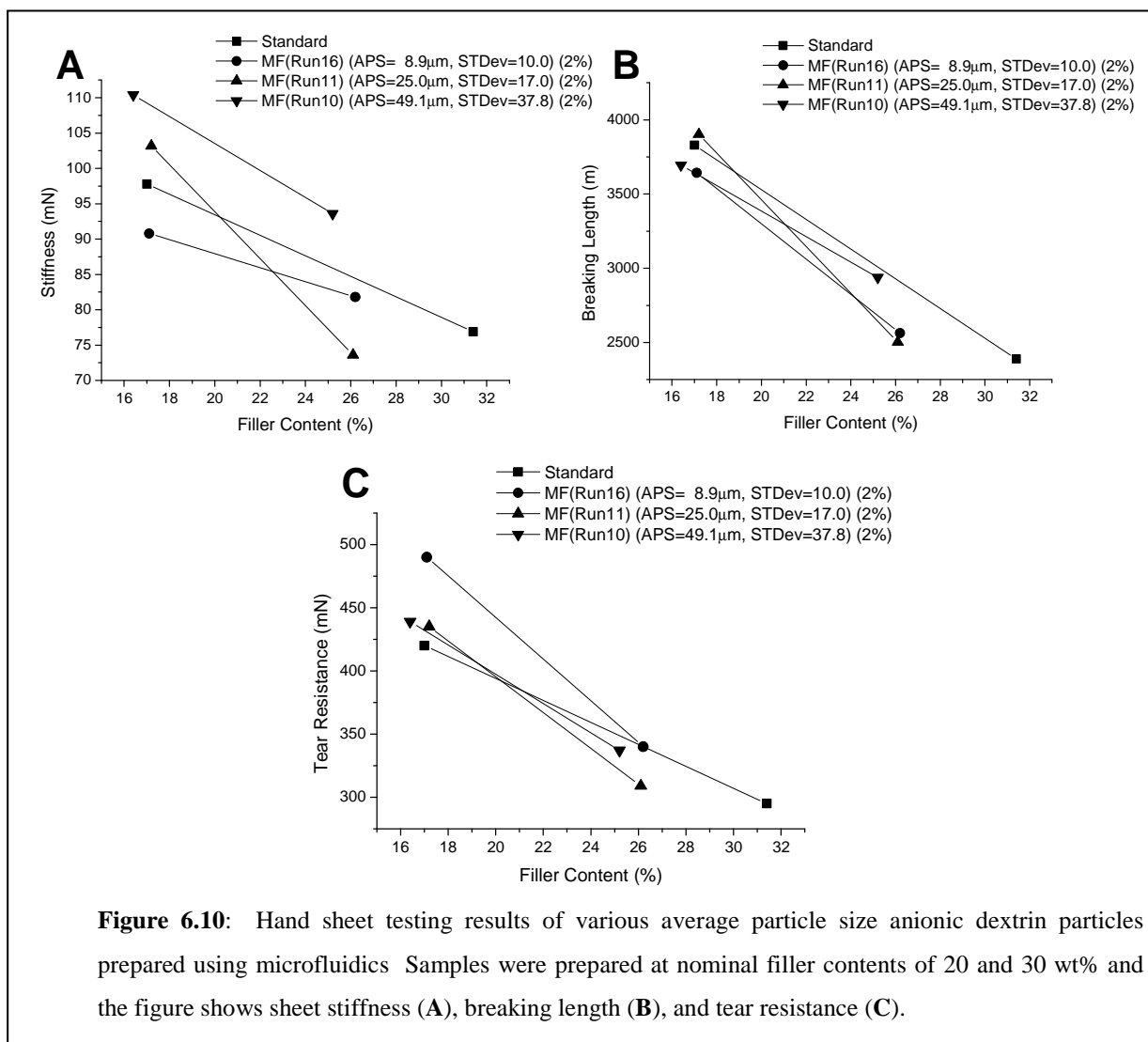
Following the study on the preparation of anionic dextrin particles using microfluidics, as described in Section 5.3, three selected samples were sent for hand sheet testing trials. These

samples consisted of particles with different average size and distribution and highlighted in Table C1, Appendix C. Particles were tested for stiffness, breaking length, and tear resistance in sheets prepared at nominal filler content levels of 20 and 30 wt% and results are shown in Figure 6.10 (also refer to Table D9, Appendix D).

Mechanical properties of sheets prepared with samples did not show overall improvement, though the smaller particles (APS = 8.9 µm) contributed to some improvement in tear resistance at a lower filler loading. A very promising improvement in bending stiffness for sheets prepared with particles possessing an average particle size of 49.1 µm was gained and it appears that values systematically declined as the particle size decreased. The larger particles may be contributing to the bulk of the sheets, explaining the gain in stiffness. An even greater increase in particle size may result in further improvement in stiffness, but only to a certain extent since the increase is limited to the thickness of a sheet of paper (roughly about 100 µm). Too large particle will result in inhomogeneity of the paper matrix (which is called formation in papermaking) or result in picking of paper sheets. This can typically occur when adhesive particles adhere to the sheet press, causing fibres to be pulled out from the surface and resulting in a loss in paper strength. This should be considered as an important factor in any further investigations.

6.5 Summary

The percentage improvement in strength properties (versus the standard) of hand sheets prepared using selected samples from each synthesis approach was used for comparison. The samples used included the following:

- Macrogel particles - Sample MG020-6 (Figure 6.4)
- Designer particles – Sample DP1 (Figure 6.5)
- LbL modified PCC – Sample PCC-LBL040 (3 layers) (Figure 6.6)
- In-situ cross-linked anionic maize starch – Sample ISXL6 (Figure 6.9)
- Microfluidic processed anionic dextrin particles – Sample MF(Run10) (Figure 6.10)

Since the actual filler loading varied in each sample, the data points, including those of the standards, were first extrapolated to filler loadings of 20, 25, and 30 wt% in order to allow a

comparative study. The extrapolated data points appear in Table D10, Appendix D, and the percentage improvements presented in Figure 6.11.

Figure 6.11: Comparison of percentage improvement in hand sheet properties achieved using LbL modified PCC, macrogel particles, designer particles, ISXL particles, and dextrin particles prepared with the microfluidic device. Data points were extrapolated to filler contents of 20, 25, and 30 wt% and the figure shows improvements in sheet stiffness (**A**), breaking length (**B**), tear resistance (**C**), and folding endurance (**D**).

The LbL modified PCC, and most notably the microfluidic processed dextrin particles improved stiffness at lower filler content, with similar improvements obtained as the loading was increased. Stiffness in sheets prepared with macrogel and ISXL particles did not show any effect at lower loadings, but significant improvement was gained at higher loadings, with an almost 14% improvement at 30 wt% filler content where the latter sample was used. Designer particles only showed a slight improvement in stiffness at lower filler loadings.

The mechanical properties of sheets prepared with microfluidic processed particles did not indicate any improvement, whereas the remaining samples showed very positive behaviour. Breaking length improvement for each of these samples remained fairly consistent across the loading range with the LbL modified PCC (up to 50%) and designer particles showing the highest increases. Most samples also showed a definite increase in tear resistance as the filler loadings increased with the LbL modified PCC once again showing the best performance with improvements up to 45% at the 30 wt% loading. The layered PCC also outperformed the other particles in enhancing folding endurance up to 650% at 20 wt% filler content and about 500% at 30 wt%, with the remaining particles reaching values up to 450% at 20 wt% loadings. Only the ISXL particles (apart from the microfluidic processed particles) did not succeed in improving endurance at higher filler levels.

6.6 Conclusions

Commencing this study, the concept of using ionic modified particles to improve paper strength was investigated. This was achieved using a known method for preparing polyester particles (suitable for use as pigment replacer), but modifying it either cationic or anionic. These particles were used as paper additives individually as well as in combination (cationic particles treated to the anionic charged fibres and anionic particles blended with PCC).
Very promising improvements in sheet stiffness and tear resistance were shown and the study was considered as successful. It further demonstrated potential future application as a multifunctional additive for improving paper strength while acting as synthetic pigment replacement.

Anionic polysaccharide particles tested in hand sheets included those prepared by macrogel methods, W/W emulsification (designer particles), in-situ cross-linking and anionisation, microfluidic emulsification, as well as filler particles encapsulated in layers of maize starch.

The most significant improvement in paper stiffness was observed where the following polysaccharide particles were used:

- LbL modified PCC (3 layers): The percentage improvement remained very consistent over the filler loading range tested. The method allowed higher starch concentrations to be retained in the system, while improving filler/fibre surface adhesion.

- Microfluidic processed dextrin particles: The larger dextrin particles appear to improve the bulk of the paper and the most significant improvement in stiffness was obtained at lower filler loadings.

- In-situ cross-linked particles: The most significant improvement was obtained at higher filler loading levels and the inherent retention of granule crystallinity (at lower degrees of anionic substitutions) was identified as a possible contributing factor.

The mechanical properties of hand sheets prepared with most of the modified particles, except those prepared on the microfluidic device, showed improvements compared to the standards. The most notable increases of all strength properties was those obtained using the LbL modified PCC (3 layers).

6.7 References

1.   N. Schall; E. Kruger; R. Blum, et al., *TAPPSA Journal (www.TAPPSA.co.za)*, **2008**.

2.   K. M. Almgren; E. K. Gamstedt; P. Nygard, et al., *International Journal of Adhesion & Adhesives*, **2009**, 29, 551-557.

3.   B. Drouin; R. Gagnon; C. Cheam, et al., *Composites Science and Technology*, **2001**, 61, 389-393.

4.   R. E. Mark; C. C. Habeger; J. Borch, et al., *Handbook of Physical Testing of Paper*. 2nd ed.; Marcel Dekker: **2001**; Vol. 1.

5.   *Sheet Forming - a complete instruction*; Mondi Competence Center Innovation: 2007.

6. A. Vanerek; B. Alince; T. G. M. van de Ven, *Colloids and Surfaces*, **2006**, 280, 1-8.

7. F. Marin; J. L. Sanchez; J. Arauzo, et al., *Bioresource Technology*, **2009**, 100, 3933-3940.

8. R. H. Gunning; B. C. Henshaw; F. J. Lubbock, Polyester Granules and Process, Patent: US 4,137,380, **1979**.

9. M. Karickhoff, Vesiculated Beads, Patent: US 4,489,174, **1984**.

Chapter 7: Conclusions and recommendations

7.1 Introduction

The main objective of this study was to increase the PCC filler loading in paper above 18 wt% without causing substantial deterioration in paper strength properties with the major focus on sheet stiffness. This was achieved through the introduction of a dual additive multifunctional polysaccharide system where at least one of these additives was in particulate form. Presently the paper industry largely relies on a single cationic starch solution addition to (a limited extent) improve properties and therefore the principal focus was on developing a supplementary anionic polysaccharide particles that would allow strong interaction with PCC and fibre (treated with cationic starch). Several techniques for modifying the polysaccharides were investigated as well as processes for preparing the gel particles. The performance of selected samples was tested in paper hand sheets at different filler loadings and improvements in stiffness and strength properties compared.

7.2 Conclusions

There were 7 major objectives as outlined in Chapter 1, and the following conclusions can be drawn from these:

7.2.1 Background and theoretical considerations

Following a literature study on the physicochemical properties and chemical modification of polysaccharides as well as established techniques for preparing microgel particles, the following were found:

- Maize starch, the most significant industrial polysaccharide, consists of semi-crystalline granules in its native form and is cold water soluble as a result of hydrogen bonding of free hydroxyl groups located on the macromolecular backbone. These hydrogen groups are readily available for preparing ionised and/or cross-linkable

starch derivatives by adopting, for example, a substitution reaction mechanism with functional halide compounds under alkali conditions (Williamson's ether synthesis).

- Chemically modified polysaccharide solutions (eg. cationic starch) are widely used in papermaking processes to flocculate and retain anionic charged fibres, but its benefit in improving mechanical properties is limited to the amount of polysaccharide retained in the sheet matrix.

- Polysaccharide particle processing has gained widespread interest predominantly for its application as drug carrier system in the pharmaceutical industry and flavourant delivery vehicle in food industries. The application of multifunctional polysaccharide particles in the paper industry remains specifically unknown.

7.2.2 Concept of using ionic particulates for paper strengthening

Cross-linked anionic and cationic polyester particles were prepared to illustrate the concept of incorporating modified particulates in the paper process and to determine its effect on sheet stiffness and mechanical properties. Ionic modification was achieved by blending the polyester with either acrylic acid (anionic monomer) or 3-[(methacryloylamino)propyl]-trimethylammonium chloride (cationic monomer) prior to O/W emulsification in a colloid-stabilised aqueous phase and cross-linking with a redox initiation system.

The addition of anionic polyester particles showed a significant improvement in paper bending stiffness at filler loadings below 25%. Improvements in breaking length and tear resistance were also observed. Where the cationic starch solution was replaced with cationic polyester particles, only a marginal improvement in stiffness was shown with negligible effect on other mechanical properties. A combination of these particles increased stiffness values at higher filler loadings and also had a positive effect on tear resistance and, most notably, folding endurance.

7.2.3 Modification of polysaccharides and characterisation

By applying the Williamson's ether synthesis anionic, cationic, and allyl starch solutions were prepared using sodium monochloroacetate, 3-chloro-2-hydroxypropyltrimethyl-ammonium

chloride, and allyl bromide, respectively. The degree of substitution of each was determined using ^{1}H-NMR spectroscopy.

The substitution reaction during the carboxymethylation of starch solutions proceeded very slowly due to its enhanced hydrophilicity, which promoted swelling and increased solution viscosity.

7.2.4 Interaction of ionic modified polysaccharides with fibre/filler

Fluorecein isothiocyanate was successfully attached onto the backbone of both cationic and anionic starch in order to investigate their interaction with filler and fibre, making use of fluorescence microscopy. Anionic starch indicated exclusive adsorption onto PCC, while the cationic starch adsorbed onto the negatively charged fibre as well as the filler. The non-selective ionic interaction with PCC was attributed to the filler's calco-carbonic equilibration system.

7.2.5 Conventional ionic modified polysaccharide particle synthesis

Anionic modified polysaccharide particles were successfully synthesised using conventional processing techniques and included the following:

- *Macrogel particles*: Carboxymethylated maize starch solutions were cross-linked with epichlorohydrin to form a stiff gel followed by homogenisation and then ultrasonication in water to break down the gel particulates to smaller size. Although the process formed non-uniform, highly poly-disperse particles and required high intensity mixing principles, the system was essentially solvent-free thus making it easier to purify the particles.

- *Water-in-water emulsified (designer) particles*: Modified dextrin solutions were found to remain immiscible in aqueous solutions of poly(ethylene glycol) and homogenisation yielded a stable particle suspension. Unsaturated groups attached onto the backbone of dextrin could be cross-linked using free radical polymerisation. Although the dextrin had to be modified with both anionic and allyl groups prior to particle preparation, the system was solvent free and since no salt formed as by-product during polymerisation (compared to using epichlorohydrin), purification of

particles was significantly easier, allowing the continuous phase to be readily recycled for further use.

- *Layer-by-layer (LbL) modified PCC*: Alternate and consecutive adsorption of oppositely charged starch solutions onto PCC was utilised to encapsulate the filler in multiple starch layers (anionic outer layer). Fluorescence microscopy was used to observe individual layer formations. Thermogravimetric analysis indicated increased starch adsorption occurred where the degrees of ionic modification was lower. Electrokinetic methods can be used to determine the net colloidal charge of bulk solutions, which enables individual layer treatment to just beyond the onset of zeta potential. This should eliminate potential polyelectrolyte under- or overcharge, which may have a detrimental effect on layer properties.

- *In-situ cross-linked anionic granules*: Partial swelling of native starch granules allowed modification to be performed while its inherent structure was retained below its rupture point. The granules were cross-linked with epichlorohydrin followed by carboxymethylation, where the latter indicated enhanced substitution rates, compared to carboxymethylation of starch gel solutions. They became increasingly amorphous as the degree of carboxymethyl substitution was increased. The recovered granules were easily purified by filtration.

  This process is superior to other conventional processes investigated since pre-gelatinisation is avoided which significantly reduces handling complexities.

7.2.6 Preparation of ionic modified polysaccharide particles using microfluidics

A study on microfluidics was conducted where a multi-channel interdigital micro-mixer was used to prepare W/O emulsified anionic dextrin particles of controlled particle size and distribution. The solvent phase consisted of heptane containing Hypermer B246 as emulsifier and the aqueous phase comprised of allyl modified dextrin and sodium acrylate which, after emulsification, was copolymerised (at 70 ^{o}C) with potassium persulfate as initiator and *N,N'*-methylene bisacrylamide as cross-linking agent.

Response surface methodology was applied to study the effect of aqueous and solvent flow rates as well as emulsifier level on average particle size and distribution. In general, smaller particles, with corresponding narrower distribution, were formed where the solvent flow rate was increased and the aqueous flow rate was decreased.

7.2.7 Hand sheet testing

Hand sheets were prepared and the performance of the various modified polysaccharide particles tested at nominal filler loadings varying between 20 and 30%. Overall, the introduction of anionic polysaccharide particles, regardless of processing approach, was accompanied with some improvement in sheet stiffness and/or mechanical properties. The following can be concluded from each addition:

- *Macrogel particles*: Low anionic degrees of substitution (DS_{th} = 0.2) were shown to progressively improve stiffness as filler loading was increased from 20 to 30 wt%. Lower percentage cross-linked (ECH = 1%) macrogels imparted enhanced improvement in breaking length and folding endurance.

- *Water-in-water emulsified (designer) particles*: Only a marginal improvement in stiffness was observed at 20 wt% filler loading. However, significant and very consistent increases were gained in all of the mechanical properties.

- *Layer-by-layer (LbL) modified PCC*: A superior increase in all properties was obtained using filler particles coated with 3 layers maize starch (DS_{th} = 0.4). Consistent stiffness improvements were reported at all filler levels tested. Mechanical properties improved drastically, especially folding endurance.

- *In-situ cross-linked anionic granules*: A very promising improvement in stiffness using most samples (different degrees of modification) was observed, especially where the anionic degree of substitution (DS_{th} = 0.2) was low at 30 wt% filler loadings. Mechanical properties also improved, especially at lower loading levels.

- *Microfluidic processed particles*: Larger particle size and distribution were shown to cause a significant improvement in stiffness, possibly since it contributes to the bulk of the paper sheet. However, these particles had a negligible effect on improving the mechanical properties of hand sheets.

7.3 Major contributions

In summary, the major contributions of this study are:

- Stiffness and mechanical properties of paper hand sheets were improved using filler loadings above 20 wt% by the addition of cross-linked and carboxymethylated poysaccharide particles to PCC. This, together with the cationic starch added to the fibre, acted as a multi-functional additive system for enhancing inter-surface bonding.

- A process for preparing anionic modified water-insoluble granular starch for use in paper has been proposed whereby partially swollen maize starch granules are cross-linked using epichlorohydrin prior to anionisation with sodium monochloroacetate. The process is simple and economical since it does not require the pre-gelatinisation of starch. Low degrees of anionisation ($DS_{th} = 0.2$) have been shown to be the most effective in improving stiffness and mechanical properties.

- Sequential layering of ionic modified starch solutions (as polyelectrolyte) onto PCC was shown to be a unique and attractive technique to increase the starch retention in paper. The attachment of individual fluorescent markers onto the polyelectrolyte backbones was effective in indicating the sequential layers deposited on the filler surface. Layer thickness was also shown to be dependent on the degree of ionic substitution. It is serendipity that the LbL modified PCC showed exceptional improvement in stiffness and especially mechanical properties. The mono-layering of soluble polymers on the filler indicates that introduction of nanotechnology to the papermaking process could potentially be of great benefit to the industry.

- The use of microfluidics for preparing W/O emulsified anionic polysaccharide particles was shown to be novel and the potential application of these additives for improving paper stiffness was shown. This approach is still in its infancy, but many changes and gains can be expected for the future.

Patents emanating from this research (Appendix E):

1. A. Kornherr, F. Eder, B.J.H. Janse, R.D. Sanderson, J.C. Terblanche, M. Zou, *Process and device for preparing starch microgel particles for the paper industry*, Applicant: Mondi Limited South Africa, European Patent Application No. 09450062.6-2115.

2. A. Kornherr, F. Eder, B.J.H. Janse, R.D. Sanderson, J.C. Terblanche, M. Zou, Process *for preparing polysaccharide gel particles and pulp furnish for use in paper making*, Applicant: Mondi Limited South Africa, European Patent Application No. 09450061.8-2115.

7.4 Recommendations for future research

On completion of this study, the following recommendations can be made:

- The scale-up of modified polysaccharide particles must be studied. The preparation of in-situ cross-linked granules should be strongly considered, as this process is fairly simple and only requires the use of a single batch reactor system with a filtration unit. The successful scale-up would also ensure more material is available for testing in paper. Particles should then be tested in paper prepared using a continuous papermaking pilot plant in order to simulate production processing.

- More comprehensive hand sheet testing should be conducted in order to find the optimal polysaccharide particle size using the microfluidic process. The hand sheet properties can then be included as separate responses using response surface methodology.

- More comprehensive hand sheet testing can also be conducted in order to find the optimum ratio cationic starch to anionic particles that must be incorporated to produce the strongest paper sheets.

- In paper board manufacture the mechanical properties in certain applications (eg. corrugated boards) is of extreme importance. A study on the performance of ionic modified polysaccharide particles (using some of the techniques described in this study) in these systems should prove to be very interesting.

- The recycling of paper inevitably causes fibres to weaken as a result of successive chemical treatments and processing. This will ultimately result in paper becoming progressively weaker as it is recycled. A similar study on recycled paper can be performed in an attempt to compensate for the deterioration in sheet strength, ultimately extending the use and application areas of these types of products.

Appendices

Appendix A

Formulations

Table A1: Carboxymethyl starch reaction efficiencies and formulations for different DS values

Sample	Theoretic Degree of Substitution (DS_{th})	Experimental Degree of Substitution (DS_{exp})	Reaction Efficiency (RE) (%)	Addition (g)					
				Starch	Acetone	Water	SMCA	NaOH	HCl
CMS1	0.05	0.013	26	20	20	100	0.72	1.65	4.01
CMS2	0.15	0.042	28	20	20	100	2.16	2.16	4.05
CMS3	0.2	0.042	21	20	20	100	2.88	2.42	4.07
CMS4	0.3	0.099	33	20	20	100	4.31	2.92	4.12
CMS5	0.4	0.14	35	20	20	100	5.75	3.43	4.16
CMS6	0.6	0.19	32	20	20	100	8.63	4.45	4.24

Table A2: Cationic starch reaction efficiencies and formulations for different DS values

Sample	Theoretic Degree of Substitution (DS_{th})	Experimental Degree of Substitution (DS_{exp})	Reaction Efficiency (RE) (%)	Addition (g)					
				Starch	Acetone	Water	CHPTMAC	NaOH	HCl
CS1	0.05	0.037	74	20	20	100	1.93	1.65	3.99
CS2	0.4	0.25	63	20	20	100	15.47	3.38	3.99

Table A3: In-situ cross-linked carboxymethyl starch granule formulations for different DS values and percentage cross-linking agent additions.

Sample	Theoretic Degree of Substitution (DS_{th})	Experimental Degree of Substitution (DS_{exp})	Reaction Efficiency (RE) (%)	Epichlorohydrin (ECH) (%)	Addition (g)							
					Starch	ECH	NaOH	Acetone	Water	SMCA	NaOH	HCl
ISXL1	0	0	-	3	20	0.60	1.26	91.00	9.00	0.00	0	2.85
ISXL2	0.2	0.15	75	3	20	0.60	1.26	91.00	9.00	2.88	8.31	26.55
ISXL3	0.8	0.55	69	3	20	0.60	1.26	91.00	9.00	11.51	8.31	26.55
ISXL4	1	0.65	65	3	20	0.60	1.26	91.00	9.00	14.38	8.31	26.55
ISXL5	0.5	0.3	60	1	20	0.20	1.09	91.00	9.00	7.19	8.31	26.55
ISXL6	0.5	0.37	74	3	20	0.60	1.26	91.00	9.00	7.19	8.31	26.55
ISXL7	0.5	0.3	60	5	20	1.00	1.43	91.00	9.00	7.19	8.31	26.55
ISXL8	0.5	0.35	70	10	20	2.00	1.86	91.00	9.00	7.19	8.31	26.55
ISXL9	0.2	0.14	70	1	20	0.20	1.09	91.00	9.00	2.88	8.31	26.55
ISXL10	0.8	0.51	64	1	20	0.20	1.09	91.00	9.00	11.51	8.31	26.55
ISXL11	0.2	0.15	75	6	20	1.20	1.52	91.00	9.00	2.88	8.31	26.55
ISXL12	0.5	0.35	70	6	20	1.20	1.00	91.00	9.00	7.19	8.31	26.55
ISXL13	0.8	0.51	64	6	20	1.20	1.52	91.00	9.00	11.51	8.31	26.55

Table A4: "Self-crosslinked" carboxymethyl starch granule formulations for different DS values.

Sample	Theoretic Degree of Substitution (DS_{th})	Experimental Degree of Substitution (DS_{exp})	Reaction Efficiency (RE) (%)	Addition (g)						
				Starch	Acetone	Water	SMCA	NaOH	HCl	Acetone
SISXL1	0.2	0.14	70	20	91.00	9.00	2.88	8.31	17.42	174.25
SISXL2	0.4	0.25	63	20	91.00	9.00	5.75	8.31	14.99	149.91

Table A5: Dextrin-in-heptane particle formulations with various dextrin concentrations.

Sample	Span 80 conc. based on solvent phase (wt%)	Dextrin (Type II) conc. in water (wt%)	Epichlorohydrin (ECH) conc. based on total sample weight (wt%)	Addition (g)						
				Dextrin (20wt%)	Water	NaOH	ECH	Heptane	Span 80	HCl
DEX1	6.7	1	3	1.00	19.00	0.50	1.50	30.00	2.0	1.2
DEX2	6.7	2	3	2.00	18.00	0.50	1.50	30.00	2.0	1.2
DEX3	6.7	3	3	3.00	17.00	0.50	1.50	30.00	2.0	1.2
DEX4	6.7	4	3	4.00	16.00	0.50	1.50	30.00	2.0	1.2
DEX5	6.7	5	3	5.00	15.00	0.50	1.50	30.00	2.0	1.2
DEX6	6.7	10	3	10.00	10.00	0.50	1.50	30.00	2.0	1.2
DEX7	6.7	15	3	15.00	5.00	0.50	1.50	30.00	2.0	1.2
DEX8	6.7	20	3	20.00	0.00	0.50	1.50	30.00	2.0	1.2

Appendix B

Microfluidic Set-up

Figure B1: Process and instrumentation diagram of microfluidic system used for evaluation at TU/e, Eindhoven.
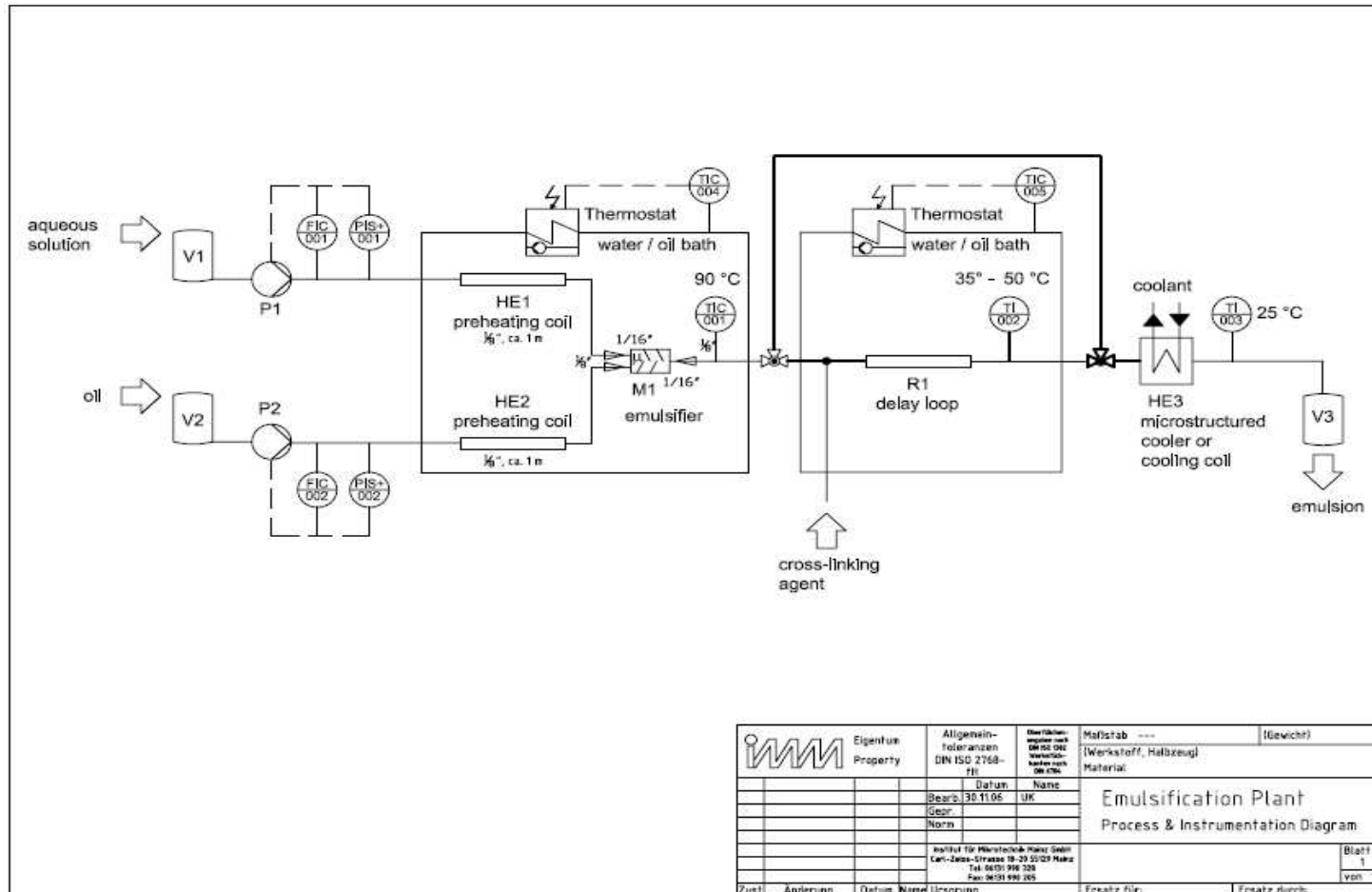
Appendix C

Design-Expert® response surface methodology

Table C1: Experimental conditions and response values (actual and predicted) of D-optimal RSM design for preparing anionic dextrin particles using microfluidics.

Standard order[a]	Run order[b]	Actual values			Coded values			Response 1 (R1)		Response 2 (R2)	
		Factor 1 (X_1)	Factor 2 (X_2)	Factor 3 (X_3)	Factor 1 (X_1)	Factor 2 (X_2)	Factor 3 (X_3)	Average particle size (µm)		Standard deviation	
		Aqueous flowrate (ml/min)	Solvent flowrate (ml/min)	Emulsifier level (%)	Aqueous flowrate (ml/min)	Solvent flowrate (ml/min)	Emulsifier level (%)	Actual	Predicted	Actual	Predicted
1	5	1	40	1	-1	1	-1	10.1	6.5	25.3	21.7
2	10	1	2	1	-1	-1	-1	49.1	48.5	37.8	38.5
3	9	20	21	1	1	0	-1	53.3	53.9	62.3	55.8
4	4	10.5	25.75	1	0	0.25	-1	39.9	37.3	46.2	42.9
5	8	10.5	11.5	2	0	-0.5	0	38.2	41.2	39.0	42.5
6	16	1	40	3	-1	1	1	8.9	11.3	10.0	10.4
7	1	1	2	3	-1	-1	1	59.3	53.3	68.8	69.3
8	6	20	40	2	1	1	0	32.4	32.6	29.6	36.2
9	14	1	21	2	-1	0	0	22.5	29.9	29.3	35.0
10	11	20	21	3	1	0	1	25.0	23.9	17.0	22.5
11	13	10.5	32.875	2.5	0	0.625	0.5	26.4	22.7	25.9	24.0
12	3	20	40	1	1	1	-1	47.3	47.6	59.1	63.4
13	18	20	40	3	1	1	1	16.0	17.6	18.0	9.0
14	15	1	21	1	-1	0	-1	25.3	27.5	35.2	30.1
15	2	1	2	3	-1	-1	1	54.2	53.3	74.9	69.3
16	12	1	40	1	-1	1	-1	9.9	6.5	19.2	21.7
17	7	1	40	3	-1	1	1	9.8	11.3	8.5	10.4
18	17	1	2	1	-1	-1	-1	46.1	48.5	34.9	38.5

[a] Not randomised

[b] Randomised

Appendix D

Hand sheet testing results

Table D1: Hand sheet testing results of cationic and anionic modified polyester particles (Section 3.2).

Sample	Filler (nominal) (%)	Filler content (actual) (%)	Grammage (g/m$^{2)}$)	Bending stiffness (mN)	Breaking length (m)	Tear resistance (mN)	Folding Endurance (-)
Standard	20	18.8	79.5	102	4278	392	41
Standard	25	26.4	80.5	97	2862	353	
Standard	30	31.8	82.5	94	2385	334	
Anionic Polpar	20	18.1	81.8	127	3865	628	31
Anionic Polpar	25	26.2	82	98	3363	432	
Anionic Polpar	30	30.5	80.25	82	2917	353	
Cationic Polpar	20	17.0	81.3	111	3980	432	31
Cationic Polpar	25	22.8	78.6	105	3394	392	
Cationic Polpar	30	26.5	79.6	103	2442	353	
Combined	20	18.6	79.5	97	4662	549	148
Combined	25	21.1	81.4	97	4300	510	
Combined	30	25.3	82.6	118	3298	432	

Table D2: Hand sheet screening results of anionic macrogel maize starch particles prepared with various theoretical degrees of substitution and ECH cross-linking percentages (Section 4.3) at 25% nominal filler content.

Sample	Theoretic Degree of Substitution (DS_{th})	Experimental Degree of Substitution (DS_{exp})	Epichlorohydrin (ECH) (%)	Filler (nominal) (%)	Filler content (actual) (%)	Grammage (g/m$^{2)}$)	Bending stiffness (mN)	Breaking length (m)	Tear resistance (mN)	Folding Endurance (-)
Standard				25	25.9	81.5	86.0	3250	423	18
MG 020-1	0.2	0.08	1	25	26.0	81.4	87.0	5059	368	857
MG 050-1	0.5	0.14	1	25	24.0	81.0	87.6	5026	528	363
MG 080-1	0.8	0.23	1	25	24.6	82.3	90.8	5154	593	350
MG 020-3	0.2	0.07	3	25	25.7	81.5	87.2	4507	517	259
MG 050-3	0.5	0.19	3	25	25.3	80.9	84.1	4517	532	280
MG 080-3	0.8	0.25	3	25	26.6	82.0	85.4	4645	507	271
MG 020-6	0.2	0.08	6	25	25.1	81.0	94.1	4350	502	104
MG 050-6	0.5	0.18	6	25	25.0	81.5	85.5	4542	526	218
MG 080-6	0.8	0.23	6	25	25.7	81.8	90.8	4489	504	147

Table D3: Hand sheet screening results of anionic (DS_{th} = 0.2) macrogel maize starch particles cross-linked with 6 wt% ECH (Section 4.3).

Sample	Theoretic Degree of Substitution (DS_{th})	Experimental Degree of Substitution (DS_{exp})	Epichlorohydrin (ECH) (%)	Filler (nominal) (%)	Filler content (actual) (%)	Grammage (g/m$^{2)}$)	Bending stiffness (mN)	Breaking length (m)	Tear resistance (mN)	Folding Endurance (-)
Standard				20	19.6	81.8	98.4	3932	446	26
Standard				25	24.7	81.3	81.2	3346	409	16
Standard				30	30.2	81.3	73.3	2835	328	11
MG 020-6	0.2	0.08	3	20	19.8	81.3	94.0	4834	582	162
MG 020-6	0.2	0.08	3	25	24.0	81.0	84.2	4212	468	65
MG 020-6	0.2	0.08	3	30	30.5	81.3	78.4	3241	413	27

Table D4: Hand sheet testing results of anionic designer dextrin particles (Section 4.4).

Sample	Filler (nominal) (%)	Filler content (actual) (%)	Grammage (g/m$^{2)}$)	Bending stiffness (mN)	Breaking length (m)	Tear resistance (mN)	Folding Endurance (-)
Standard	20	22.0	80.0	96.2	3328	453	15
Standard	25	27.6	80.5	86.8	3069	333	9
Standard	30	33.8	80.3	75.6	2318	232	4
DP1	20	22.0	79.8	100.3	4540	489	83
DP1	25	27.8	79.8	82.8	3760	449	35
DP1	30	33.7	80.0	76.4	3030	382	14

Table D5: Hand sheet testing results of PCC encapsulated with starch (3 layers) (Section 4.5).

Sample	Filler (nominal) (%)	Filler content (actual) (%)	Grammage (g/m$^{2)}$)	Bending stiffness (mN)	Breaking length (m)	Tear resistance (mN)	Folding Endurance (-)
Standard	20	21.8	80.9	105.9	3868	430	17
Standard	25	27.4	80.5	93.4	3193	329	6
Standard	30	32.6	80.3	82.8	2713	271	3
PCC-LBL0.40 (3 layers)	20	20.7	80.9	114.5	6038	564	135
PCC-LBL0.40 (3 layers)	25	26.4	80.3	100.7	4925	510	51
PCC-LBL0.40 (3 layers)	30	31.2	80.3	92.5	4158	418	25

Table D6: Hand sheet testing results of PCC encapsulated with anionic starch ($DS_{th} = 0.40$) (1 layer) (Section 4.5).

Sample	Filler (nominal) (%)	Filler content (actual) (%)	Grammage (g/m$^{2)}$)	Bending stiffness (mN)	Breaking length (m)	Tear resistance (mN)	Folding Endurance (-)
Standard	20	21.1	81.0	85.4	3658	450	28
Standard	25	26.5	79.8	78.0	3106	370	12
Standard	30	32.7	79.8	63.2	2518	298	5
PCC-LBL0.40 (1 layer)	20	23.2	80.4	82.6	3259	410	17
PCC-LBL0.40 (1 layer)	25	27.4	80.6	79.1	2669	340	16
PCC-LBL0.40 (1 layer)	30	34.8	80.1	62.4	2328	294	7

Table D7: Hand sheet testing results of in-situ cross-linked anionic maize starch (ISXL) particles prepared with various theoretic degrees of substitution and ECH cross-linking percentages (Section 4.6).

Sample	Theoretic Degree of Substitution (DS_{th})	Epichlorohydrin (ECH) (%)	Filler (nominal) (%)	Filler content (actual) (%)	Grammage (g/m$^{2)}$)	Bending stiffness (mN)	Breaking length (m)
Standard			20	21.5	80.5	82.0	3730
Standard			25	26.0	81.0	85.6	2770
Standard			30	32.0	81.0	73.7	2200
ISXL1	0	3	20	19.0	80.3	92.0	4720
ISXL1	0	3	25	23.6	80.8	96.9	4840
ISXL1	0	3	30	28.5	80.1	90.5	3530
ISXL2	0.2	3	20	17.8	80.3	113	5160
ISXL2	0.2	3	25	24.1	80.3	96	4000
ISXL2	0.2	3	30	28.3	80.9	95.9	3730
ISXL3	0.8	3	20	19.4	80.1	111	4700
ISXL3	0.8	3	25	23.9	80.8	109	4140
ISXL3	0.8	3	30	30.7	80.9	71.9	2900
ISXL5	0.5	1	20	19.1	81.3	111	4600
ISXL5	0.5	1	25	23.9	79.9	96.4	3880
ISXL5	0.5	1	30	28.8	80.1	82.7	3470
ISXL6	0.5	3	20	19.1	79.8	110	4600
ISXL6	0.5	3	25	23.9	80.6	99.9	4170
ISXL6	0.5	3	30	29.4	79.8	79.6	3630
ISXL7	0.5	5	20	19.6	80.1	96	4500
ISXL7	0.5	5	25	24.9	80.6	87.3	3960
ISXL7	0.5	5	30	29.3	80.5	90.1	3440
ISXL8	0.5	10	20	18.8	80.1	98.4	4780
ISXL8	0.5	10	25	23.9	80.3	91.8	3950
ISXL8	0.5	10	30	29.1	80.4	86.8	3530

Table D8: Hand sheet testing results of in situ cross-linked anionic maize starch (ISXL) particles prepared with anionic $DS_{th} = 0.5$ and cross-linked with 3 wt% ECH (Section 4.6).

Sample	Theoretic Degree of Substitution (DS_{th})	Epichlorohydrin (ECH) (%)	Filler (nominal) (%)	Filler content (actual) (%)	Grammage ($g/m^{2)}$)	Bending stiffness (mN)	Breaking length (m)	Tear resistance (mN)	Folding Endurance (-)
Standard			20	19.6	81.8	98.4	3932	446	26
Standard			25	24.7	81.3	81.2	3346	409	16
Standard			30	30.2	81.3	73.3	2835	328	11
ISXL6	0.5	3	20	18.2	80.3	95.0	4857	507	180
ISXL6	0.5	3	25	23.5	80.3	89.0	3917	449	57
ISXL6	0.5	3	30	28.7	80.8	84.0	3358	464	27

Table D9: Hand sheet testing results of various average particle size anionic dextrin particles prepared using microfluidics (Section 5.3).

Sample	Average Particle Size (μm)	Standard Deviation (-)	Filler (nominal) (%)	Filler content (actual) (%)	Grammage ($g/m^{2)}$)	Bending stiffness (mN)	Breaking length (m)	Tear resistance (mN)
Standard			20	17.0	80.1	97.8	3829	420
Standard			30	31.4	79.0	76.9	2389	295
MF(Run 16)	8.9	10.0	20	17.1	78.8	90.8	3644	490
MF(Run 16)	8.9	10.0	30	26.2	79.1	81.8	2564	340
MF(Run 11)	25.0	17.0	20	17.2	79.5	103.2	3902	435
MF(Run 11)	25.0	17.0	30	26.1	78.0	73.6	2503	309
MF(Run 10)	49.1	37.8	20	16.4	79.0	110.4	3695	439
MF(Run 10)	49.1	37.8	30	25.2	80.4	93.6	2938	337

Table D10: Hand sheet results (extrapolated to 20, 25, and 30% filler content) of samples prepared with different processing techniques.

Particles	Sample	Filler (%)	Extrapolated data points			
			Bending stiffness (mN)	Breaking length (m)	Tear resistance (mN)	Folding Endurance (-)
Macrogel	Standard	20	96	3870	448	24
	Standard	25	84	3352	392	17
	Standard	30	72	2834	336	10
	MG 020-6	20	92	4806	560	142
	MG 020-6	25	85	4065	485	82
	MG 020-6	30	78	3323	409	22
Designer	Standard	20	100	3582	486	16
	Standard	25	91	3150	392	12
	Standard	30	82	2718	299	7
	DP1	20	103	4788	512	90
	DP1	25	92	4144	466	61
	DP1	30	82	3500	420	31
LbL modified PCC	Standard	20	110	4032	450	18
	Standard	25	99	3496	376	11
	Standard	30	88	2960	302	5
	PCC-LBL0.40 (3 layers)	20	115	6136	581	135
	PCC-LBL0.40 (3 layers)	25	105	5241	513	82
	PCC-LBL0.40 (3 layers)	30	94	4345	444	29
In-situ cross-linked	Standard	20	96	3870	448	24
	Standard	25	84	3352	392	17
	Standard	30	72	2834	336	10
	ISXL6	20	93	4540	488	138
	ISXL6	25	88	3822	467	65
	ISXL6	30	82	3105	446	-
Microfluidic processed	Standard	20	93	3528	394	-
	Standard	25	86	3029	351	-
	Standard	30	79	2530	307	-
	MF(Run 10)	20	104	3386	397	-
	MF(Run 10)	25	94	2954	339	-
	MF(Run 10)	30	84	2522	281	-